MODEL BASED APPROACH FOR THE PLANT-WIDE ECONOMIC CONTROL OF FLUID CATALYTIC CRACKING UNIT

by

REDAH MOUSA ALSABEI

A Doctoral Thesis submitted in partial fulfilment of the requirements for the award of the degree of Doctor of Philosophy in Chemical Engineering

ABSTRACT

Fluid catalytic cracking (FCC) is one of the most important processes in the petroleum refining industry for the conversion of heavy gasoil to gasoline and diesel. Furthermore, valuable gases such as ethylene, propylene and isobutylene are produced. The performance of the FCC units plays a major role on the overall economics of refinery plants. Any improvement in operation or control of FCC units will result in dramatic economic benefits. Present studies are concerned with the general behaviour of the industrial FCC plant, and have dealt with the modelling of the FCC units, which are very useful in elucidating the main characteristics of these systems for better design, operation, and control. Traditional control theory is no longer suitable for the increasingly sophisticated operating conditions and product specifications of the FCC unit. Due to the large economic benefits, these trends make the process control more challenging. There is now strong demand for advanced control strategies with higher quality to meet the challenges imposed by the growing technological and market competition.

According to these highlights, the thesis objectives were to develop a new mathematical model for the FCC process, which was used to study the dynamic behaviour of the process and to demonstrate the benefits of the advanced control (particularly Model Predictive Control based on the nonlinear process model) for the FCC unit. The model describes the seven main sections of the entire FCC unit: (1) the feed and preheating system, (2) reactor, (3) regenerator, (4) air blower, (5) wet gas compressor, (6) catalyst circulation lines and (7) main fractionators.

The novelty of the developed model consists in that besides the complex dynamics of the reactor-regenerator system, it includes the dynamic model of the fractionator, as well as a new five lump kinetic model for the riser, which incorporates the temperature effect on the reaction kinetics; hence, it is able to predict the final production rate of the main products (gasoline and diesel), and can be used to analyze the effect of changing process conditions on the product distribution. The FCC unit model has been developed incorporating the temperature effect on reactor kinetics reference construction and operation data from an industrial unit. The resulting global model of the FCC unit is described by a complex system of partial-differential-equations, which was solved by discretising the kinetic models in the riser and regenerator on a fixed grid along the height of the units, using finite differences. The resulting model is a high order DAE, with 942 ODEs (142 from material and energy balances and 800 resulting from the discretisation of the kinetic models).
The model offers the possibility of investigating the way that advanced control strategies can be implemented, while also ensuring that the operation of the unit is environmentally safe. All the investigated disturbances showed considerable influence on the products composition. Taking into account the very high volume production of an industrial FCC unit, these disturbances can have a significant economic impact. The fresh feed coke formation factor is one of the most important disturbances analysed. It shows significant effect on the process variables. The objective regarding the control of the unit has to consider not only to improve productivity by increasing the reaction temperature, but also to assure that the operation of the unit is environmentally safe, by keeping the concentration of CO in the stack gas below a certain limit.

The model was used to investigate different control input-output pairing using classical controllability analysis based on relative gain array (RGA). Several multi-loop control schemes

were first investigated by implementing advanced PID control using anti-windup. A tuning approach for the simultaneous tuning of multiple interacting PID controllers was proposed using a genetic algorithm based nonlinear optimisation approach. Linear model predictive control (LMPC) was investigated as a potential multi-variate control scheme applicable for the FCCU, using classical square as well as novel non-square control structures. The analysis of the LMPC control performance highlighted that although the multivariate nature of the MPC approach using manipulated and controlled outputs which satisfy controllability criteria based on RGA analysis can enhance the control performance, by decreasing the coupling between the individual low level control loops operated by the higher level MPC. However the limitations of using the linear model in the MPC scheme were also highlighted and hence a nonlinear model based predictive control scheme was developed and evaluated.

Results demonstrate that using modern nonlinear model predictive control (NMPC) approaches based on state-of-the-art optimization algorithms and software the advanced control of complex chemical processes, such as the FCCU can be brought into the realm of possibility. The proposed nonlinear control scheme was applied to the control of the highly nonlinear FCC process. Simulations showed that the non-linear model-based MPC is highly effective, and coped well with the complexity and nonlinearities of the FCC process. Both NMPC and LMPC were superior to PID control, and it was shown that the NMPC provided better performance compared to LMPC. A novel economic criteria-based NMPC (ENMPC) was proposed and demonstrated the benefits of controlling the plant based on economic criteria rather than following predetermined setpoint trajectories. The new concept of differentiating between beneficial (good) and harmful (bad) disturbances was introduced and it was shown that regulating the plant at it predetermined operating conditions when beneficial disturbances occur can actually decrease control performance. The novel ENMPC scheme is inherently able to differentiate between good and bad disturbances and exploit potential beneficial disturbances continuously adapting the plant operating conditions to achieve economic optimisation and satisfy environmental and operating constraints.

These results have demonstrated that the control structures proposed may be applied in industry in the form of a new scheme for controlling highly complex chemical processes with significant economic benefits.

Acknowledgments

First and foremost, I thank Almighty Allah (God) for blessing me with success and prosperity. I would like to thank all the people who have supported me in various ways throughout the period of this doctoral research. In particular, I would like to thank my supervisors, Prof. Zoltan Nagy and Prof. Nassehi for their enthusiasm, guidance and continuous encouragement throughout the research. Special recognition is also paid to their incredible patience, their many fruitful discussions and excellent ideas.

I would like to take this golden opportunity to show my appreciation, gratitude and deep thanks to all those people who helped me in carrying out my research and provided all kinds of support in the Department of Chemical Engineering; from the administrative staff: Yasmin, Anna, Liz, Ann, Janey and Becky; from support and technical staff Paul and Tony.

I would like to express sincere thanks is extended to my friends in S158: Hakem, Fahd, Saleemi, Dr. Bahareh, Dr. Matthew and Alhajji for their support and encouragement.

Thanks and gratitude to my parents and my parents-in-law, who have been the greatest driving force behind my PhD, and I absolutely could not have finished without their support, love and prayers. To all my family; my brothers and sisters you have inspired me to go far and get the PhD.

Last but not least, I would like to extend my sincere gratitude to my wife, my daughters and my son, you have always there for me and there is no way I can repay you, my thesis dedication is the smallest gesture I can offer.

Contents

List of Figures

List of Tables

LIST OF NOMENCLATURE

A_{lp}	cross sectional area of lift pipe (ft^2)
A_{reg}	cross sectional area of regenerator (ft^2)
A_{ris}	cross sectional area of the reactor riser (ft^2)
A_{sp}	cross sectional area of catalyst circulation line (ft^2)
$A_{stripper}$	cross sectional area of the reactor stripper (ft^2)
A_{sv}	cross sectional area of regenerated/spent catalyst slide valve at completely open position (in^2)
a_1	furnace heat loss parameter (B.t.u/s F)
a_2	furnace heat loss parameter (B.t.u/s F)
a_j	activity of the catalyst in reaction *j*
B	bottom product (kmol)
C	random fluctuating velocity of an individual particle, (m/s)
C_{cat}	coke fraction on catalyst at the reactor outlet (kg/kg)
cCO_{sg}	concentration of carbon monoxide in stack gas (ppm)
C_H	weight fraction of hydrogen in coke (lb/lb)
$cO_{2,sg}$	concentration of oxygen in regenerator stack (mol%)
C_p	specific heat at constant pressure ([kJ/kg K)
$c_p(z)$	average heat capacity (B.t.u/mol F)
c_{pair}	heat capacity of air (B.t.u/mol F)
c_{pc}	heat capacity of catalyst (B.t.u/mol F)
c_{pCO}	heat capacity of carbon monoxide (B.t.u/mol F)
c_{pCO2}	heat capacity of carbon dioxide (B.t.u/mol F)
c_{pfl}	heat capacity of fresh liquid (B.t.u/mol F)

c_{pf}	heat capacity of fresh vapour (B.t.u/mol F)
c_{pH2O}	heat capacity of steam (B.t.u/mol F)
c_{pN2}	heat capacity of nitrogen (B.t.u/mol F)
c_{pO2}	heat capacity of oxygen (B.t.u/mol F)
c_{psv}	heat capacity of slurry (B.t.u/mol F)
C_p^s	concentration of the reactant lump in path *p* (%)
C_{rgc}	weight fraction of coke on regenerated catalyst (lb/lb)
C_{rw}	wet gas compressor compression ratio (lb/lb)
C_{sc}	weight fraction of coke on spent catalyst (lb/lb)
C_1	wet gas production constant (mol/lb)
C_2	wet gas production constant (mol/lb)
c_c	coke content on catalyst (wt%)
CTO	COR catalyst-to-oil ratio (gcat/gfeed)
D	distillate product flow (kmol/min)
E	deactivation function parameter
$E_{oil,\ inlet}$	elevation where oil enters the reactor riser (ft)
E_{tap}	pressure tap elevation on standpipe (ft)
E_{cf}	activation energy of coke formation (kJ/kg)
Ep	activation energy for reaction path *p*, J/mol
F	feed rate (kmol/min)
F_{air}	air flow rate into regenerator (mol/s)
F_{cat}	flow rate of spent or regenerated catalyst (lb/s)
F_{cc}	catalyst flow in the regenerator (lb/s)
F_b	effect of feed type on coke production
f	deactivation function parameter

F_{coke}	production of coke in reactor riser (lb/s)
F_f	flow of feedstocks entering the reactor (kg/s)
F_H	burning rate of hydrogen (lb/s)
f_{of}	overflow factors
$fpp(x)$	nonlinear valve flow rate function
f_{rgc}	force exerted by regenerated catalyst (lb_f)
F_{rgc}	flow rate of regenerated catalyst (lb/s)
F_s	flow of catalyst entering in reactor (kg/s)
f_{sc}	force exerted by spent catalyst (lb_f)
F_{sc}	flow rate of spent catalyst (lb/s)
F_{sg}	stack gas flow (mol/s)
$F_{sucn,\ comb}$	combustion air blower inlet suction flow (ICFM)
$Fsucn,\ wg$	wet gas compressor inlet suction flow (ICFM)
F_T	air flow rate into regenerator (lb/s)
F_t^{set}	set point to total air flow controller (lb/s)
$f_{ubend,\ rgc}$	regenerated catalyst friction factors (lb s/ft^2)
$f_{ubens,sc}$	spent catalyst friction factors (lb s/ft^2)
F_{V6}	flow through combustion air blower suction valve (lb/s)
F_{V7}	flow through combustion air blower vent valve (lb/s)
F_{V11}	flow through wet gas compressor suction valve (lb/s)
F_{V12}	flow through wet gas flare valve (lb/s)
F_{V13}	flow through wet gas compressor anti-surge valve (lb/s)
F_{wg}	flow of wash oil to reactor riser (lb/s)
F_1	flow of wash oil to reactor riser (lb/s)
F_1^{set}	set point to wash oil flow controller (lb/s)

F_2	flow of diesel oil to reactor riser (lb/s)
F_2^{set}	set point to diesel oil flow controller (lb/s)
F_3	flow of fresh feed to reactor riser (lb/s)
F_3^{set}	set point of fresh feed flow controller (lb/s)
F_4	flow of slurry to reactor riser (lb/s)
F_4^{set}	set point of slurry flow controller (lb/s)
F_5	flow of fuel to furnance (lb/s)
F_5^{set}	set point to wash oil flow controller (lb/s)
F_6	combustion air blower throughput (lb/s)
F_7	combustion air flow to the regenerator (lb/s)
F_{11}	wet gas flow to the vapour recovery (lb/s)
g	acceleration due to gravity (ft/s^2)
h_{ris}	height of reactor riser (ft)
H_{wg}	wet gas compressor head (psia)
K	flow coefficient for the slide valve
KK	light gas scaling constant
k_{comb}	combustion air blower discharge pipe flow resistance factor (lb/s psia)
K	kinetic constant of feedstocks cracking (s^{-1})
K_2	kinetic constant of feedstocks cracking (s^{-1})
K_h	absorption coefficient of lump F_h
k_{ij}	rate constant in the four-lump model [m3/(kg s)]
k_i	reaction rate constant (s^{-1})
k_1	reaction rate constant for reaction I (s^{-1})
k_2	reaction rate constant for the reaction II (s^{-1})
k_3	reaction rate constant for the reaction III (mol s^{-1})

k_6	combustion air blower suction valve flow rating (lb/s psia)
k_7	combustion air blower vent valve flow rating (lb/s psia)
k_{11}	wet gas compressor suction valve flow rating (lb/s psia)
k_{12}	wet gas flare valve flow rating (lb/s psia)
k_{13}	wet gas compressor anti-surge valve flow rating (lb/s psia)
k_{14}	regenerator stack gas valve flow rating (lb/s psia)
k_c	kinetic constant of coke formation in Kurihara's expression (s^{-1})
kp	reaction rate coefficient for reaction path p, m^3/ s kgcat
k_d	deactivation constant for conversion (wt%)
L	reflux (kmol/min)
L_T	condenser's liquid flow (kmol)
$L_{ubend,\ rgc}$	length of regenerated catalyst u-bend (ft)
$L_{ubend,s}$	length of spent catalyst u-bend (ft)
M	molecular mass of the lump (kg/kmol)
m_1	polytrophic exponent
M	total liquid holdup (kmol)
M_1	effective heat capacity of regenerator mass (B.t.u/ F)
Mcp_{eff}	effective heat capacity of riser vessel and catalyst (B.t.u/ F)
M_e	flow rate of entrained catalyst from dense bed into dilute phase (lb/s)
Mow	liquid holdup over weir (kmol)
M_{rgc}	inertial mass of regenerated catalyst (lb s^2/ft)
Muw	liquid holdup under weir (kmol)
M_{sc}	inertial mass of spent catalyst (lb s^2/ft)
M_{wi}	molecular weight of species i (kg/kmol)
n	quantity of gas (mol)

n_1	exponential of the coke generation kinetics
n_2	deactivation function parameter
N^*	integer value representing a constant for pressure drop on catalyst pipes
NC	number of components
NT	number of stages
NF	feed stage
P_{atm}	atmospheric pressure (psia)
P_{base}	combustion air blower base discharge pressure (psia)
P_{rb}	pressure at bottom of reactor riser (psia)
P_{rgb}	pressure at bottom of regenerator (psia)
P_{vru}	discharge pressure of wet gas compressor to vapour recovery unit (psia)
P_1	combustion air blower suction pressure (psia)
P_2	combustion air blower discharge pressure (psia)
P_4	reactor pressure (psia)
P_5	reactor fractionator pressure (psia)
P_6	regenerator pressure (psia)
P_7	wet gas compressor suction pressure (psia)
P	deactivation function parameterQ_{air} = enthalpy of air to regenerator (B.t.u/s)
Q_c	total heat of burning carbon (B.t.u/s)
Q_{catout}	enthalpy of catalyst out of reactor riser (B.t.u/s)
$Q_{cracking}$	heat generated from cracking (B.t.u/s)
Q_e	total heat loss from regenerator to environment (B.t.u/s)
Q_{ff}	heat required to bring fresh feed to reactor riser temperature (B.t.u/s)
Q_{fg}	enthalpy of outgoing regenerator stack gases (B.t.u/s)
Q_{fr}	heat required to raise temperature of fresh feed (B.t.u/s)

Q_H	enthalpy of hydrogen to regenerator (B.t.u/s)
Q_{in}	enthalpy into regenerator, reactor (B.t.u/s)
Q_{loss}	heat loss from furnance (B.t.u/s)
Q_{out}	enthalpy out of regenerator, reactor (B.t.u/s)
Q_{rgc}	enthalpy of regenerated catalyst (B.t.u/s)
Q_{sc}	enthalpy of spent catalyst (B.t.u/s)
Q_{slurry}	heat required to bring slurry to reactor riser (B.t.u/s)
qF	feed liquid fraction (kmol/kmol)
R	universal gas constant (ft^3 psia/lbmol)
R_j	net production rate of component *j*/species *l*, (mol/s kg)
R_i	rate of reaction *i* in the kinetic model (s^{-1})
Rp	reaction rate for path *p*, (mol/s kg)
R_{pm}	net production rate of a lump (mol/kg s)
t_c	residence time of catalyst in the reactor (s)
T	gas-solid phase temperature (K)
T_{air}	temperature of air entering regenerator (F)
T_{atm}	atmospheric temperature (F)
T_{base}	base temperature (F)
$T_{base,f}$	base temperature of reactor fresh feed (F)
$T_{comb,d}$	combustion air blower discharge temperature (F)
T_{cy}	regenerator stack gas temperature at cyclone (K)
T_{lm}	furnance log mean temperature difference (F)
T_r	temperature of reactor riser (F)
T_{ref}	base temperature for reactor riser energy balance (F)
T_{reg}	temperature of regenerator bed (F)

T_{sc}	temperature of spent catalyst entering regenerator (F)
T_1	temperature of fresh feed entering furnance (F)
T_2	temperature of fresh feed entering reactor riser (F)
T_3	furnance firebox temperature (F)
U_{af}	furnance overall heat transfer coefficient (B.t.u/s)
V	boil up (kmol/min)
$V_{comb,d}$	combustion air blower suction system volume (ft^3)
$V_{comb,s}$	combustion air blower suction system volume (ft^3)
V_{reg}	regenerator volume occupied by gas (ft^3)
v_{rgc}	velocity of regenerated catalyst (ft/s)
v_{ris}	volumetric flow rate in reactor riser (ft/s)
v_s	superficial velocity in regenerator (ft/s)
v_{sc}	velocity of spent catalyst (ft/s)
V_6	combustion air blower vent valve position
V_7	combustion air blower vent valve position
V_{11}	wet gas compressor suction valve position
V_{12}	wet gas flare valve position
V_{13}	wet gas compressor vent valve position
V_{14}	stack valve position
W	catalyst hold-up (ton)
W_c	inventory of carbon in regenerator (lb)
W_r	inventory of catalyst in reactor (lb)
W_{reg}	inventory of catalyst in regenerator (lb)
W_{ris}	inventory of catalyst in reactor riser (lb)
wt_{ir}	weight fraction of ten lump species (lb/lb)

$WHSV$	weight hourly space velocity (1/h)
XCO	molar ratio of CO to air (mol/mol)
XCO_{sg}	molar ratio of CO to air in stack gas (mol/mol)
XCO	molar ratio of CO_2 to air (mol/mol)
$XCO_{2,\,sg}$	molar ratio of CO_2 to air in stack gas (mol/mol)
XN_2	molar ratio of N_2 to air (mol)
XO_2	molar ratio of O_2 to air (mol/mol)
$XO_{2,sg}$	molar ratio of O_2 to air in stack gas (mol/mol)
X_v	volume fraction conversion
x_i	column liquid composition (kmol/kmol)
y_f	feedstocks mass fraction (kg/kg)
y_g	gasoline mass fraction (kg/kg)
y_i	column vapor composition (kmol/kmol)
yj	mass fraction for the jth component (kg/kg)
z	vertical position in regenerator (ft)
z_{bed}	regenerator dense bed height (ft)
z_{cyc}	height of cyclone inlet (ft)
zF	column feed mass fraction (kmol/kmol)
z_{lp}	height of lift pipe discharge (ft)
z_{top}	O_2, CO measured point (ft)
V_{ij}	stoichiometric coefficient for the reaction from i to j lump determined by the molecular weight of lumps i and j.
k_{ij}	kinetic constant for the reaction from i to j lump
W	weight hour space velocity
dz	dimensionless length

α_i	the deactivation parameter for the cracking of i lump.
MWc	molecular weight of coke.

Greek notations

δ_z	Dirac delta function
ΔH_{crack}	heat of cracking (B.t.u/s)
ΔH_{fu}	heat of combustion of furnance fuel (B.t.u/SCF)
ΔHH	heat of combustion of hydrogen (B.t.u/lb)
ΔH_1	heat of formation of CO (B.t.u/mol)
ΔH_2	heat of formation of CO (B.t.u/mol)
ΔP_{frac}	pressure drop across reactor main fractionator (psia)
$\Delta P_{elb,rgc}$	pressure drop of the different elements of regenerated catalyst pipe (psia)
$\Delta P_{elb,sc}$	pressure drop of the different elements of spent catalyst pipe (psia)
ΔP_{RR}	differential pressure between regenerator and reactor (psia)
ΔP_{svrgc}	pressure drop regenerated catalyst slide valve (psia)
ΔP_{svsc}	pressure drop spent catalyst slide valve (psia)
$\Delta T_{stripper}$	temperature drop across reactor stripper (F)
ε_e	effective void fraction in regenerator dense phase bed
ε_f	apparent void fraction in regenerator dense phase bed
η_p	polytrophic efficiency
ρ	density (lb/ft^3)
ρ_{airg}	density of air at regenerator conditions

ρ_b	volume fraction of catalyst
ρ_c	density of catalyst in spent and regenerator catalyst circulation line (lb/ft^3)
$\rho_{c,dilute}$	density of catalyst in dilute phase (lb/ft^3)
$\rho_{c,dense}$	density of catalyst in dense phase (lb/ft^3)
ρ_f	density of feedstocks (kg/m3)
ρ_g	density of exit gas (mol/ft^3)
ρ_{lift}	density of catalyst in lift pipe (lb/ft^3)
ρ_{part}	settled density of catalyst (lb/ft^3)
ρ_{ris}	average density of material in reactor riser (lb/ft^3)
ρ_v	vapour density of at reactor riser conditions (lb/ft^3)
τ_{fb}	furnance firebox time constant (s)
τ_{fill}	riser fill time (s)
τ_{fo}	furnance time constant (s)
τ_r	catalyst residence time in riser (min)
Ψ_f	effective coke factor for gas-oil feed (psif)
α	deactivation constant for coke formation (s^{-1})
α_1	crack ability factor for the feedstocks
α_i	relative volatilities of components
α_j	deactivation parameter in reaction *j*
φ	fraction of original activity of the catalyst (dimensionless)
φ_c	coke deactivation function

ϕ_{coke}	activity function for coke formation
ϕ_{conv}	activity function for conversion
τ	residence time (s)
γ	stoichiometric factor of a lump
$\sum a$	sum of molar concentrations (a_i: mol/g of gas) of all the gaseous lumps

CHAPTER 1
INTRODUCTION

1.1 Background

Worldwide, the fluid catalytic cracker (FCC) is the workhorse of the modern refinery. Its function is to convert heavy hydrocarbon petroleum fractions into a slate of more usable range of products, and must adapt to seasonal, environmental and other changing demand patterns, such as for gasoline, LPG and diesel. Furthermore, valuable gases such as ethylene, propylene and isobutylene are produced. The performance of the FCC units plays a major role in the overall economics of refinery plants (Alhumaizi and Elnashaie, 1997). Any improvement in operation or control of FCC units will result in dramatic economic benefits. First commercialised over half a century ago, the FCC is still evolving. Improvements in the technology, as well as changing feed stocks and product requirements continue to drive this evolution. Control of the FCC has been, and continues to be, a challenging and important problem. As will be seen, its steady state behaviour is highly nonlinear, leading to multiple steady states and input multiplicities. In earlier years, before the development of zeolite catalysts, the major control problem was one of stabilisation, of just keeping the unit running. Later with zeolite catalysts, the emphasis shifted to increasing production rates in the face of unit constraints and to handling heavier feeds (Arbel et al., 1995). New world trends in product demands, and to meet more severe legislation about fuel compositions raised the significance of controlling FCC product selectivity. The different product slates of the FCC process are the consequence of the complex interplay between reactions, such as cracking, isomerisation, hydrogen transfer, oligomerisation, etc. The complexity of gas oil mixtures, which are the typical FCC feeds, makes it extremely difficult to characterise and describe the inherent kinetics at a molecular level. Hence, one is forced to examine generalities rather than the details. One of the methods used to do this, is to consider the behaviour of groups of compounds as a unit. In this way, similar components are grouped into a few “cuts” or “lumps”. Therefore, the study of the reactions involved in the catalytic cracking process has followed the lumping methodology (Serti-Bionda et al., 2010).

The FCC unit consists of two interconnected gas-solid fluidised bed reactors. The riser reactor, where almost all the endothermic cracking reactions and coke deposition on the catalyst occur, and

the regenerator reactor, where air is used to burn off the coke accumulated on the catalyst. The heat produced is carried by the catalyst from the regenerator to the reactor (Emad and Elnashaie, 1997). Thus, in addition to reactivating the catalyst, the regenerator provides the heat required by the endothermic cracking reactions. The region of economically attractive operational conditions is determined by both the properties of the feed stocks, catalyst and the desired product distribution requirements. In practice, the optimisation of the FCC unit to the desired range of products is usually carried out by trial and error. The disadvantage of this approach is that the transition from one state to the other must be gradual, and is not always successful, because of the complex interactions between the two reactors. As a result, it could lead to loss of production and consequently affect profits. Most of the economic gain from FCC control development has come from the optimisation level, with the regulation system simply providing stable, responsive, and safe operation. The problem is to find regulator schemes that are effective, economically justified, related to existing practice, and able to provide an adequate operator interface when desired. Most studies (Kurihara, 1967; Iscoll, 1970; Lee and Kugelman, 1973; Eng et al., 1974; Edwards and Kim, 1988; McFarlane et al., 1990; Krishna and Parking, 1985; Elshishini and Elnashaie, 1990) concerning FCC units have dealt with the process control based on a simplified reactor-regenerator model, which in principle incorporates major observed dynamics. Any FCC control should maintain a suitable reactor temperature distribution so as to achieve good product characteristics. The regenerator temperature profile should also be bounded so as to prevent abnormal combustion and excessive temperatures. At the same time, energy and material balances must be maintained between the two parts of the unit (Lopez-Isunza, 1992).

The modelling of complex chemical systems in the simulation of process dynamics and control has been motivated by the economic incentives for improvement of plant operation and plant design. Presently, studies are concerned with the general behaviour of industrial FCC units; these research efforts deal with the modelling of FCC units, which are very useful in elucidating the main characteristics of these units for better design, operation, and control. Traditional control theory is no longer suitable for the FCC unit's increasingly sophisticated operating conditions and product specifications (Jia et al., 2003). Due to the large economic benefits, these trends make the process control more challenging. There is now a strong demand for advanced control strategies with higher control quality to meet the challenges imposed by the growing technological and market competition (Liao, 2008).

Demand in the world oil markets is primarily for motor gasoline and other high quality fuels. Gasoline and other high products can be sold at highest prices; therefore, heavy oils are less

valuable than the light fractions. Crude distillation separates crude oil into more useful fractions. However, distillation alone cannot meet the demand for high quality fuels. Figure 1.1 shows the range of products demanded by the market from a barrel of crude oil, compared with the products produced by distillation alone. An important job of modern refineries is to convert oil from the 'bottom of the barrel' to gasoline and other marketable products. Since a typical FCC unit can convert a large amount of feedstock into more valuable products, the overall economic benefits of a refinery could be considerably increased if proper control and optimisation strategies are implemented. But, analysis and control of FCC processes have been known as challenging problems due to the following process characteristics; (1) very complicated and little known hydrodynamics, (2) complex kinetics of both cracking and coke burning reactions, (3) strong interactions between the reactor and the regenerator, and (4) many operating constraints. However, the large throughput of FCCU, the change in operating conditions, and the substantial economic benefits are the motivation behind this research (Han et al., 2000).

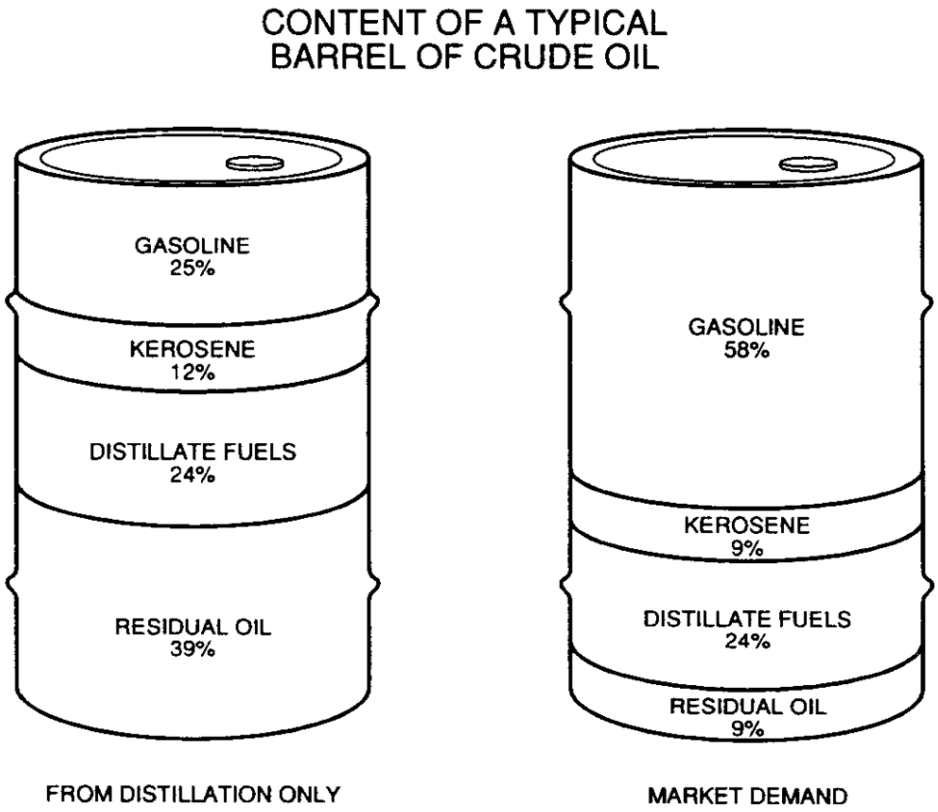

Figure 1.1: Products from typical barrel of crude oil

1.2 Research aim and objectives

The aim of this research project is to develop a mathematical model that can simulate the behaviour of the FCC unit, which consists of feed and preheat system, reactor (riser and stripper), regenerator, air blower, wet gas compressor catalyst circulation lines, and the main fractionators. The model will be subsequently used in studies of control and economic optimisation. The developed model deals with the complex dynamics of the reactor-regenerator system, and also includes the dynamic model of the fractionator, as well as a detailed five lump kinetic model for the riser (namely: gas oil, gasoline, diesel, LPG and coke). This model is able to predict and describe the compositions of the final production rate, and the distribution of the main components in the final product. This allows the estimation of economic factors, related to the operation of the FCCU.

Seven objectives have been identified that lead to a logical progression through the research:

a) to gain knowledge and understanding of FCC unit behaviour by developing a user-friendly, process simulator using an object-oriented programming environment. The simulator can be used to understand the process dynamics, and perform operator training, control structure design, controller tuning, through a comprehensive literature review;

b) implement and evaluate the 5-lump kinetic model in the FCC global model, to simulate the dynamic behaviour of open and closed loops using decoupled advanced PID control algorithms;

c) design and evaluate control schemes for controlled and manipulated variables in order to choose the best control pairs by using an analysis tool, known as relative gain array (RGA);

d) develop a PID tuning algorithm for a Multi Input Multi Output (MIMO) system by using model based optimisation;

e) design and implement linear and nonlinear Model Predictive Control (MPC);

f) derive and evaluate different economic optimisation objectives; and

g) implement a hierarchical Real Time Optimisation (RTO) algorithm and perform evaluation for different economic objectives.

1.3 Main contribution of the thesis

The main contributions of this thesis are summarised in the following lists:

a) An original mathematical model for the FCC process was developed based on the momentum, mass, and energy dynamic balances. It incorporates process hydrodynamics, heat transfer, mass transfer and catalytic cracking kinetics based on a lumping strategy, which lumps molecules and reactions according by their boiling point and treated as pseudo-components for a global description of the phenomena taking place in the reactor. The process is multivariable, strongly nonlinear, highly interactive, and subject to many operational, safety and environmental constraints, posing challenging control problems. The model was implemented in the C programming language for efficient solution, and compiled in Matlab/Simulink language programming, because it provides a convenient graphical user interface. Moreover, the model has been used to study the dynamic behaviour of the process, control the output variables and economic optimisation. The global model of the FCCU is described by a complex system of partial-differential-equations, which was solved by discretising the kinetic models in the riser and regenerator on a fixed grid along the height of the units, using finite differences. The resultant model is described by a complex system of a higher order differential-algebraic-equation (DAE), with 142 ODEs (from material and energy balances and 800 algebraic equations resulting from the discretisation of the kinetic models).

b) A flexible process simulator was developed that can be used to show how the open and closed loop control systems perform in the case of disturbances and model uncertainty. The developed simulator enables engineering and technical personnel to carry out research on the design, operation, performance, and development of a proper control system for a modern catalytic cracking unit. It could also act as an efficient tool for training operating personnel.

c) An automatic tool is proposed to tune PID controllers in a MIMO process based on a Genetic Algorithm (GA). The tuning of several interacting controllers in complex industrial plants is a challenge to process engineers and operators. The success of this task depends on complete knowledge of plant behaviour and control requirements, which can present strong interactions among variables, non-linearity and conflicting objectives. An advantage of the proposed scheme is that a coupled MIMO process with several control loops can

have all the controllers tuned in a unified way as a full MIMO controller. In the development phase, the problem of tuning *n* regulatory control loops was modelled as an optimisation problem, where tuning one control loop may damage the performance of the remaining ones. The solution of the multi-objective problem by the weighted sum approach is possible, since each loop is locally evaluated by a function that considers the integral squared error (ISE). It is worthwhile to note that this modelling is not restricted to PID control. The objective function can be used as a basis for the design and tuning of general, linear or non-linear multivariable controllers.

d) To introduce an analysis method based on the relative gain array (RGA) as a tool to help select variable pairings for decentralised multivariable control structures.

e) To evaluate the performance of Model Predictive Control (MPC) based on linearised global reactor-regenerator-main fractionator FCCU global model. Various square and non-square control structures are investigated, and the tuning of the MPC is evaluated.

f) To develop an efficient real-time nonlinear model predictive control (NMPC) strategy, based on efficient multiple shooting optimization and a real-time iteration scheme, and to evaluate the performance of the proposed scheme in the case of the simulated complete FCCU.

g) To develop a novel NMPC scheme based on the on line optimization of overall process economics related objectives. To demonstrate the benefits of controlling the FCCU based on real time economic decisions, and exploiting the beneficial effects of 'disturbances' if any, rather than simply tracking set point trajectories determined off line.

1.4 Thesis structure

An outline of the chapters in this thesis is as follows:

Chapter 1 gives an introduction to the problems in fluid catalytic cracking technology, together with the recent improvements that maximise the productivity and product quality. The aims of the current study, thesis contribution and structure of the thesis report are discussed.

Chapter 2 provides a review of relevant literature on chemical process control. The sub-sections within this chapter consist of fundamentals of crude oil processing, introduction to the FCC and its significance, process description, and FCC catalyst and process chemistry. The FCC unit is

discussed in its modelling and kinetics aspects. Moreover, various control tools and techniques are discussed. The important information that can be obtained about control, and economic process control is mentioned.

Chapter 3 presents the details of the FCC mathematical model, including the five lump kinetic model for the riser section and the main systems: feed and preheat system, reactor (riser and stripper), regenerator, air blower, wet gas compressor catalyst circulation lines and the main fractionator.

Chapter 4 presents the development of a dynamic process simulator for an open-loop system with a wide range of operating conditions and in the presence of disturbances. Also, sensitivity analyses for composition of the products are presented. The economic aspects have been described by plant gross profit and gasoline octane number, which are sensitive to the presence of disturbance.

Chapter 5 describes and discusses the implementation of a closed loop system using different regulatory controller structures. A set of FCC unit dynamic simulations have been performed and studied in response to disturbances.

Chapter 6 presents an overview of NMPC and LMPC techniques and their implementation on a very complex, industrially relevant FCC process. Software packages for advanced control simulations are studied and presented.

Chapter 7 introduces the novel NMPC approach for the hierarchical Real Time Optimisation (RTO) algorithm and provides an evaluation for different economic objectives.

Chapter 8 concludes the thesis by summarising the results of all the work that has been presented, and proposes areas of future work.

.

CHAPTER 2
LITERATURE REVIEW

2.1 Fundamentals of crude oil processing

The debate on fossil fuels and substitute energy sources is presently at a peak. In this respect, it can be seen that there are significant efforts on the global scale to develop alternatives in the form of sustainable energy sources. Yet, the currently existing alternatives to fossil fuels suffer from drawbacks (Kirby, 2004), listed in the following:

a. Water power, hydroelectric or otherwise, is a clean, non-polluting source. However, it relies on the presence of a sufficiently large water resource, and dam construction is not a sustainable activity.
b. Another option involves utilising hydrogen, which is an abundant resource. Yet, currently, requires large amounts of electrical energy for it to be generated from fossil fuels or water, and is also problematic in its transport and storage.
c. The option of energy from the sun or wind has been subject to significant work, and as such may meet a large part of the needs in some areas. However, this depends on climatic conditions, and the day/night cycle, and as such availability is variable.
d. Development of cleaner derivative fuel technologies, which produce gas from coal before burning to produce power, are said to result in less pollutants (E.ref.1).
e. The alternative of nuclear power has the benefit of zero emissions of pollutants. However, it presents huge challenges in the safe disposal of radioactive waste.
f. Biomass-derived bio-fuels rely on processing organic, vegetable matter. Such fuel is blended with conventional fossil fuel-derived diesel or petrol at low concentrations. For example, maximum 10% bio-fuel blended into petrol (E.ref. 2). A further problem lies in the amount of resources diverted from food production to bio-fuel, which raises a number of ethical questions.
g. The recovery of low-grade heat from ocean and geothermal sources offers a potential long-term solution through power generation using, for example, the Organic Rankine Cycle (14% max. efficiency). Presently, such technology is in the early stages of development, and has seen little implementation in practice.

Given these realities, it would be correct to say that there is still some time before alternative technologies can play an effective role in meeting all current and future power generation needs. Therefore, as yet, oil remains the prime energy source, providing humanity with its essential needs, including food, chemical products, therapeutic drugs, clothing, warmth and facilitating movement (Kirby, 2004).

OPEC reported that over the last forty years, fossil fuels, primarily oil, have been the main source of energy in the world (E. ref. 3).

The organisation predicts that the dependence on oil will remain the same over the next two decades, with a decline by 2030 from 39% in consumption to 36.5%. If the current trends in energy policy and technology development continue unchanged then the demand for oil could rise to 118mb/d by 2030, i.e. an increase of 34mb/d in the interval 2005-2030. Given the economic crisis, affecting the world since 2008, allied to the high price of crude oil, global consumption has fallen. This is expected to reverse as the global economy begins to recover. The demand for crude oil will be driven by the needs of the transport sector, with a predicted rise to 18mb/d by 2030. This will remain so, even with the existence of alternative sources for producing transport fuels, such as tar sand, coal, shale, and even recycled tyres and plastics. However, the process of producing petrol and diesel from crude oil remains the least expensive (E.ref. 4).

The process of producing transport fuels and other useful products involves transporting crude oil to the refinery where it is passed through a distillation column at atmospheric pressure, and fractions of jet fuel, diesel, heavy and light straight run gasoline are recovered; these high quality fuels constitute only 40% of the crude oil (E.ref. 5). The remaining 60% is composed of poor fuels that require more processing to transform them into valuable transport fuels. The atmospheric distillation column bottoms are then distilled under a vacuum, which produces gas oils. These heavy hydrocarbons are then passed as feedstock to hydrocracker or fluid catalytic cracker (FCC) units, and converted into transport fuels and light gases after sweetening.

As mentioned previously, valuable fuels are produced following vacuum distillation and cracking of the 60% crude oil part. This percentage varies with the crude oil constituents, rising in heavier crude oils, characterised by higher molecular weight constituents with less hydrogen molecules. In this case, the value of cracking units, FCC and hydrocrackers, is even greater. Therefore, refineries, in future, will require greater upgrading unit capacity, reaching 7.5mb/d in 2020, according to OPEC (E.ref. 3). It is widely recognised that one of the most efficient way to increase productivity

and efficiency is by adapting advanced controller strategies (McFarlane et al., 1990; McFarlane et al., 1993; Krishna and Parking, 1985; Elshishini and Elnashaie, 1990).

2.1.1 Process technology

Introduction to FCC and it significance

The FCC process among those used in upgrading crude oil products is characterised by its long term reliability and operation, and the variety of products resulting, such as high octane gasoline. The capability of the FCC process to produce, at low cost, high yields of gasoline with high octane number, means it plays a major role in the strategy of gasoline production in refineries (E.ref. 6).

The valuable contribution made by FCC units in gasoline production can be seen in the example of the El Segundo refinery FCC unit operated by Chevron, producing 20 gallons of gasoline per second, which represents the volume of 100,000 car fuel tanks (E.ref. 5).

FCC units vary quite significantly, in terms of where the cracking reaction occurs, and the mode of control selected. In pre-1965 FCC units, the cracking reaction occurs in the dense-phase, fluidised catalyst bed reactor, while control is established through choice of bed depth time and temperature during the process. In time, cracking reactions in the riser became more prominent, especially after introduction of potent zeolite catalysts; all this, required modifications to unit operation. New FCC unit designs have contributed to fundamental changes (Saxton and Worley, 1970), where reactor bed level was minimised; in particular, the rate of circulation of the catalyst was used to control the cracking reaction. In the same context, older units were also modified to accommodate the increased prominence of riser cracking reactions. In these scenarios, feed cracking reactions in the riser have varied in proportion to those taking place in the bed reactor, through varying the combinations of reactor and riser, between multiple or single riser feed lines, in parallel and serially (Saxton and Worley, 1970).

It is worthwhile to mention that FCC units are also capable of producing other high value oil derivatives, such as polypropylene, in addition to gasoline, extremely flexibly, meeting demand in this regard. For example, the FCC unit designed and licensed by UOP has been modified according to the target product, where the purpose of the PetroFCC unit is production of petrochemical feedstock. The UOP PetroFCC unit has the ability to generate ethylene, propylene, benzene and paraxylene, and butylenes, which represents a significant rise in yield in comparison to the traditional unit (E.ref. 7). Such production capabilities are reflected in a production capacity of

about 28% of a total production 50.2 million tons per year of PG/CG (polymer and chemical grade) propylene by FCC units. The yields of the process are shown in Table 2.1.

Table 2.1: Uses of FCC products.

FRACTION	USES
Gases	Plant fuel system Further processed into petrochemical Feedstocks LPG (Liquid Petroleum Gas)
Gasoline	Treated and blended into motor Gasolines
Naphtha	Refined into motor gasoline
Light Cycle Oil	Diesel fuel Jet fuel Fuel oil
Heavy Cycle Oil	Residual fuel Thermal cracking
Clarified Slurry Oil	Residual fuel Thermal cracking

The process results in production, in the regenerator, of waste flue gas, composed of water vapour, carbon dioxide, and carbon monoxide.

FCC units are the key producers of the majority of refinery-grade (RG) polypropylene as a result of gasoline and distillate production operations. RG polypropylene is a by-product of refineries, and annual worldwide output is 31.2 million tons. The petrochemical industry currently absorbs over 50% of this RG polypropylene output. It is predicted that output of RG polypropylene by FCC units will rise by around 5% each year (E.ref. 8).

The present discussion has reflected on the role of FCC units in the context of oil consumption in the future, where they are expected to play a significant role in accommodating expanding demand for olefins, diesel, and gasoline; FCC units will represent 47% of new refinery capacity (E.ref. 3). A technical description of the three parts of the FCC process is presented below (see Figure 2.1):

a) Pre-treatment of the feedstock: this involves the removal of sulphur as well as other contaminants;

b) Catalyst Reaction/Regeneration: the hydrocarbon feedstock is cracked after coming in contact with the hot catalyst. The coke formed on the catalyst surface is then burnt off in the regenerator section; and

c) Separation stage: based on specific boiling range, separation of hydrocarbons into different products, such as diesel, gasoline, occurs.

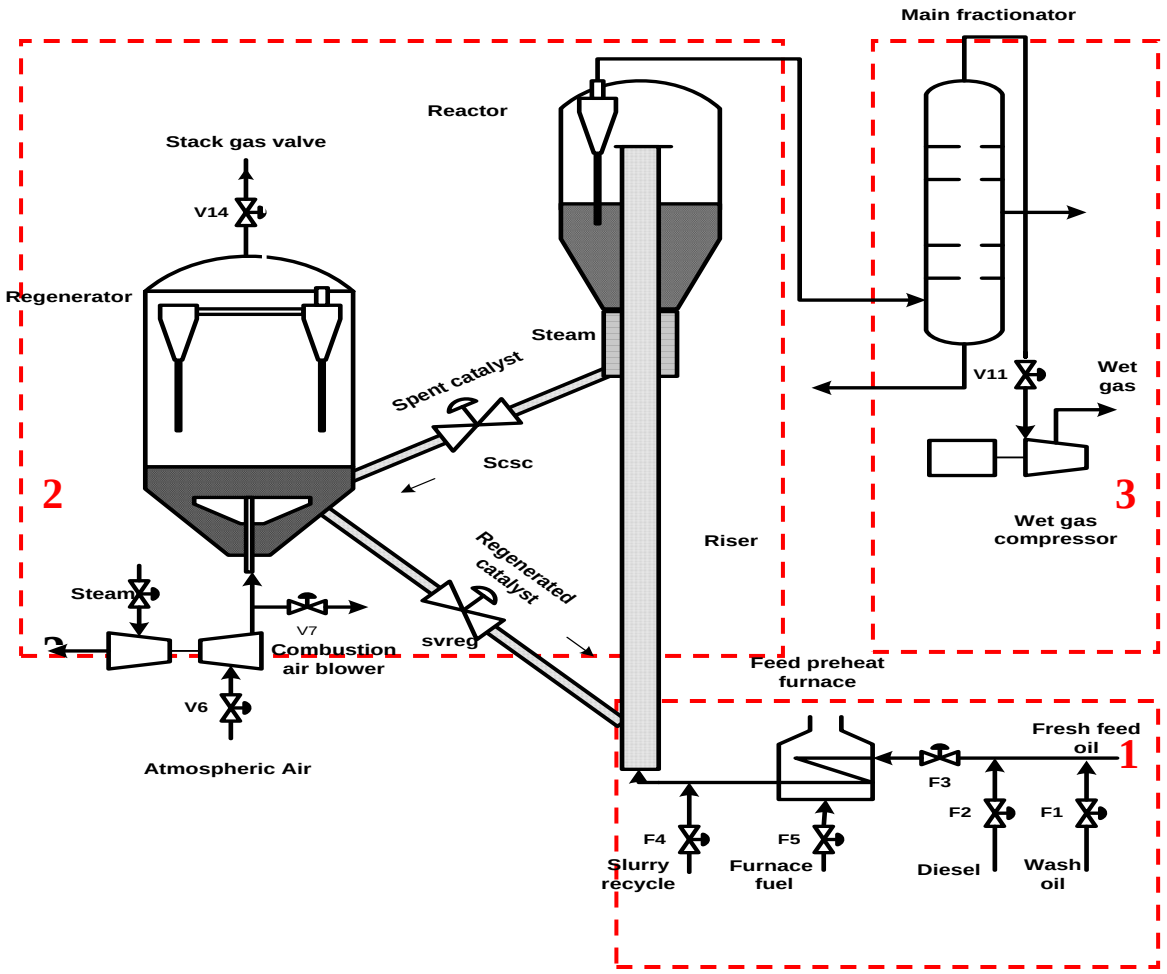

Figure 2.1: UOP type Fluid Catalytic Cracking Unit.

While the term 'mature' may be used to describe FCC technology, strictly, it is only true with respect to:

a. its existence as a commercial process for a long time; and

b. multi-phase fluidisation, as the underlying technology (Sadeghbeigi, 2000).

Otherwise, the technology continues to develop, and respond to the changing demands of the industry. In this context, understanding FCC process behaviour is key to responding to technical challenges and market demands, including environmental protection, operating conditions, higher hydrocarbon feeds processing, unit upgrading, refinery product derivatives, and feeds.

FCC unit operation may be better understood through experimental, or computer simulation studies. In comparing both approaches, experiments are very costly, given the large number of variables involved, e.g. process parameters, production strategy, feedstock type. Therefore, simulation offers a more cost effective and flexible means of studying and optimising the FCC process. The main effort lies in developing a model that accurately describes the process, after which responses can be modelled for any change in the variables of interest, without any further work on the model (Sadeghbeigi, 2000).

Process Description

The FCC process earns its name from the fluid-like behaviour of the very fine particle catalyst when mixed with vapour. The constant circulation of fluidised catalyst between reaction and regeneration zones keeps the cracking process continuous and stable. In addition, the re-circulating catalyst provides a convenient heat transfer medium between the reactor, regenerator and the oil feed. Current basic designs of operational FCC units include: "side-by-side", Orthoflow or stacked types (i.e. separate but adjacent reactor and regenerator vessels), and reactors mounted directly above the regenerator, respectively (Gary and Handwerk, 1975).

Under normal FCC operational conditions, gas-oil and any other feedstocks are heated. This heat is usually provided by the main fractionator bottoms pumparound and/or fired heaters. The FCC feed is preheated and then channelled to the reactor riser base, meeting the regenerated catalyst. Since the catalyst has been heated in the regenerator, this allows the feed to attain the desired temperature for the reactor. The catalytic reaction in the riser is endothermic, with cracking taking place in the vapour phase, and requires the feed to be vaporised. In practice, steam is the preferred means of atomising the feed. Catalyst activity is steadily degraded due to coke deposits arising from the cracking reactions while the catalyst promotes the reaction without it being chemically changed. It is at the reactor stripper stage that the catalyst and cracking products are separated. The centrifugal separation effect of cyclone stages is used to collect and return the catalyst through the diplegs and flapper/trickle valves to the stripper. On its journey into the stripper, hydrocarbons are adsorbed on the surface of the spent catalyst. Meanwhile, the porous catalyst is filled with hydrocarbon vapour; it also entrains vapours as it falls into the stripper. Steam is primarily used to strip and remove the hydrocarbons entrained by fine catalyst particles. Product vapour leaves the cyclone stage in the main fractionator, while hot product vapour from the reactor also enters close to the main fractionator base. Fractionation involves condensing and then vaporising the hydrocarbon components. Vapour/liquid contact is promoted using devices such as shed decks, disk/doughnut

trays, and grid packing. The wet gas compressor receives unstabilised gasoline and light gases exit at the top of the main fractionator. Further transformation then takes place in other refinery units.

The main fractionator produces:

- A gas phase comprising 70-90% C_3 and C_4 hydrocarbons, each containing 60% propane and 40-55% butane respectively.
- A 195 °C end distillation point gasoline fraction made up of paraffin (45-50%), alkenes (8-15%), naphtens (7-15%), and aromatics (20-30%).
- A diesel fraction (distillation range: 195-420 °C); di- and tri-aromatic molecules make up the bulk of the 30-50% of the aromatics in this fraction.
- A slurry above 420 °C.

Constant regeneration of the catalyst is needed because of coke "poisoning". This takes place in a regenerator which, in addition to restoring catalyst activity, also supplies heat that drives the endothermic feed cracking reaction. A blower brings in fresh air to burn off the coke, which is made up of carbon, hydrogen, and traces of sulphurs and nitrogen. An air distributor near the bottom of the regenerator vessel is provided for this purpose. The flue gas resulting from coke combustion passes through cyclones found at the top of the regenerator and, in some designs, is sent to a CO boiler, while in others a shell/tube or box heat exchanger harnesses the flue heat to produce steam from the boiler feed water (Sadeghbeigi, 2000).

FCC catalyst

Since there are over 140 different types of catalyst formulations in the world today, it is important that the refinery personnel involved in cat cracker operations have the fundamental understanding of catalyst technology. This is useful in areas like trouble shooting of units. The use of additives is likely to increase in the coming years due to the need to produce reformulated gasoline and to reduce SOx and NOx emissions (Scherzer, 1990).

Catalyst components

FCC catalysts are in the form of fine powders with an average particle size of 75 microns. There are four major components in the catalyst.

Zeolite

It is the key ingredient of the FCC catalyst. Its role is to provide product selectivity and much of catalytic activity. It has a well-defined lattice structure. Its basic building blocks are silica and alumina tetrahedral. Each tetrahedron consists of a silicon or aluminium atom at the center of the

tetrahedron with oxygen atoms at the corners. The activity of the zeolite comes from its acid sites. The zeolites with application to FCC are Type X and Type Y. Virtually all of the catalysts used today in FCC are of Type Y (Humphries and Skocpol**,** 2004).

Rare earth components such as lanthanum and cerium were used to replace sodium in the crystal. They form "bridges" between two to three acid sites in the zeolite framework. The rare earth exchange adds to the zeolite activity and thermal and hydrothermal stability. Low aluminium content zeolites are called Ultra stable Y or USY because of its higher stability. They are used for production of high-octane gasoline by raising the olefinicity (O'Connor et al., 2001).

The properties of zeolite play a significant role in the overall performance of the catalyst. The reactor/regenerator environment can cause significant changes in chemical and structural composition of the zeolite. For e.g., in the regenerator, the zeolite is subjected to thermal and hydrothermal treatments. The zeolite must also retain its crystallinity against feedstock contaminants such as vanadium and sodium. The three parameters, which govern zeolite behavior, are Unit Cell Size, Rare earth level, Sodium content.

The Unit Cell Size (UCS)

Is a measure of aluminium sites or the total potential acidity per unit cell. The negatively charged aluminium atoms are sources of active sites in the zeolite. Silicon atoms do not possess any activity (Cheng et al., 1998).

Rare earth

Elements serve as a "bridge" to stabilize aluminium atoms in the zeolite structure. They prevent the aluminium atoms from separating from the zeolite lattice when the catalyst is exposed to high temperature steam in the regenerator. The rare earth increases zeolite activity and gasoline selectivity with a loss in octane (Silverman et al., 1986). The insertion of rare earth maintain more and closer acid sites, which promotes hydrogen transfer reactions. In addition, rare earth improves thermal and hydrothermal stability in the zeolite.

Sodium

Is originates either from the zeolite or from the feedstock. It decreases the hydrothermal stability of the zeolite. It also reacts with the zeolite acid sites to reduce catalyst activity. In a de-aluminated zeolite, when the UCS is low, the sodium can have an adverse effect on the octane of gasoline. It is attributed to the droop in the number of strong acid sites.

Matrix

This refers to the components of the catalyst other than the zeolite. The term active matrix means the component of the catalyst other than the zeolite having catalytic activity.

Alumina is the source for an active matrix. The active matrix contributes significantly to the overall performance of the FCC catalyst. The zeolite pores are not suitable for cracking of large hydrocarbon molecules. They are too small to allow diffusion of the large molecules to the cracking sites. An effective matrix must have a porous structure to allow diffusion of hydrocarbons into and out of the catalyst. The active matrix pre-cracks heavy feed molecules for further cracking at the internal zeolite sites. The result is a synergistic interaction between matrix and zeolite in which the activity attained by their combined effects can be greater than the sum of the individual effects. An active matrix can also serve as a trap to catch some of the vanadium and basic nitrogen. The high boiling fraction of the FCC feed usually contains metals and basic nitrogen that poison the catalyst.

Catalysts and the Cracking Reaction

First, a long-chain hydrocarbon molecule is absorption on the porous surface of the catalyst. This absorption weakens the bonds between the atoms of the hydrocarbon molecule which makes the molecule more reactive (Bhattacharyya, 2010).

Inside the pores, the hydrocarbon molecule contacts the catalyst's active sites. The acidity of the active sites promotes a chemical reaction that cracks the hydrocarbon molecule apart. The cracked molecules that leave the catalyst particle are made up of shorter-chained hydrocarbons. They may form single bonds or rings. When these shorter-chained hydrocarbons are disengaged from the catalyst, they can be separated into several more valuable products: olefinic gases, liquefied petroleum gases, gasoline, and light fuel oil (Katz, 2001).

Process Chemistry

The chemistry of the fluid catalytic cracking process is complex although catalytic cracking has been subject to long and in-depth investigation. This reaction has been described as occurring because carbenium ion intermediates are produced on the acid sites of a catalyst's surface (Tominaga and Tamaki, 1997). Yet, the nature of these carbocations is still controversial. Meyers (1997) proposed the description: "classical" carbenium ions and protonated cyclopropane derivatives. In addition to C-C bond cleavage, the complex cracking process also includes other reactions:

- Isomerisation;
- Protonation, deprotonation;
- Alkylation;
- Polymerisation;
- Cyclisation,
- Condensation (due to which coke is also formed).

Complex intra- and inter-molecular reactions distinguish the catalytic cracking process, also leading to coke formation while the deactivating effect of coke on the catalyst holds the key to an elegant practical process (Sadeghbeigi, 1995; Magee and Mitchell, 1993).

Equations 2.1-2.15, describe the series of complex reactions occurring to a large gas-oil molecule in the presence of 1,200°F to 1,400°F (650°C to 760°C) FCC catalysts. The nature and strength of the acid sites on the catalyst surface feature among the many factors affecting the distribution of products. However, other factors, such as non-ideal mixing in the riser and poor separation of cracked products in the reactor, cause the majority of cracking in the FCC.

In a typical FCC unit, the main reactions occurring are (Sadeghbeigi, 2000):

a) Cracking

- paraffins cracked to olefins and smaller paraffins

$$C_{10}H_{22} \longrightarrow C_4H_{10}+C_6H_{12} \quad (2.1)$$

- olefins cracked to smaller olefins

$$C_9H_{18} \longrightarrow C_4H_8+C_5H_{10} \quad (2.2)$$

- aromatic side-chain scission

$$ArC_{10}H_{21} \longrightarrow ArC_5H_9+C_5H_{12} \quad (2.3)$$

- naphthenes cracked to olefins and smaller ring compounds

$$Cyclo\text{-}C_{10}H_{20} \longrightarrow C_6H_{12}+C_4H_8 \quad (2.4)$$

b) Isomerisation

- olefin bond shift

$$1\text{-}C_4H_8 \longrightarrow trans\text{-}2\text{-}C_4H_8 \quad (2.5)$$

- normal olefins to iso-olefin

$$n\text{-}C_5H_{10} \longrightarrow iso\text{-}C_5H_{10} \quad (2.6)$$

- normal paraffin to iso-paraffin

$$n\text{-}C_4H_{10} \longrightarrow iso\text{-}C_4H_{10} \quad (2.7)$$

- cyclo-hexane to cyclo-pentane

$$C_6H_{12} \rightarrow C_5H_9CH_3 \quad (2.8)$$

c) Hydrogen transfer

$$\text{Naphtene+Olefin} \rightarrow \text{Aromatic+Parafin} \quad (2.9)$$

- cyclo-aromatisation

$$C_6H_{12}+3C_5H_{10} \rightarrow C_6H_6+3C_5H_{12} \quad (2.10)$$

d) Trans-alkylation/alkyl-group transfer

$$C_6H_4(CH_3)_2+C_6H_6 \rightarrow 2C_6H_5CH_3 \quad (2.11)$$

e) Cyclisation of olefins to naphthenes

$$C_7H_{14} \rightarrow CH_3\text{-cyclo-}C_6H_{11} \quad (2.12)$$

f) Dehydrogenation

$$n\text{-}C_8H_{18} \rightarrow C_8H_{16}+H_2 \quad (2.13)$$

g) Dealkylation

$$Iso\text{-}C_3H_7\text{-}C_6H_5 \rightarrow C_6H_6+C_3H_6 \quad (2.14)$$

h) Condensation

$$Ar\text{-}CH{=}CH_2+R_1CH{=}CHR_2 \rightarrow Ar\text{-}Ar+{}_2H \quad (2.15)$$

2.2 Mathematical modelling concept

Given the various processes occurring in chemical plant, a multidisciplinary approach is needed in modelling such processes. A system of equations mathematically describes the intrinsic and interdependent relationships between the process variables, to form the computer model.

The benefits of simulation models are useful in (Tasoti, 2007):

- Design of the system: including optimizing the process and its parameters, performing dynamic analysis, and analyzing the effect of key factors, as well as unit upgrade.
- Process control: analysing the possible control strategies, identifying the best control scheme; developing predictive control model and expert system.
- Potential failure mode identification: includes determining factors disturbing the process, or those that reduce performance of the plant.
- Personnel training: enabling realistic training simulation of plant start-up, operation, and shutdown, including operation at the plant design limits.
- Developing safety procedures and determining the environmental impact: allows dangerous regimes of operation to be identified with associated risk assessment leading to accident prevention controls, and quantifying social and economic impacts.

The mathematical models for a system may be described as stochastic / statistical (empirical) or analytical, based on the type of relations existing among the system variables. A statistical model is built on measurements, and observations of system operation, and has the advantage of:

- mathematical simplicity, and so requires basic mathematics treatment
- Knowledge of the system does not need to be deep, concerning the underlying phenomena, and processes

However, statistical models also present several major disadvantages, where:

- A large amount of data, obtained from experiments on the system to be modelled, is required
- It is not possible to extrapolate and extend mathematical models beyond the range of experimental data used to build them
- A unique and new model must be built to fit each new system or variant developed, using new data derived from experiments performed on these systems

In contrast, analytical mathematical models are built on equations for the laws of conservation of mass, energy, and momentum, as well as those laws governing the physics and chemistry of processes occurring in the system. Such models offer a number of advantages:

- The ability to extend them easily to take account of changes, i.e. their domain of validity is extended,
- Provide greater flexibility,
- Analytical models can be extended to fit new systems with similar processes.

However, analytical models also present disadvantages, in that:

- Knowledge of the system's underlying processes and phenomena must be quite good
- Specialist skill is required to derive those equations that describe the physics and chemistry of the system to be modeled
- A model validation/verification stage, involving experiment, is needed; the experimental data is input into the model to compare output with reality.

Additionally, the system models may reflect either the steady state, or unsteady (dynamic) state; in the former, the model algebraic equations are independent of time, i.e. do not change with time; while in the latter, the model equations are time-dependent, differential equations describing continuous system variables. In addition, the relationships in either case may be linear or non-

linear. The analytical model of the chemical system is built by specifying appropriate energy, momentum, and mass conservation equations coupled to the equations of chemical equilibrium and the physical state of the system.

- The statistical model is built by recording the process variables in experiments, and applying statistical methods to determine the equations relating the process inputs to the output
- A mixed statistical and analytical model may be defined by coupling empirical and analytical equations

2.2.1 FCC cracking kinetics modelling

Prior to the 1930s, hydrocarbon cracking was achieved by applying high temperature to effectively break the bonds in the high molecular weight compounds resulting in lower molecular weight hydrocarbons. However, this thermal cracking process was superseded by catalytic cracking, which would occur rapidly, and at lower temperature.

Currently, key components of modern refinery infrastructure are fluid catalytic crackers, which facilitate the conversion of high molecular weight hydrocarbons into desired products, LPG, gasoline, and diesel. Given the high value products of cracking, any development that increases FCC process yields, by as little as 1%, is welcomed (Das et al., 2003). However, such advances can only be achieved by deep understanding of FCC operations, typically, residence times, temperatures, catalysts, feedstocks, and catalyst-to-oil (C/O) ratio. Optimisation of unit operation for maximum yield in particular modes of operation requires models for the reactor and reaction kinetics that are highly accurate, regardless of the feedstock used.

Review of FCCU Modelling

The importance of the FCCU has led to the development of many models over time, based on varying assumptions regarding reaction kinetics, and component hydrodynamics, including generator and riser. The focus in some models has been the regenerator only (Ford et al., 1976; Errazu et al., 1979; de Lasa et al., 1981; Guigon and Large, 1984; Krishna and Parkin, 1985; Lee et al., 1989a), while others have been restricted to the cracking process or reactor (Weekman and Nace, 1970; Paraskos et al., 1976; Jacob et al., 1976; Shah et al., 1977; Lee et al., 1989b; Larocca et al., 1990; Takatsuka et al., 1987), and yet others that included both reactor and regenerator (Kumar et al., 1995; Lee and Kugelman, 1973; McGreavy and Isles-Smith, 1986; Bozicevic and Lukec, 1987; Arandes and de Lasa, 1992; McFarlane et al., 1993; Arbel et al., 1995; Arandes et al., 2000). These models have been summarised in Table 2.2, with a breakdown of feedstock/product combinations with respect to each component.

Table 2.2: Review of kinetic models used in FCCU with different lump components.

<table>
<tr><td rowspan="4">Kinetic Models</td><td colspan="17">Components</td><td colspan="2" rowspan="3"></td></tr>
<tr><td colspan="8">Feed</td><td colspan="9">Product</td></tr>
<tr><td>1</td><td>2</td><td>3</td><td>4</td><td>5</td><td>6</td><td>7</td><td>8</td><td colspan="4">9</td><td colspan="2">10</td><td colspan="2">11</td><td>12</td></tr>
<tr><td>P_l</td><td>N_l</td><td>As_l</td><td>Ar_l</td><td>As_h</td><td>Ar_h</td><td>P_h</td><td>N_h</td><td colspan="4">Gasoline</td><td colspan="2">LPG</td><td colspan="2">Gas</td><td>Coke</td><td>Approach</td><td>Ref.</td></tr>
<tr><td>3 – Lump</td><td colspan="8">Gas Oil</td><td colspan="4">G</td><td colspan="5">Gas + Coke</td><td>PF</td><td>1</td></tr>
<tr><td>4a – Lump</td><td colspan="8">Gas Oil</td><td colspan="4">G</td><td colspan="4">Gas</td><td>Coke</td><td>PF</td><td>2,3</td></tr>
<tr><td>4b – Lump</td><td colspan="8">Gas Oil</td><td colspan="4">G</td><td colspan="4">LPG + Gas</td><td>Coke</td><td>PF</td><td>4,5.19</td></tr>
<tr><td>5a – Lump</td><td colspan="8">Gas Oil</td><td colspan="4">G</td><td colspan="2">LPG</td><td colspan="2">Gas</td><td>Coke</td><td>PF</td><td>6,7</td></tr>
<tr><td>5b – Lump</td><td colspan="4">LCO</td><td colspan="4">HCO</td><td colspan="4">G</td><td colspan="4">LPG + Gas</td><td>Coke</td><td>PF</td><td>8,9,10</td></tr>
<tr><td>6a – Lump</td><td colspan="4">LCO</td><td colspan="4">Gas Oil</td><td colspan="4">G</td><td colspan="2">LPG</td><td colspan="2">Gas</td><td>Coke</td><td>PF</td><td>11</td></tr>
<tr><td>6b – Lump</td><td colspan="4">LCO</td><td colspan="4">Gas Oil</td><td colspan="4">G</td><td colspan="2">LPG</td><td colspan="2">Gas</td><td>Coke</td><td>PF</td><td>12</td></tr>
<tr><td>7 – Lump</td><td colspan="8">HCO</td><td colspan="4">G + Diesel</td><td>Propene + butene</td><td>Propane + butane</td><td>Ethene</td><td>Other gases</td><td>Coke</td><td>PF</td><td>13</td></tr>
<tr><td>8a – Lump</td><td colspan="4">Non-Aromatic Carbons</td><td colspan="4">Aromatic carbons</td><td colspan="4">G + Diesel</td><td>Propene + butene</td><td>Propane + butane</td><td>Ethene</td><td>Other gases</td><td>Coke</td><td>PF</td><td>14</td></tr>
<tr><td>8b – Lump</td><td colspan="8">LCO</td><td>P</td><td>O</td><td>N</td><td>A</td><td colspan="2">LPG</td><td colspan="2">Gas</td><td>Coke</td><td>PF</td><td>15</td></tr>
<tr><td>8c – Lump</td><td colspan="8">Gas Oil</td><td>P</td><td>O</td><td>N</td><td>A</td><td colspan="2">LPG</td><td colspan="2">Gas</td><td>Coke</td><td>PF</td><td>16</td></tr>
<tr><td>10 - Lump</td><td>P_l</td><td>N_l</td><td>As_l</td><td>Ar_l</td><td>As_h</td><td>Ar_h</td><td>P_h</td><td>N_h</td><td colspan="4">G</td><td colspan="5">Gas + Coke</td><td>FF</td><td>17,18,19,20,21</td></tr>
<tr><td>12 – Lump</td><td>P_l</td><td>N_l</td><td>As_l</td><td>Ar_l</td><td>As_h</td><td>Ar_h</td><td>P_h</td><td>N_h</td><td colspan="4">G</td><td colspan="2">LPG</td><td colspan="2">Gas</td><td>Coke</td><td>FF</td><td>22</td></tr>
</table>

Where : PF: Product Focus, FF: Feed Focus, AG : Aromatic Gasoline, Ar_h : Heavy Aromatic Rings, Ar_l : Light Aromatic Rings, As_h : Heavy Aromatic Substituents, As_l : Light Aromatic Substituents, Gas : (Light Gas, Dry Gas, Fuel Gas), HCO : Heavy Cycle Oil (P_h, N_h, As_h, Ar_h), HGO : Heavy Gas Oil (As_h, Ar_h), LCO : Light Cycle Oil (P_l , N_l , As_l , Ar_l), LGO : Light Gas Oil (As_l , Ar_l), LPG : Liquid Petroleum Gas, N_h : Heavy Naphthene, N_l : Light Naphthene, P_h : Heavy Paraffin, P_l : Light Paraffin, VGO : Vacuum Gas Oil, P, O, N, A: Paraffin, Olefins, Naphthene, Aromatic.

A common assumption regarding the flow in the reactor riser is to consider that it follows a plug regime (Arbel et al., 1995), allied to a uniform distribution temperature in the cross-section, and a gradient over the riser height. Further assumptions include adiabatic conditions, quasi-steady state, temperature uniformity irrespective of position for the two phases, no slip conditions, and oil vapour/catalyst constant heat capacities. Another assumption is that the riser has isothermal conditions, as in the CSTR type, despite the non-isothermal conditions existing in the riser bottom, given the finite time for mixing (McFarlane et al., 1993). Therefore, the main difference among these models of the riser is in the treatment of the kinetics of reaction.

The study of catalytic cracking involves two key areas: (i) catalytic cracking reaction mechanism; and (ii) the approach chosen for describing the kinetics of complex, multi-component mixtures (the level of kinetic expression complexity selected must be balanced with the financial, resource, and computational cost, etc. of the model). A reduced modelling overhead may be secured by employing correlations of cracking kinetics, given the availability of several, such as The saturates, aromatics, resins and asphaltenes SARA (Xu et al., 2005), lumps like the 5 lump model (Bozicevic and Lukec, 1987), and a mechanistic approach to reactions as in single-event kinetics (Feng et al., 1993).

The Lumped Approach to Kinetic Modelling

Feedstocks passed through a cracking unit vary in component species, which are typically a huge amount of different hydrocarbons, beyond the ability of models to account for the kinetics of each one. Overcoming this obstacle involves the introduction of lumping, in which species are grouped together based on their boiling range, where it is thought that their reaction kinetics will be the same. These lumped groups represent pseudo-components that are treated as though they are individual components. An example of lumped components is that of C_6 to C_8 paraffins, which share the same physical and chemical properties. In gas oil cracking, reactions take place sequentially along a series of paths, where the resulting primary products are lumped into pseudo-components, such as gasoline, coke, LCO, and LPG (Gomez-Prado et al., 2006).

Kinetic Models based on Products

Blanding (1953) presented the first model of catalytic cracking kinetics using a two lump approach, where the first lump contained all the components with boiling points above that of gasoline, and the second lump contained those below. Nearly two decades later, a 3-lump model Figure 2.2 was proposed; the first lump contained gas oil that was not cracked, the second grouped the components of gasoline, and the third light gas and coke (Weekman and Nace, 1970). This model was

distinguished by being simple as it had three components resulting in only three reactions, and allowed the yield of gasoline, and conversion of gasoil to be calculated at the same time (Lee et al., 1989).

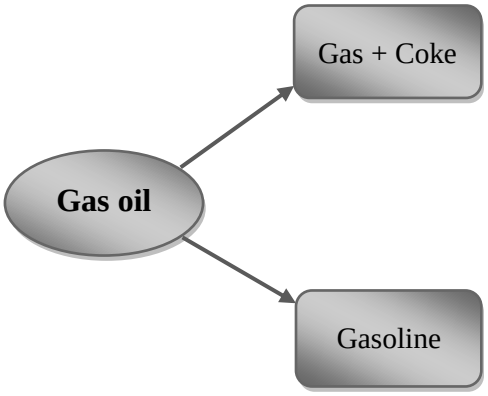

Figure 2.2: 3-lump Model.

However, this model also presented some disadvantages, including the need to calculate a new kinetics set, whenever the feedstock changed (Weekman and Nace, 1970). This major disadvantage was overcome with the development of a 10-lump model, which was more complex (Figure 2.3), but allowed feedstock composition and kinetic constants to remain independent (Jacob et al., 1976). This model was made up of lumps, in which groups with similar molecular structure were grouped together. These lumps are the products: (i) gasoline (G) and (ii) coke with gases (C). Then the reaction groups: (iii) naphthtenes (N), (iv) paraffins (P), (v) aromatic rings (Ar), (vi) aromatic substituent groups (As); these reaction groups are further subdivided into light and heavy fractions, where the former have boiling ranges below 343 °C, and are denoted by the subscript, $_l$, and the latter have boiling ranges above 343 °C, and are denoted by the subscript, $_h$.

The 10-lump model provided a number of advantages, as it enabled estimates of the rate of light and heavy oils, as well as gasoline production, as well as gas oil conversion to be calculated. However, the model required the composition of feedstock to be determined, and also further data from experiments (Jacob et al., 1976). In common with the 3-lump model, it was not possible to independently estimate coke formation (Feng et al., 1993).

The concept of lumping feedstock components and products has become well-established and progressed over time (Weekman and Nace, 1970). In catalytic cracking models proposed by Yen et al. (1988) and Lee et al. (1998), the three lump model was developed into a 4-lump model (Figure 2.4) by creating two separate lumps from the coke with gas oil lump.

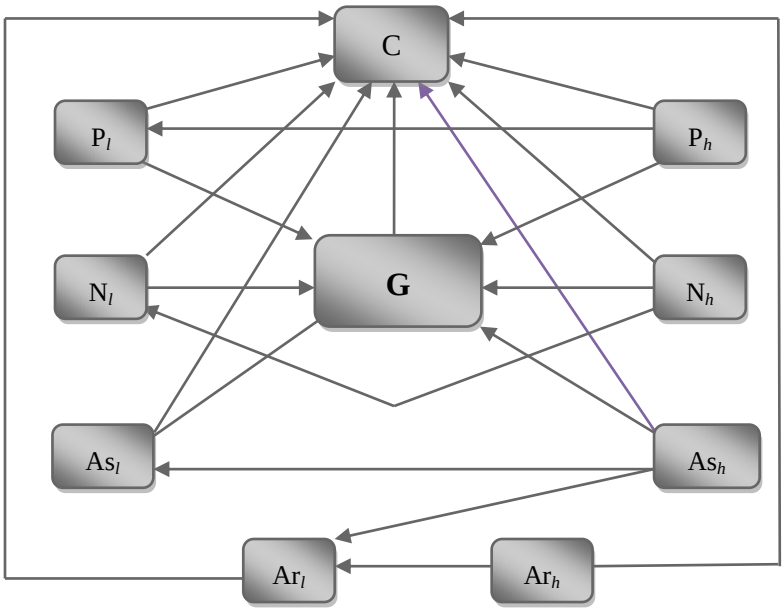

Figure 2.3: 10-lump model.

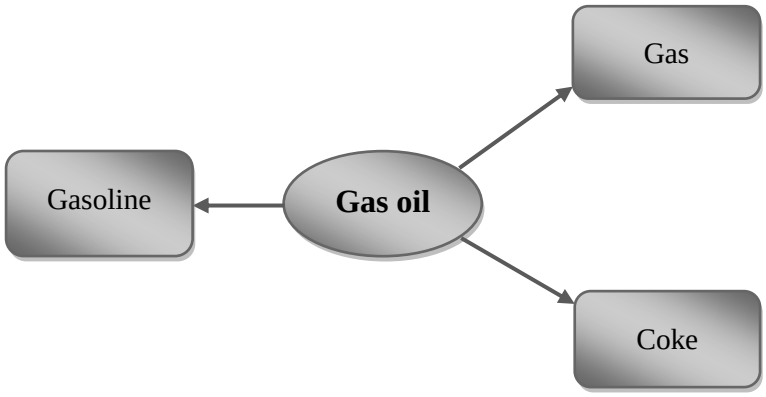

Figure 2.4: 4-lump Mode.

A 5-lump model was proposed (Figure 2.5), where the gas oil lump was further sub-divided into light and heavy fractions (Corella and Frances, 1991). For the case of aromatic gas oil cracking, this 5-lump model was made simpler by Dupain et al. (2003) in modelling less reaction. The Weekman and Nace (1970) 3-lump model was extended into a 5-lump model by dividing the gas oil lump into three new lumps comprising paraffins, naphthtenes, and aromatics by Larocca et al. (1990). The 5-lump model by Ancheyta-Juarez et al. (1999) was different in that rather than divide the gas oil lump, they split the gas lump into two dry gas and liquefied product gas lumps. The model describing the distribution of the products of catalytic cracking was proposed by John and

Wojciechowski (1975). In the model, primary and secondary products were n-butane, propylene, and butane, and secondary products were represented by iso-butane, ethylene, ethane, methane, and coke. Corma and Martinez-Triguero (1984) proposed modifications to the model in adding isobutene and propane to the primary and secondary products group.

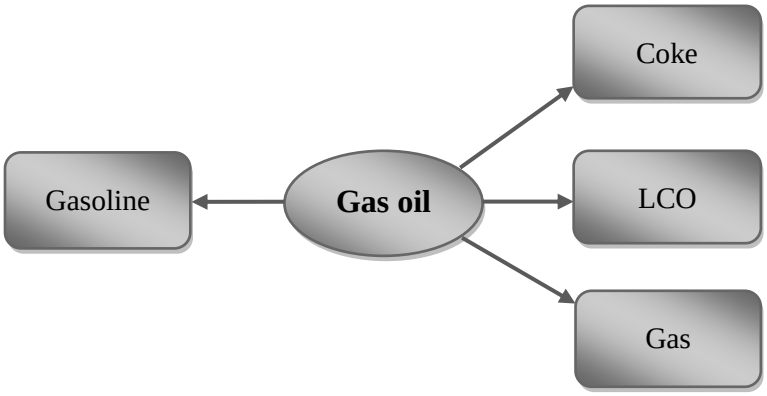

Figure 2.5: 5-lump Model.

6-lump models were proposed by Takatsuka *et al*. (1987), who added a new lump for the residual oil, and Oliveira and Biscaia (1989), who focused on paraffinic gas oils and gasoline. An 8-lump model was derived from the Ancheyta-Juarez *et al*. (1999) 5-lump model by Hagelberg *et al*. (2002) (Figure 2.6). The gasoline lump was split into olefin, paraffin, naphthene, and aromatic components lying in the $343^{o}C^{+}$ boiling temperature range, and also those components with boiling temperatures in the range, $220^{o}C$ to $343^{o}C$, comprising light naphthenes, light paraffins, and light aromatics. The assumption was that the cracking the heavy hydrocarbon lumps would result in gasoline, light gas oil, coke, and light gases lumps. Furthermore, the light gas oil lump would be cracked to give gasoline, coke, and light gases. Further cracking was considered possible, where gasoline would be converted into coke and light gases. The model is easier to deal with given the reduced set of kinetic parameters. Additionally, data to fit the kinetic rates of the model were obtained from short contact reactor experiments.

An advance in the area of 5-lump model was presented in the work of Dupain et al. (2006), in taking account of thermal cracking in producing coke and gas. However, despite the simplicity of kinetic models based on products, they are dependent on the feedstock conceptualised as one component. Such dependence on the feedstock in the model kinetics is a significant disadvantage, as new experiments must be performed for any change to the feedstock composition to derive the appropriate kinetic parameters.

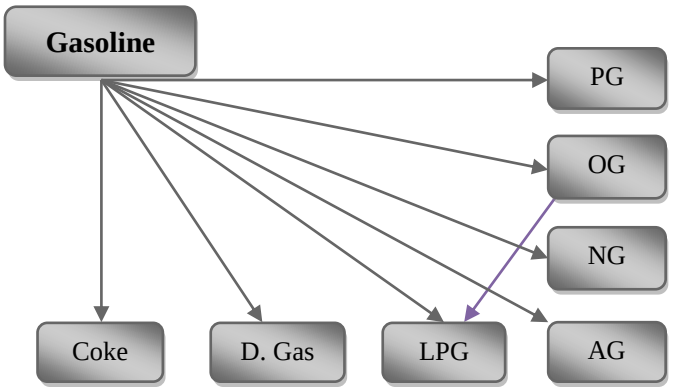

Figure 2.6: 8-lump model.

Kinetic Models based on the feed

As was discussed previously for those models based on products, a number of models have also been proposed that are based on the feedstock, beginning with the Jacob et al. (1976) 10-lump model, where the spectrum of products was treated in a better way. The composition of the feedstock was studied from the perspective of its influence on the gasoline product composition. The feedstock was considered to be a combination of napthtenes, paraffins, and aromatics, while gasoline was considered to be composed of olefins, naphthenes, paraffins, and aromatics (Pitault et al., 1994). This model also considered the LPG, light cycle oil, coke, and dry gas product groups. All this led to the inclusion of 25 reactions, such as cyclisation of olefins to naphthenes, hydrogen transfer, ß-scission, and condensation with hydrogen transfer between olefins and aromatics.

Data for the reaction rate constants were determined by experiments on the microactivity-test (MAT) system. However, this may introduce errors to the model given the limitations associated with the MAT system in the kinetic modelling of catalytic cracking (Farag, 1993). It is argued that the time allocated (1-2 min) for catalyst contact is shorter than is the case in practice in the riser. In addition, feed vaporisation, and the endothermic nature of cracking may lead to a significant drop in reactor temperature, which is not accounted for (Hagelberg et al., 2002).

A 13-lump model (Figure 2.7) presented by SINOPEC (Chen and Cao, 1995) shares the same features as the 10-lump model. Feedstock components are grouped by family, i.e. naphthtenes (N), paraffins (P), asphaltenes (Fa), and aromatics (Ca), and also based on range of boiling temperature denoted by $_l$ for diesel (205 - 320°C), $_m$ for gas oil (320 - 500°C), and $_h$ for residue (500°C and above). Products are then split into a gasoline lump (G), coke lump (Ck), and a lump including all C_1 to C_4 gases (Gs) (Gomez-Prado et al., 2006).

In another model, the gas products lump is divided into a primary lump composed of 46.7g/gmol average molecular weight (LPG) gases, and secondary lump composed of 18.4 g/gmol average molecular weight dry gaseous constituents to give a 12-lump model (Olivera, 1987).

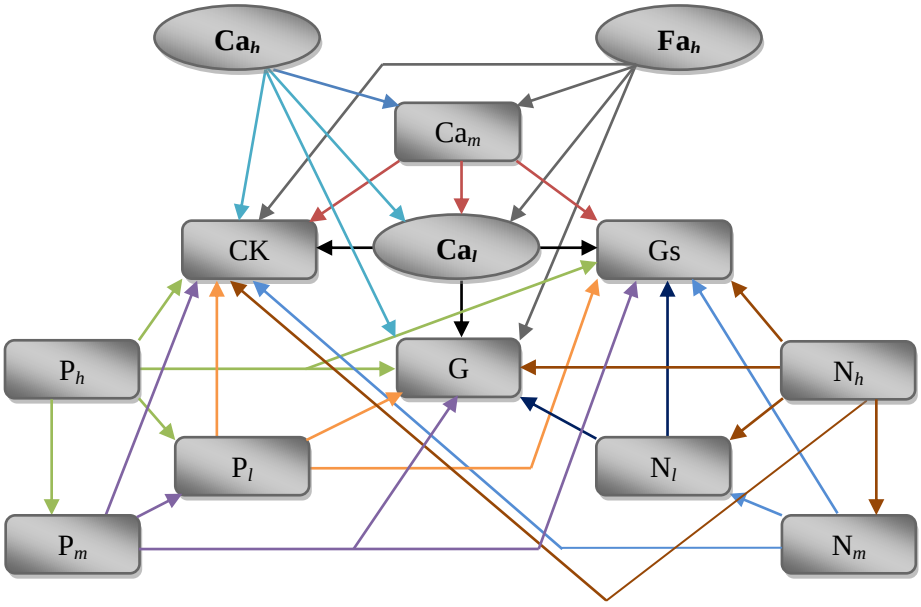

Figure 2.7: 13-lump model.

These 10, 12 and 13 lump models cannot include the whole spectrum of products, and so further treatment is needed to provide estimates of coke and light gas yields. In the case where coke is not presented in the kinetic model component balance, catalyst coke deposits may be estimated by the correlation given by Kambreck (1991).

Gas oil cracking was represented in a kinetic model using the lumping approach, where the gas oil feed is converted into lower boiling point products, namely gasoline, liquid petroleum gas (LPG), light cycle oils (LCO), coke, and light gases (LG). Further conversion of these products results in lower cut point products, such as LPG, gasoline and LG from LCO, as well as coke (Araujo-Monroy and Lopez-Isunza, 2006).

This kinetic model is distinct given that the dependence of kinetic parameters on feedstock type is taken care of through frequency factor functions representing the ratio of feed aromatics/naphthenes. Moreover, an innovative feature is that each feedstock component is converted into its constituent species that are adsorbed and cracked on the catalyst surface to give the lower level component. For example, the paraffins component of gas oil, at the LCO level, is transformed into, and adsorbed as olefins, paraffins, aromatics, and naphthtenes.

However, a number of disadvantages are present, where the basis of this model is claimed to be Gates (1979) catalytic cracking reactions, but this is not so clear in the actual model. Furthermore, light gas and LPG components are treated as lumps, rather than individually.

Feed/Product-focus Kinetic Models

Since the models discussed above focused either on the product spectrum or the feedstock, their limitations led workers to propose models that integrated both, e.g. Gomez-Prado (2003). In the model, four families are considered to form the feedstock, namely olefins, paraffins, aromatics, and naphthenes. In addition to asphaltenes, these are split by boiling range into cuts comprising light gasoline (50 to 120°C), heavy gasoline (120 to 205°C), diesel (205 to 320°C), gasoil (320 to 500°C), and residue (greater than 500°C). The product spectrum is defined to include the key refinery products of interest, i.e. gases, gasoline, and diesel, as well as coke, which represents a major component in the model since it is the source of heat for vaporising the feed, and maintaining the endothermic cracking reactions. The full model is made up of 294 reactions for the 32 components (Gomez-Prado et al., 2006).

2.3 Introduction to advanced chemical process control

2.3.1 Why advanced process control?

From its beginnings in antiquity until the early 1960s, the field of process control was based almost entirely on mechanical, electrical, or pneumatic analog controllers, which were usually designed using linear single-input, single-output considerations. Hardware limitations, economic cost, and the dearth of applicable theory usually precluded anything more complex then these simple schemes. Because many large-scale industrial processes are endowed by nature with large time constants, open-loop stability, and significant damping of fluctuations through mixing and storage tanks such simple control schemes work well for perhaps 70 percent of the control loops one might encounter. For the remaining 30 percent more difficult control problems, most controllers were considered marginally acceptable during this early period because there were few environmental regulations, product specifications were quite loose, and intermediate blending tanks could cover many of the sins of inadequate control. Thus the costs of even small sophistications in control were high and the economic incentives for improved control were comparatively low (Agachi et al., 2006).

Over the last 25 to 30 years, there has been a dramatic change in these factors. Industrial processes are now predominantly continuous with large throughputs, highly integrated with respect to energy and material flows, constrained very tightly by high-performance process specifications, and under intense governmental safety and environmental emission regulations. All these factors combine to produce more difficult process control problems as well as the requirement for better controller performance. Significant time periods with off-specification product, excessive environmental emissions, or process shut-down due to control system failure can have catastrophic economic consequences because of the enormous economic multipliers characteristic of high throughput continuous processes. This produces large economic incentives for reliable, high-quality control systems in modern industrial plants.

Another recent development in process control is that the performance of real-time digital computers suitable for on-line control has improved significantly, while prices have fallen drastically. Figure 2.8 shows an example of the price trends for small minicomputers in spite of the inclusion of more reliable electronics and increasing inflation. With the process control computer now such a small part of the overall process capital costs, the installation of a fast minicomputer with large amounts of storage can often be easily justified on the basis of improved safety and manpower savings. Once in place, the computer is usually operating in a timesharing mode with large numbers of input/output operations, so that the central processing unit (CPU) is typically in use only about 5 percent of the time. Thus many installations have 95 percent of the computing power of a highly capable minicomputer, programmable in a high-level languages such as Fortran, C, Visual Basic, LabVIEW etc., already available for implementing sophisticated computer control schemes.

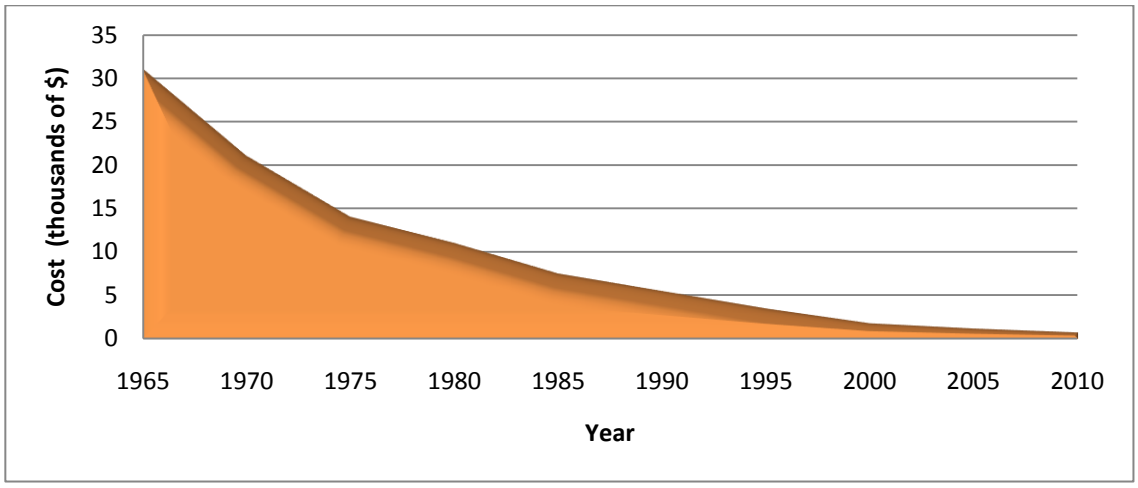

Figure 2.8: An example of price trends for real time minicomputers.

At the same time, modern control theory is undergoing intense development, with many successful applications in the chemical industry. Recently, a number of process control research groups have been applying new and more sophisticated control of algorithms and schemes to simulated, laboratory-scale, and even full-scale processes. The process control engineer must design an economically optimal process control scheme based on a judicious comparison of the available control algorithms. The present work offers help in this and strives to present a brief introduction to the theory and practice of the most important modern process control strategies, using the industrially relevant chemical processes as the subjects of control performance studies (Lu, J. 2001 and Agachi et al., 2006).

2.3.2 Concepts of process control

A *control system* comprises a number of elements, and is used to bring and maintain a process variable at a specified level or trajectory-the set point or reference. Control system analysis is based on *linear system theory*, whereby the cause-effect relationship between the various system elements is assumed linear. Figure 2.9 is a schematic representation of the variables in a process. These variables can be classified into input, and output, and further sub-divided into disturbance, manipulated, associated, and controlled variables. An input variable is one governed by the system "environment" including *disturbance* inputs and *manipulated* or *control* inputs, which in turn, affect the output; these include mass or energy flows, environmental variables etc. Output variables include technological parameters, yield, etc. Output variables comprise *controlled variables* that need to be held at specific set points, and *associated variables* that are controlled within a specified range (Agachi et al., 2006).

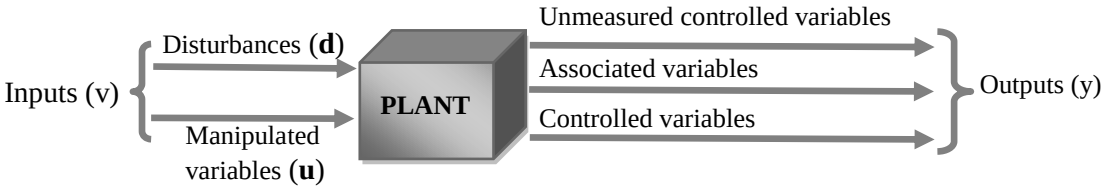

Figure 2.9: Definition of input and output variables considered for control system design.

Control systems are classified into open and closed loop. Figure 2.10 shows a schematic of an *open-loop* system, in which a controller or control actuator achieves the desired response. On the other hand, the *closed-loop* control system utilises a measure of the output-the *feedback signal*-to see how far this differs from the desired output.

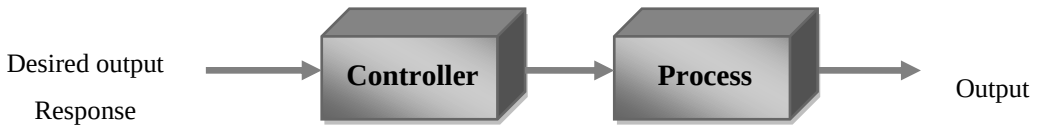

Figure 2.10: Open-loop control system.

Figure 2.11 represents a simple *closed-loop feedback control system*. In this type of system, the process is controlled by a function describing the relationship between the output and the reference input. Generally, the difference between the reference input and actual process output is amplified. This is fed back into the control system, with the objective of constantly reducing this difference. This concept of feedback control forms an important basis of system design and analysis (Agachi et al., 2006; Nagy, 2001).

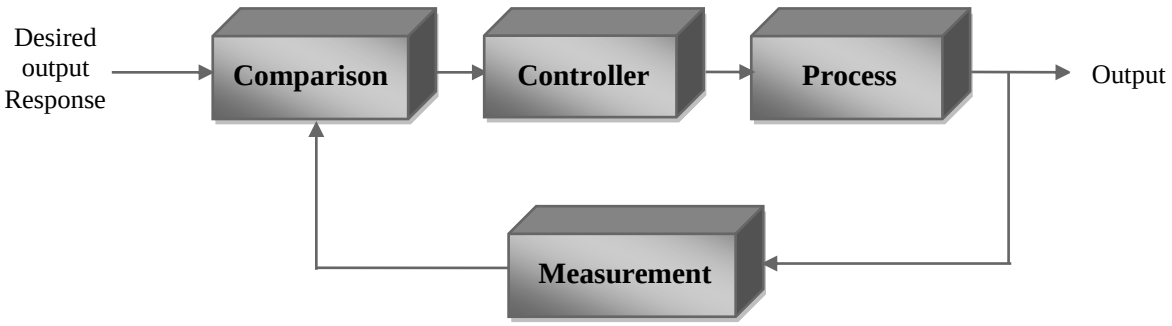

Figure 2.11: Closed-loop feedback control system.

2.3.3 History of automatic control

The concept of *feedback control* was one of the most important contributions in the history of automatic control (Mayr, 1970). The use of feedback in order to control a system has had a fascinating history. The first applications of feedback control rest in the development of float regulator mechanisms in Greece in the period 300 to 1 B.C. The water clock of Ktesibios used a float regulator. An oil lamp devised by Philon in approximately 250 B.C. used a float regulator in the oil lamp for maintaining a constant level of fuel oil. Heron of Alexandria, who lived in the first century A.C., published a book entitled *Pneumatica*, which outlined several forms of water-level mechanisms using float regulators (Mayr, 1970).

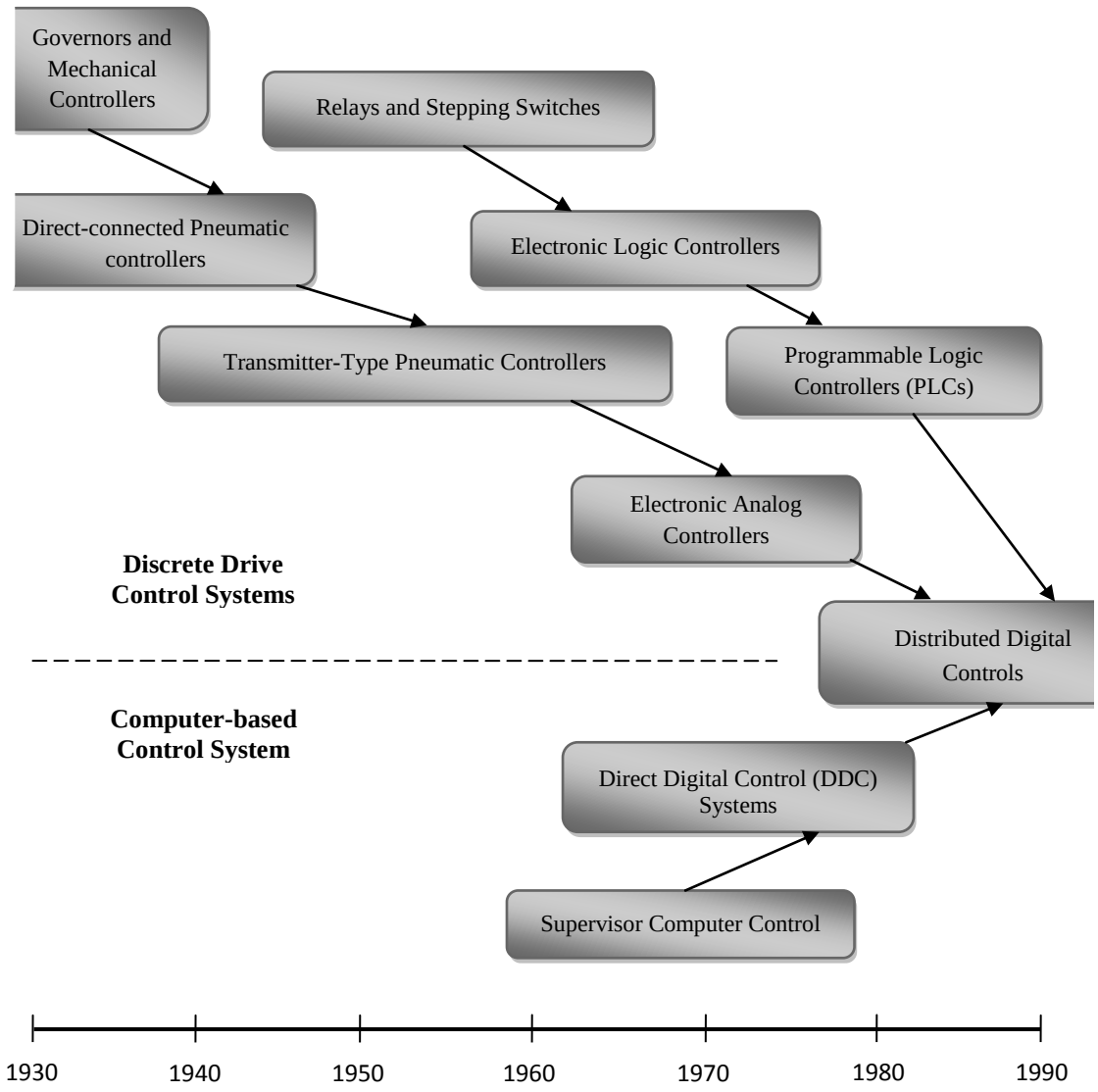

Figure 2.12: Evolution of industrial control technology.

The lines of technological development can be divided into two separate streams, as illustrated in Figure 2.12. The upper stream with its two branches is the more traditional one, and includes the evolution of analog controllers and other discrete devices such as relay logic and motor controllers. The second stream is a more recent one that includes the use of large-scale digital computers and their mini and micro descendants in industrial process control. These streams have merged into the current mainstream of distributed digital control systems.

The dates of several key milestones in the evolutionary process of the development of control theory and practice are shown in Table 2.3.

Table 2.3: Selected historical developments of control systems.

1769	James Watt's steam engine and governor developed. The Watt steam engine is often used to mark the beginning of the Industrial Revolution in Great Britain. During the industrial revolution, great strides were made in the development of mechanization, a technology preceding automation.
1800	Eli Whitney's concept of interchangeable parts manufacturing demonstrated in the production of muskets. Whitney's development is often considered as the beginning of mass production.
1868	J. C. Maxwell formulates a mathematical model for a governor control of a steam engine.
1913	Henry Ford's mechanized assembly machine introduced for automobile production.
1927	H. W. Bode analyzes feedback amplifiers.
1932	H. Nyquist develops a method for analyzing the stability of systems.
1934	Direct-connected pneumatic controls dominate market.
1938	Transmitter-type pneumatic control systems emerge, making centralized control rooms possible.
1952	Numerical control (NC) developed at Massachusetts Institute of Technology for control of machine-tool axes.
1954	George Devol develops "*programmed article transfer*" considered to be the first industrial robot design.
1958	First computer monitoring in electric utility
1959	First supervisory computer in refinery
1960	First solid-state electronic controllers on market.
1960	First Unimate robot introduced, based on Devo1's designs. Unimate installed in 1961 for tending die-casting machines.
1963	First direct digital control (DDC) system installed.
1970	First programmable logic controllers (PLCs) on market.
1970	Sales of electronic controllers surpass pneumatic
1975	First distributed digital control system on market.

Computer-based Control System Developments

In addition to the evolution of the traditional types of control systems described above, a more recent (and equally important) evolution of computer-based process control systems has been taking place, as shown in the lower part of Figure 2.12. The first application of computers to industrial processes was in the areas of plant monitoring and supervisory control. In September 1958, the first industrial computer system for plant monitoring was installed at an electric utility power generating station. This innovation provided an automatic data acquisition capability not available before, and freed the operator from much drudgery by automatically logging plant operating conditions on a periodic basis. Shortly thereafter (in 1959 and 1960), supervisory computer control systems were installed in a refinery and in a chemical plant. In these applications, analog controllers were still the primary means of control. The computer used the available input data to calculate control set points that corresponded to the most efficient plant operating conditions. These set points then were sent to the analog controllers, which performed the actual closed-loop control. The ability of supervisory control computers to perform economic optimization as well as to acquire, display, and log plant data provided the operator with a powerful tool for significantly improving plant operations.

The next step in the evolution of computer process control was the use of the computer in the primary control loop itself, in a mode usually known as *direct digital control*, or DDC. In this approach, process measurements are read by the computer directly, the computer calculates the proper control outputs then sends the outputs directly to the actuation devices. The first DDC system was installed in 1963 in a petrochemical plant. For security, a backup analog control system was provided to ensure that the process could be run automatically in the event of a computer failure. This proved to be a wise precaution, because this early DDC installation (as well as many others) was plagued with computer hardware reliability problems. Despite these problems, it demonstrated many of the advantages digital control has over analog control: tuning parameters and set points do not drift, complex control algorithms can be implemented to improve plant operation, and control loop tuning parameters can be set adaptively to track changing operating conditions.

2.3.4 Economical importance of process control

Control engineering is concerned with the analysis and design of goal-oriented systems. Modern control theory is concerned with systems with the self-organizing, adaptive, robust, learning, and optimum qualities. The control of an industrial process (manufacturing, production, and so on) by

automatic rather than human means is often called *automation.* Automation is prevalent in the chemical, electric power, paper, automobile, and steel industries, among others. The concept of automation is central to our industrial society. Automatic machines are used to increase the production of a plant per worker in order to offset rising wages and inflationary costs. Thus industries are concerned with the productivity per worker of their plant. *Productivity* is defined as the ratio of physical output to physical input. In this case we are referring to labour productivity, which is real output per hour of work. In a study conducted by the U.S. Commerce Department it was determined that labour productivity grew with an average annual rate of 2.8% from 1948 to 1984. In order to continue these productivity gains, expenditures for factory automation in the United States have increased from 8.0 billion dollars in 1992 to 20.0 billion dollars in 2000. Worldwide, expenditures for process control and manufacturing plant control have grown from 22.0 billion dollars in 1992 to 45.0 billion dollars in 2000. The U.S. manufacturers currently supply approximately one-half of worldwide control equipment (Brittain, 1977).

The transformation of the U.S. labour force in the country's brief history follows the progressive mechanization of work that attended the evolution of the agrarian republic into an industrial world power. In 1820 more than 70% of the labour force worked on the farm. By 1900 fewer than 40% were engaged in agriculture. Today, less than 5% work in agriculture.

The easing of human labour by technology, a process that began in prehistory, is entering a new stage. The acceleration in the pace of technological innovation inaugurated by the Industrial Revolution has until recently resulted mainly in the displacement of human muscle power from the tasks of production. The current revolution in computer technology is causing an equally momentous social change: the expansion of information gathering and information processing as computers extend the reach of the human brain. The work week in U.S. manufacturing industries shortened from 67 hours in 1860 to about 39 hours in 1984 and even less nowadays. Control systems are used to achieve (1) increased productivity and (2) improved performance of a device or system. Automation is used to improve productivity and obtain high quality products. Automation is the automatic operation or control of a process, device, or system. Automatic control of machines and processes is used in order to produce a product within specified tolerances. The term *automation* first became popular in the automobile industry but nowadays none of the industries can survive to the very strict economical and ecological requirements and the process complexities without automation. There are about 350,000 control engineers in the United States and also Japan, and over 200,000 control engineers in the states of former Soviet Union and Eastern Europe. In the United States alone, the control industry does a business of over 30 billion dollars per year!

2.3.5 What is "modern" control theory?

In response to an input perturbation, a system is considered *stable* if it settles to a steady state; however, it is *unstable* if it remains unsteady, with outputs varying. In a stable integrating system, the output asymptotically approaches a ramp, while it changes in an exponential manner in an exponentially unstable system.

Classical control theory only addresses single-input, single-output (SISO) systems represented by constant coefficient linear differential equations, also described by Laplace as transforms. However, *modern control theory* is able to address general multivariable systems, whether defined by variable-coefficient linear, nonlinear, and partial differential equations, as well as by integral equations. Moreover, *optimal control theory* has been developed so that control schemes can be implemented to minimise a specified function, such as cost etc.

- Furthermore, methods for process identification and state estimation have also been developed. *Process identification* algorithms determine the structure of the process model and can then provide estimates of process parameters. *State estimation* techniques are applied in real-time systems to estimate those state variables that are not measured, or to improve estimates of state-variables given measurement errors. Nagy and Agachi (2004) describe a typical advanced control scheme as consisting of (see Figure 2.13):

- a *process* subjected to control inputs (u), natural process disturbances (d_1), and special input disturbances (d_2) used for the purpose of identification;

- *measurement devices:* these monitor a number of system state variables or a combination of these, with measurement error included;

- *state estimator:* this provides a best estimate of process state (x_{est}), based on the noisy measurements (y) and the process model;

- a *controller:* this takes account of the state estimates (x_{est}), setpoints (r) and controller parameters (K) and generates appropriate control actions;

- a *process identification block:* its function is to identify the process model parameters (α) from user measurements of the process. Provided the parameters do not change with time, this identification is unique. However, if process parameters vary with time, identification has to be undertaken periodically, in order to adapt to these changes.

In most applications only a few of the components of this control structure are required.

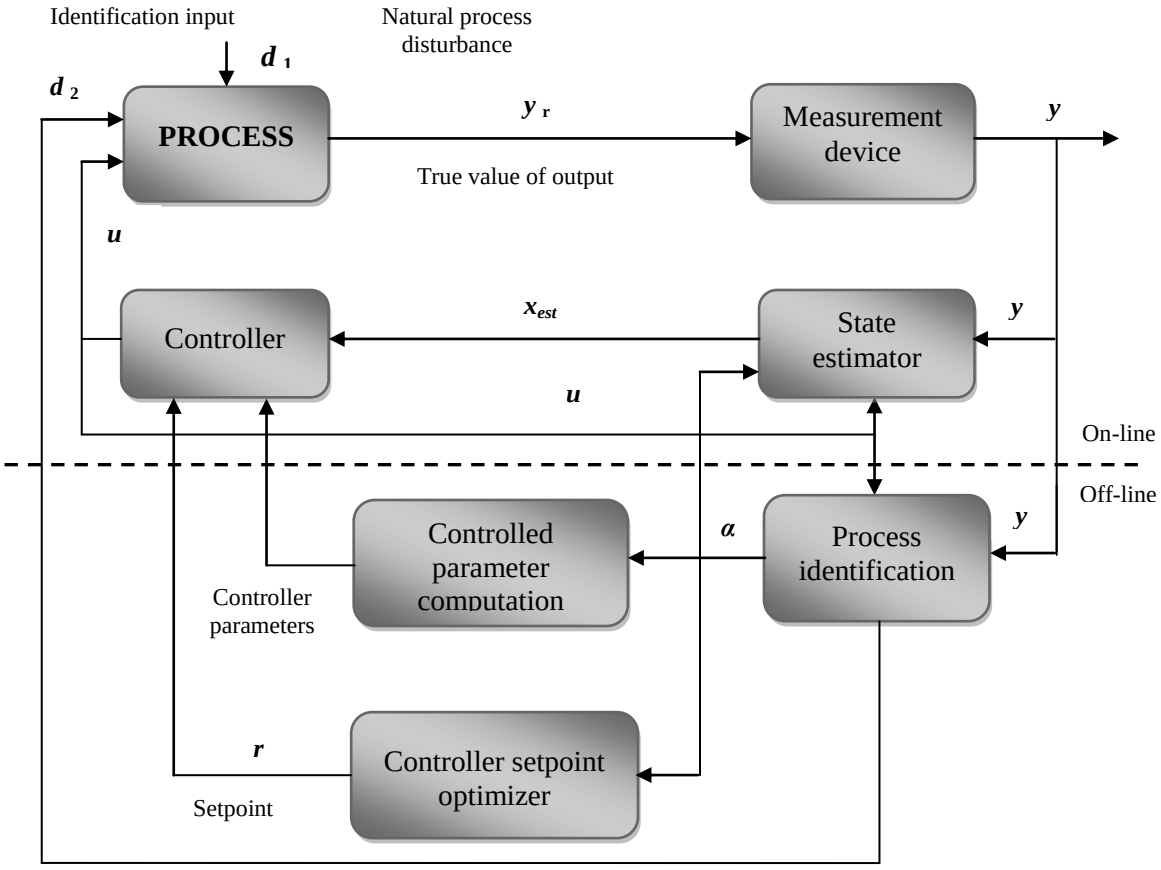

Figure 2.13: Advanced computer control scheme.

2.3.6 Advanced process control techniques

Key problems in Advanced Control of Chemical Processes

Figure 2.14 outlines the main features of chemical processes in relation to the challenges they pose in terms of control. Chemical processes are mainly characterised by (Nagy and Agachi, 2004):

These characteristics have revealed the implementation of various advanced control strategis to maximize process performance.

The chemical industry is characterized as having very dynamic and unpredictable marketplace conditions. For instance, in the course of the last 15 years we have witnessed an enormous variation in crude and product prices.

The demands of chemical products vary also widely, imposing different production yields. It is generally accepted that the most effective way to generate the most profit out of the plants while

responding to marketplace variations with minimal capital investment is provided by the integration of all aspects of automation of the decision making process (Garcia et al., 1989), which are:

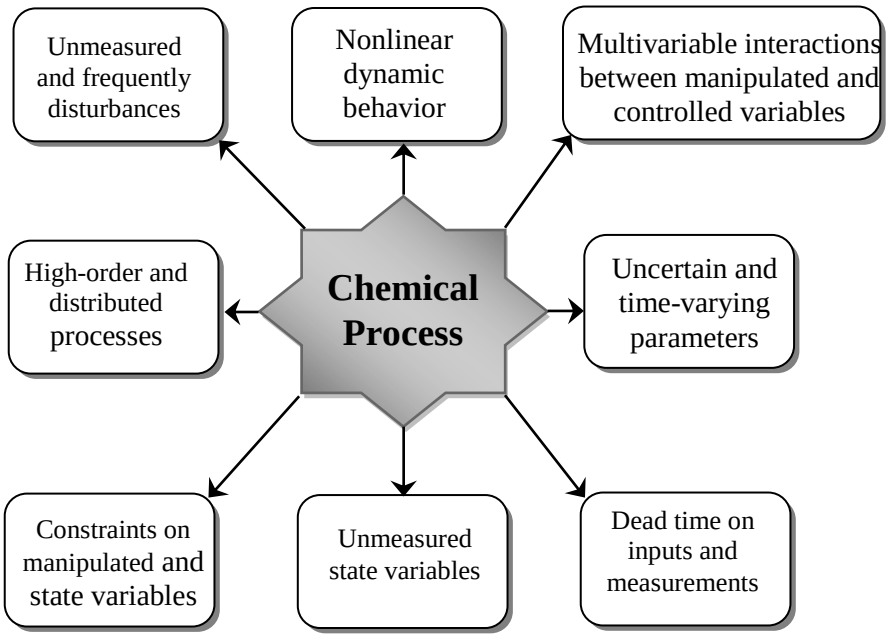

Figure 2.14: Common process characteristics, important in the choice of control strategy

- *measurement* (acquiring measurements and monitoring process variables and states using appropriate instrumentation);
- *control* (satisfying operating criteria by manipulating degrees of freedom in the process);
- *optimisation* (satisfying economic objectives by manipulating degrees of freedom in the process);
- *logistics* (maximising profits and realising company objectives through the appropriate allocation of raw materials and the scheduling of the operating plants).

Currently, practical performance criteria must be achieved by control systems in one or more of the following aspects:

- *economic*: these are related to holding process variables at the targets defined by the optimisation phase or through dynamically minimising an operating cost function.
- *safety and environmental*: where process variables are not permitted to pass specific limits dictated by the safety of personnel or equipment, or environmental regulations.
- *equipment*: process operations may not exceed physical limitations of the equipment.

- *product quality*: products must satisfy set specifications.
- *human preference*: these may be dictated by the tolerance of the plant operator: e.g. variable oscillation levels that are not tolerable.

In addition, the implementation of such integrated systems is forcing the processes to operate over an ever-wider range of conditions. As a result, we can state the control problem that any control system must solve as follows (Garcia et al., 1989):

> *"Update on-line the manipulated variables to satisfy multiple, changing performance criteria in the face of changing plant characteristics."*

The whole spectrum of process control methodologies in use today is faced with the solution of this problem. The difference between these methodologies lies in the particular assumptions and compromises made in the mathematical formulation of performance criteria and in the selection of a process representation. These are made primarily to simplify the mathematical problem so that its solution fits the existing hardware capabilities. The natural mathematical representation of many of these criteria is in the form of dynamic objective functions to be minimized and of dynamic inequality constraints. The usual mathematical representation for the process is a dynamic model with its associated uncertainties.

At the moment there are an important number of advanced control techniques from *ad hoc* algorithms for particular systems to very general methods with wide application area and well-developed theory. A classification of these techniques is difficult because many of the algorithms are very similar, being obtained from some more general methods via usually minor changes concerning the performance criteria, optimization method, prediction horizon, constraint handling, etc. However, all these algorithms have a common feature: all are based on a process model, described in different ways. The proposed classification, based on this feature is presented in Figure 2.15. According to this, the advanced control techniques can be classified first in four conceptually different categories. The first and most important approach, the Model Predictive Control (MPC), can be classified further, for example, according to different model types used for prediction in the controller. This feature being usually the most significant difference among MPC algorithms.

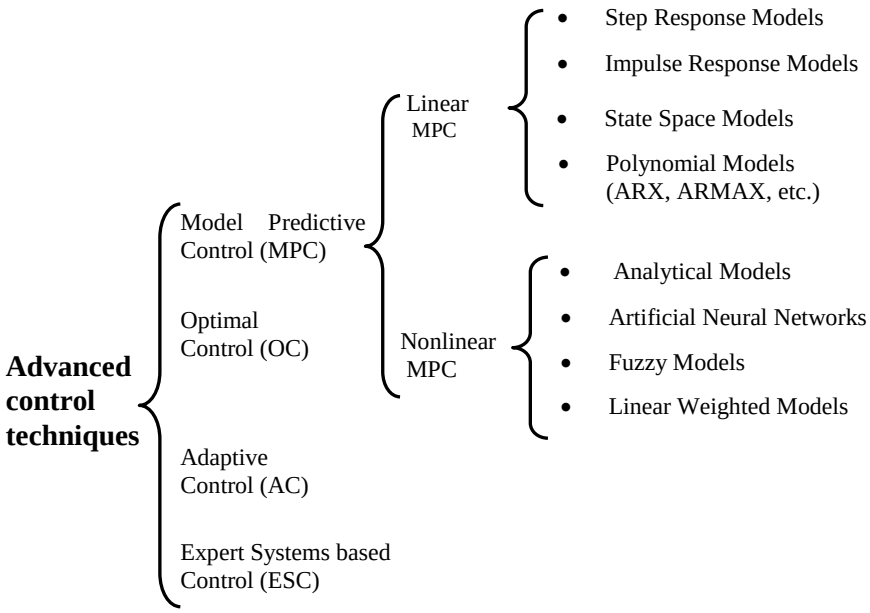

Figure 2.15: Classification of advanced control techniques.

2.3.7 Historical development of LMPC

The current interest of the processing industry in MPC can be traced back to a set of papers, which appeared in the late 1970s. In 1978 Richalet et al. described successful applications of "*Model Predictive Heuristic Control*" and in 1979 engineers from Shell outlined "*Dynamic Matrix Control*" (DMC) (Cutler and Ramaker, 1980) and reported applications to a fluid catalytic cracker (Prett and Gillette, 1979). In both algorithms an *explicit* dynamic model of the plant is used to predict the effect of future actions of the manipulated variables on the output (thus the name "Model Predictive Control"). The future moves of the manipulated variables are determined by optimization with the objective of minimizing the predicted error subject to operating constraints. The optimization is repeated at each sampling time based on updated information (measurements) from the plant. Thus, in the context of MPC the control problem including the relative importance of the different objectives, the constraints, etc. is formulated as a dynamic optimization problem. While this by itself is hardly a new idea (Clarke, 1994; Chang, 1961), it constitutes one of the first examples of large-scale dynamic optimization applied routinely in real time in the process industries. The MPC concept has a long history (Kwon, 1994). The connections between the closely related minimum time optimal control problem and Linear Programming were recognized first by Zadeh and Whalen in 1962. Propoi (1963) proposed the moving horizon approach, which is at the core of all MPC

algorithms. It became known as *"Open Loop Optimal Feedback"*. The main idea of this approach is presented on Figure 2.16.

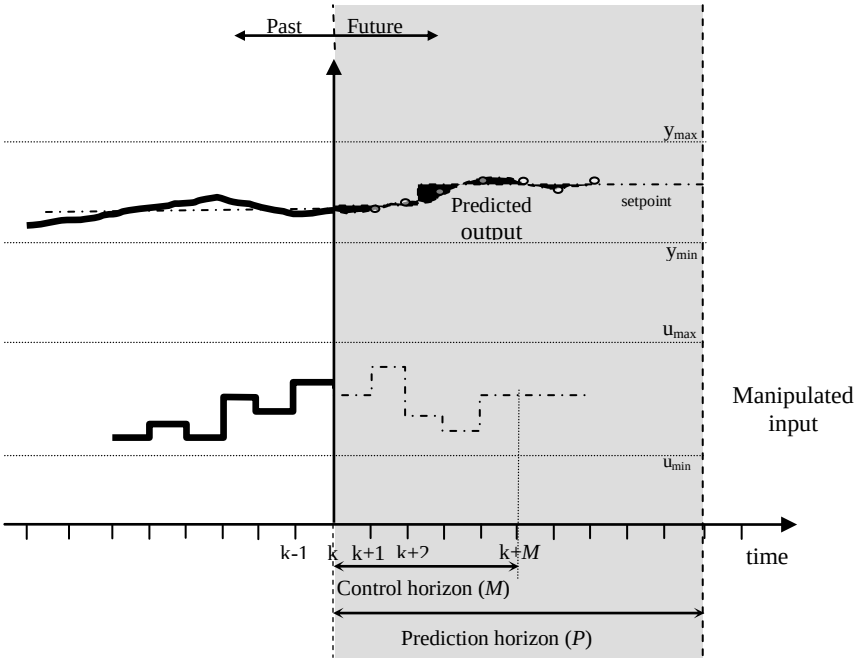

Figure 2.16: The moving horizon approach of MPC techniques.

The extensive work on this problem during the 1970s was reviewed in the thesis by Gutman (1982). The connection between this work and MPC was discovered by Chang and Seborg in 1983.

Since the rediscovery of MPC in 1978 and 1979, its popularity in the Chemical Process Industries has increased steadily. Mehra et al. (1982) reviewed a number of applications including a superheater, a steam generator, a wind tunnel, a utility boiler connected to a distillation column and a glass furnace. Shell has applied MPC to many systems, among them a fluid catalytic cracking unit (Prett and Gillette, 1979) and a highly non-linear batch reactor (Garcia, 1984). Matsko (1985) summarized several successful implementations in the pulp and paper industries Matsko (1985).

Several companies (Bayley, DMC, Profimatics, Setpoint) offer MPC software. Cutler and Hawkins (1987) reported a complex industrial application to a hydrocracker reactor involving seven independent variables (five manipulated two disturbances) and four dependent (controlled) variables including a number of constraints. Martin et al. (1986) cited seven completed applications and ten under design. They include: fluid catalytic cracker-including regenerator loading, reactor severity and differential pressure controls; hydrocracker (or hydrotreater) bed outlet temperature

control and weight average bed temperature profile control; hydrocracker recycle surge drum level control; reformer weight average inlet temperature profile control; analyzer loop control. The latter has been described in more detail by Caldwell and Martin (1987). Setpoint has applied the MPC technology to: fixed and ebulating bed hydrocrackers (Grosdidier, 1988); fluid catalytic crackers; distillation columns; absorber/stripper bottom C_2 composition control, polymerization reactors and other chemical and petroleum refining operations (Meadows et al., 1995; Nagy and Agachi 1997; Marques and Morari 1986; Matsko 1979; Prett and Gillette 1979).

In academia, MPC has been applied under controlled conditions to a simple mixing tank and a heat exchanger (Arkun et al., 1986) as well as a coupled distillation column system for the separation of a ternary mixture (Levien and Morari, 1987). Parrish and Brosilow (1985) compared MPC with conventional control schemes on a heat, exchanger and an industrial autoclave Parrish and Brosilow (1985).

2.3.8 Industrial MPC development

An excellent review of the industrial development of MPC, was presented by Allgower et al. (1999) in their review paper. They presented the most important commercial software for industrial implementation of MPC as follows:

IDCOM

The first description of MPC control applications was presented by (Richalet et al., 1976; Richalet 1993; Richalet et al., 1978). They described their approach as Model Predictive Heuristic Control (MPHC). The commercial software was referred to as IDCOM, an acronym for *Identification and Command*. The distinguishing features of IDCOM are:

1. finite impulse response (FIR) model for the plant;
2. quadratic performance objective over a finite prediction horizon;
3. future output behavior specified by a reference trajectory;
4. input and output constraints included in the formulation;
5. optimal inputs computed using a heuristic iterative algorithm.

The MPHC algorithm drives the predicted future output as closely as possible to a reference trajectory, defined as a first order path from the current output value to the desired setpoint. The speed of the desired closed loop response is set by the time constant of the reference trajectory.

Richalet et al. (1978) maked the important point that dynamic control must be embedded in a hierarchy of plant control functions in order to be effective. They describe four levels of control.

- Level 3 - Time and space scheduling of production
- *Level 2* - Optimization of setpoints to minimize costs and ensure quality and quantity of production
- *Level l* - Dynamic multivariable control of the plant
- *Level 0* - Control of ancillary systems; PID control of valves.

They pointed out that significant benefits do not come from simply reducing the variations of a controlled variable through better dynamic control at level 1. The real economic benefits come at level 2 where better dynamic control allows the controlled variable setpoint to be moved closer to a constraint without violating it. This argument provides the basic economic motivation for using MPC technology. This concept of a hierarchy of control functions is fundamental to advanced control applications and seems to have been followed by many practitioners.

DMC

Engineers at Shell Oil developed MPC technology independently in the early 1970's, with an initial application in 1973. Cutler and Ramaker presented details of an unconstrained multivariable control algorithm which they named Dynamic Matrix Control (DMC) at the 1980 Joint Automatic Control Conference (Cutler and Ramaker, 1980; Cutler et al., 1983). In a companion paper Prett and Gillette (1979) described an application of DMC technology to a FCCU reactor/regenerator in which the algorithm was modified to handle nonlinearities and constraints. Key features of the DMC control algorithm include:

1. linear step response model for the plant;
2. quadratic performance objective with move suppression over a finite prediction horizon;
3. future output behavior specified by following the setpoint;
4. optimal inputs computed as the solution to a least-squares problem.

By using the step response model one can write predicted future output changes as a linear combination of future input moves. The matrix that ties the two together is the so-called *Dynamic Matrix.* Using this representation allows the optimal move vector to be computed as the solution to

a least-squares problem. Feedforward control is readily included in this formulation by modifying predicted future outputs.

The objective of a DMC controller is to drive the output as close to the setpoint as possible in a least-squares sense with a penalty term on the input moves. This results in smaller computed input moves and a less aggressive output response. As with the IDCOM reference trajectory, this technique provides a degree of robustness to model error. Move suppression factors also provide an important numerical benefit in that they can be used to directly improve the conditioning of the numerical solution.

The initial IDCOM and DMC algorithms represent the *first generation* of MPC technology; they had an enormous impact on industrial process control and served to define the industrial MPC paradigm (Garcia and Prett, 1986).

QDMC

The original IDCOM and DMC algorithms provided excellent control of unconstrained multivariable processes. Constraint handling, however, was still somewhat ad-hoc. Engineers at Shell Oil addressed this weakness by posing the DMC algorithm as a *Quadratic Program* (QP) in which input and output constraints appear explicitly (Garcia and Morshedi, 1986). A distinguishing feature of QDMC over DMC is that the control moves are solved as a QP with hard constraints rather than least squares without constraints.

The default QDMC algorithm requires strict enforcement of input and output constraints at each point of the prediction horizon. Constraints that are strictly enforced are referred to as *hard constraints.* Constraints for which violations are allowed are referred to as *soft constraints.* In practice Garcia and coworkers (Garcia and Morari, 1982; Garcia and Morshedi, 1986) report that hard output constraints are typically required to be satisfied over only a portion of the horizon which they refer to as the *constraint window.* The constraint window generally starts at some point in the future and continues on to steady state. They report that if non- minimum phase dynamics are present, performance is improved by pushing the constraint window farther into the future. This amounts to ignoring hard output constraints during the initial portion of the closed loop response. The QDMC algorithm can be regarded as representing a *second generation* of MPC technology, comprised of algorithms, which provide a systematic way to implement input and output constraints. This was accomplished by posing the MPC problem as a QP.

IDCOM-M, SMOC, and PCT

As MPC technology gained wider acceptance, and problems tackled by MPC technology grew larger and more complex, control engineers implementing second generation MPC technology ran into other practical problems. The QDMC algorithm provided a systematic approach to incorporate hard input and output constraints, but there were several obvious, limitations:

1. there was no clear way to handle an infeasible solution. For example it is possible for a feedforward disturbance to lead to an infeasible QP; what should the control do to recover from infeasibility?
2. the soft constraint formulation is not completely satisfactory because it means that all constraints will be violated to some extent, as determined by the relative weights. Clearly some output constraints are more important than others, however, and should never be violated.
3. process models are still limited to step response models, which are incapable of representing unstable processes.
4. the constant-disturbance output feedback is sub-optimal and unrealistic especially when low-level PID controllers are in place.

Fault tolerance is also an important practical issue. Rather than simply turning itself off as signals are lost, a practical MPC controller should remain online and try to make the best of the sub-plant under its control. It also became increasingly difficult to translate control requirements into relative weights for a single objective function. Including all the required tradeoffs in a single objective function means that relative weights have to be assigned to the value of output setpoint violations, output soft constraint violations, inputs moves, and optimal input target violations.

These issues motivated engineers at Shell (France), Adersa and Setpoint Inc. to develop new versions of MPC algorithms. The version marketed by Setpoint was called IDCOM-M, while the Adersa version was referred to as HIECON (Hierarchical Constraint Control). The IDCOM-M controller was first described in a paper by Grosdidier et al. (1988). Distinguishing features of the IDCOM-M algorithm include:

1. controllability supervisor to screen out ill-conditioned plant subsets;
2. multi-objective function formulation; quadratic output objective followed by a quadratic input objective;
3. controls a single future point in time for each output, called the coincidence point, chosen from a reference trajectory;

4. constraints can be hard or soft, with hard constraints ranked in order of priority.

The SMOC algorithm (Marquis and Broustail, 1988) developed at Shell France is very close to the "modern" development of MPC with the following distinguishing features:

1. state space models are used which can represent both stable and unstable processes.
2. full state estimation known as *extended close-loop observer* is used for output feedback; constant output disturbance is simply a special case.
3. a distinction is introduced between *controlled variables* that are in the control objective and *feedback variables* that are used for state estimation, resolving the difficulty for interdependent output variables.
4. input and output constraints are observed via a QP formulation.

The SMOC and IDCOM-M algorithms are two of several that represent a *third generation* of MPC technology; others include the PCT algorithm sold by Profimatics, the RMPCT controller developed by Honeywell, and the PFC algorithm developed by Adersa. This generation distinguishes between several levels of constraints (hard, soft, ranked), provides some mechanism to recover from an infeasible solution, addresses the issues resulting from a control structure that changes in real time, uses state estimation as optimal output feedback, and allows for a wider range of process dynamics (stable and unstable) and controller specifications.

While MPC theory has advanced to the point where nominal stability can be guaranteed with several schemes, the majority of the current industrial MPC algorithms are based on ideas inherited from the original DMC and IDCOM algorithms. Products sold by Adersa, Aspen Technology, Continental Controls, Honeywell, and Pavilion Technology share such features as a finite prediction horizon and options for impulse or step response models. The main emphasis in recent years has been to allow for a wider range of model types, including nonlinear models, state space models (e.g., SMOC from Shell), and better integration of the controller interface into existing distributed control hardware (Qin and Badgwell, 2000).

2.3.9 Unconstrained Linear Model Predictive Control (LMPC) with step response and impulse response models

Step Response Models

To derive the step response model for a general multi-input-multi-output (MIMO) it was assumed that y_l, $l=1,...,n_y$, were stable and deal with an output *vector* at each time interval:

$$y(k-1) = [y_1(k-1),...,y_{n_y}(k-1)]^T \tag{2.16}$$

and can be define the state vectors

$$Y(k-1) \overset{\Delta}{=} [y(k-1)^T, y(k)^T,..., y(k+n-3)^T, y(k+n-2)^T]^T \; for \;\; \Delta v(k+i) = 0; \quad i \geq -1 \tag{2.17}$$

and

$$Y(k) \overset{\Delta}{=} [y(k)^T, y(k+1)^T,..., y(k+n-2)^T, y(k+n-1)^T]^T \; for \;\; \Delta v(k+i) = 0; \quad i \geq 0. \tag{2.18}$$

The output vector evolution is described by:

$$Y(k) = M^S \cdot Y(k-1) \tag{2.19}$$

where

$$M^S = \begin{bmatrix} 0 & I & 0 & ... & ... & 0 & 0 \\ 0 & 0 & I & 0 & ... & 0 & 0 \\ : & & & & & & : \\ 0 & 0 & ... & ... & ... & 0 & I \\ 0 & 0 & ... & ... & ... & 0 & I \end{bmatrix}. \tag{2.20}$$

And the identity matrix I is of dimension n_y x n_y.

Each step response coefficient S_i is a vector of dimension n_y

$$S_i = [s_{1i}, s_{2i},..., s_{n_y i}]^T. \tag{2.21}$$

The step response model becomes:

$$Y(k) = M^S Y(k-1) + S\Delta v(k-1) \tag{2.22}$$

where S is an $n \cdot n_y$ vector.

Assume next that there are n_v inputs v_m, $m=1,...,n_v$. Because of linearity, the effects of the individual inputs can simply be added up:

$$Y(k) = M^S Y(k-1) + \sum_{m=1}^{n_v} S_m \, \Delta v_m(k-1) \tag{2.23}$$

This can be defined as an input vector $\Delta v(k-1) = [\Delta v_1(k-1),..., \Delta v_{n_v}(k-1)]^T$ and the step response coefficient matrix:

$$S_i = \begin{bmatrix} s_{1,1,i} & s_{1,2,i} & \dots & s_{1,n_v,i} \\ s_{2,1,i} & & & \\ \vdots & & & \\ s_{n_y,1,i} & s_{n_y,2,i} & \dots & s_{n_y,n_v,i} \end{bmatrix} \tag{2.24}$$

where $s_{l,m,i}$ is the i^{th} step response coefficient relating the m^{th} input to the l^{th} output. Then the MIMO step response model becomes:

$$Y(k) = M^s Y(k-1) + S\,\Delta v(k-1) \quad . \tag{2.25}$$

The recursive expression (2.26) is initialized (*k=0*) assuming that there were no changes *Δv(-l)* cu *l=1,...,n* (which put the system at steady state) and that the steady state output $\hat{y}\ 0$ is known (measured). Then the vector *Y(0)* can be set equal to the steady state system output $\hat{y}\ 0$ repeated *n* times:

$$Y(0) = [\hat{y}(0)^T, \hat{y}(0)^T, \dots, \hat{y}(0)^T]^T. \tag{2.26}$$

The recursive formula (2.26) was proposed in the original formulation of DMC.

If all the outputs are integrating, then (2.26) holds with M^S replaced by:

$$M^I = \begin{bmatrix} 0 & I & 0 & \dots & \dots & 0 & 0 \\ 0 & 0 & I & 0 & \dots & 0 & 0 \\ \vdots & & & & & & \vdots \\ 0 & 0 & \dots & \dots & \dots & 0 & I \\ 0 & 0 & \dots & \dots & \dots & -I & 2I \end{bmatrix}. \tag{2.27}$$

Consequently, both the stable and integrating outputs lead to the general formula:

$$Y(k) = MY(k-1) + S\,\Delta v(k-1). \tag{2.28}$$

Impulse Response Models

For stable SISO (single-input-single-output) systems equation (2.19) in an expanded form is:

$$\begin{bmatrix} y(k-1) \\ y(k) \\ y(k+1) \\ \vdots \\ y(k+n-1) \end{bmatrix} = \begin{bmatrix} 0 & 1 & 0 & \dots & \\ 0 & 0 & 1 & \dots & \\ 0 & 0 & 0 & \dots & \\ & & & \dots & \\ & & & 0 & 0 & 1 \\ & & & 0 & 0 & 1 \end{bmatrix} \begin{bmatrix} y(k-2) \\ y(k-1) \\ y(k) \\ \vdots \\ y(k+n-2) \end{bmatrix} + \begin{bmatrix} 0 \\ s_1 \\ s_2 \\ \vdots \\ s_n \end{bmatrix} \Delta v(k-1). \tag{2.29}$$

and by taking the differences between the adjacent rows the following can be obtaind:

$$\begin{bmatrix} \Delta y(k) \\ \Delta y(k+1) \\ \Delta y(k+2) \\ : \\ \Delta y(k+n-1) \end{bmatrix} = \begin{bmatrix} 0 & 1 & 0 & \dots & \\ 0 & 0 & 1 & \dots & \\ 0 & 0 & 0 & \dots & \\ & & & \dots & \\ & & & 0 & 0 & 1 \\ & & & 0 & 0 & 0 \end{bmatrix} \begin{bmatrix} \Delta y(k-1) \\ \Delta y(k) \\ \Delta y(k+1) \\ : \\ \Delta y(k+n-2) \end{bmatrix} + \begin{bmatrix} h_1 \\ h_2 \\ h_3 \\ : \\ h_n \end{bmatrix} \Delta v(k-1) \tag{2.30}$$

where

$$\Delta y(k+i) = y(k+i) - y(k+i-1) \tag{2.31}$$

and

$$h_i = s_i - s_{i-1}; \tag{2.32}$$

$$H = [h_1 \; h_2 \; \dots \; h_n]^T; \tag{2.33}$$

are the impulse response coefficients of the system.

Analogous to the development of the step response the model can be derived as:

$$\Delta y(k+l) = N \Delta Y(k+l) = N M^l \Delta Y(k) + \sum_{i=1}^{l} N M^{i-1} H \Delta v(k+l-i) \quad . \tag{2.34}$$

Note that

$$N M^{i-1} H = \begin{cases} h_i & i \le n \\ 0 & i > n \end{cases} \tag{2.35}$$

and therefore for $l > n$,

$$\Delta y(k+l) = \sum_{i=1}^{n} h_i \Delta v(k+l-i) \quad . \tag{2.36}$$

Or, $\Delta y(k) = \sum_{i=1}^{n} h_i \Delta v(k-i)$ (2.37)

which is referred to as the *input-output form of the impulse response model.*

Estimation and prediction

The objective for using a model is to predict the effect of future manipulated variable moves on the output. This will allow finding the "best" future moves to reach some desired output behavior. To obtain a more general form of the model in which the measured disturbances are also accounted thy modeled system can be represented by the block diagram in Figure 2.17. It is assumed that P^u (the

effect of *u* an *y*) is described by the step response coefficients and P^d (the effect of the disturbances *d* on *y*) by a similar dynamic matrix:

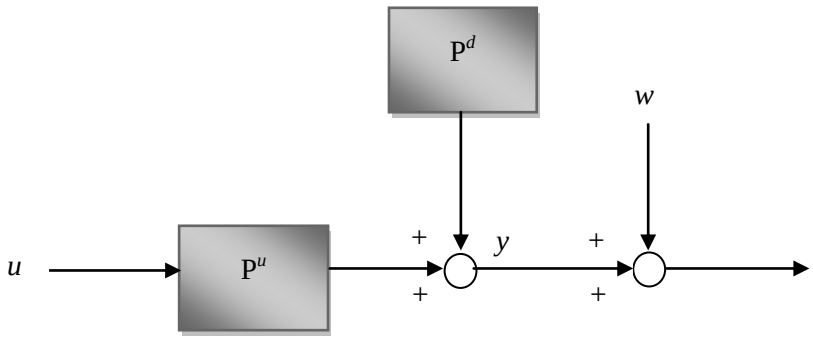

Figure 2.17: Plant with manipulated variable *u*, measured disturbance *d* and effect of unmeasured disturbance *w*.

$$S^u = \begin{bmatrix} S_1^u \\ S_2^u \\ \vdots \\ S_{n-1}^u \\ S_n^u \end{bmatrix} \quad ; \quad S^d = \begin{bmatrix} S_1^d \\ S_2^d \\ \vdots \\ S_{n-1}^d \\ S_n^d \end{bmatrix}. \tag{2.38}$$

The straightforward generalization of (2.28) is given as follows:

$$Y(k \mid k-1) = M^S Y(k-1 \mid k-1) + S^u \, \Delta u(k-1) + S^d \, \Delta d(k-1) \tag{2.39}$$

Using this general linear model, the following operations have to be performed to obtain a *p*-step-ahead prediction vector:

1. *Preparation.* Do not vary the manipulated variables for at least n time intervals (*Δu(-1)=Δu(-2)=...= Δu(-n)=0*) and assume the measured disturbance changes are zero (*Δd(-1)=Δd(-2)=...= Δd(-n)=0*) during that time. Then the system will be at rest at *k=0.*
2. *Initialization (k=0).* Measure the output $\hat{y}(0)$ and initialize the model prediction vector as

$$Y(0 \mid 0) = [\hat{y}(0)^T, \hat{y}(0)^T, ..., \hat{y}(0)^T]^T \tag{2.40}$$

Measure Δd(0), obtain measurement at next sampling time ($\hat{y}(1)$, Δd(1)); and set k=1.

3. *Model Prediction*

$$Y(k \mid k-1) = MY(k-1 \mid k-1) + S^d \Delta d(k-1) + S^u \Delta u(k-1) \tag{2.41}$$

where

$$Y(k \mid k-1) \stackrel{\Delta}{=} [y(k \mid k-1)^T, y(k+1 \mid k-1)^T, ..., y(k+n-2 \mid k-1)^T, y(k+n-1 \mid k-1)^T]^T \tag{2.42}$$

Correction:

$$Y(k \mid k) = Y(k \mid k-1) + K_F(\hat{y}(k) - y(k \mid k-1)) \quad . \tag{2.43}$$

4. Compute the *p*-step-ahead prediction vector:

$$\mathbf{Y}(k+1 \mid k) = \mathbf{M}\mathbf{Y}(k \mid k) + \mathbf{S}^{\mathbf{d}} \Delta d(k) + \mathbf{S}^{\mathbf{u}} \Delta \mathbf{u}(k) \tag{2.44}$$

where

$$\mathbf{Y}(k \mid k-1) \stackrel{\Delta}{=} [y(k+1 \mid k)^T, y(k+2 \mid k)^T, ..., y(k+p-1 \mid k)^T, y(k+p \mid k)^T]^T; \tag{2.45}$$

$$\text{estimated for} \quad \Delta u(k+i) = 0; \quad i \geq m;$$

$$\Delta \mathbf{u}(k) = [\Delta u(k)^T, \Delta u(k+1)^T, ..., \Delta u(k+m-1)^T]^T.$$

5. Obtain measurements $\hat{y}(k+1)$, *Δd(k+1)* at the next sampling time, set *k:=k+1* and go to step 3.

Least Squares Solution of the Control Problem

The algorithm presented before to compute the *p*-step-ahead prediction vector for *m* present and future input moves allow expressing the control problem as an optimization problem of the form:

$$\begin{aligned} &\min_{\Delta u(k)} \{ || \Gamma^y [\mathbf{Y}(k+1 \mid k) - \mathbf{R}(k+1)] ||^2 + || \Gamma^u \Delta \mathbf{u}(k) ||^2 \} \\ &s.t. \quad \mathbf{Y}(k+1 \mid k) = \mathbf{M}\mathbf{Y}(k \mid k) + \mathbf{S}^{\mathbf{d}} \Delta d(k) + \mathbf{S}^{\mathbf{u}} \Delta \mathbf{u}(k) \end{aligned} \tag{2.46}$$

where

$$\begin{aligned} &\Gamma^u = diag\{\Gamma^u_1, ..., \Gamma^u_m\} \quad ; \\ &\Gamma^y = diag\{\Gamma^y_1, ..., \Gamma^y_p\}; \end{aligned} \tag{2.47}$$

are the weight matrices in block diagonal form.

This optimization problem can be solved by the least squares algorithm. For this the problem can be rewritten as the following set of linear equations:

$$\begin{bmatrix}\Gamma^{y}\mathbf{S}^{\mathbf{u}}\\ \Gamma^{u}\end{bmatrix}\Delta\mathbf{u}(k) = \begin{bmatrix}\Gamma^{y} & 0\\ 0 & I\end{bmatrix}\begin{bmatrix}\mathbf{R}(k+1)-\mathbf{MY}(k\mid k)-\mathbf{S}^{\mathbf{d}}\Delta d(k)\\ 0\end{bmatrix}\overset{\Delta}{=}\begin{bmatrix}\Gamma^{y}E_{p}(k+1\mid k)\\ 0\end{bmatrix} \tag{2.48}$$

where:

$$E_{p}(k+1\mid k)=\begin{bmatrix}e(k+1\mid k)\\ e(k+2\mid k)\\ \vdots\\ e(k+p\mid k)\end{bmatrix}\overset{\Delta}{=}\mathbf{R}(k+1)-[\mathbf{MY}(k\mid k)+\mathbf{S}^{\mathbf{d}}\Delta d(k)]. \tag{2.49}$$

$E_p(k+1|k)$ is the measurement corrected vector of future output deviations from the reference trajectory (i.e. errors), assuming all future moves are zero. Note that this vector contains the effect of measurable disturbances ($\boldsymbol{S^d\Delta d(k)}$) on the prediction.

For practical choices of $p \leq n$ and weights this system of equations is *over specified:* the total number of independent equations is greater than or equal to the dimension of the vector of unknowns $\boldsymbol{\Delta u(k)}$. That is, the total number of controlled variable projections is larger than the total number of manipulated variable projections.

The vector of residuals of the system (2.48) is

$$\rho=\begin{bmatrix}\Gamma^{y}[\mathbf{MY}(k\mid k)+\mathbf{S}^{\mathbf{d}}\Delta d(k)+\mathbf{S}^{\mathbf{u}}\Delta\mathbf{u}(k)-\mathbf{R}(k+1)]\\ \Gamma^{u}\Delta\mathbf{u}(k)\end{bmatrix} \tag{2.50}$$

or

$$\rho=\begin{bmatrix}\Gamma^{y}[\mathbf{Y}(k+1\mid k)-\mathbf{R}(k+1)]\\ \Gamma^{u}\Delta\mathbf{u}(k)\end{bmatrix} \tag{2.51}$$

It should be noted that minimizing the sum of squares of the residuals of (2.48) is equivalent to solving the optimal control problem (2.46). The solution that minimizes the sum of squares of the residuals of (2.48) is given by

$$\Delta\mathbf{u}(k)=(\mathbf{S}^{\mathbf{u}T}\Gamma^{yT}\Gamma^{y}\mathbf{S}^{\mathbf{u}}+\Gamma^{uT}\Gamma^{u})^{-1}\mathbf{S}^{\mathbf{u}T}\Gamma^{yT}\Gamma^{y}E_{p}(k+1\mid k) \quad . \tag{2.52}$$

At a given interval of time *k*, having implemented moves in the past and having measured the most current values of the output variables $\hat{y}(k)$, a set of future manipulated variable moves $\boldsymbol{\Delta u(k)}$ up to *m* intervals of time is computed. This set of moves into the future could be implemented as such

and the solution repeated after m intervals of time have elapsed. However, using this implementation measurement information would be used only every *m* intervals of time.

The output measurement $\hat{y}(k)$ is used for the correction of the present state estimate *Y(k|k)*. Because at time *k* future measurement information is not available, we judge it to be best to omit the correction step in the *p*-step-ahead predictor. However, at time *k*+1 new measurement information becomes available and can be used to obtain improved state estimates *Y(k*+1|*k*+1*)* and output predictions *Y(k*+1|*k*+1*)*. Thus the available measurement information is better used if only the moves corresponding to the present time are implemented and if the whole procedure is repeated at the next time interval when a new measurement becomes available. That is, as a new measurement is obtained, a new value for *Y* (*k*+1|*k*+1) is computed, accounting for measurement errors and changes in disturbances. Such a controller implementation is denoted as the *moving horizon* or *receding horizon* approach.

Moving Horizon and Closed Form Control Law

As explained above, the MPC control problem is solved at each time interval to allow the controller to compensate effectively for disturbances on the outputs and for model errors. The resulting control law becomes:

$$\Delta u(k) = [I \quad 0 \quad 0...0]\,(\mathbf{S}^{\mathbf{u}T}\Gamma^{yT}\Gamma^{y}\mathbf{S}^{\mathbf{u}} + \Gamma^{uT}\Gamma^{u})^{-1}\mathbf{S}^{\mathbf{u}T}\Gamma^{yT}\Gamma^{y}E_{p}(k+1\mid k) \tag{2.53}$$

where only the first move (at time *k)* is computed. Note that the only part of the algorithm that changes at each execution of the controller is the projected error $E_p(k+1|k)$. Therefore, for implementation the constant matrix pre-multiplying $E_p(k+1|k)$ can be computed off-line:

$$K_{MPC} = [I \quad 0 \quad 0...0]\,(\mathbf{S}^{\mathbf{u}T}\Gamma^{yT}\Gamma^{y}\mathbf{S}^{\mathbf{u}} + \Gamma^{uT}\Gamma^{u})^{-1}\mathbf{S}^{\mathbf{u}T}\Gamma^{yT}\Gamma^{y} \quad . \tag{2.54}$$

The on-line algorithm is summarized in the following:

1. *Preparation.* Do not vary the manipulated variables for at least *n* time intervals (*Δu(-1)=Δu(-2)=...=Δu(-n)=0*) and assume the measured disturbance changes are zero (*Δd(-1)=Δd(-2)=...=Δd(-n)=0*) during that time. Then the system will be at rest at *k* = 0.
2. *Initialization (k* = 0). Measure *Δd(0)* and the output $\hat{y}(0)$ and initialize the model prediction vector as

$$Y(0\mid 0) = [\hat{y}(0)^{T}, \hat{y}(0)^{T}, ..., \hat{y}(0)^{T}]^{T}. \tag{2.55}$$

Obtain measurement at next sampling time ($\hat{y}(1)$, *Δd(1))*. Set *k* = 1.

3. *Model Prediction:*

$$Y(k \mid k-1) = M^{S} Y(k-1 \mid k-1) + S^{u}\, \Delta u(k-1) + S^{d}\, \Delta d(k-1) \quad . \tag{2.56}$$

where the first element of *Y(k|k-*1), *y(k|k-*1), is the model prediction of the output at time *k*. The value of *Δu(k-1)* should be the actual value implemented on the plant, rather than the value computed by the controller at the last time step. This value may be different because of actuator saturation.

Correction:

$$Y(k \mid k) = Y(k \mid k-1) + K_{F}(\hat{y}(k) - y(k \mid k-1). \tag{2.57}$$

4. *Compute the reference trajectory error vector:*

$$E_{p}(k+1 \mid k) = \mathbf{R}(k+1) - \mathbf{M}\, Y(k \mid k) - \mathbf{S^{u}} \Delta d(k). \tag{2.58}$$

5. *Compute the manipulated variable move:*

$$\Delta u(k) = K_{MPC}\ E_{p}(k+1 \mid k) \tag{2.59}$$

which is implemented on the plant.

6. Obtain measurements $\hat{y}(k+1)$, *Δd(k+1)* at next sampling time, set *k:=k+*1 and go to step 3.

The dynamic behaviour of this algorithm will be determined by the choice of adjustable parameters. These include the weights Γ^{y} and Γ^{u} and the number of moves *m*. These parameters will influence, among other things, the speed of response and specifically, the *stability* of the inputs and outputs (i.e. whether the algorithm produces bounded *u* and/or *y* signals). Note that, if any of these parameters needs to be changed on-line, it is necessary to recompute the matrix K_{MPC}, thus imposing additional on-line computational requirements.

2.3.10 General tuning guidelines of MPC

The most significant tuning parameters that must be selected for MPC controllers are *prediction horizon*, *control horizon*, *sampling interval*, *penalty weight matrices*, and if the control engineer decided to use a *filter*, the parameters of this.

The choice of these parameters has a profound effect on the nominal stability, robustness, and controller performance of the MPC algorithms. In practical applications the most important criteria

that have to be satisfied by controllers are: stability and robustness. Thus, ideally one should know a range of the control parameters, which provide stability and robustness, and then select from this interval the values for the parameters, which give the best control performance in accordance to certain control objectives. For linear systems there are developed algorithms to obtain the sufficient conditions, which guarantee nominal stability and robustness (Garcia and Morari, 1985a; Garcia and Morari, 1985b; Shridar and Cooper, 1997). However for nonlinear systems the known sufficient conditions (Allgower, 1999) are usually much too strong to be met for practical implementation and one must resort to a set of heuristics based on the extrapolation of linear systems, simulations and experiments.

According to this, the following effects of the tuning parameters on the control performance were observed from the author experience and the examples from the literature:

Prediction horizon. Usually longer prediction horizon leads to more aggressive control action and faster response. With longer prediction horizons the closed-loop system is less robust to model-plant mismatch, however this effect can be reduced by including a filter in the feedback loop. Nominal stability is strongly affected by the horizon length. Usually there is a critical minimum horizon length to achieve a stable closed-loop system.

Control horizon. When the number of control moves is increased a more aggressive control action can be observed. In this case the system response is faster and more sensitive to disturbances. Additionally, increasing the control horizon leads to much more complicated optimization problems, especially in the nonlinear case. Usually there is an upper band on the control horizon established by the controller performance and the computational complexity of the problem.

Sampling time. To ensure good closed-loop performance, the sampling time should be small enough to capture adequately the dynamics of the process, and at the same time large enough to permit the feasibility of real-time implementation (the computational time necessary to solve one open-loop control problem should be smaller than the sampling interval). Zafiriou and Morari (1986) proposed some criteria to select the sampling interval for stable linear SISO systems (Zafiriou and Morari, 1986). For unstable systems robustness depends on the sampling time and there is an inverse relationship between the model error and the maximum allowable size of the sampling time.

Weight matrices. Some attempts to obtain these parameters have been presented in the literature (Kalra and Georgakis, 1994). The results of the author simulations show that the smaller the weight on the control inputs the better is the control performance with regards of the controlled outputs.

However, to avoid aggressive control action small penalties (usually 5-15 % of the output penalty) on the control action should be used, too. Finally there is the possibility of making the weights time varying. Because there are no easy guidelines this is rarely pursued in practice.

Feedback filter. The use of a well-tuned filter on the feedback signal provides good disturbance rejection and fast systems response. However, the choice and the effects of the filter are strongly dependent on the certain system (Luenberger, 1971). An example of the effects of the Extended Kalman Filter (EKF) used in the NMPC of a high purity distillation column is presented later.

2.4 Interaction analysis and multiple single-loop designs

2.4.1 The Relative Gain Array (RGA)

In the control of multi-parameter plant, a common technique is the Relative Gain Array (RGA), which was first developed by Bristol (1966), with other workers (Shinskey, 1979, 1984; McAvoy, 1983) contributing to its further development and wider adoption. The relative gain array forms the basis of the analysis, and is defined as a matrix containing all possible combinations of Single Input Single Output (SISO) variable pairs expressed in the form of interactive measures (Bristol, 1966).

As such, considering the defined interactions for control of decentralised (multiloop SISO) systems, a set of preferred variable pairs are indicated in the RGA. While the RGA technique was initially developed for steady state systems, it was relatively easy to account for dynamic systems (Witcher and McAvoy, 1977).

However, with further improvements, the RGA included other than simple interaction measures, and also included fundamental property data, i.e. robustness against errors in the model and uncertainties in the input, as well as stability of the closed loop (Grosdidier et al., 1985; Yu and Luyben, 1987; Skogestad and Morari, 1987).

The RGA has been well described, in terms of properties and uses (Hovd and Skogestad, 1992), and while it enjoys wide use, suffers a number of disadvantages, where interactions between control loops may occur in the steady and dynamic states, but these are not captured in the RGA (Friedly, 1984). This is explained in that the RGA does not provide the true closed loop interaction measures (Jensen et al., 1986). In addition, for greater than 2x2 systems, the RGA is not capable of providing the response satisfying the variable pairing problem (Bristol, 1979), and is the case where there is total dependence on other control loops of feasibility of the variable pairing (Shinskey, 1984; Haggblom, 1994).

The influence of other output variables on the transfer function governing the input and output variables (u_j) and (y_i) respectively has been defined in a proposed interaction measure (Bristol, 1966). This interaction measure represented by the ratio of the two transfer functions; one defines the relation between the given two input and output variables, while others are uncontrolled, and the other transfer function of the same two variables, but with all others controlled, denoted by λ_{ij}; where:

$$\lambda_{ij} = \frac{\left.\frac{\partial y_i}{\partial u_j}\right|_{u_k \text{constant}, k \neq j}}{\left.\frac{\partial y_i}{\partial u_j}\right|_{y_k \text{constant}, k \neq i}} = \frac{gain\ with\ other\ loops\ open}{gain\ with\ other\ loops\ closed} \tag{2.60}$$

The relative gains λ_{ij} for all possible variable pairings define a matrix, the relative gain array (RGA), Λ. The partial derivatives in eq. (2.60) can be related to the open-loop transfer functions of a system. Consider a 2x2 system described by the model:

$$y_1(s) = G_{11}(s)u_1(s) + G_{12}(s)u_2(s) \tag{2.61}$$

$$y_2(s) = G_{21}(s)u_1(s) + G_{22}(s)u_2(s) \tag{2.62}$$

The transfer function between y_1 and u_1 with y_2 uncontrolled (i.e., $u_2 = 0$) is G_{11}. The corresponding transfer function when y_2 is perfectly controlled is obtained by the elimination of u_2 with $y_2 = 0$. This gives the relative gain:

$$\lambda_{11}(s) = \left(1 - \frac{G_{12}(s)G_{21}(s)}{G_{11}(s)G_{22}(s)}\right)^{-1} \tag{2.63}$$

The value for λ must be computed for every possible combination of i and j. After every value is found, the RGA matrix can then be formed:

$$RGA = \Lambda = \begin{bmatrix} \lambda_{11} & \lambda_{12} \cdots & \lambda_{1n} \\ \lambda_{21} & \lambda_{22} \cdots & \lambda_{2n} \\ & \vdots & \\ & \vdots & \\ \lambda_{n1} & \lambda_{n2} \cdots & \lambda_{nn} \end{bmatrix} \tag{2.64}$$

Interpreting the RGA

There are certain important properties and guidelines used in understanding and analysing the RGA, and what the different values of the RGA mean:

1. All elements of the RGA across any row, or down any column will sum up to one:

$$\sum_{i=1}^{n} \lambda_{ij} = \sum_{j=1}^{n} \lambda_{ij} = 1 \qquad (2.65)$$

This makes calculating the RGA easier because:

in a 2x2 case, only 1 element must be calculated to determine all elements,
in a 3x3 case, only 4 elements must be calculated to determine all elements and so on.

2. The λ_{ij} calculated from a steady-state matrix is dimensionless and unaffected by scaling.
3. Each of the rows in the RGA represents one of the outputs. Each of the columns represents a manipulated variable.

- **If λ_{ij} = 0:** The manipulated variable (m_j) will have no effect on the output or the controlled variable (y_i).
- **If λ_{ij} = 1:** The manipulated variable m_j affects the output y_i without any interaction from the other control loops in the system. From the definition of λ_{ij} this implies that the gain loop with all loops open is equal to the gain loop with all other loops closed: i.e. $g_{11} = g^*_{11}$.
- **f λ_{ij} < 0:** The system will be unstable whenever m_j is paired with y_i, and the opposite response in the actual system may occur if other loops are opened in the system.
- **f 0 < λ_{ij} < 1:** This implies that other control loops (m_j- y_i) are interacting with the manipulated and controlled variable control loop.

Three different relationships based on λ=0.5 imply different interpretations of pairing and the RGA:

- **If λ_{ij} = 0.5:** The control pairing effect is equal to the retaliatory effect of other loops.
- **If λ_{ij} < 0.5:** The other control loops are influencing the control pair, and the influence of the other control loops is greater than the influence of the control pair.
- **If λ_{ij} > 0.5:** This means that the control pair has a greater influence on the system than the other control loops.

- **If λ_{ij} >1:** The open-loop gain of the control pair is greater than the gain with all other loops closed: i.e. $g_{11} > g^*_{11}$. The positive value of RGA indicates that the control pair is dominant in the system, but the other loops are still affecting the control pair in the opposite direction. The higher the value of λ_{ij} the more correctional effects the other control loops have on the pair (Haggblom, 1995).

Table 2.4: Summary of the interpretation of the RGA.

λ_{ij}	**Possible Pairing**
λ_{ij} **= 0**	Avoid pairing m_j with y_i
λ_{ij} **= 1**	Pair m_j with yi
λ_{ij} **< 0**	Avoid pairing m_j with y_i
λ_{ij} **= or < 0.5**	Avoid pairing m_j with y_i
λ_{ij} **>1**	Pair m_j with y_i

2.5 Nonlinear Model Predictive Control (NMPC) and industrial applications

2.5.1 Introduction

During in the last decade nonlinear model predictive control (NMPC) techniques have become increasingly important and accepted in chemical industries. The NMPC paradigm encompasses a significant number of different approaches, each one with its own special feature, all NMPC techniques rely on the idea of generating values for process inputs as solutions of an on-line (real-time) optimization problem using a nonlinear process model. The nonlinear dynamic model can be used in different ways and in different phases of the control algorithm depending on the particular nonlinear model predictive control approach. Excellent reviews have been published in the literature recently, indicating the current and continuously increasing interest directed toward this control strategy (Allgower et al., 1999; Qin and Badgwell, 2000; Henson, 1998; Imsland et al., 2003; McAvoy, 2002; Nikolaou and Michael, 2001; Poloski et al., 2003; Mayne, 2000). Our intention is not to review these reviews here. The objective of this is rather to provide a motivation

of the study, identify potential benchmark processes categories, and to bring up key problems that need to be addressed in industrial NMPC applications. For details about the applications and NMPC products the reader is referred to the aforementioned review papers and the references therein.

In the wide variety of chemical processes nonlinearity is the rule rather than the exception. There are processes which present many challenging control problems including: nonlinear dynamic behaviour, multivariable interactions between manipulated and controlled variables, unmeasured state variables, unmeasured and frequent disturbances, high-order and distributed processes, uncertain and (variable) dead time on inputs and measurements. Further, reliable measurements of important variables to be controlled, such as quality related variable, are often difficult to obtain on-line. The economic benefits of applying advanced process control (APC) approaches in chemical industry had been widely recognized, first in academia but nowadays in industry, too. The theoretical economical optimal operating condition of a chemical process usually lies on active constraints. Therefore in practice the operating region has to be chosen such that constraints are not violated even in the case of strong disturbances. Quality of control determines how close the process can be pushed to the boundary. APC approaches allow the tighter control of process variables, hence permitting the operation of processes closer to the limits, yielding higher profit. A simple graphical explanation of the economical advantages of APC is shown in Figure 2.18 and 2.19. The schematic representation on Figure 2.19 shows that the optimal operating region given by APC is usually on active constraints but provides higher quality with lower variability then typical operating regions with classical control approaches.

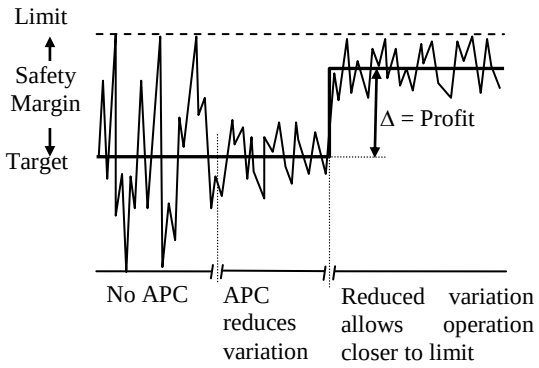

Figure 2.18: Economical benefit given by the use of APC.

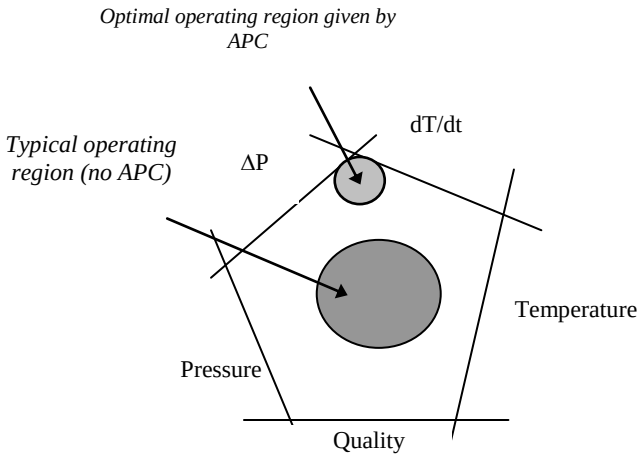

Figure 2.19: Typical operating regions with and without APC.

A number of APC approaches and algorithms that are able to handle some of the aforementioned process characteristics have been presented in the recent years. Many of these approaches are not able to handle the various process characteristics and requirements met in industrial applications resulting in a large gap between the number of industrial and academic NMPC products. Although, it is well recognized, that the performance of a control system is mostly inherent in how successfully it can cope with the *nonlinearity of the process*, chemical processes have been traditionally controlled by using algorithms based on a linear time-invariant approximate process model the most common being step and impulse response models derived from the convolution integral. One reason for this is that in most LMPC applications reported the goal is largely to maintain the process at a desired steady-state (regulator problem, disturbance rejection) (e.g. in refinery processing), rather than moving rapidly from one operating point to another (setpoint tracking problem). A carefully identified linear model, which usually can be identified in a fairly straightforward manner from process test data, is sufficiently accurate in the neighborhood of a single operating point. In addition, by using a linear model and a quadratic objective, the nominal MPC algorithm takes the form of a highly structured convex Quadratic Program (QP), for which reliable solution algorithms and software can easily be found. This is important because the solution algorithm must converge reliably to the optimum in no more than a few tens of seconds to be useful in manufacturing applications. For these reasons, in many cases a linear model will provide the majority of the benefits possible with MPC technology (Bequette, 1991; Morari and Lee, 1997; Lee and Cooley, 1996).

Nevertheless, there are cases where nonlinear effects are significant enough to justify the use of nonlinear model predictive control (NMPC) technology. These include at least two broad categories of applications (Qin and Badgwell, 2000); i.e., disturbance rejection control problems where the process is highly nonlinear and subject to large frequent disturbances (pH control, bioreactor, etc.) (Galan et al., 2000; Nagy and Agachi, 1998; De Oliveira, 1996), or setpoint tracking problems where the operating points change frequently and incorporate a sufficiently wide range of nonlinear process dynamics (batch process control, start-up problems, polymer manufacturing, etc.) (Muske et al., 2000a; Muske et al., 2000b; Nagy and Agachi, 1997; Brengel and Geider, 1989).

A rough distribution of the number of MPC applications versus the degree of process nonlinearity is shown on Figure 2.20, (Qin and Badgwell, 2000). MPC technology has not yet penetrated deeply into areas where process nonlinearities are strong and market demands require frequent changes in operating conditions. It is these areas that provide the greatest opportunity for NMPC applications (Morari and Lee, 1997; Qin and Badgwell, 2000).

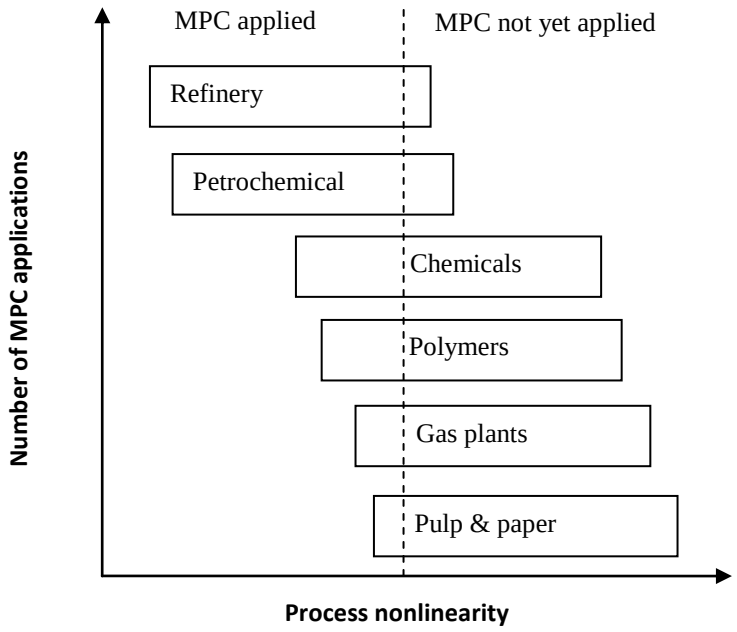

Figure 2.20: Distribution of MPC application versus the degree of process nonlinearity.

2.5.2 Generic NMPC problem formulation

A direct extension of the LMPC methods results when a nonlinear dynamic process model is used, rather than the linear convolution or state space model.

Nonlinear model predictive control is an optimization-based multivariable constrained control technique using a nonlinear dynamic process model for the prediction of the process outputs (Allgower et al., 1999; Bequette, 1991). At each sampling time the model is updated on the basis of new measurements and state variable estimates. Then the open-loop optimal manipulated variable moves are calculated over a finite prediction horizon with respect to some cost function, and the manipulated variables for the subsequent prediction horizon are implemented. Then the prediction horizon is shifted by usually one sampling time into the future and the previous steps are repeated. This generic moving horizon approach of model predictive control algorithms (both nonlinear and linear) is given in Figure (2.16).

The optimal control problem to be solved on-line in every sampling time in the NMPC algorithm can be formulated as:

$$\min_{u(t)\in\mathcal{U}} \mathcal{H}(x(t), u(t), p) \tag{2.67}$$

subject to:

$$\dot{x}(t) = f(x(t), u(t), p)\,, \tag{2.68}$$

$$y(t) = g(x(t), u(t), p)\,, \tag{2.69}$$

$$x(t_k) = \hat{x}(t_k), \quad x(t_0) = \hat{x}_0\,, \tag{2.70}$$

$$h(x(t), u(t), p) \le 0, \quad t \in [t_k, t_F]\,, \tag{2.71}$$

where $\mathcal{H}$ is the performance objective, t is the time, t_k is the time at sampling instance k, t_F is the final time at the end of prediction, $x(t) \in \mathbb{R}^{n_x}$ is the n_x vector of states, $u(t) \in \mathcal{U}$ is the n_u set of input vectors with $\mathcal{U} = \mathcal{U}_1 \times \mathcal{U}_2 \times \ldots \times \mathcal{U}_{n_u}$ representing the set of all possible trajectories of each control input, $y(t) \in \mathbb{R}^{n_y}$ is the n_y vector of measured variables used to compute the estimated states $\hat{x}(t_k)$, $p \in \mathcal{P} \subset \mathbb{R}^{n_p}$ is the n_p vector of uncertain parameters, where the set $\mathcal{P}$ can be either defined by hard

bounds or probabilistic, characterized by a multivariate probability density function. The function $f : \mathbb{R}^{n_x} \times \mathcal{U} \times \mathcal{P} \rightarrow \mathbb{R}^{n_x}$ is the vector function of the dynamic equations of the system, $g : \mathbb{R}^{n_x} \times \mathcal{U} \times \mathcal{P} \rightarrow \mathbb{R}^{n_y}$ is the measurement equations function, and $h : \mathbb{R}^{n_z} \times \mathcal{U} \times \mathcal{P} \rightarrow \mathbb{R}^{c}$ is the vector of functions that describe all linear and nonlinear, time-varying or end-time algebraic constraints for the system, where *c* denotes the number of these constraints. The objective function can have the following general form:

$$\mathcal{H}(x(t),\, u(t),\, p) = \mathcal{M}(x(t_F), p) + \int_{t_k}^{t_F} \mathcal{L}(x(t),\, u(t),\, p)dt \tag{2.72}$$

The form of (2.72) is general enough to express a wide range of objectives encountered in NMPC applications (moving or shrinking horizon approach on regulation and/or setpoint tracking, direct minimization of the operation time, optimal initial conditions, multiple simultaneous objectives, treatment of soft constraints, etc.). For batch processes with end-point optimization the objective usually reduces to the Mayer form ($\mathcal{L}(\cdot) = 0$), however the Lagrange term ($\mathcal{L}(\cdot)$) still may be used, e.g. to implement soft constraints on control rate.

2.5.3 Industrial implementation of NMPC

In the past 20-30 years LMPC has become a preferred control strategy for a large number of processes mainly due to the reasons mentioned in the introduction. While the development of LMPC approaches and industrial products has reached the fourth generation with more than 4500 applications (see Figure 2.21), there are only few NMPC providers (Table 2.6) with rather limited number of applications (Table 2.6).

Table 2.5 lists several commercial NMPC products and the companies supplying them. This list is by no means exhaustive. There are several other approaches but these are either mainly applications to a particular process or the NMPC products are too new (Fischer-Rosemount, ABB, Ipcos, etc.) and were not included here due to lack of information. However the technology sold by the companies in Table 2.6 is representative of the current state-of-the-art.

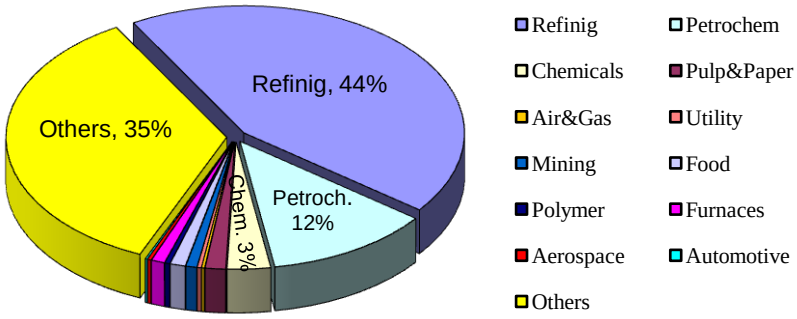

Figure 2.21: Summary of industrial LMPC applications by areas.

Table 2.5: NMPC companies and product names.

Company	Product Name (Acronym)
Adersa	Predictive Functional Control (PFC)
Aspen Technology	Aspen Target (Apollo)
Continental Controls	Multivariable Control (MVC)
DOT Products	NOVA Nonlinear Controller (NOVA-NLC)
Pavilion Technologies	Process Perfecter

An excellent review and description of these NMPC products is given in (Qin and Badgwell, 2000). Table 2.6 provides information on the details of each algorithm, including the model types used, options at each step in the control calculation, and the optimization algorithm used to compute the solution.

Table 2.6: Comparison of industrial NMPC control technology.

Company	Adersa	Aspen Technology	Continental Controls	DOT Products	Pavilion Technologies
Algorithm	PFC	Aspen Target	MVC	NOVA-NLC	Process Perfect
Model Forms[1]	NSS-FP S ,I, U	NSS-NNN S, I, U	SNP-ARX S	NSS-FP S, I	NNN-ARX S, I, U
Feedback[2]	CD, ID	CD, ID, EKF	CD	CD	CD, ID
Rem. Ill-cond.[3]	-	IMS	IMS	IMS	-
SS. Opt. Obj.[4]	Q[I,O]	Q[I,O]	Q[I,O]	-	Q[I,O]
SS. Opt. Const.[5]	IH, OH	IH, OH	IH, OS	-	IH, OH, OS
Dyn. Opt. Obj.[6]	Q[I,O], S	Q[I,O,M]	Q[I,O,M]	(Q,A)[I,O,M]	Q[I,O]
Dyn. Opt. Const.[7]	IA, OH, OS, R	IH, OS-l1	IH, OS	IH, OH, OS	IH, OS
Output Traj.[8]	S, Z, RT	S, Z, RT	S, Z, RT	S, Z, RTUL	S, Z, TW
Output Horiz.[9]	CP	CP	FH	FH	FH
Input Param.[10]	BF	MM	SM	MM	MM
Sol. Method[11]	NLS	QPKWIK	GRG2	NOVA	GRG2

[1]*Model Form:* (ARX) autoregressive with exogeneous inputs (input-output model), (FP) First-Principles, (NSS) Nonlinear State-Space, (NNN) Nonlinear Neural Net, (SNP) Static Nonlinear Polynomial, (S) Stable, (I) Integrating, (U) Unstable

[2]*Feedback:* (CD) Constant Output Disturbance, (ID) Integrating Output Disturbance, (EKF) Extended Kalman Filter

[3]*Steady-State Optimization Objective:* (Q) Quadratic, (I) Inputs, (O) Outputs

[4]*Removal of ill-conditioning:* (IMS) Input move suppression

[5]*Steady-State Optimization Constraints:* (IH) Input Hard maximum, minimum, and rate of change constraints, (OH) Output Hard maximum and minimum constraints

[6]*Dynamic Optimization Objective:* (Q) Quadratic, *(A)* One norm, (I) Inputs, (O) Outputs, (M) Input Moves

[7]*Dynamic Optimization Constraints:* (IH) Input Hard maximum, minimum, and rate of change constraints, (IA) IH with input acceleration constraints, (OH) Output Hard maximum and minimum constraints, (OS) Output Soft maximum and minimum constraints, (OS-l1) Output soft constraints with l_1 exact penalty treatment

[8]*Output Trajectory:* (S) Setpoint, (Z) Zone, (RT) Reference Trajectory, (TW) Trajectory Weighting, (TRUL) Upper and lower reference trajectories

[9]*Output Horizon:* (FH) Finite Horizon, (CP) Coincidence Points

[10]*Input Parameterization:* (SM) Single Move, (MM) Multiple Move, (BF) Basis Functions

[11]*Solution Method:* (NLS) Nonlinear least squares, (QPKWIK) multi-step Newton method, (GRG2) Generalized reduced gradient, (NOVA) Mixed complimentary nonlinear program

An approximate summary of industrial NMPC application is presented in Table 2.8 with the breakdown on different areas of application shown on Figure 2.22.

Table 2.7: Approximate summary of NMPC applications by application areas.

Company Area	Adersa	Aspen Technology	Continental Controls	DOT Products	Pavilion Technologies	Total
Air and Gas			18			18
Chemicals	2		15		5	22
Food Processing					9	9
Polymers		1		5	15	21
Pulp and Paper					1	1
Refining					13	13
Utilities		5	2			7
Unclassified	1		1			2
Total	3	6	36	5	43	93

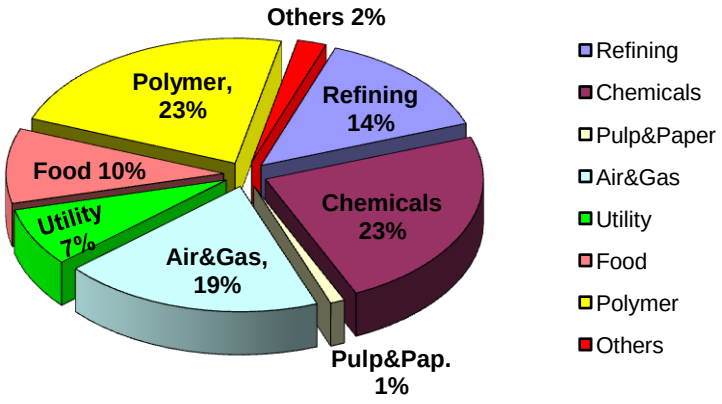

Figure 2.22: Summary of NMPC applications by areas.

It is interesting to note that the distribution of NMPC applications has changed significantly compared to LMPC applications. In refining where processes are operated around a steady-state LMPC can do the job, and the additional burden related to NMPC is probably not necessary. However in polymers and chemicals (e.g. pharmaceuticals) NMPC seem to be the right approach. Half of the NMPC applications are in these two areas, while we can find only a very small percentage of LMPC applications in these processes. The explanation for this could be in the fact that these industries are dominated by highly nonlinear and unstable batch processes, where LMPC

approaches usually fail. The analysis of the LMPC approaches in these areas shows that those applications are for continuous processes where LMPC approaches (sometimes with gain scheduling) can work around the operating points. For example INCA® (the product of IPCOS Technology (Van Brempt et al., 2001) in the actual control calculations uses linear models carefully identified for the operating points, approach which is however more difficult to use efficiently for batch processes. Also for polymers and chemicals (e.g. pharmaceuticals) the objectives are in terms of distribution control of the final product quality which is difficult to express in the LMPC framework. An interesting observation from the analysis of the NMPC applications shows that almost all reported applications (those which were found in the literature) are for continuous processes and many of the presented products do not even work for discontinuous highly nonlinear and unstable processes with large variation in process gain. The need of NMPC for continuous polymerization processes can be explained by the frequent grade changeover operations of the reactors in order to meet diversified demands of the market. However even in these cases relatively simpler NMPC approaches based on linear model scheduling can work and are applied. In the case of batch polymerization and certain fine chemical processes the physico-chemical properties of the system (viscosity, density, heat capacity) can change dramatically during the process leading to change in the gain sometimes even with two order of magnitudes. In these cases the controller has to cover a wide range of operating conditions and cope with highly nonlinear process dynamics. This motivates the use of batch polymerization (Park et al., 2003; Pan and Lee, 2003; Sekia et al., 2001; Dulce and Silva, 2002) or fine chemical processes (Le Lann et al., 1999) as good benchmark problems for NMPC assessments. These processes also allow a broad variation in the control problem formulation from simple setpoint tracking to shrinking horizon online optimizing control, or end-point performance control, product property distribution control, etc. Although the above statistics shows the contrary, it should be mentioned however, that in the fine chemicals industry frequent changes in products, lower production rates can make the implementation of NMPC more difficult to be accepted, due the high rate of return needed in the case of short product lifetime.

2.5.4 Challenges in industrial NMPC

The flow of tasks which need to be performed in generic industrial NMPC applications is presented in Figure 2.23. Each block represents its specific problem which need to be discussed in more detail and can represent the main framework of industrial NMPC assessments. Even the link of the NMPC to the process through the input/output devices (I/O) is an important issue where communication protocols between process and controller or even between different task-blocks

within the NMPC need to be compared (OPC, DDE, UDP, TCP/IP, etc.). Obviously not all blocks are present for all NMPC applications. However if the goal is the development of generic NMPC tools adequate for SISO, or thin (CVs > MVs), fat (CVs < MVs), or square (CVs = MVs) MIMO plants all components need to be considered, and those components which are not needed for a certain application will be turned off. For example for SISO control systems the determination of process subsets and ill-conditioning is not an issue and the corresponding modules will be by-passed in the controller.

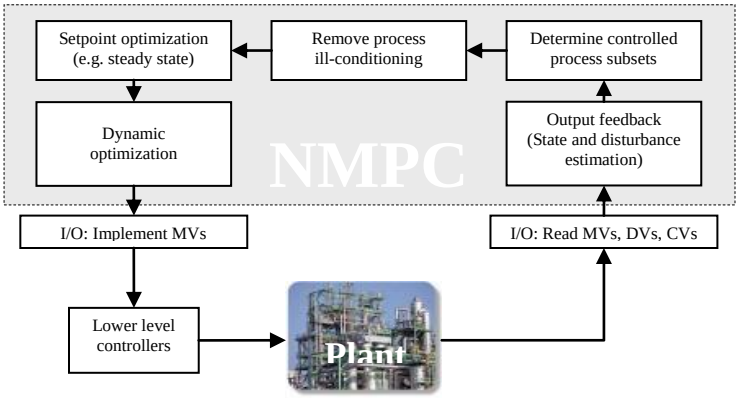

Figure 2.23: Sequence of tasks involved in a generic NMPC application.

Some of the major challenges related to industrial NMPC applications in my opinion are:

- *Efficient development and identification of control-relevant model.* The importance of modeling in NMPC applications is straightforward. Unlike traditional control where modeling and analysis represent a small part of the effort in the application development, it is estimated that up to 80% of time and expense in designing and installing a NMPC is attributed to modeling and system identification. Figure 2.24 schematically represents the design effort involved in NMPC design versus traditional control.

  All LMPC and most of the NMPC products use empirical models identified through plant tests. Figure 2.25 shows the distribution of industrial MPC algorithms based on the model type used. It is attractive to use first-principles (FP) models (in following section details for FP), which give the most inside about the process. First principles models are globally valid and therefore well suited for optimization that can require extrapolation beyond the range of data used to fit the model. Despite the clear advantages of using FP models most of the NMPC approaches are based on empirical nonlinear models. The reasons for this are in the difficulty of the development of proper process models and in the increased computational

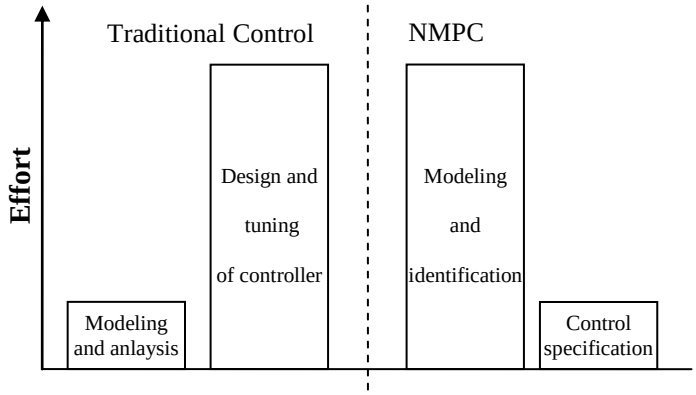

Figure 2.24: Design effort of NMPC versus traditional control.

burden required for the solution of FP models. Since the modelling is a time consuming part of the NMPC design the choice of proper modelling environment is crucial. Almost all industrial NMPC approaches try to beneficiate form the power of chemical modelling software (ASPEN, gPROMS, Hysys, etc.) rather than building and solving the models from scratch. The model identification is important even if first principle models are used. In this case usually offline parameter identification has to be performed. It is very important to keep in mind (however often overlooked) that models (whether empirical or FP) are imperfect (both in term of structure and parameters). Therefore robustness is a key issue in NMPC applications. Robustness has also been identified as one of the major deficiencies of current NMPC products (actually none of the products presented here has any systematic treatment of robust performance except the inherent robustness due to feedback, and penalization of excessive control movements). How to choose the proper plant tests to identify the best model is an important question (Gopaluni et al., 2003, Shouche et al., 2002). For example many vendors believe that the plant test is the single most important phase in the implementation of DMC-plus controllers. *Optimal experimental design* even if it is not *the*, but it can be *a* answer/recipe to the model identification question. Additionally, robust NMPC design can lead to significant performance improvement (Nagy and Braatz, 2003; Wang and Romagnoli, 2003). Another important problem which need to be assessed in case of FP model based NMPC approaches, is the tradeoff between the model accuracy (hence complexity) and computational requirement. Often the control-relevant model does not necessarily have to be the most accurate and finding the proper balance between the

accuracy of the model and computational burden is usually very challenging. Including many details into the model can lead to large number of states resulting in unobservable models based on available measurements besides the prohibitively large computational burden. The determination of the control-relevant model always has to be done in conjunctions with the observer design.

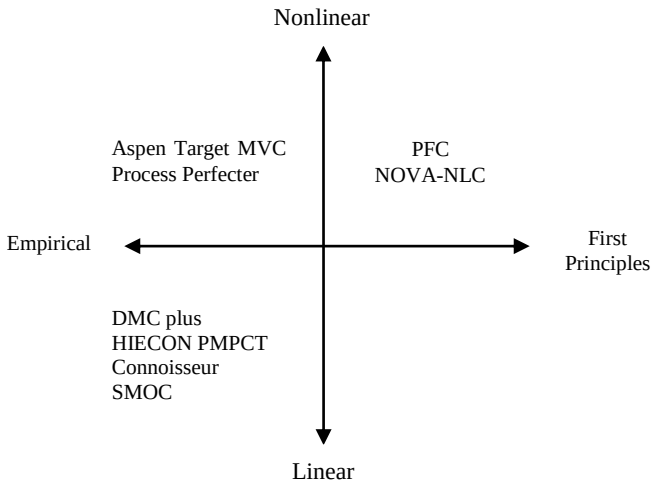

Figure 2.25: Classification of model types used in industrial MPC algorithms.

- *State and parameter estimation.* The lack of reliable *sensors* is one of the major bottlenecks in industrial NMPC applications. This problem is crucial when FP models are used (Allgower et al., 1999). This problem needs to be assessed in detail in the project. In many industrial applications software sensors need to be developed based on additional empirical models (most often neural networks are used for this purpose, e.g. INCA, (Van Brempt et al., 2001).

- *Managing the on-line computational load.* In NMPC approaches exorbitant computational load is involved. The use of efficient optimization approach is crucial (Biegler, 2000; Biegler, 1984, Biegler and Rawlings, 1991; Bock et al., 1999; Hassapis, 2003). There are other important problems here which need to be discussed such as robustness of optimization, or the choice of proper objective functions and optimization problem setup for efficient solution. These will be discussed in more detail in the final report.

- *Design as an integrated system.* In industrial NMPC optimization is involved in several steps of the controller presented in Figure 2.23 (steady-state optimization, dynamic optimization, state estimation, and model identification). An efficient approach to design

model, estimator (of model parameters and states), and optimization algorithm as an **integrated system** (that are simultaneously optimized) rather than independent components could be the capstone in NMPC design.

- *Long-term maintenance of control system.* It is clear the implementation complexity of NMPC approaches is high. But it is important to assess how long term maintenance can be performed and what the limits of the approach in face of changing process and operating conditions are.

2.5.5 First principle (analytical) model based NMPC

The objective of NMPC is to calculate a set of future control moves (control horizon, T_c or M) by minimization of a cost function, like the squared control error on a moving finite horizon (prediction horizon, T_P or P). The optimization problem is solved on-line based on prediction obtained from a nonlinear model. One can use different empirical nonlinear models for prediction in the controller, but the most attractive approach is the use of first principle models, which are globally valid and therefore well suited for the optimization that can require extrapolation beyond the range of data used to fit the model (De Oliveira and Biegler, 1994; Lee, 1998).

A general mathematical formulation of the nonlinear model predictive control problem, when the process is described by ordinary differential equations (ODEs), is:

- *objective function*:

$$\min_{u(\cdot),P,M} J\ x\ t\ ,u\ .\ ,P,M \tag{2.73}$$

- *constraints:*

$$\frac{dx}{dt} = f\ \ x,u,q,d \tag{2.74}$$

$$x(t_k) = \hat{x}(t_k) \tag{2.75}$$

$$0 = g_1\ \ x \tag{2.76}$$

$$y_p = g_2\ \ x \tag{2.77}$$

$$u_{\min}\ \ k+i\ \le u\ \ k+i\ \le u_{\max}\ \ k+i \tag{2.78}$$

$$u\ \ k+i-1\ \ -\Delta u_{\max} \le u\ \ k+i\ \le u\ \ k+i-1\ \ +\Delta u_{\max} \tag{2.79}$$

$$u\ k+i\ = u\ k+M-1 \qquad \text{for all} \quad i=\overline{M-1,P} \tag{2.80}$$

$$x_{\min}\ k+i\ \le x\ k+i\ \le x_{\max}\ k+i \tag{2.81}$$

$$y_{\min}\ k+i\ \le y_p\ k+i\ \le y_{\max}\ k+i \tag{2.82}$$

Where x = state variables, u = manipulated variables, q = parameters, d = measured and unmeasured disturbances, y = output variables.

Generally, the prediction and control horizon, respectively, are considered fixed for an open loop optimization. The objective function usually is chosen as the sum of the squares of the differences between the predicted outputs and the setpoint values over the prediction horizon of P time steps:

$$J\ x(t),u(\cdot)\ = \int_{t_k}^{t_k+T_P} \left\| Q\cdot E \right\|^2 dt \ \Leftrightarrow J\ x(k),u(\cdot)\ = \sum_{i=1}^{P} \left\| Q_i\ r\ k+i\ - y_p\ k+1\ \right\|^2 \tag{2.83}$$

continuous form *discrete form*

Often the objective function (2.83) includes a second term, which is the squared sum of the manipulated variable changes over the control horizon (M):

$$J\ x(t),u(\cdot)\ = \sum_{i=1}^{P} \left\| Q_i\ r\ k+i\ - y_p\ k+1\ \right\|^2 + \sum_{i=1}^{M} \left\| R_i \Delta u\ k+i-1 \right\|^2 \tag{2.84}$$

The second term was originally introduced by the unconstrained formulation of LMPC in which constraints are handled artificially through the weighting factors (matrices Q_i and R_i). Since the constrained LMPC algorithms likewise the NMPC methods explicitly include constraints there is no need of the second term in the objective function, however in many of the constrained LMPC and NMPC applications authors use this term, too. Instead of, or additionally to the second term of the objective function, we can assure a smooth control action by introducing another term to minimize the deviations of the manipulated inputs from their setpoints. In this way a more general formulation of the performance function is obtained and the optimization problem to be solved at each sampling time can be written as follows:

$$\min_{u\ k\ \ldots u\ k+M-1} \left\{ \sum_{i=1}^{P} \left\| Q_i\ r\ k+i\ - y_p\ k+1\ \right\|^2 + \sum_{i=1}^{M} \left\| R_i \Delta u\ k+i-1 \right\|^2 + \sum_{i=1}^{M} \left\| R_l^{'}\ u\ k+i-1\ - u^{ref}\ k+i-1\ \right\|^2 \right\} \tag{2.85}$$

The predicted values of the output variables (y-$_p$) can be considered equal to the value obtained from the model (y_m), but usually a correction is made to reduce the cumulative error effect of the

measurement errors and the model/plant mismatch. The correction equation usually has the following form:

$$y_p\ k+i\ = y_m\ k+i\ + K(k+i)\cdot\ y_m\ k\ - y_p\ k \tag{2.86}$$

The decision variables in the optimization problem expressed by equations (2.73)-(2.82) are the control actions, *M* sampling time steps into the future (control horizon). Generally, $1 \le M \le P$ and it is assumed that manipulated variables are constant beyond the control horizon (equation 2.80). Although the optimization provides a profile of the manipulated input moves over a control horizon (*M*), only the first control action is implemented. After the first control action is implemented, new measurements are obtained which are used for the compensation of plant/model mismatch and the estimation of unmeasured state variables. Finally the prediction horizon is shifted by one sampling time into the future and the optimization is performed again.

In the NMPC approaches absolute (2.78) and velocity (2.79) constraints as well as state- and output-variable constraints are explicitly included.

Since a constrained nonconvex nonlinear optimization problem has to be solved on-line, the major practical challenge associated with NMPC is the computational complexity that increases significantly with the complexity of the models used in the controller. There has been a significant progress in the field of dynamic process optimization. Fast on-line optimization algorithms that exploit the specific structure of optimization problems arising in NMPC have been developed and real-time applications have been proven to be feasible for small-scale processes. However, the global solution of the optimization cannot be guaranteed and the development of fast and stable optimization techniques is one of the major objectives in the NMPC research (De Oliveira and Biegler, 1995).

2.5.6 Nonlinear model predictive control with guaranteed stability

Besides the constraints described in the previous section, another important requirement that the nonlinear model predictive controllers have to meet (however seldom taken into consideration for practical implementation) is that it should assure a stable closed-loop system.

The most straightforward way to achieve guaranteed stability is to use an infinite horizon cost functional ($P = M = \infty$) (Campo and Morari, 1986; Keerthi and Gilbert, 1988). In this case, from the Bellman's principle of optimality results that the open loop input and sate trajectories obtained as the solution of the optimization problem are equal to the closed loop trajectories of the nonlinear

system. Consequently, any feasible predicted trajectory goes to the origin. However, using infinite horizon in the performance criterion leads to practically unsolvable optimization problem. To cope with this disadvantage, and guarantee stability, besides the input and state constraints, so-called stability constraints have to be included into the finite horizon open-loop optimization problem (Chen and Allgower, 1996; Chen and Allgower, 1998a; Findeisen and Allgower, l999; Findeisen and Rawlings, 1997; Sistu and Bequette, 1996).

The most widely suggested stability constraint is the terminal equality constraint, which forces the states to be zero (equal to their steady state values) at the end of the finite horizon:

$$x\ t+T_p\ =0 \tag{2.87}$$

Using the terminal equality constraint to guarantee stability is an intuitive approach, however it increases significantly the on-line computation necessary to solve the open loop optimization problem and often causes feasibility problems (De Nicolao et al., 1996; De Nicolao et al., 1997; De Nicolao et al., 1998).

Another approach to guarantee stability is the so-called ***quasi-infinite horizon nonlinear MPC* (QIHNMPC)**, in which the prediction horizon is approximately extended to infinity by introducing a terminal penalty term in the objective function (Chen and Allgower, l997; Chen et al., 1997; Chen et al., 1998; Findeisen and Allgower, 2000a; Mayne and Michalska, 1990; Michalska and Mayne, 1993). The basic idea of this approach consists of the approximation of the infinite horizon prediction to achieve closed-loop stability, while the input function to be determined on-line is of finite horizon only. The terminal penalty term is determined off-line such that it bounds from above the infinite horizon objective function of the nonlinear system controlled by a local state feedback law in a terminal region Ω (Chisci et al., 1996; Mayne, 1996; Mayne et al., 2000; Mayne and Michalska, 1990; Meadows et al., 1995; Meadows and Rawlings, 1993).

2.6 Conclusions

For modern refiners, the catalytic cracker is the key to profitability in that the successful operation of the unit determines whether or not the refiner can remain competitive in today's market. The major objective of FCC units is to convert low-value, high-boiling feedstocks into valuable products such as gasoline and diesel. The three dominant reactions are cracking, isomerisation, and hydrogen transfer. The catalyst acid sites have a major influence on the reaction chemistry. The introduction of zeolites into the FCC catalyst drastically improved the performance of the catalytic cracker reaction products. The zeolite catalysts are active and selective. The higher activity and

selectivity translate into more profitable liquid product yields and additional cracking capacity. The need to produce reformulated gasoline will increase demand for the shape-selective zeolite; the additive technology is continuously expanding.

The benefits of the new catalyst technologies is the achievement of deep bottoms cracking with low coke; high conversion and high yields of gasoline and light olefins. These benefits have been verified in many successful commercial applications.

Selective modifications of the unit's components (feed injection, riser termination, air distribution, catalyst cooling, stripper design), flexibility of operations, mechanical improvements are improving the unit's reliability, and increasing the quantity and quality of valuable products, and operating flexibility. However, these modifications also increase the complexity of controlling the highly interacting and strongly nonlinear FCCU.

It is well recognized that the economic effectives on the performance of the control system applied for its operation suitable control system can increase efficiency and reduce the environmental impact of an FCCU.

This chapter provides an overview of the development of linear and nonlinear model predictive control strategies .The detailed evaluation of the trends of industrial applications and preparation of the model predictive control approaches indicate that linear and nonlinear MPC are suitable technologies for the FCCU, with significant potential to increase the profit a ability and efficiency of the unit.

The FCCU high degree of efficiency will continue to play a key role in meeting future market demands, in which the application of advanced control approaches will be undoubtedly a key element.

CHAPTER 3
MATHEMATICAL MODELING OF A FLUID CATALYTIC PROCESS

3.1 Analytical mathematical model of the FCCU

In current refineries, the FCC unit plays a prominent role, producing gasoline and diesel, as well as valuable gases, such as ethylene, propylene and isobutylene, from feedstocks that comprise atmospheric gas oils, vacuum gas oils and hydrocracker bottoms. The significant economic role of the FCC unit in modern-day petroleum refining has attracted great interest in academia and industry in terms of developing and modelling control algorithms for efficient FCC application. Figure 3.1 depicts the unit to which the mathematical model relates. The main parts of the FCC unit that have been modelled are:

1. Feed and preheat system
2. Reactor
3. Catalyst circulation lines
4. Regenerator
5. Air blower
6. Wet gas compressor
7. Main fractionators.

The modelling of this unit is sufficiently complex to capture the major dynamic effects that occur in an actual FCCU system; it is multivariable, strongly interacting and highly nonlinear.

The FCCU dynamic model presented in this chapter includes the main systems as well as a kinetic model based on a five-lump system, capable of predicting the yields of valuable products. While the five-lump kinetic model is a significant simplification of the actual cracking kinetics; it is sufficiently complex to describe the yields of valuable products and gasoline octane value. The resulting global model of the FCCU is described by a complex system of partial-differential-equations, which were solved by discretising the kinetic models in the riser and regenerator on a

fixed grid along the height of the units, using finite differences. The resulted model is a high order DAE, with 942 ODEs (142 from material and energy balances and 800 resulting from the discretisation of the kinetic model).

The body of literature relating to the modelling of the FCC process is quite large, reporting strong interactions and a variety of operating, security and environmental constraints. The prospect of realising even greater yields of high-demand products through increased production and more stable operation have motivated the search for models that are practical and more accurate, allied to control strategies that are flexible, better performing, and more cost effective. Ford et al. (1976) proposed a distributed parameter model of the FCC unit regenerator based on a detailed kinetic combustion model. This was followed by Lee and Groves (1985), who modelled an FCC unit by employing macroscopic models to describe the reactor and regenerator. However, it was only until McFarlane et al. (1993) described a dynamic FCC unit model with constraints that a problem which was challenging the chemical process control community was overcome.

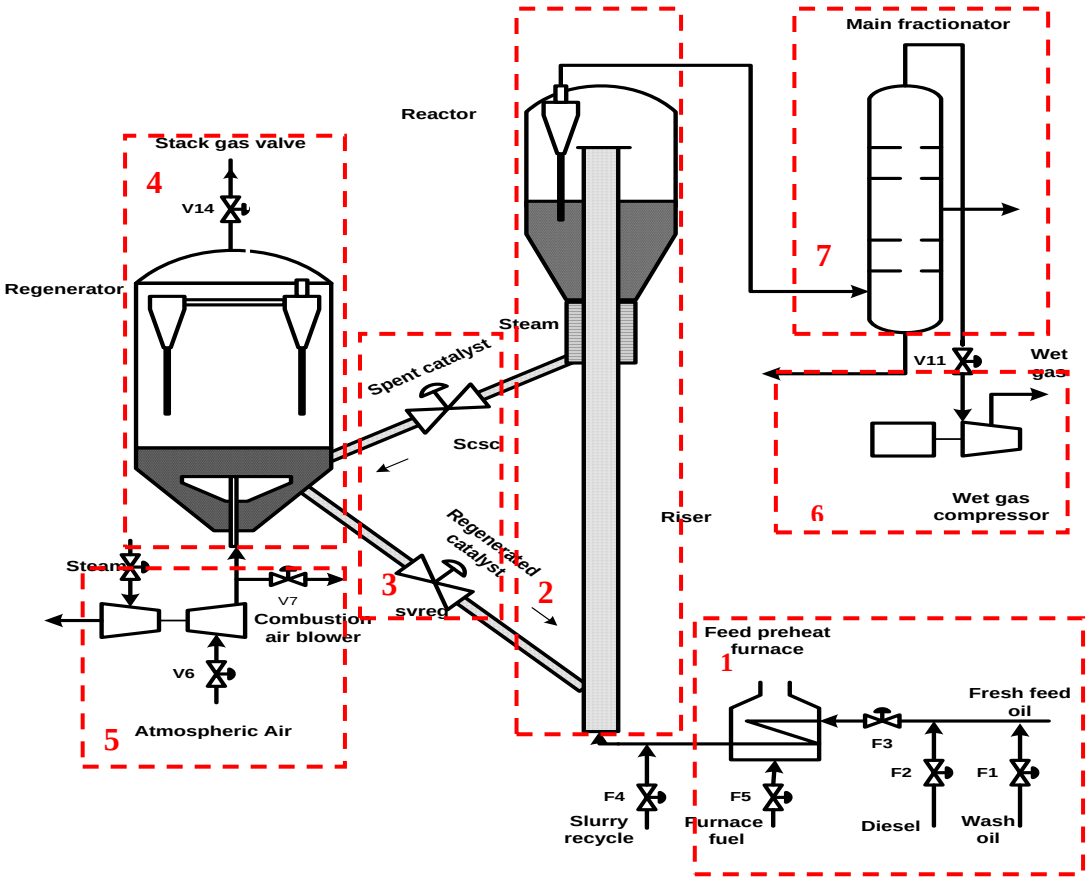

Figure 3.1: UOP fluid catalytic cracking unit.

Their work proposed a distributed parameter model for the regenerator, yet used a continuous stirred-tank reactor (CSTR) without a yield model for the reactor section. In order to achieve effective FCC optimisation, it is quite important that a detailed yield model, which will predict gasoline octane value and yields of valuable products, is applied, as declared in the literature in Section 2.2. In this context, there are many kinetic models, which can be categorised as: heavy lumped models and molecular based models. Despite being more generic, molecular models require analysis at a molecular level. Since such an analysis is very complex, one strategy has been to lump different groups of molecules by boiling point. These are then treated as pseudo-components, allowing the phenomena occurring in the reactor to be described globally. Regarding modelling for the riser section, different kinetic schemes were proposed: from three kinetic lumps, up to thirteen or more (Jacob et al., 1976). Secchi et al. (2001) dynamically simulated the UOP stacked FCC unit by modelling the regenerator as a bubble–emulsion–freeboard model, while the riser was represented by a 10-lump dynamic model. This was validated against experimental data obtained from a working industrial unit. Han and Chung (2001) also proposed a detailed dynamic FCC process simulator, including models of catalyst liftlines, stripper, feed preheater and cyclones. The riser reactor was described as a distributed parameter 4-lump model and the regenerator as a two-regime, two-phase model.

Accurately modelling industrial FCC units is very complicated owing to the strong interactions between process variables, the significant uncertainty surrounding the kinetics of the cracking reactions, coke deposition leading to catalyst deactivation in the riser reactor, and the coke burning process in the regenerator.

3.1.1 Feed system model

The fresh feed stream is transported through the preheat furnace; after exiting, slurry recycled from the main fractionator bottom is mixed with it. The model presented by McFarlane et al. (1993) and Cristea et al. (2003) assumed that, at all times, actual flows were equal to the controller's set point by disregarding controller dynamics and those of the flow streams:

$$F_1 = F_1^{set} \tag{3.1}$$

$$F_2 = F_2^{set} \tag{3.2}$$

$$F_3 = F_3^{set} \tag{3.3}$$

$$F_4 = F_4^{set} \tag{3.4}$$

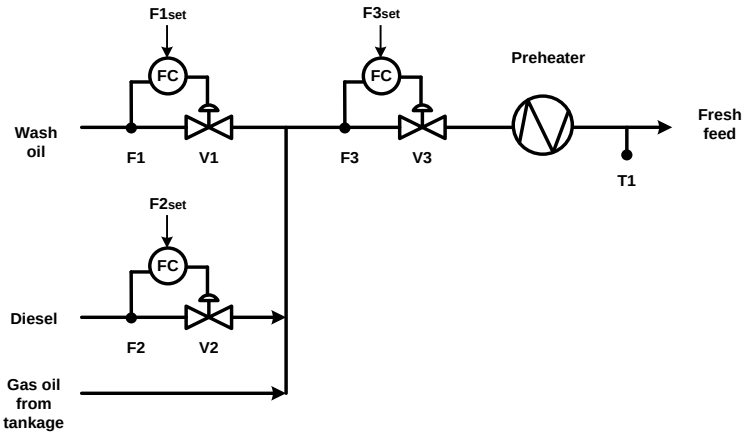

Figure 3.2: Feed system.

3.1.2 Preheat system model

According to McFarlane et al. (1993), the feed pre-heater is represented as a furnace with a fixed flame temperature in the combustion chamber, regardless of spatial position. Moreover, air supply to the pre-heater is assumed to be at the temperature of the surroundings.

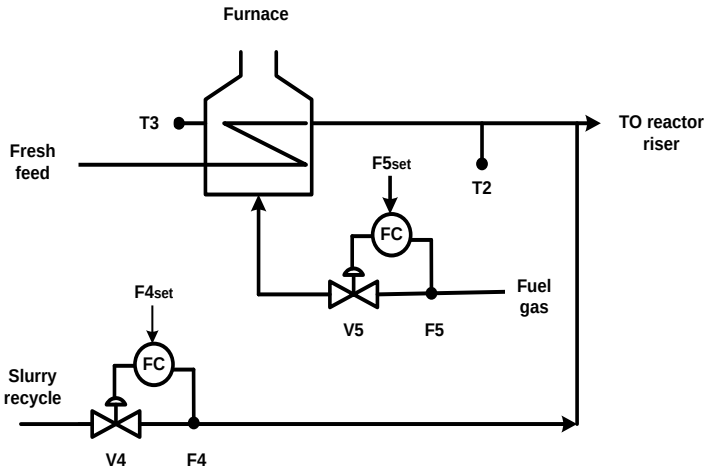

Figure 3.3: Preheat systems.

Based on the assumption that fresh feed, F_3, enters the preheat furnace at temperature T_1, the dynamic energy balance returns furnace firebox and outlet temperatures using the following models (McFarlane et al., 1993; Cristea et al., 2003):

$$\frac{dT_3}{dt} = \frac{1}{\tau_{fb}}\left(F_5 \Delta H_{fu} - UA_f T_{lm} - Q_{loss}\right) \tag{3.5}$$

$$T_{lm} = \frac{(T_3 - T_1) - (T_3 - T_2)}{\ln\left(\frac{T_3 - T_1}{T_3 - T_2}\right)} \tag{3.6}$$

$$Q_{loss} = a_1 F_5 T_3 - a_2 \tag{3.7}$$

$$F_5 = F_5^{set} \tag{3.8}$$

$$\frac{dT_2}{dt} = \frac{1}{\tau_{fo}}(T_{2,ss} - T_2) \tag{3.9}$$

$$T_{2,ss} = T_1 + \frac{UA_f T_{lm}}{F_3} \tag{3.10}$$

Reactor Model

Figure 3.4 presents the two parts of the reactor: the riser and the stripper.

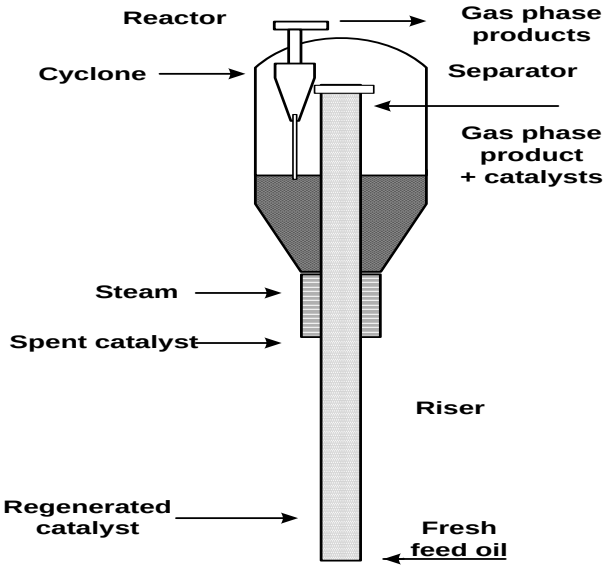

Figure 3.4: Schematic diagram of the industrial riser reactor and the stripper.

In gasoline and olefin refinery production, FCC units are the main conversion units. FCC reactor models typically represent the riser using lump-kinetic schemes with varying numbers of lumps to simulate the two-phase (i.e. constant slip between phases) plug-flow transported bed. These models are used to simulate FCC operation and predict product yields.

The reactor riser model

The complexity inherent in the riser is due to complicated hydrodynamics, heat transfer, mass transfer and catalytic cracking kinetics. Moreover, influential parameters vary along the riser height (Gupta and Rao, 2003):

- Feed is injected into the riser, as are particles of hot catalyst from the regenerator; the liquid feed vaporises and entrains catalyst and liquid drops along the riser height.
- Vaporisation of liquid feed increases gas velocity.
- The varying gas velocity affects axial (and radial) catalyst volume fractions.
- Gas and catalyst particles exhibit significant slip between each other.
- Vaporised hydrocarbons undergo cracking on the surfaces of catalyst particles, resulting in lighter hydrocarbons and coke. The coke is deposited on the catalyst surface steadily deactivating it. The reactant and product hydrocarbons continue to diffuse to and away from the catalyst surface.
- Heat is transferred from the hot catalyst, vaporising liquid feed and providing heat to the endothermic cracking reactions.

The lumping approach is applied to FCC unit modelling given that it is not feasible to treat all species and reactions, because the complex reaction network comprises a huge number of unknown rate constants. Therefore, molecules and reactions are lumped by their chemical nature, i.e. the number of carbon atoms, while different molecular groups are lumped by their boiling points. For this purpose, kinetic models have been found to describe cracking behaviour adequately (Carabineiro et al., 2004).

In modelling the riser for this study, the following assumptions were made:

- Cracking reactions take place exclusively in the reactor,
- The riser wall is adiabatic,
- Negligible dispersion and adsorption occur inside catalyst particles,
- The catalyst and coke are given the same properties,
- The riser reactor is taken as being tubular, one-dimensional, and with no axial or radial dispersions.

Kinetic model of riser reactor

The following representative models describing riser kinetics were investigated:

Five-lump kinetic model

When it is important to predict yields of coke, gasoline and dry gas, a five-lump kinetic model is used. Knowledge of coke yields allows heat integration to be studied, together with air blowers and the design and simulation of the main fractionator. While predicting yields of gasoline and dry gas separately from other lumps, it allows the effects at main components in the FCC unit (e.g. gas compressors) to be analysed. Therefore, this catalytic cracking kinetic model separates gasoline, dry gas and coke from other lumps (Ancheyta-Juarez and Sotelo-Boyas, 2000).

The following scheme simplifies five-lump kinetic models (Dupain and Gamas, 2003; Dupain et al., 2006): A number of assumptions are made in this model: coke forms at initial catalyst-oil contact, diesel only cracks to gas, and it is not converted into gasoline where a small quantity of uncrackable gas oil exists.

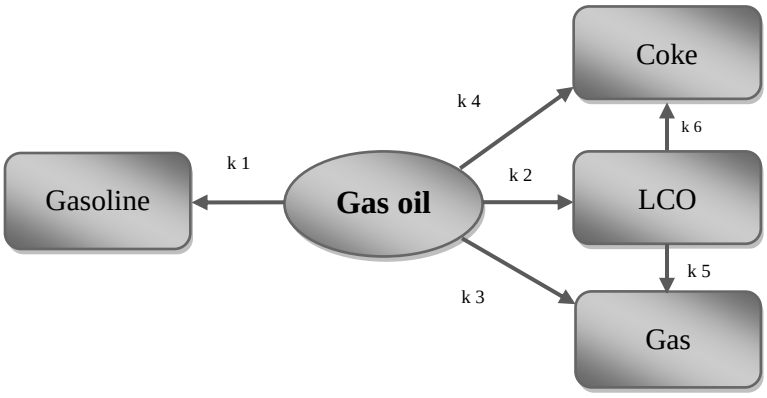

Figure 3.5: The five-lump kinetic model for cracking.

All the cracking reactions are assumed to occur only in the reactor riser. Sensible heat, heat from vaporisation, and the heat driving the endothermic cracking reactions are provided by the hot catalyst. The riser is modelled by mass balance, describing the production of gasoline, diesel, slurry, coke and gases. The following sets of differential equations describe this model:

$$\frac{dy_{feed}}{dt_c} = ((-(k_1 + k_2 + k_3)(y_{slurry} - x_{slurry}))\psi_{conv} - (k_5(y_{slurry} - x_{slurry})CTO \quad (3.11)$$

$$\frac{dy_{diesel}}{dt_c} = ((k_1(y_{slurry} - x_{slurry}) - k_4 y_{diesel})\psi_{conv} - (k_6 y_{diesel})\psi_{coke})CTO \quad (3.12)$$

$$\frac{dy_{gasoline}}{dt_c} = ((k_2(y_{slurry} - x_{slurry}))\psi_{conv} CTO \quad (3.13)$$

$$\frac{dy_{gas}}{dt_c} = ((k_3(y_{slurry} - x_{slurry}) + k_4 y_{diesel})\psi_{conv} CTO \quad (3.14)$$

$$\frac{dy_{coke}}{dt_c} = ((k_5(y_{slurry} - x_{slurry}) + k_6 y_{diesel})\psi_{coke} CTO \quad (3.15)$$

The catalyst-to-oil ratio *(CTO)* is expressed as follows:

$$CTO = \frac{Frgc}{f3 + f4} \quad (3.16)$$

The activity function of coke formation describes this process:

$$\frac{d\psi_{coke}}{dt_c} = -\alpha\psi_{coke} \quad (3.17)$$

Coke deposits "poison" the catalyst and reduce cracking activity. The activity function of catalyst conversion can be described as a function of coke content; it is assumed to be the same for all the reactions.

$$\frac{d\phi_{conv}}{dc_c} = -kd\phi_{conv} \quad (3.18)$$

Catalyst deactivation model

The catalyst deactivation model is used in kinetic studies conducted on catalytic cracking/pyrolysis lumping models, and is typically based on a function dependent on time-on-stream, represented by the catalyst residence time, or a function dependent on coke content of catalyst, represented by the catalyst coke mass fraction. While the former catalyst deactivation functions are in use, the latter are particularly appropriate, since a main cause of catalyst deactivation is coke (Alsabei et al., 2008).

The aim in this work was to develop a coke content-dependent, catalyst deactivation function. Among the estimated function variables, coke content of the catalyst is independent, and represents an operating parameter, with unknown value at any particular point in time. As such, to prevent a new unknown from being introduced, direct measurement to deduce the parameter, and consequently the deactivation function, was performed. The function of coke content in the catalyst was derived from least squares regression analysis, varying with the prevailing operating conditions and properties of the feed. The catalyst deactivation function was then derived.

As shown in Eq. (3.29), the catalyst coke content (C_c) in heavy oil pyrolysis is a function varying with feed atomic ratio C/H, temperature of reaction (T), oil gas residence time (t), catalyst residence time (t_c), and weight ratios of catalyst-to-oil (R_{co}) and steam-to-oil (R_{so}).

Least squares regression analysis is performed on experimental results to yield the parameters needed in Eq. (3.29), resulting in Eq. (3.30). In turn, experimental data applied to the catalyst deactivation function described by Eq. (3.31), yields the function used in this work. This function is independent of reaction temperature, and does not vary, compared to a deactivation function based time-on-stream, as the function already accounts for the effect of temperature (Roman et al., 2009).

$$C_c = a\left(\frac{C}{H}\right)^b T^c t^d \left(1-R_{co}\right)^e \left(1-R_{so}\right)^f t_c^g 100 \tag{3.19}$$

$$C_c = 3.5248\left(\frac{C}{H}\right)^{4.3889} T^{0.2838} t^{-0.1774} \left(1-R_{co}\right)^{-0.4795} \left(1-R_{so}\right)^{-0.3963} t_c^{0.2276} 100 \tag{3.20}$$

$$\varphi = \exp\left(-\alpha \cdot C_c\right) \tag{3.21}$$

$$\varphi = \exp\left(-2.55\left(\frac{C}{H}\right)^{4.3889} T^{0.2838} t^{-0.1774} \left(1-R_{co}\right)^{-0.4795} \left(1-R_{so}\right)^{-0.3963} t_c^{0.2276}\right) \tag{3.22}$$

Assumptions regarding riser energy balance include stirred tank dynamics, negligible heat loss to the environment, and the heat of cracking being proportional to riser temperature. Hence, the energy balance is (Cristea et al., 2003):

$$M Cp_{eff} = \frac{dT_r}{dt} = Q_{in} - Q_{out} \tag{3.23}$$

where:

$$Q_{in} = Q_{rgc} + F_3 Cp_{fl}\left(T_2 - T_{base,f}\right) \tag{3.24}$$

$$Q_{out} = Q_{catout} + Q_{slurry} + Q_{cracking} + Q_{ff} \tag{3.25}$$

$$Q_{catout} = F_{rgc} Cp_c (T_r - T_{base}) \tag{3.26}$$

$$Q_{slurry} = F_4 [Cp_{sv}(T_r - T_{ref}) + Q_{sr}] \tag{3.27}$$

$$Q_{ff} = F_3 [Cp_{fv}(T_r - T_{ref}) + Q_{fr}] \tag{3.28}$$

$$Q_{cracking} = F_3 + F_4 \ \Delta H_{crack} \tag{3.29}$$

$$\Delta H_{crack} = 172{,}7 + 3(T_r - T_{ref}) \tag{3.30}$$

The bottom of the reactor riser pressure is needed in the force balance on the regenerated catalyst bend. This is expressed by:

$$P_{rb} = P_4 + \frac{\rho_{ris} h_{ris}}{144} \tag{3.31}$$

where

$$\rho_{ris} = \frac{F_3 + F_4 + F_{rgc}}{\nu_{ris}} \tag{3.32}$$

$$\nu_{ris} = \frac{F_3 + F_4}{\rho_v} + \frac{F_{rgc}}{\rho_{part}} \tag{3.33}$$

The inventory of the catalyst in the riser is:

$$W_{ris} = \frac{F_{rgc} A_{ris} h_{ris}}{\nu_{ris}} \tag{3.34}$$

3.1.3 The reactor stripper model

This part of the FCC unit is represented as a continuous tank with perfect mixing, where reactions do not occur. This is justifiable, since the catalyst and product vapour are separated immediately by the cyclones; thus, usually, no cracking reaction occurs in this disengaging-stripping section. The factors affecting coke yield in the riser in the form of deposits on the catalyst, are assumed exclusively to be: weight hourly space velocity in the riser (WHSV), carbon concentration on the regenerated catalyst, residence time of the catalyst in the riser, and the coking characteristics of the various feeds (Cristea et al., 2003).

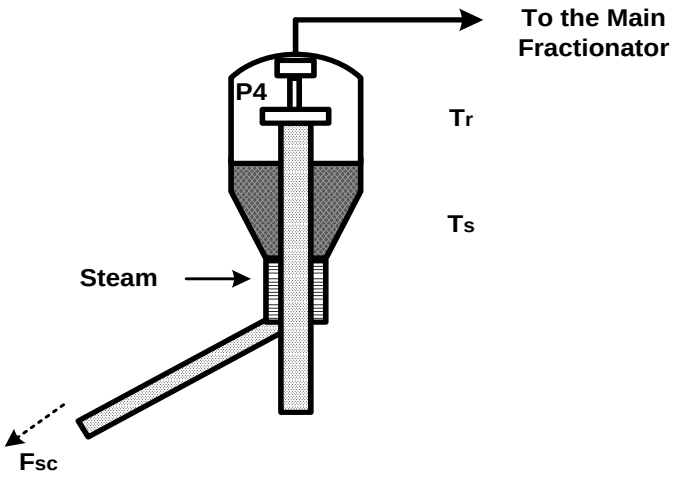

Figure 3.6: Scheme of the FCCU stripper.

The production of coke is given by:

$$F_{coke} = \frac{1.3557 \quad F_3 + F_4 \quad F_B \tau_r^{-1.9843}}{100 WHSV} \tag{3.35}$$

where

$$\tau_r = \frac{W_{ris}}{60 F_{rgc}} \tag{3.36}$$

$$WHSV = \frac{3600(F_3 + F_4)}{W_{ris}} \tag{3.37}$$

$$F_B = \frac{\Psi_f F_3 + 5F_4 + 3F_1 - 0.8F_2}{F_3 + F_4} \tag{3.38}$$

and Ψ_f = 1 for normal gasoil

> 1 for heavier than normal gasoil

< 1 for lighter than normal gasoil

> 0

Wet gas yield is given by:

$$F_{wg} = (F_3 + F_4)[C_1 + C_2(T_r - T_{ref})] \quad (3.39)$$

The coke balance in the stripper also includes any carbon on the regenerated catalyst entering the reactor. This is expressed by:

$$\frac{dC_{sc}}{dt} = \frac{1}{W_r}(F_{rgc}C_{rgc} + F_{coke} - F_{sc}C_{sc} - C_{sc}\frac{dW_r}{dt}) \quad (3.40)$$

In the stripper, catalyst balance is given by:

$$\frac{dW_r}{dt} = F_{rgc} - F_{sc} \quad (3.41)$$

The pressure drop between the main fractionator and the reactor is assumed constant; hence, the reactor pressure is given by:

$$P_4 = P_5 + \Delta P_{frac} \quad (3.42)$$

3.1.4 Regenerator model

For the regenerator model, the assumptions are that the catalyst phase is perfectly mixed, that coke deposits on the catalyst consist of carbon and hydrogen, and that all the hydrogen is burned off in the regenerator. Moreover, it is assumed that the conversion of hydrogen is complete following these reactions:

$$4H + O_2 = 2H_2O \quad (3.43)$$

where oxygen and carbon in the coke react to produce CO and CO_2:

$$2C + O_2 = 2CO \quad (3.44)$$

$$C + O_2 = CO_2 \quad (3.45)$$

Furthermore, carbon monoxide reacts to produce carbon dioxide:

$$2CO + O_2 = 2CO_2 \quad (3.46)$$

Mass and heat transfer in the reactor and regenerator are complex. Hence, the regenerator is typically described as two zones: a dense bed zone (with a dense phase and a gaseous phase), and an entrained catalyst zone (Figure 3.8). Two phases are assumed to make up the fluidised bed: gaseous reactants first giving a bubble phase and including products moving up the bed in plug-

flow; and a second, perfectly mixed, dense phase comprising solid catalyst and gas (Bollas et al., 2007; Han and Chung, 2001).

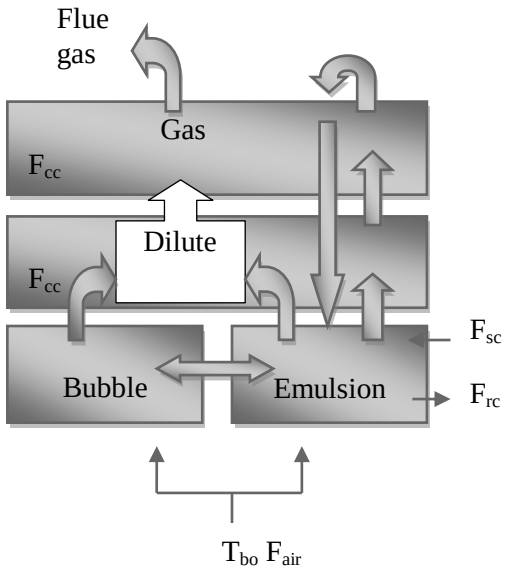

Figure 3.7: Regenerator phases.

Along the bed, gas moves and mass transfer between the two phases occurs. In order to allow modelling of the dense bed, a number of assumptions, as follow, are made:

- bubbles do not contain any catalyst particles within them;
- the cyclones restore all the particles of the ejected catalyst in the freeboard to the dense bed;
- perfect mixing of the catalyst particles in the dense bed occurs due to the cyclone recycling action and circulation in the bed;
- thermal equilibrium exists between the catalyst in the dense bed and the gases;
- the gas densities of the bubble and emulsion phases are both the same;
- gases follow a tubular flow regime in both the bubble and emulsion phases;
- regenerator gas consists of oxygen, carbon monoxide, carbon dioxide, water vapour, and nitrogen.

The gaseous and dense phases of the bed are assumed to be in internal equilibrium. Due to entrainment in the flows, catalyst is to be found in the zone above the dense bed (the disengaging zone). The quantity of catalyst decreases with vertical distance. In the presence of the catalyst, heat is generated by reactions (3.43), (3.44) and (3.45); this influences the energy balance in the regenerator. Only reaction (3.46) is significant in the region above the disengaging zone (the dilute phase) since there is very little catalyst there (Han et al., 2000; Ansari and Tade, 2000).

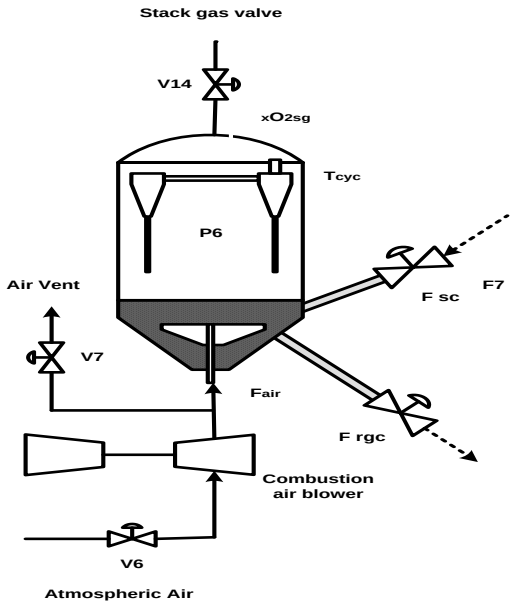

Figure 3.8: Scheme of the FCCU regenerator.

The following equations describe the energy balance for the reactor bed (McFarlane et al., 1993; Cristea et al., 2003):

$$[W_{reg}Cp_c + M_I]\frac{dT_{reg}}{dt} = Q_{in} - Q_{out} \tag{3.47}$$

where

$$Q_{in} = Q_{air} + Q_H + Q_C + Q_{sc} \tag{3.48}$$

$$Q_{out} = Q_{fg} + Q_{rgc} + Q_e \tag{3.49}$$

$$Q_{air} = F_{air}Cp_{air}(T_{air} - T_{base}) \tag{3.50}$$

$$Q_H = F_H \Delta H_H \tag{3.51}$$

$$Q_c = F_{air}(XCO_{sg}\Delta H_1 + XCO_{2,sg}\Delta H_2 \tag{3.52}$$

$$Q_{sc} = F_{sc} Cp_c (T_{sc} - T_{base}) \tag{3.53}$$

$$Q_{rgc} = F_{rgc} Cp_c (T_{reg} - T_{base}) \tag{3.54}$$

$$F_H = F_{sc}(C_{sc} - C_{rgc})C_H \tag{3.55}$$

$$Q_{fg} = [F_{air}(XO_{2,sg} CpO_2 + XCO_{sg} CpCO + XCO_{2,sg} CpcO_2 + 0.79 CpN_2) + 0.5 F_H CpH_2O](T_{cyc} - T_{base}) \tag{3.56}$$

The energy balance of the regenerator is expressed by:

$$\frac{dT_{reg}(z)}{dt} = 0 \qquad 0 \le z \le z_{bed} \tag{3.57}$$

$$\frac{dT_{reg}(z)}{dt} = (\Delta H_1 \cdot \frac{dXCO(z)}{dz} + \Delta H_2 \frac{dXCO_2(z)}{dz}) \cdot \frac{1}{Cp(z)} \qquad z_{bed} < z \le z\_ \tag{3.58}$$

$$Cp(z) = 0.79 \cdot CpN_2 + XCO(z) \cdot CpCO + XCO_2(z) \cdot CpCO_2 + XO_2(z) \cdot CpO_2 + \ldots [0.5 \cdot CpH_2O \cdot F_H + \delta_z \cdot Cp_c \cdot M_e] \cdot \frac{1}{F_{air}} \qquad \delta_z = 0 \quad z \ge Z_{cyc} \qquad \delta_z = 1 \quad z < z_{cyc} \tag{3.59}$$

The carbon balance is given by:

$$\frac{dC_{rgc}}{dt} = \frac{1}{W_{reg}} \cdot (\frac{dW_c}{dt} - C_{rgc} \cdot \frac{dW_{reg}}{dt}) \tag{3.60}$$

$$\frac{dW_{reg}}{dt} = F_{sc} - F_{sp} \tag{3.61}$$

$$\frac{dw_c}{dt} = (F_{sc} C_{sc})\left[F_{rgc} C_{rgc} + 12 F_{air}(XCO_{sg} + XCO_{2,sg})\right] \tag{3.62}$$

Mass balances of oxygen, carbon monoxide, carbon dioxide are expressed as:

$$\frac{dXO_2}{dz} = [100 \cdot (-0.5 \cdot k_1 - k_2) \cdot \rho_B(z) \cdot C_{rgc} - k_3 \cdot XCO(z)] \cdot \frac{XO_2(z)}{\nu_s} \tag{3.63}$$

$$\frac{dXCO(z)}{dz} = [100 \cdot k_1 \cdot \rho_B(z) \cdot C_{rgc} - 2 \cdot k_3 \cdot XCO(z)] \cdot \frac{XO_2(z)}{\nu_s} \tag{3.64}$$

$$\frac{dXCO_2(z)}{dz} = -\frac{dXO_2(z)}{dz} - 0.5 \cdot \frac{dXCO(z)}{dz} \tag{3.65}$$

$$XCO_2(z) = XO_2(0) - XO_2(z) - 0.5 \cdot XCO(z) \tag{3.66}$$

$$XO_2(0) = \frac{1}{F_{air}} \; 0.21F_{air} - 0.25F_H \tag{3.67}$$

$$k_1 = 6.9547 \cdot e^{19.88\frac{34000}{T_{reg}(z)+459.6}} \tag{3.68}$$

$$k_2 = 0.69148 \cdot e^{15.06-\frac{25000}{T_{reg}(z)+459.6}} \tag{3.69}$$

$$k_3 = 0.6412 \cdot P_6 \cdot e^{25.55-\frac{45000}{T_{reg}(z)+459.6}} \tag{3.70}$$

The output concentrations are:

$$cO_{2,sg} = \frac{100 \cdot F_{air} \cdot XO_2}{F_{sg}} \tag{3.71}$$

$$cCO_{sg} = \frac{10^6 \cdot 28 \cdot XCO}{28 \cdot XCO + 44 \cdot XCO_2 + 32 \cdot XO_2 + 22.12} \tag{3.72}$$

The following empirical formula gives volume fractions of catalyst in the regenerator bed:

$$\frac{d\rho_B(z)}{dz} = 0 \tag{3.73}$$

$$\rho_B(z) = 1 - \varepsilon_e \qquad 0 \le z \le z_{bed} \tag{3.74}$$

$$\frac{d\rho_B(z)}{dz} = \frac{-1000 \cdot F_{air} \cdot \rho_B(z)}{A_{reg} \cdot \nu_s \cdot \rho_{c,dilute}} \qquad z_{bed} < z \le z_{cyc} \tag{3.75}$$

$$\varepsilon_e = \min[1, \quad \max(\varepsilon_f, \varepsilon_f + \frac{1.904 + 0.363 \cdot \nu_s - 0.048 \cdot \nu_s^2}{z_{bed}})] \tag{3.76}$$

$$\varepsilon_f = 0.332 + 0.06 \cdot v_s \tag{3.77}$$

The empirical equations describing the mass flow rate of entrained catalyst exiting the bed are:

$$M_e = A_{reg}\rho_{c,dilute}v_s \tag{3.78}$$

where:

$$\rho_{c,dilute} = -0.878 + 0.582 \cdot v_s \tag{3.79}$$

$$\nu_s = \frac{F_{sg} + F_{air}}{2} \cdot \frac{1}{\rho_g \cdot A_{reg}} \tag{3.80}$$

where

$$\rho_g = \frac{520 \cdot P_6}{379 \cdot 14.7 \cdot (T_{reg} + 459.6)} \tag{3.81}$$

Ideal gas behaviour is assumed to give regenerator pressure balance:

$$\frac{dP_6}{dt} = \frac{R}{V_{reg,g}} \cdot [n \cdot \frac{dT_{reg}}{dt} + (T_{reg} + 459.6) \cdot \frac{dn}{dt}] \tag{3.82}$$

$$\frac{dn}{dt} = F_{air} - F_{sg} \tag{3.83}$$

$$V_{reg,g} = A_{reg} \cdot z_{cyc} - A_{reg} \cdot z_{bed} \cdot (1 - \varepsilon_e) \tag{3.84}$$

$$P_{rgb} = P_6 + \frac{W_{reg}}{144 \cdot A_{reg}} \tag{3.85}$$

$$\Delta P_{RR} = P_6 - P_4 \tag{3.86}$$

Stack gas flows through the stack valve from the regenerator are given by:

$$F_{sg} = k_{14} \cdot V_{14} \cdot \sqrt{P_6 - P_{atm}} \tag{3.87}$$

Empirically, the regenerator bed height is expressed as:

$$z_{bed} = \min[z_{cyc}, (2.85 + 0.8 \cdot \nu_s + \frac{W_{reg} - \rho_{c,dilute} \cdot A_{reg} \cdot z_{cyc}}{A_{reg} \cdot \rho_{c,dense}}) \cdot (\frac{\rho_{c,dense}}{\rho_{c,dense} - \rho_{c,dilute}})] \tag{3.88}$$

where

$$\rho_{c,dense} = \rho_{part}(1 - \varepsilon_f) \tag{3.89}$$

3.1.5 Air blower model

A single-stage centrifugal compressor, driven by a variable speed steam turbine, is used to simulate the air blower system. For the anti-surge control system, an atmospheric vent line and valve are available on the discard line (Cristea et al., 2003).

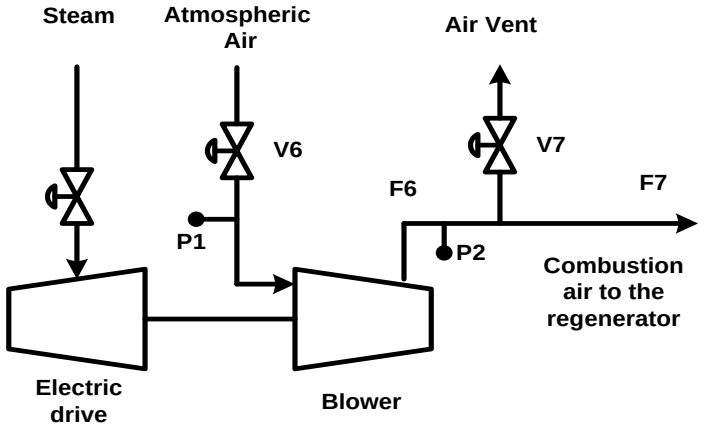

Figure 3.9: Combustion air blower.

Head capacity performance is given by:

$$F_{sucn,comb} = 45000 + \sqrt{1.581 \cdot 10^{9} - 1.249 \cdot 10^{6} \cdot P_{base}^{2}} \tag{3.90}$$

$$P_{base} = \frac{14.7 \cdot P_{2}}{P_{1}} \tag{3.91}$$

Suction and discharge pressure are given by:

$$\frac{dP_{1}}{dt} = \frac{R \cdot (T_{atm} + 460)}{29 \cdot V_{comb,s}} \cdot (F_{v6} - F_{6}) \tag{3.92}$$

$$\frac{dP_{2}}{dt} = \frac{R \cdot (T_{comb,d} + 460)}{29 \cdot V_{comb,d}} \cdot (F_{6} - F_{V7} - F_{7}) \tag{3.93}$$

where

$$F_{6} = \frac{520 \cdot 29 \cdot P_{1} \cdot F_{sucn,comb}}{14.7 \cdot 379 \cdot 60 \cdot (T_{atm} + 460)} \tag{3.94}$$

$$F_7 = k_{comb}\sqrt{P_2 - P_{rgb}} \tag{3.95}$$

$$F_{V6} = k_6 \cdot f_{pp}(V6) \cdot \sqrt{P_{atm} - P_1} \tag{3.96}$$

$$F_{V7} = k_7 \cdot f_{pp}(V7) \cdot \sqrt{P_2 - P_{atm}} \tag{3.97}$$

3.1.6 Model of catalyst circulation lines

The rate of catalyst circulation through the lines' system between the regenerator and riser is controlled by two slide valves; the pressure drop across each governs the catalyst circulation rate. Spent and regenerated catalyst circulation is represented as a single-phase flow, driven by simple force balances. For the purpose of simplification, factors affecting catalyst circulation in an operational FCCU are disregarded in the model. These include carbon concentration on the regenerated catalyst and stream injection at various points in bends (Cristea et al., 2003):

$$144(P_6 - P_{rb}) + z_{bed}\rho_c + (E_{tap-}E_{oil})\rho_c - \Delta P_{svrgc} - \Delta P_{elb,rgc} - \frac{F_{rgc}L_{rgc}f_{rgc}}{A_{rgc}^2\rho_c} = 0 \tag{3.98}$$

The force balance on the spent catalyst line is expressed as:

$$144(P_4 - P_6) + (E_{str-}E_{lift})\rho_c + \frac{W_r}{A_{str}} - \Delta P_{svsc} - \Delta P_{elb,sc} - \frac{F_{sc}L_{sc}f_{sc}}{A_{sc}^2\rho_c} = 0 \tag{3.99}$$

where

$$\Delta P_{sv} = \left[\frac{50F_{cat}}{KA_{sv}sv}\right]^2 \frac{144}{\rho_c} \tag{3.100}$$

$$\Delta P_{elb} = \frac{1}{2}N^*\rho_c v^2 \tag{3.101}$$

3.1.7 Main fractionator model

Distillation technology is quite prevalent in the refining industry, which counts as one of the largest users. A key refinery process, fractionating, occurs in the distillation unit so modelling the distillation unit is vital in predicting the composition of products derived from various gas oils processed under different operating conditions.

Among separation processes, FCC distillation stands out as one of the most complex. Distillation typically results in a mixture of various hydrocarbon compounds which cannot be characterised in

terms of individual components. This has given rise to the practice of substituting a finite number of pseudo-components to express the composition of crude feedstocks and resulting products. Each pseudo-component is a complex hydrocarbon mixture characterised by an average boiling point and an average specific gravity; this is then treated as a single component (Kumar and Sharma, 2001).

The FCCU global model includes a nonlinear model representing a continuous 38-stage distillation column with a reboiler and a total condenser; feed flow enters the column at stage 8. The following assumptions were made with respect to the 117th order model for the main fractionator:

- There are three pseudo-components (multicomponent hydrocarbon mixture) representing gasoline, diesel and slurry(the heavy component)
- relative volatilities are constant,
- there is no vapour holdup,
- molar flows are constant (vapour flow is the same for all stages),
- Franci's Weir Formula describes liquid flow dynamics,
- there is a total condenser,
- energy balance and hydrodynamics are neglected.

Hence, the pressure balance for the main fractionator is expressed by:

$$\frac{dP_5}{dt} = 0.833(F_{wg} - F_{V11} - F_{V12} + F_{V13}) \tag{3.102}$$

where $$F_{V12} = k_{12}V_{12}\sqrt{P_5 - P_{atm}} \tag{3.103}$$

Liquid flows according to Franci's Weir Formula:

$$M = M_{ow} + M_{uw} \tag{3.104}$$

The liquid flow L depends only on holdup over the weir, M_{ow}; total holdup is the sum of the holdup over the weir and the holdup below the weir:

$$M = M_{ow} + M_{uw} \tag{3.105}$$

In the rectifying section, vapour flows are given by:

$$V = V_b + (1 - g_F)F \tag{3.106}$$

The equations of the derived model are given (Halvorsen et al., 2000; Halvorsen and Skogestad, 2003) by:

- the liquid holdup at each column stage *j* except the feed stage is given by:

$$\frac{dM_j}{dt} = L_{j+1} - L_j + V_{j-1} - V_j \tag{3.107}$$

- the material balance for component *i* at stage *j* except the feed stage:

$$\frac{dM_j x_{i,j}}{dt} = L_{j+1}x_{i,j+1} - L_j x_{i,j} + V_{j-1}y_{i,j-1} - V_j y_{i,j} \tag{3.108}$$

- the liquid holdup at the feed stage *NF*:

$$\frac{dM_{NF}}{dt} = L_{NF+1} - L_{NF} + V_{NF-1} - V_{NF} + F \tag{3.109}$$

- the material balance for component *i* at the feed stage:

$$\frac{dM_{NF}x_{i,NF}}{dt} = L_{NF+1}x_{i,NF+1} - L_{NF}x_{i,NF} + V_{NF-1}y_{i,NF-1} - V_{NF}y_{i,NF} \tag{3.110}$$

- for the reboiler (stage *j=1*), the liquid holdup is:

$$\frac{dM_1}{dt} = L_2 - V_1 - B \tag{3.111}$$

- the material balance for component *i* in the reboiler (stage *j=1*):

$$\frac{dM_1 x_{i,1}}{dt} = L_2 x_{i,2} - V_1 y_{i,1} - B x_{i,1} \tag{3.112}$$

- for the condenser (stage $j=N_T$)

$$\frac{dM_{NT}}{dt} = V_{NT-1} - L_T - D \tag{3.113}$$

- the material balance for component *i* in the reboiler (stage $j=N_T$):

$$\frac{dM_{NT}x_{i,NT}}{dt} = V_{NT-1}y_{i,NT-1} - LTx_{i,NT} - Dx_{i,NT} \tag{3.114}$$

- Vapour-liquid equilibrium in each stage *j* for the multicomponent mixture *i*:

$$y_j = \frac{\alpha_i x_j}{1 + (\alpha_i - 1)x_j} \tag{3.115}$$

3.1.8 Wet gas compressor model

This component of the FCC process is represented by a single-stage centrifugal compressor. The compressor is driven by a constant speed electric motor and is assumed to pump against a constant pressure created by the vapour recovery unit (Cristea et al., 2003).

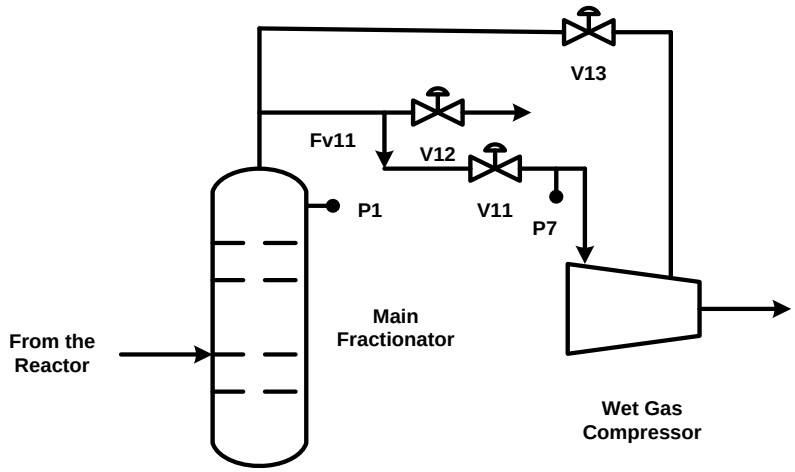

Figure 3.10: Wet gas compressor.

Wet gas compressor performance is given by:

$$F_{sucn,wg} = 11{,}600 + \sqrt{1.366\,.10^{8} - 01057\,H_{wg}^{2}} \tag{3.116}$$

Where

$$H_{wg} = 182.922(C_{rw}^{0.0942} - 1) \tag{3.117}$$

$$C_{rw} = \frac{P_{vru}}{P_{7}} \tag{3.118}$$

The ideal gas law provides the relation for molar flow rate through the compressor:

$$F_{11} = \frac{520 \cdot F_{sucn,wg} \cdot P_{7}}{379 \cdot 60 \cdot 590 \cdot 14.7} \tag{3.119}$$

Pressure balance around the compressor is given by:

$$\frac{dP_7}{dt} = 5 \cdot (F_{V11} - F_{11}) \tag{3.120}$$

$$F_{V11} = k_{11} \cdot f_{pp}(V11) \cdot \sqrt{P_5 - P_7} \tag{3.121}$$

$$F_{V13} = k_{13} V_{13} P_{vru} \tag{3.122}$$

The nonlinear valve flow characteristics are expressed by:

$$f_{pp}(x) = e^{2\ln[0.15(1-x)]} \quad \text{for } x > 0.5 \tag{3.123}$$

$$f_{pp}(x) = 0.3x \qquad \text{for } x \leq 0.5 \tag{3.124}$$

The geometric and functional parameters of the model were adjusted to provide simulation outputs in the range of the real plant data, shown in Table 3.1. The Matlab function with the implemented model equations and use constants is in Appendix.

Table 3.1 provides data for the global model of a complex reactor-regenerator-fractionator process plant.

Table 3.1: Construction and operation data.

Experimental data	**Value**	**Unit of measure**
Riser diameter	1.2	m
Riser height	39.4	m
Striper diameter	2.9	m
Striper height	5.6	m
Elevation of the feed inlet in the riser	2.4	M
Cross sectional area of regenerated catalyst pipe	0.6	m^2
Cross sectional area of spent catalyst pipe	0.7	m^2
Length of regenerated catalyst pipe	7.3	m
Length of spent catalyst pipe	5.4	m

Experimental data	Value	Unit of measure
Cross sectional area of regenerated catalyst, slide valve at completely open position	0.58	m^2
Cross sectional area of spent catalyst, slide valve at completely open position	0.7	m^2
Regenerator diameter	8.5	m
Regenerator height	13.7	m
Height of cyclone inlet	15.2	m
Height of O_2 measurement point	17	m
Elevation of the pipe for regenerated catalyst, outlet from regenerator	12.2	m
Elevation of the pipe for spent catalyst, inlet in the regenerator	18.5	m
Temperature of the fresh feed entering the regenerator	143	C
Atmospheric pressure	1	bar
Location of the feed stage tray	8	-
Spent catalyst valve position	55	%
Regenerated catalyst valve position	65	%
Fresh feed flow rate	170	m^3/h
Slurry recycle flow rate	9.6	m^3/h
Furnace fuel flow rate	34	scf/s
Gasoil density	0.8915	t/m^3
Slurry density	0.968	t/m^3
Gasoline density	0.7372	t/m^3
Diesel density	0.862.6	t/m^3

3.2 Conclusions

This chapter proposes a complex nonlinear dynamic model for the FCCU. The model describes the 7 main sections of the entire FCCU; including (1) the feed and preheating system, (2) reactor, (3) regenerator, (4) air blower, (5) wet gas compressor, (6) catalyst circulation lines and (7) main fractionators.

The novelty of the model consists in that besides the complex dynamics of the reactor-regenerator system, it includes the dynamic model of the fractionator, as well as a new five lump kinetic model for the riser which incorporates the temperature effect an reaction kinetics; hence, it is able to

predict the final production rate of the main products (gasoline and diesel) and can be used to analyze the effect of changing process conditions on the product distribution.

The FCCU model has been developed on the basis which incorporates the temperature effect on reactor kinetics reference construction and operation data from an industrial unit. The resulting global model of the FCCU is described by a complex system of partial-differential-equations, which was solved by discretising the kinetic models in the riser and regenerator on a fixed grid along the height of the units, using finite differences. The resulting model is a high order DAE, with 942 ODEs (142 from material and energy balances and 800 resulting from the discretisation of the kinetic models).

CHAPTER 4
DEVELOPMENT OF A DYNAMIC PROCESS SIMULATOR FOR THE FCCU

In this system the main operation and considerations for the FCCU are analysed. In the development of the process simulation these aspect must be taken into consideration to provide a tool that enables operators to analyse realistic process conditions. The following operational and control aspects will determine the key input and output parameters used in the simulations.

4.1 Considerations of process operation

The primary purpose of FCCU is to convert the heavy oils such as vacuum gasoil, coker gasoil, etc into lighter and more valuable products such as LPG, gasoline, distillate and diesel. This particular unit is designed to maximize the production of LPG and gasoline while the distillate product stream is used either in the diesel pool or the fuel oil pool. The aim of operation of the unit depends on the specific requirements of each of these products. The control of operation of the unit depends on a few selected parameters, which are closely monitored to achieve the optimum mix of products that satisfy all the requirements. They also depend on the various unit constraints such as equipment limitations, etc. The FCCU is a complex multivariate system with strong interactions between the parameters. This interaction is a natural consequence of heat balance. This heat balance refers to a steady state condition of the process where energy, or heat, requirements are met by the combustion of coke. This heat gets transferred from the regenerator to the reactor by hot circulated catalyst. For e.g., if reactor temperature is increased, at constant feed preheat temperature, then there will be a corresponding increase in the catalyst circulation rate and in the regenerator temperature, which will have its own effect on the yields and product quality.

The most important and common term that describes the operation of FCCU is conversion. This gives a broad picture of the performance of the unit. It is defined as the weight percent of the feedstock that has been converted to gasoline or lighter than gasoline products. It also includes the coke formation during the cracking reactions.

Conversion (%) = [Feed rate (vol.) – (Distillate + LCO + HCO) /Feed rate (vol.)] 100

The conversion is also represented as apparent conversion and true conversion based on seasonal demands of gasoline. Normally, the end point of gasoline distillation range would be between 380 ^{o}F and 450 ^{o}F, i.e. 193 ^{o}C to 232 ^{o}C. Any undercutting of gasoline would result in that portion of gasoline dropping down to the LCO pool.

Hence apparent conversion is the conversion calculated before allowing for the adjustment and true conversion is the one calculated on actual yields. It should, however, be noted that the fractionator is operated in a fixed temperature profile and no cut point adjustments are done in the normal operation of the unit.

Another term used for comparison of the different operating variables is the kinetic conversion. This is defined as conversion divided by 100 minus conversion.

Kinetic conversion = Conversion / (100-conversion)

The second order values of kinetic conversion are useful in generating straight-line relationships between the variables. This term is used generally for the process monitoring and catalyst evaluation of the unit and is not widely used by the operating personnel in the routine operation of the unit.

For purpose of discussion, the unit can be broadly divided into the reactor-regenerator and the rest, i.e. fractionator, gas concentration and power recovery sections. Most of the major parameters in these sections are adjusted independent of each other. Normally the reactor section is operated and stabilized in a fixed pattern before adjusting the rest of the unit. Any change in the reactor-regenerator operation parameters will subsequently need the fractionation and other sections to be re-stabilized.

4.1.1 Reactor-regenerator section

The major operating parameters that are adjusted in the reactor-regenerator section include the charge rate, combined feed temperature, combustion air rate, pressure balance, reactor temperature, recycle ratio, catalyst inventory, fresh catalyst addition rate, dispersion steam and stripping steam rates, etc. The parameters, which cannot be adjusted directly, include catalyst activity, catalyst circulation rates, feed quality, conversion, regenerator temperature, etc.

Feed charge rate

The feed charge rate to the unit is normally decided on a long-term basis and is not subjected to frequent changes during routine operation. However, the unit operates best when the feed rate is

close to design. The flexibility of feed rate is usually dependent on constraints of equipments and its capacity limitations rather than the process itself. For effective unit operation, change of feed rate involves restoration of the original conversion levels by adjusting the severity of operation. This is achieved by maintaining the reactor temperature at the required level. The various means of maintaining the required reactor temperature is discussed in detail later.

Combined feed temperature

Any FCCU in operation will automatically adjust its parameters to maintain its heat balance. One of the major inputs of heat to the reactor is the feed. The temperature of the combined feed, i.e. fresh feed and the recycle together, is directly related to the heat input to the reactor.

Any change in the feed temperature will correspondingly lead to changes in the catalyst circulation rate and thereby conversion levels if the reactor temperature is to be maintained constant. If, for example, the feed temperature is increased slightly, then in order to maintain the same reactor temperature, less heat is required from the catalyst. So the catalyst circulation rate gets reduced. As a result of that, conversion level decrease as there is less contact between feed and catalyst. Also coke generation is reduced when catalyst circulation rate reduces. Regenerator temperature tends to rise slightly as catalyst circulation rate reduces. If there is any limitation in the catalyst circulation rates and in maintaining the required reactor temperature, then it is advisable to increase the feed temperature. If, on the other hand, there is no limitation in catalyst circulation, then it is advisable to reduce feed temperature and maintain same reactor temperature to increase conversion level. When conversion is increased in this manner, the gas yield is also reduced.

The effects of an increase in the feed temperature are:

- Reduction in catalyst to oil ratio
- Reduction in coke yield
- Reduction in conversion
- Increase in regenerator temperature

Combustion air rate

This is the most important parameter in the regenerator and can vastly affect the operation of the unit. The main purpose of the regenerator is to burn off all the coke that has been formed during the course of the cracking reactions. The heat that is produced during the burning of coke in the regenerator is used for providing the required temperature in the reactor for normal operation of the

unit. It is also essential to ensure that the entire coke is burnt off or else the activity of the catalyst gets reduced and also maintaining the reactor temperatures become difficult. The air rate to the regenerator is set to maintain a slight amount of excess oxygen in the regenerator flue gases. About 1-2% excess oxygen is maintained so as to ensure that the entire coke in the spent catalyst is burnt off in the regenerator.

Reactor temperature

The reactor temperature is the most important parameter in the reactor structure during the normal operation of the unit. The conversion level of the unit is dependent on the reactor temperature. Increase in reactor temperature will result in an increase in the conversion. Higher reactor temperature will also result in a slightly higher octane number of gasoline produced. This controller acts on the regenerated catalyst slide valve, thereby adjusting the catalyst circulation rate to meet the required reactor temperature. Generally, reactor temperature can also be adjusted by varying the other parameters of heat balance in the system like the feed preheat, the coke make, recycle ratio, airflow, etc. However, the best method of adjusting the reactor temperature would depend on individual scenario taking into consideration the flexibility available in the feed preheat circuit, main air blower capacity, catalyst regeneration, slide valve opening, etc.

The effects of an increase in the reactor temperature are:

- Increase in catalyst to oil ratio
- Increase in regenerator temperature
- Increase in conversion
- Increase or decrease in gasoline yield depending on over-cracking point
- Increase in C4– yield and olefins
- Increase in gasoline octane and bromine number
- Increase in cycle oil aromaticity
- Slight increase in coke yield

CO combustion

During the course of the cracking reactions in the riser, coke is formed as a by product, which gets deposited on the catalyst. This coke is burnt off in the regenerator to evolve the heat required to carry out the reactions in the riser. It is also required to retain its activity, as the coke deposition on the catalyst will prevent the oil particles from coming in contact with the active sites of the catalyst. Coke comprises of carbon and hydrogen in varying proportions. In the regenerator, the entire

carbon is converted to carbon dioxide, either directly from the carbon state or in steps where the carbon is first converted to carbon monoxide and then carbon monoxide to carbon dioxide. The hydrogen in the coke gets converted to water.

The reactions that take place in the regenerator can be summarized as given below:

$$C + O_2 \rightarrow CO_2 + \text{heat} \quad (4.1)$$

$$C + ½\, O_2 \rightarrow CO + \text{heat} \quad (4.2)$$

$$CO + ½\, O_2 \rightarrow CO_2 + \text{heat} \quad (4.3)$$

$$H_2 + ½\, O_2 \rightarrow H_2O + \text{heat} \quad (4.4)$$

Maximum heat is generated from the combustion of carbon monoxide to carbon dioxide. Flow of air to the regenerator is increased to such an extent that complete oxidation to carbon dioxide is ensured. This also confirms that the catalyst has been regenerated to the maximum possible extent thus regaining its activity. CO combustion to CO_2 is also promoted by adding additional agents such as CO promoters in the fresh catalyst being added into the system. The process of regeneration of the spent catalyst in the regenerator requires great attention because of the after effects of either excess air or less air than what is required. They are called afterburning and behind in burning, which is discussed below.

Behind in burning / afterburning

It is very important to burn off all the coke that is produced during the cracking reactions. The flow of air to the regenerator has to be enough so as to ensure that all the coke has been burnt off. This can be done by maintaining a slight excess amount of oxygen in the flue gas exiting out of the top of the regenerator. The amount of coke burnt should be equal to the amount of coke generated during the reactions. If the coke burnt is less than the coke being deposited on the catalyst, then there will be net accumulation of coke. This will result in loss of activity of the catalyst. The regenerator temperature will also start coming down slightly. The difference in temperature between the dense phase of the catalyst and the dilute phase of the catalyst or the flue gas temperature will come down as there is no more air available for further combustion of coke. The sample of catalyst, if checked periodically, will tend to get darker and darker. The material balance of the unit gets affected as a result of the lower activity of the catalyst with conversion levels coming down. This phenomenon is called behind in burning. Care should be taken not to let the

unit go behind in burning. In case the unit does go behind in burning, then the flow of air should be increased in very slow steps keeping constant watch over the regenerator temperatures. There will be a sharp rise in the temperatures leading to a corresponding decrease in the catalyst circulation rates. This will lead to further temperature rise in the regenerator, which in turn will have to be compensated by decreasing the combined feed temperature to increase catalyst circulation rates. Once all the accumulated coke in the catalyst has been confirmed as burnt off by physically checking the sample of catalyst and verifying with the expected improvement in conversion, then the unit can be brought back to the normal state. The catalyst absorbs about 70% of the heat that is generated in the regenerator during the course of burning of coke. Hence it is essential that most of the coke burning take place in the combustor zone so that the catalyst present in the dense phase can absorb the heat that is generated. In case of excessive air to the regenerator, the velocity of catalyst will increase resulting in transfer of the burning location from the dense phase to the dilute phase of catalyst. When coke burning takes place in the dilute phase then the heat that is liberated cannot be fully absorbed as there will be very less catalyst around that location. As a result the heat liberated will increase the temperatures of the cyclones and the flue gas lines leading to possible damage to the equipment.

Regenerator temperatures

Regenerator temperature is as such not a directly controlled parameter. It however gives a fair idea of the operation of the unit. The change in regenerator temperature indicates the change in the process of reaction in the riser. An increase in the regenerator temperature indicates either a heavier feedstock, i.e. more coke formation, lower catalyst circulation rate, higher operating pressures, higher combined feed temperatures, etc. The difference in temperatures within the dense phase and dilute phase of catalyst in the regenerator also gives an idea of the extent of behind in burning or afterburning.

Regenerator catalyst re-circulation

The high efficiency regenerator operation involves complete oxidation of carbon and carbon monoxide to carbon dioxide within the dense phase of catalyst. The regenerator can be divided into two sections; the lower regenerator and the upper regenerator connected by a riser through which the catalyst is transported up from the lower to the upper zone. There is also another line, which sends the catalyst from the upper regenerator section to the lower zone. The re-circulation slide valve is located on this line. This line is utilized to send back some of the hot catalyst from the upper zone to the lower zone to maintain the required minimum temperature so that complete

combustion is ensured. This is essential because if the combustion is incomplete, then the balance coke in the catalyst will start burning in the dilute phase of the catalyst in the upper zone and in the flue gas lines. The heat that will be liberated during that burning will not be absorbed fully as the density of catalyst in that area is very low. This will result in the cyclone and other hardware getting exposed to very high temperatures causing mechanical damage. This phenomenon, as explained earlier, is called afterburning. In such cases, the re-circulation slide valve is opened so that the hot catalyst flows back to the lower section of the regenerator, thereby increasing temperature, which will result in more combustion taking place and the entire C and CO gets converted to CO_2.

Catalyst circulation rate

This is also not a directly controlled parameter. It depends on the overall operation of the reactor and regeneration. The rate of catalyst circulation is dependent on the feed rate, reactor temperature, combined feed temperature and the regenerator temperature. The catalyst circulation rate is the main driver for maintaining the reactor temperature. It is also dependant on the pressure differentials across the slide valves. The opening of the regenerated catalyst slide valve gives a fair picture of the relative performance of the unit. This should be in a "floating" range and not too close or too wide open.

Catalyst to oil ratio (CTO ratio)

This is similar to catalyst circulation rate in that it is not a directly controlled parameter. This is defined as the tones per hour of catalyst circulated divided by the tones per hour of feed charge rate. This parameter is dependent on the catalyst circulation rate and is affected by the changes in the process parameters, which affect the circulation rate. An increase in the catalyst to oil ratio occurs as a result of an increase in the reactor temperature, a decrease in the regenerator temperature or a reduction in the combined feed temperature. If, for the same reactor temperature, the CTO ratio is increased, it will lead to an increase in conversion resulting in higher gas and LPG yield, more coke formation and a slight decrease in regenerator temperature. However, the rate of increase in conversion with increasing CTO ratio becomes less when high levels of conversion are reached. The relationship of kinetic conversion with CTO ratio is linear and keeps on increasing without change.

Feed quality

The feed quality itself is not a parameter that can be controlled or changed. It keeps on changing over a period of time due to the varying proportions and the quality of the individual components

like vacuum gas oil, coker gas oil, unconverted bottoms from hydrocracker unit, etc. Hence the feed sample is tested for its properties and then the appropriate process conditions are maintained to get the desired results from the unit.

Effect of reactor-regenerator variables on products

Dry gas

At a constant feed temperature and reactor temperature, the reactor energy requirement will remain the same. Some operating variables can be changed without altering the energy requirements of the reactor like regenerator temperature and feed preheat temperature. This is because the energy input is a combination of catalyst circulation rate and temperature. To maintain a constant reactor temperature, if the feed temperature or regenerator temperature is raised, then the catalyst circulation rate is reduced. Although the reactor temperature doesn't go up, the riser-mix temperature goes up because lower quantity of hotter catalyst mixing with feed. It has been accepted that dry gas yield increases with higher reactor temperatures. It has also been noted that the dry gas yield varies even at constant reactor temperatures. Whenever the riser-mix temperature increases, it has been seen that dry gas yield increases. Hence increase in regenerator temperature or feed preheat temperature also increases the dry gas yield. It goes to show that the dry gas yield is not a function of conversion but is a thermally driven process. Decreasing the reactor temperature, regenerator temperature or the feed temperature can reduce dry gas generation but its effect on the other sections and products should also be considered.

LPG

Normally, the yield of C_3s and C_4s are dependant only on conversion levels. That is to say that the yield of LPG will increase as conversion increases no matter how it is achieved, increasing reactor temperature or catalyst to oil ratio, etc. The ratio of isobutane to butylenes yields drops sharply as the reactor temperature is increased. This is because at higher reactor temperatures, higher olefins will be generated with little effect on the C4 yield. This is of relevance to estimate the amount of isobutane in feed to the alkylation unit.

Gasoline

At constant conversion levels, increasing the reactor temperature decreases gasoline yield. When the reactor temperature is increased, to hold constant conversion the C/O ratio also has to be adjusted. Hence there will be more dry gas yield and coke formation. So the liquid yield, including gasoline, will come down. Generally it is accepted that a 10% increase in conversion or a 10oC rise

in reactor temperature will increase the RON of gasoline by 1.0 number from the base octane number. As the temperatures go higher, the rate of increase in octane goes down. Since gasoline yield and gasoline octane are both dependant on reactor temperature in different ways, an optimum operating range has to be decided to maximize octane-barrels. The increase in octane due to higher reactor temperature is due to the increase in the olefin content of gasoline. The olefin content of gasoline is reflected in the bromine number. Lowering conversion level at the same reactor temperature can reduce olefins in gasoline. Gasoline octane sensitivity, defined as the difference between RONC and MONC is a function of reactor temperature only and is not affected by any change in the conversion level.

Cycle oils

Like LPG, the yield of cycle oils is also a function of conversion level only.

4.2 Implementations and simulation procedure

The FCC model comprises algebraic equations coupled with ordinary differential equations and differential algebraic equations of high order.

The set of algebraic and differential equations describing the 7 main parts of the FCCU were implemented in simulators using the Matlab differential algebraic equation solvers. Matlab ODE functions are used to solve the spatial ordinary differential equations for the riser, yielding the output variables of gas temperature at the riser exit, and the distribution of product in the stream. The spatial differential equations for the reactor riser and regenerator are solved using an Eulis discretization method in space, and then applying adoptive predictions ODE integrators (implemented in Matlab ODE solvers) to the discretized equations for the time-domain integration.

For the dynamic model, the solution in that the first step involves calculating the variables at the steady state. Once this is accomplished, these values are used to define the open loop initial conditions. The C++ programming language was used to write the code for the plant model simulator. The Matlab MEX compiler was used to compile the C-function used in the simulation. Although, source files can be compiled and linked within a Matlab executable shared library by MEX, the model was run on MATLAB SIMULINK to ensure solution efficiency. The dynamic process simulator achieves 3 key aims:

1. Exploring the dynamic behaviour of the process
2. Development and evaluation of facilitates the control schemes based on the model for the whole process unit.

3. Serves as the predictive model in the nonlinear model predictive schemes developed in this study.

4.2.1 Open loop simulations for the investigations of the dynamic behaviour of the FCCU

The major manipulated variables (MV) in this FCC unit are: fresh feed flow, recycled slurry flow, spent catalyst valve, regenerated catalyst valve, furnace fuel flow, air temperature, coke formation factor and air flow rate. A set of process outputs were investigated in this section, as shown in Table (4.1).These inputs and outputs correspond to the most frequently used manipulated and controlled outputs, corresponding to most industrial FCC units (Arbel et al., 1996; Grosdidier et al., 1993). Other manipulated variables and output variables can be added to the simulator according to specific industrial practice by implementing it in a SIMULINK block diagram, as shown in Figure (4.1).The step change analysis is shown in this chapter in Figures (4.3 to 4.8). These figures show the widely different dynamic characteristics of the variables, including inverse response and other important non-linearities with different disturbance scenarios (Table 4.1). All the disturbances reflect possible upsets that affect the normal operation of the unit, and have been selected from a practical point of view (Alsabei et al., 2008).

Table 4.1: Process input and base case operating conditions with disturbances.

Type	variable	Description	Base case operating conditions	Disturbance		%
				Step change value		
				+	-	
Manipulated variable	F_3	Flow of fresh feed to reactor riser (lb/s)	120	132	108	±10
	F_{air_c}	Air flow rate into regenerator (lb/s)	69.92	73.41	66.42	±5
				76.91	62.92	±10
	svsc	Spent catalysis valve (%)	0.3			-
	svrgc	Regenerator catalyst valve (%)	0.3			-
	F_5	Flow of fuel to furnace (lb/s)	32			-
	psif	Effective coke factor for gas-oil feed	1	1.05	0.95	±5
				1.1	0.9	±10
	F_4	Flow of slurry to reactor riser (lb/s)	3	3.6	2.4	±20
	t_{air}	Temperature of air entering regenerator (F)	416			-

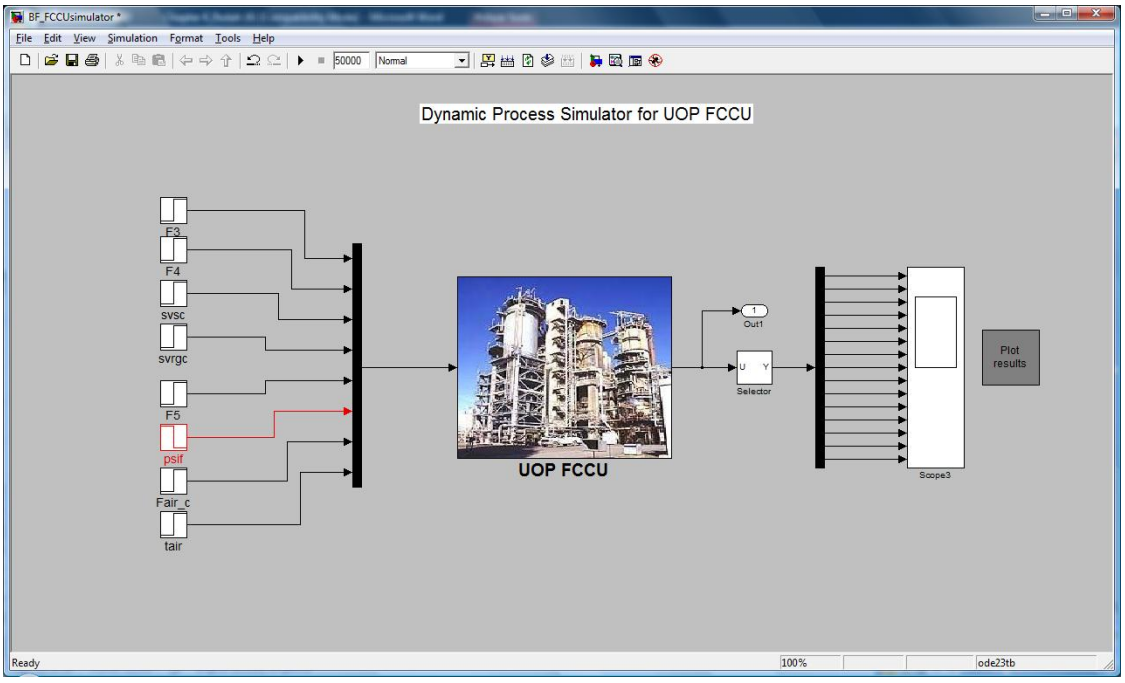

Figure 4.1: SIMULINK block diagram used for the open-loop simulation.

Sensitivity analysis for composition of the products

The objective of the simulations is to investigate whether small errors in the parameters can have consequences for products composition. In the riser section (described by the five-lump kinetic model as described in Chapter 3), a sensitivity analysis for composition of the products at different catalyst-raw material-ratios, i.e. the ratio of catalyst circulated to fresh feed (CTO), was performed. The CTO is not an independent variable, and increases with an increase in reactor temperature; moreover, it decreases with higher regenerator or combined feed temperatures. Therefore a high sensitivity of the product composition to variations in the CTO indicates that the reactor and regenerate temperatures must be tightly controlled for smooth operation of the FCCU.

Figures (4.2) illustrate that CTO has an important influence on the composition of coke, gases and diesel resulting in the riser. It also has a small influence on the gasoline yield at the outlet from the riser. The increase of the CTO leads to an increased cracking rate. The coke amount is formed very fast during the first 0.4 seconds. During the first 0.4 seconds, a rapid decrease in the rate of conversion of raw material is found due to coke formation. After 4 seconds, no net diesel is formed; it only disappears. Gas, formed from both gas oil and diesel, rapidly forms within 0.4 seconds and then starts to saturate. During the first 4 seconds, the gas is predominantly formed from gasoil, but

afterwards is taken over by diesel. This indicates that diesel is a stable fraction, which displays hardly any cracking activities.

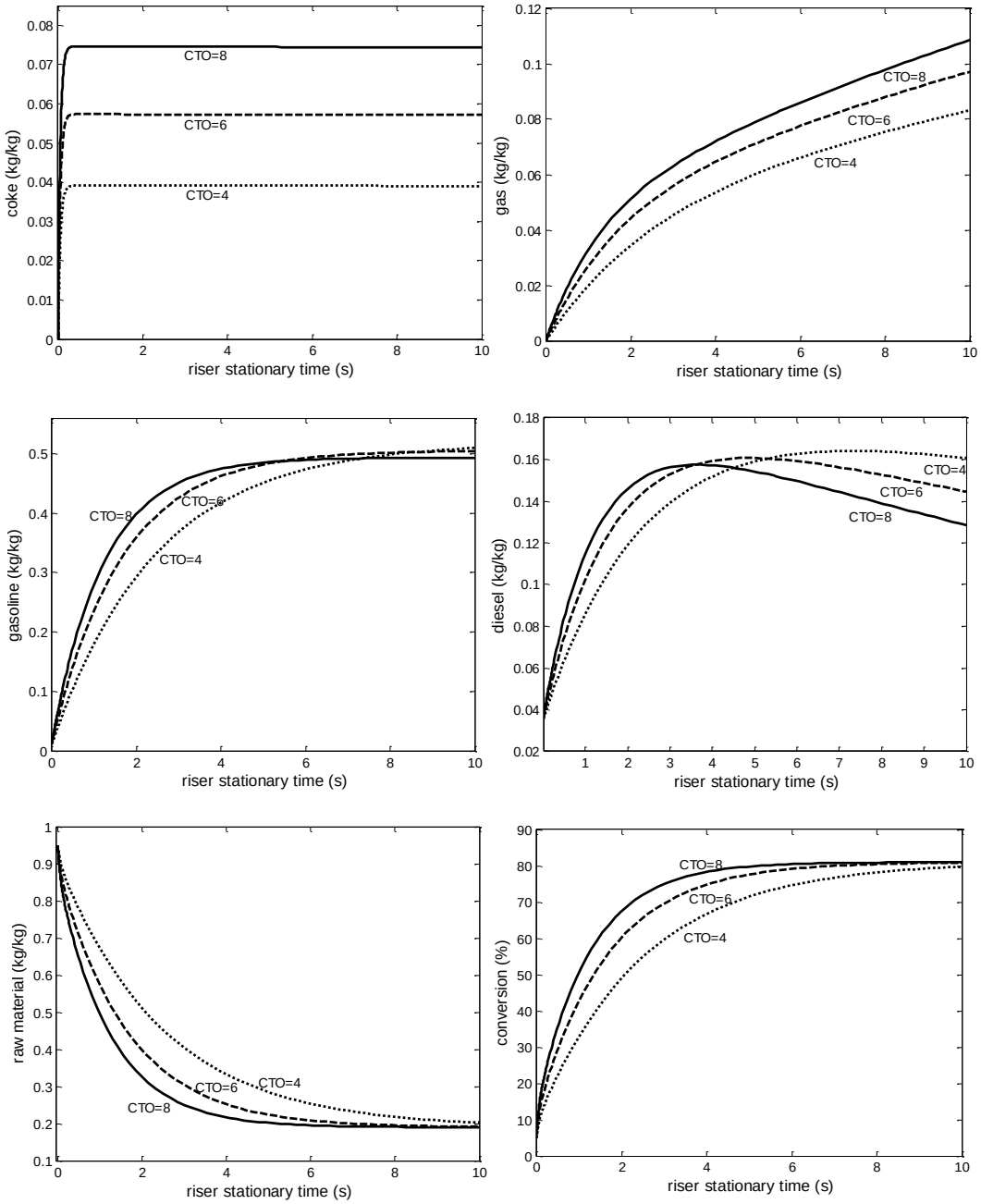

Figure 4.2: Distribution of products and raw material, and raw material conversions in the riser at different CTOs.

The fact that diesel is a fairly inactive phase is because the gasoil molecules are more reactive a result of longer side-chains attached to the polycyclic aromatic cores; diesel is less reactive due the

short side-chains, which are attached to these cores. The raw-material conversion at different CTOs is shown in Figure 4.2. The CTO has a small influence on the raw-material conversion; an increase in CTO leads to approximately the same value of conversion (~ 80%).

Analysis of the dynamic response of the FCCU to various process disturbances

Dynamic simulation of the FCC process was performed according to the simulation design shown in Table (4.1). Gas oil feed rate, air flow rate, and stem positions of the slide valves at both catalyst transport lines were chosen as simulation variables to whose changes the dynamic responses are demonstrated. Each simulation run started from the steady state corresponding to the base case operating conditions, and the subsequent transient response was obtained as each simulation variable went through a series of step changes shown in Table (4.1).

Change in fresh feed rate (F_3)

Disturbance could appear due to the raw-material rate changes. Figure (4.3) shows that a 10% increase in the fresh feed rate determines the decrease in the regenerator temperature, and also in the reactor, after a peak.

Figure (4.3) shows the dynamic responses to the changes in fresh feed rate. After the fresh feed rate is increased by10% at time equal to 1.5 h, the reactor temperature drops because of an increase in heat consumption to vaporise the additional amount of fresh feed. The lowered riser temperature (T_r) results in a considerable decrease in feed conversion, while the increased feed rate leads to a sharp rise in coke on spent catalyst (C_{sc}), and subsequently on regenerated catalyst (C_{rgc}). The increased feed rate also raises the density of hydrocarbon gases in the reactor, and so there is a jump in gas pressure, as well as in the pressure at the reactor (not shown). This jump will trigger a jump in spent catalyst flow rate, but has an opposite effect on regenerated catalyst flow rate. Therefore, the catalyst holdup in the reactor steadily decreases, until a new steady state is reached, where the two catalyst circulation rates balance each other. Regenerator temperatures (T_{reg}) start to decrease due to increased spent catalyst inflow from the reactor. Since the fixed air flow does not supply enough oxygen to burn of the increased coke in the dense bed nor to sustain after-burning reactions in the freeboard, CO concentration (cCO_{sg}) in the stack gas steadily rises. The oxygen deficiency in the regenerator also leads to no further rises in the temperature at the new steady state.

A 10% step decrease in the fresh feed rate at 1.5 h causes the system to move in the opposite direction to the case of the 10% step increase, but the detailed responses show quite different aspects due to process nonlinearity. The feed conversion increases due to increased catalyst-to-oil ratio in the riser as well as better regeneration of catalyst in the regenerator. Contrary to the oxygen

deficiency encountered before, oxygen surplus prevails throughout the regenerator, because of the decreased spent catalyst inflow from the reactor. This causes a rise in the regenerator temperature due to after-burning of CO, and a consequent drop in the CO concentration (cCO_{sg}) of stack gas. It was found in the simulations described above that the step changes in fresh feed rate immediately alter the reactor pressure, which subsequently triggers a series of changes in the process dynamics.

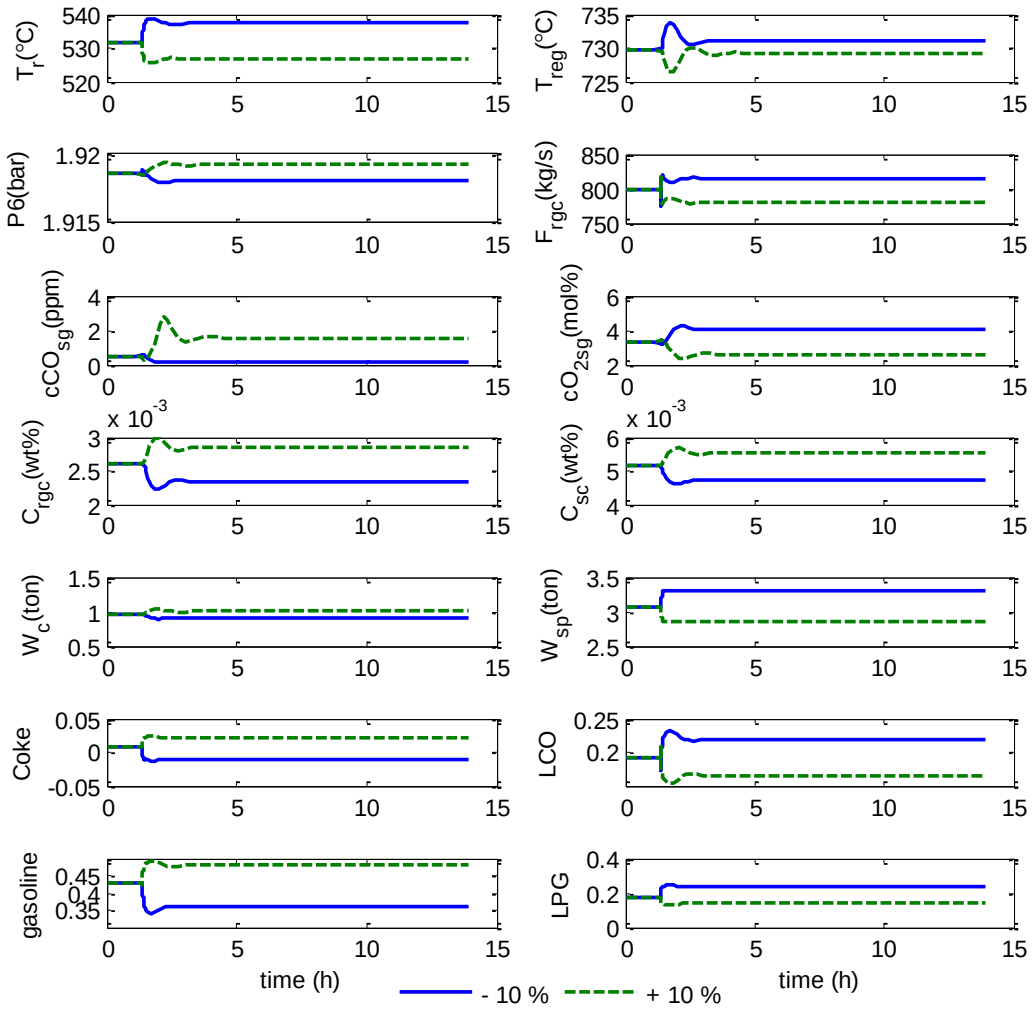

Figure 4.3: Simulation of FCCU dynamic response in the presence of step change in flow fresh feed disturbance (F_3 = ±10% increase at t = 1.5 h).

Change in air flow rate (F_{air_c})

The air flow rate is the most important parameter in the regenerator, and can vastly affect the operation of the unit. Figure (4.4) shows the dynamic responses to the changes in the air flow rate

to the regenerator. A 5% step increase in air flow causes a sharp increase in the regenerator pressure (P_6), as well as in the regenerated catalyst flow rate (f_{rgc}) to the riser bottom. On the other hand, the spent catalyst flow rate (not shown) has inverse response behaviour of initial decrease followed by ultimate increase. This behaviour can be explained by a steady increase in the reactor pressure due to increasing static pressure exerted by the rising catalyst holdup in the reactor. The increased air flow rate also accelerates coke burning, and thus raises temperature in every part of the unit and reduces the CO concentration (cCO_{sg}) in the stack gas. It also causes the coke concentrations on both spent and regenerated catalyst to steadily drop to their respective steady state values. The conversion of feed is increased by the elevated riser temperature and cleaner regenerated catalyst.

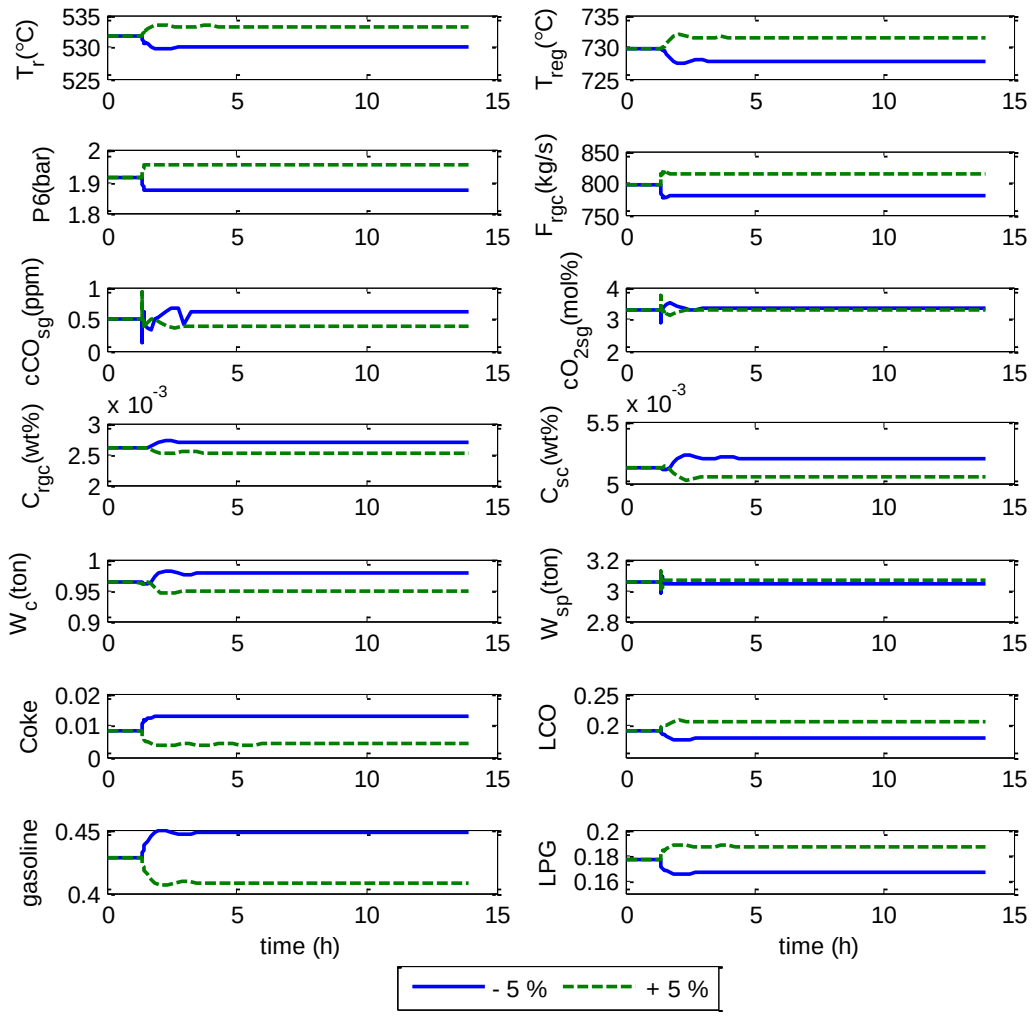

Figure 4.4: Simulation of FCCU dynamic response in the presence of step change in air flow rate disturbance (F_{air_c} = ± 5% decrease at t = 1.5 h).

A 5% step decrease in the air flow rate at time equal to 1.5 h brings about the state of oxygen deficiency in the regenerator. A large amount of coke cannot be burnt, resulting in gradual accumulation on catalyst surfaces in both vessels over a long time. Such a long response time is characteristics of the composition dynamics in the regenerator that has large mass and thermal holdups and strong interactions with the reactor. *CO* concentration (cCO_{sg}) also shows a considerable increase, because of poor afterburning reactions in the regenerator. This oxygen deficiency lowers the temperatures of both vessels as well as the conversions, but gasoline yield is significantly increased.

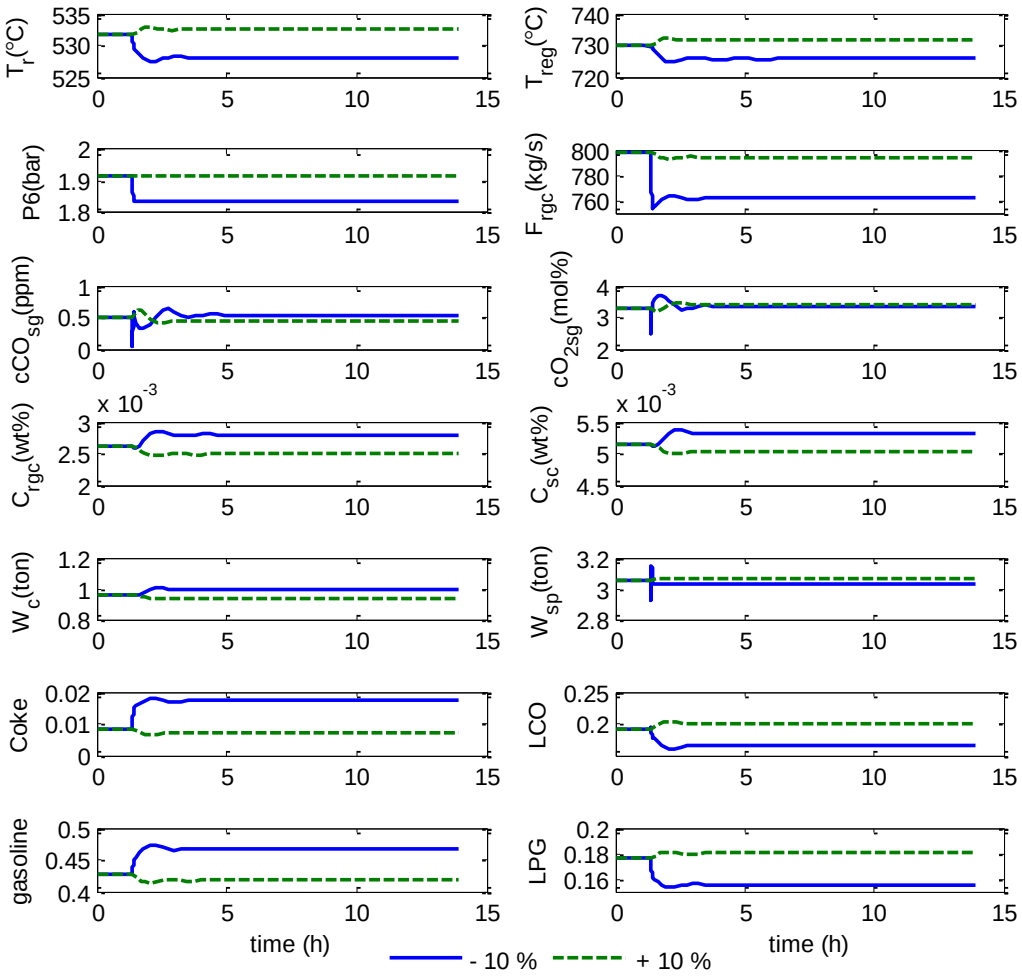

Figure 4.5: Simulation of FCCU dynamic response in the presence of step change in air flow rate disturbance (F_{air_c} = ± 10% decrease at t = 1.5 h).

Figure (4.5) shows the dynamic responses to the changes in the air flow rate to the regenerator. A 10% step increase in air flow causes an effect on air blower efficiency, because of its limitations. This can be clearly noted as there are no significant changes in the variables; the conversion of feed is also affected.

A 10% step decrease in the air flow rate at time equal to 1.5 h resulted in similar behaviour as seen for 5% step degrees as shown in figure (4.4).

Change in coke formation factor (Ψ_f)

Heat is required to make the cracking reaction work and achieve satisfactory conversion. The quality of the FCC feedstock impacts the concentration of coke on the catalyst entering the regenerator. Coke formation is a necessary by product of the FCC operation, the heat released from burning coke in the regenerator supplies the heat for the reaction.

Figure (4.6) shows the dynamic responses to the (5%) increase in Ψ_f, fresh feed coke formation factor, at time equal to 1.5 h.

This simulation run with a 5% increase represents a realistic unmeasured disturbance to the feed composition. The increase in Ψ_f affects the cracking reactions, and coke is deposited on the catalyst, reducing catalyst activity. This led to a rapid increase in coke deposition in the riser and concentration of coke on spent catalyst (C_{sc}). This additional coke is transported to the regenerator on the spent catalyst resulting in higher combustion rates in the regenerator, and thus an increase in regenerator temperature (T_{reg}). However, the initial increase in combustion rates is insufficient to burn off all additional coke arriving from the reactor, and so the concentration of carbon on regenerated catalyst (C_{rgc}) increases. Consumption of oxygen increases, while total air flow rate to the regenerator is held constant by the total air controller, so excess oxygen concentration in the stack gas ($cO_{2,sg}$) decreases and stack carbon monoxide concentration ($cCO_{,sg}$) peaks and begins to decline. As regenerator temperature increases, combustion rates increase and more of the coke transported from the reactor is consumed. The concentration of carbon on regenerated catalyst peaks and begins to decline. It eventually reaches steady state at a level only slightly higher than the initial concentration. Taking into account the fact that the heat generated by CO formation is about three times less than CO_2 heat formation, the global effect is to reduce the net heat contribution in the regenerator with the consequence that the temperature decreases in the last part of the simulation.

During regeneration, the coke level on the catalyst is typically reduced (C_{rgc}). The carbon also decreases during the process (W_c). Moreover, the catalyst inventory stand pipe entering the

regenerator (W_{sp}) increases, and the regenerator pressure (P_6) is also increased. The pressure has little effect on conversion, so it is not adjusted to change product yields, but is important for catalyst circulation phenomena.

From the regenerator, the catalyst flows down through a transfer line commonly referred to as a standpipe, where (f_{rgc}) is the catalyst circulation rate. The amount of carbon that remains on the regenerated catalyst is an operating variable, and more carbon on the regenerated catalyst results in less conversion.

Increasingly hotter regenerated catalyst is transported back to the riser, affecting its energy balance. As riser temperature (T_r) increases, wet gas production increases due to higher cracking rates.

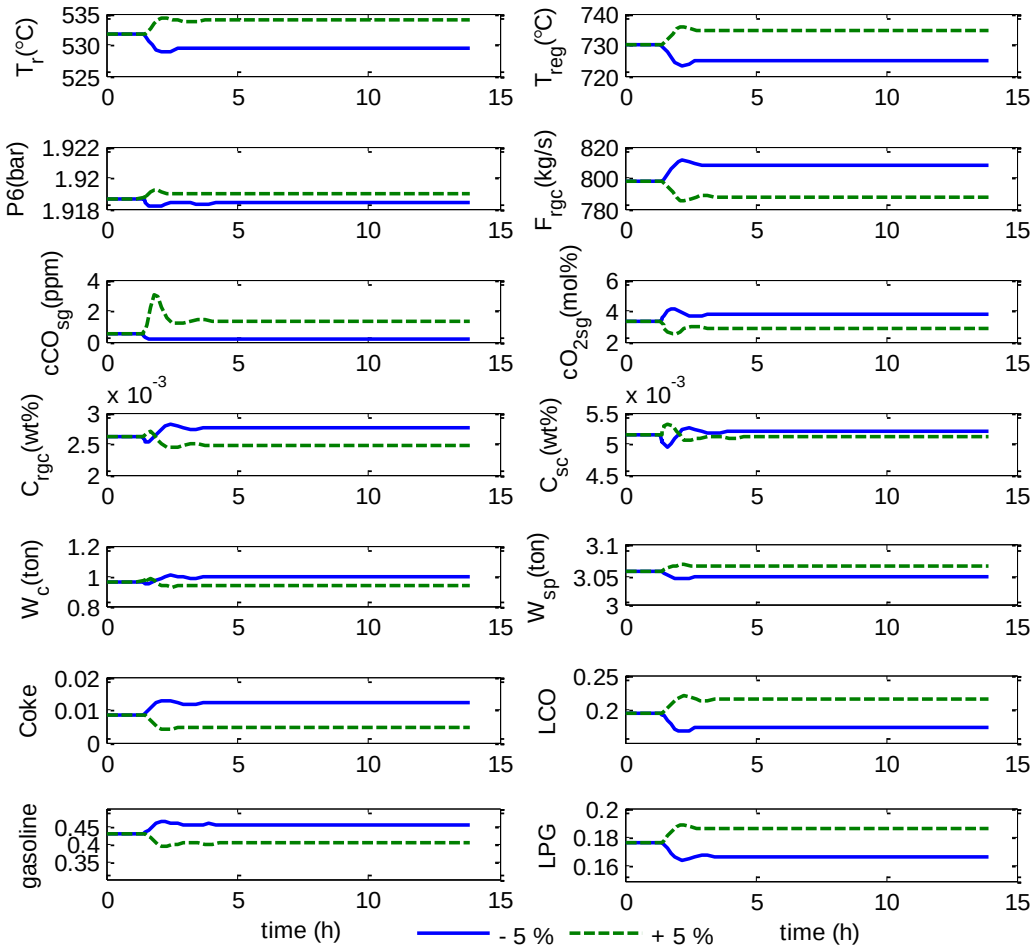

Figure 4.6: Simulation of FCCU dynamic response in the presence of step change in fresh feed coke formation factor disturbance (Ψ_f = ±5% decrease at t = 1.5 h).

With this magnitude of disturbance, the carbon on the regenerated catalyst can be reduced by increasing the regenerator temperature. It is important, however, to keep a constant percentage of carbon on the regenerated catalyst, because carbon yields increase in the reactor when the regeneration is incomplete. If this additional carbon is not burned off in the regenerator, the carbon yields will again increase when the catalyst passes through the reactor. This can lead to carbon runaway, i.e. more carbon is produced than burned off (Sadeghbeigi, 2000; Bollas et al. 2007).

The composition of the products and raw material along the riser is also influenced in both either a positive or negative way by this disturbance; the increase in the coking rate leads to an increase in the flow of the regenerated catalyst, which then increases the catalyst-to-oil ratio, is not an independent variable. It increases with an increase in reactor temperature and decreases with higher regenerator temperature; this then leads to a decrease in gasoline and coke yield, but an increase in LCO and LPG yield. The disturbance would be considered positive, if the objective is to have more LCO or LPG than gasoline, and negative if gasoline is the desired product.

A 5% step decrease in coke formation factor, Ψ_f, at 1.5 h causes the system to move in the opposite direction to the case of the 5% step increase, but the detailed responses show quite different aspects due to process non-linearity with inverse responses.

The dynamic responses to the disturbance test of (10%) increase in Ψ_f **(**fresh feed coke formation factor) at time equal to 1.5 h, is shown in Figures (4.7). These figures show the widely different dynamic characteristic of the variables, including inverse response and other important non-linearities.

However, it can be noted in the scenario of (10%) decrease in coke formation factor, Ψ_f, which the gasoline products increase hugely. This determines two facts, in that the disturbance could be a positive sign, and that feed quality affects the gasoline production.

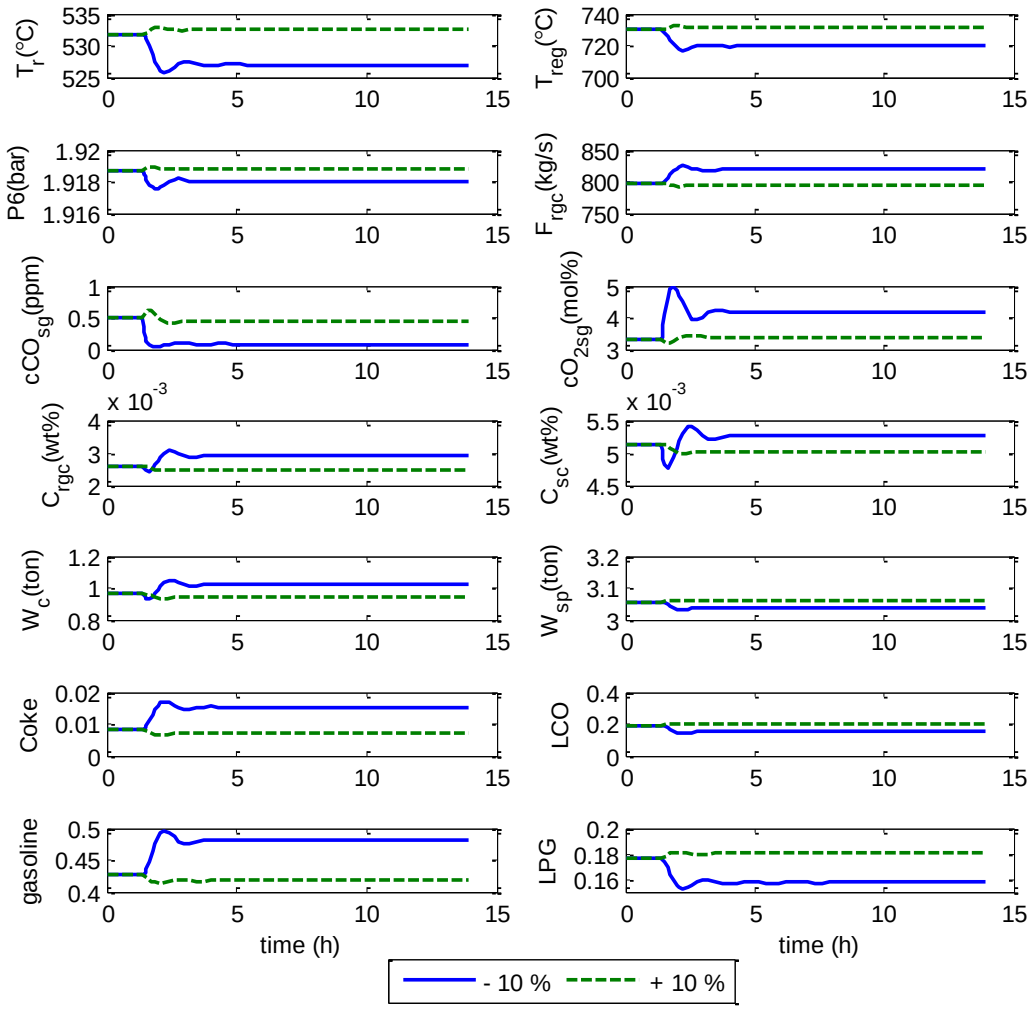

Figure 4.7: Simulation of FCCU dynamic response in the presence of step change in fresh feed coke formation factor disturbance (Ψ_f = ±10% decrease at t = 1.5 h).

Change in slurry recycle rate (F_4)

Dynamic responses are shown in Figure (4.8). Slurry recycling could appear as a result of change in the raw-material fresh feed rate, or because of changes in the valve position on the slurry circulation line. Heavier feeds than gas oil result in deposits of greater quantities of coke upon cracking. A given change, i.e.(20% increase in flow rate of slurry at time equal to 1.5 h, is expected to have a greater effect on system response than an equal size change in gas oil feed.

As demonstrated in this run, small changes in slurry flow rate produce significant temperature responses, and therefore slurry flow rate is a useful manipulated variable. The reduction in slurry flow rate causes an immediate and rapid drop in the concentration of coke on spent catalyst (C_{sc}). With lower C_{sc}, less coke arrives at the regenerator on spent catalyst, reducing the rate of combustion reactions occurring in the bed. Regenerator temperature (T_{reg}) drops slightly, excess oxygen ($cO_{2,sg}$) rises and concentration of carbon monoxide in the stack gas ($cCO_{,sg}$) falls. The flow rate of regenerated catalyst (F_{rgc}) falls a small amount, for reasons described previously; this leads to increases of carbon inventory in the regenerator (W_c) and inventory of catalyst in regenerator stand pipes (W_{sp}). With falling regenerator bed temperature and flow rate of regenerated catalyst, reactor riser temperature (T_r) also increases after initial falls caused by the sudden drop in slurry flow rate.

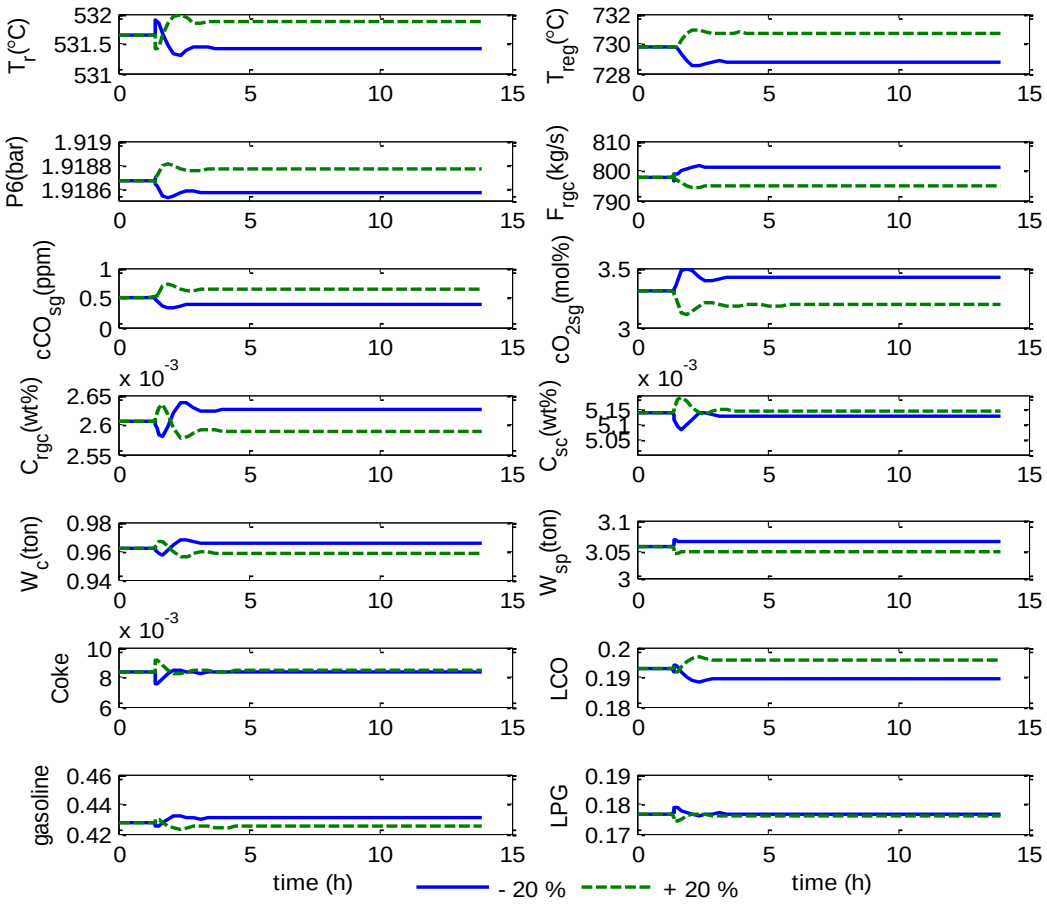

Figure 4.8: Simulation of FCCU dynamic response in the presence of step change in slurry flow recycle rate disturbance (F_4 = ± 20% decrease at t = 1.5 h).

Disturbance in slurry recycle flow rate leads to a decrease in the flow of the regenerated catalyst, which decreases the catalyst-to-oil ratio, then leading to a small increase in LCO yield, but decreases gasoline or LPG yield.

In figure (4.8), it can clearly be observed that a 20% decrease in slurry recycle flow rate, F_4, has an opposite effect on all the other variables. In addition, the same disturbance caused nonlinear behaviour and inverse response for most of the variables.

4.3 Conclusions

Cracking reactions are endothermic, and therefore, to achieve higher productivity, the reactor should be operated at as high a temperature as possible. Assuring the regeneration of the catalyst (the burning of the deposited coke), the regenerator, as with the reactor, must be operated as close as possible to its metallurgical limit in terms of temperature. Restrictions concerning the concentration of carbon monoxide in the stack gas are very important from an environmental point of view. A dynamic simulator was developed, which implemented the detailed dynamic model for an FCC process and the model solver (these were presented in chapter 3). The correlations were developed for the thermodynamic properties and transport parameters contained in the model either by literature survey, or by nonlinear regression of literature data. The steady-state behaviour was investigated and the results showed good match with those in the literature, and real plant data.

All the investigated disturbances showed considerable influence on the products composition. Taking into account the very high volume production of an industrial FCCU, these disturbances can have a significant economic impact. The fresh feed coke formation factor is one the most important disturbances analysed. It shows significant effect on the process variables. Moreover, the objective regarding the control of the unit has to consider not only to improve productivity by increasing the reaction temperature, but also to assure that the operation of the unit is environmentally safe, by keeping the concentration of *CO* in the stack gas below a certain limit.

The dynamic simulations show the nonlinear and multivariable behaviour of the FCC process. The simulation results also show that the FCC model is sufficiently complex to capture the major dynamic effects that occur in an actual unit. The process outputs exhibited a series of complex dynamic behaviours, such as inverse response behaviour, variations different time scales, impulse response, indicating difficulties in controller designs.

The model offers the possibility of investigating the way that advanced control strategies can be implemented, while also ensuring that the operation of the unit is environmentally safe.

CHAPTER 5
ADVANCED PID CONTROL OF THE FCCU PROCESS

5.1 Introduction

Over the course of six decades, significant developments have been achieved in catalytic cracking, which is a key petroleum refining process. As a result, the fluid catalytic cracking unit (FCCU) has been the test bed for many new control schemes, and both the industry and academics have worked steadily to develop and implement efficient algorithms for this purpose. The FCC process presents many challenges due to its (i) complex and poorly understood hydrodynamics, (ii) complicated reaction kinetics for cracking and coke burning, (iii) significant reactor/regenerator interactions, and (iv) multiple constraints in operation (Elamurugan and Kumar, 2010). Moreover, the process is characterised by behaviour in the steady and dynamic states that is highly nonlinear, which results in many potential states and input levels, etc. Prior to the introduction of zeolite catalysts, stabilising and maintaining the process was the key control objective. However, with the use of zeolite catalysts attention focused on raising production output, and coping with heavy feedstocks. As a desirable product, reformulated gasoline has added the challenge of controlling the product chemistry, which is a complicated undertaking as those variables that can be manipulated are very few compared to the large number of actual process variables (Han et al., 2001).

5.2 Controllability analysis and control structure selection for the FCCU

5.2.1 General considerations for the control of the FCCU

In general, the key objective of controlling the FCCU is to keep the process running within acceptable safety, environmental, and staff workload limits, etc, while simultaneously guaranteeing economic plant operation. Typically, a conventional hierarchical control system satisfies these criteria, where each level performs a specific task or tasks (see Figure 5.1). In the schematic not all the logic control functions are presented, e.g. startup/shutdown and safety systems, as these do not feature in normal plant operation. There are various ways for the concept to be implemented in a control system, but more importantly the idea of distributing control to the different levels is key.

This chapter discusses the regulatory control level, which is the lowest in the hierarchy, and solely tasked with maintaining smooth running of the process. In contrast, economic optimisation is handled by higher levels in the hierarchy. Typically, such a control system is both decentralised and cascaded, where specific measurements for set points are acquired in the implementation of the former, and then set point values commanded by the upper levels or the human operator, in the latter. Cascaded loops may also be found within the regulatory control level, in that a valve position is cascaded into a measurement of flow, in which case, flow is a manipulated variable not the position of the valve. Henceforth, "regulatory control system" and "lower-level control system" are used interchangeably.

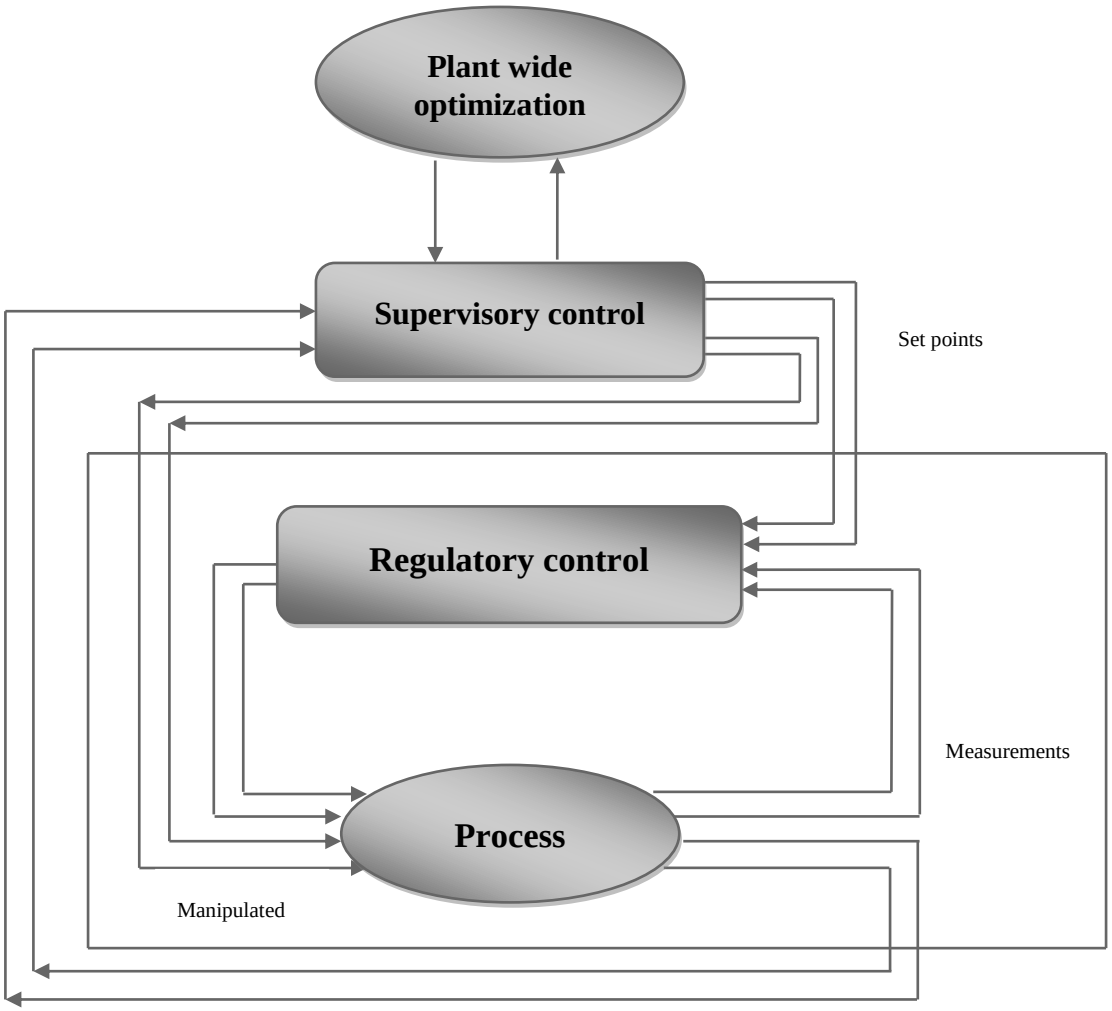

Figure 5.1: Hierarchical control system.

Within this control hierarchy, an **intermediate** or supervisory level may hold a multivariable, process model-based system that computes optimised plant operating parameters according to a specific objective. This supervisory level is characterised by the capability to handle constrained manipulated and controlled variables, especially in avoiding saturation of the manipulated variables. This preventative action may require coordination between control loops through assigning set values, or perhaps directly introducing more degrees of freedom.

The control hierarchy upper or **top level** is concerned with optimisation across the entire process plant, which is typically in the steady state and taking place regularly off-line. Even though this top level is where the most significant economic gains are realised, proper functioning of the lower levels is necessary for this to happen. This fact is often not properly understood.

5.2.2 Objectives for regulatory control

A control system regulating process plant should satisfy several criteria or objectives:

1. Control quality needs to be at a level where operating personnel are able to maintain the plant operating in safety, without need for action on part of the control system higher hierarchical levels. This enables simple recovery from failures, where no expensive backup is needed for the higher levels.
2. The system needs to be easily understood and tuned, which is usually solved by using control loops that are simple and decentralised. However, where significant interactions exist, multivariable control may be introduced.
3. At the top level, the system should as far as practicable use simple models, in order to enhance reliability and reduce cost in formulating and implementing a complex dynamic plant model, which will have a computation overhead applied at the top level. This is resolved by ensuring that the regulatory control level is at the lower level of the system hierarchy, which has the advantage of minimising model uncertainty and facilitating local linearization.
4. The system should allow the upper levels in the hierarchy to have longer sampling times, which would lessen the computational burden at those levels. Distinct sampling times should be used, with faster times at the lower levels, and so higher levels will not wait for responses from the lower levels.

Therefore, based on the criteria or objectives above, a set of four further objectives for the regulatory control may be formulated:

5. Rapid control should be possible, particularly in the case of some variables.
6. The control system should operate the process closely following the set values commanded by the hierarchy top levels. These set values sent to the bottom level represent manipulated variables, where the aim is to move the process to these new values directly with minimum interaction, avoiding the need to map interactions and process dynamics in a model residing at the top levels.
7. The system should effectively reject local perturbations, which is an extension of the second objective, and aims at maintaining the controlled parameters at the set points. The system needs to include extra degrees of freedom or additional manipulated variables (unused) that are directly changed by the top levels in the system hierarchy.
8. The system must be robust, i.e. it should not be unnecessarily limited in performance due to, for example, significant sensitivity to perturbations, or have RGA elements. This remaining control problem is that which is seen by the top level, and contains manipulated inputs, both used and unused, as well as lower level set values. The unnecessary performance limitations refer those which are not part of the original control problem formulation in the absence of the control system lower level (Hovd and Skogestad, 1993).

The first three objectives (5,6,7) above relating to rapid control, set point following, and perturbation rejection are discussed here, and relate to system controllability at the lower level. The criterion of simplicity is satisfied by the system lower level being completely decentralised.

5.2.3 Control structure selection for the FCCU using RGA

The criteria or objectives presented in the previous section are satisfied primarily by choosing the appropriate control strategy or structure, and then deciding the following:

- Outputs *y*: the regulatory system controlled variables, both primary and secondary, or control objectives, are chosen. Primary outputs can normally be chosen easily, as they represent key process variables, or those needed to achieve a control objective. Such variables may need rapid control, as previously discussed in the system objectives (5), and include liquid levels, and specific pressures and temperatures to be maintained within strict limits. On the other hand, secondary outputs are variables, which can normally be measured

easily, but are not essential to control. They are chosen to satisfy some of the objectives (1, 2, and 4) discussed previously. Such variables are usually pressures and temperatures at specific points in the process plant. Hence, the choice of regulatory control system output variables is closely linked to the problem of measurement choices.

- Inputs ***u***: regulatory control system manipulated variables are chosen. The chosen inputs represent a subset of the whole range of manipulated inputs, while any "unused" variables represent manipulated inputs that can be used ether by the top control hierarchy, or the plant operating personnel.
- Pairing: the controlled and manipulated variables selected are paired to achieve decentralised control. Such pairing will affect the nature of system interactions and disturbances. Moreover, in this decentralized control system, the tolerance to failure in one or many loops is also determined by pairing.

Selection of the outputs

Generally several variables are controlled in an FCCU. However, in this work controlling two or three variables at the regulatory level will be considered, which represent the most important output parameters and also exemplify the difficulties of the multivariable controller design for interacting systems. These parameters are: T_r, T_{reg}, and $cO_{2,sg}$ (Grosdidier et al., 1993). The justification for trying to control these three variables is as follows:

The product distribution is determined by the reaction conditions inside the riser, which are therefore very important for the economic performance of the FCC process. There is then an incentive to control *both* T_r and T_{reg} which are directly related to the riser outlet and inlet temperature, respectively. A secondary controlled variable is not necessarily less important than a primary controlled variable. For example, although T_r is classified as a secondary controlled variable because it in itself is not very interesting, the importance of T_r as a controlled variable comes from the close connection between T_r and conversion. The need to avoid afterburning should be obvious and makes it reasonable to control directly $cO_{2,sg}$.

Based on this discussion, the primary controlled variables considered in this work is the $cO_{2,sg}$., whereas the secondary variables are T_r and T_{reg}, for which measurements are generally available.

Independent variables (manipulating inputs and disturbances)

The following nine independent variables were considered:

svrgc = regenerated catalyst slide valve position.

svsc = the spent catalyst slide valve position.

F_{air_c} = flow rate of air to the regenerator

F_5 = furnace fuel flow rate

F_3 = fresh feed gas oil flow rate

F_4 = slurry recycle flow rate

V_{14}= stack gas valve

t_{air} = air temperature

Ψ_f = feed oil composition; here represented by the coke production rate factor

The feed oil composition may be adjusted by changing the ratio between recycled and fresh feed. There are actually several additional manipulating variables, but we have assumed that these are already used by the regulatory control level to control holdups and pressure. These variables include:

F_{sc} = spent catalyst flow rate

F_{fg} = flue gas flow rate

W_{wg} = wet gas compressor throughput, as the wet gas compressor is situated downstream of the distillation column receiving the reaction products.

F_{sc} is used to control the catalyst holdup in the separator, whereas F_3 is used to control the regenerator pressure P_6. W_{wg} indirectly controls the separator pressure P_4. In practice the pressures P_6 and P_4 may have to be adjusted when the catalyst slide valve position *svsc* is changed, in order to avoid reversal of the catalyst flow *(F_{sc})*.

All the nine independent variables above may be used as manipulating variables *(u's)* for control, but in most cases we will only use two: the regenerated catalyst flow rate, F_{rgc} and the air flow rate F_{air_c} .The remaining independent variables may then be regarded as *disturbances* (*d*'s) in the regulatory control system. The variables Ψ_f , F_5, F_4 and F_3 are all related to the oil feed. The

variable Ψ_f *is* the coke production rate factor and depends on the feed composition. Immediately downstream of the FCC there is a distillation column which separates the products from the cracking reactions. The heavy fraction from the distillation column, "slurry," has a large coke producing tendency. The coke production rate factor can therefore be changed indirectly by changing the amount of slurry, which is recycled to the riser. The air temperature t_{air} is generally a disturbance since there is usually no air preheater in the system.

Consideration of typical operational constraints for the FCCU

The constraints that apply to plant operation must be carefully considered in making choices regarding the manipulated input and controlled output variables. For the FCC, one or more constraints determine the optimal operating point, and so the preferred control structure is the one that operates the plant nearest to these constraints. The plant optimal operating point will vary according to the properties of the feedstock, and the product range aimed for, which obviously influences the relative importance of the different constraints. This encourages the development of a different control structure for each optimal operating state. Yet, it may not be practical to formulate a different control structure for different operating conditions. Control constraints that are commonly encountered, may include:

- Flue gas minimum oxygen concentration *($cO_{2,sg}$)*: The concentration of oxygen in flue gas needs to be minimum in that complete combustion will have taken place previously within the dense regenerator bed, where *CO* is converted into CO_2 (*complete combustion mode*). This is an important constraint that ensures that no afterburning takes place, as there is insufficient oxygen in the flue gas.
- Wet gas compressor maximum capacity: The FCC unit wet gas compressor compresses the output products ready to be taken for gas treatment downstream.
- Air blower maximum capacity *(F_T)*: The blower capacity needs to be at the maximum required to supply air for combustion within the regenerator.

Implications for Regulatory Control

For the purpose of operating the plant close to the constraints, it is worthwhile to choose the constrained outputs (measurements) to be controlled by the regulatory system. Therefore, in the complete combustion mode, flue gas oxygen concentration, $cO_{2,sg}$, may be adopted as a controlled variable.

At the same time, in the control system, it is wise to avoid those manipulated inputs that may cause constraints to be easily reached. For example, wet gas production is affected significantly by feed flow rate F_3, and so in a process state nearing the wet gas compressor constraint, feed flow rate F_3, should not be adopted as a manipulated variable. A similar scenario involves the air flow rate F_{air_c} and air blower capacity constraint. However, a number of workers (Pohlenz, 1963; Hicks et al., 1966) have proposed air flow rate, F_{air_c}, as a manipulated variable. Therefore, the control system should prevent the process from violating the air blower capacity constraint. This may be achieved, for example, by modifying the feedstock or the conditions of reaction leading to less coke formation. FCC constraints were treated in detail by Grosdidier et al. (1993), of which a key selection is presented in Table 5.1.

Table 5.1: Operating constraints and their relative importance (0: low; 10: high).

No.	Process variable	Notation	Constraints	Importance
1.	Temperature of reactor riser	T_r	T_r < 537 °C	10
2.	Temperature of regenerator bed	T_{reg}	720 °C < T_{reg} < 745 °C	10
3.	Concentration of O_2 in stack gas	$cO_{2,sg}$	$cO_{2,sg}$ > 2 %	9
4.	Concentration of CO in stack gas	$cCO_{,sg}$	$cCO_{,sg}$ > 350 ppm	9.5
5.	Differential pressure between regenerator and reactor	*dprr*	0.15 bar < *dprr* < 0.2 bar	8

Controller and manipulated variable pairing

The complexity of manipulated and controlled variable pairing is such that systematic mathematical analysis is needed to account for more than physical or process parameters. A well-configured control system would be capable of keeping the process within specified constraints, and rapidly restore it to its nominal operating state. In the context of choosing the appropriate control structure, related to multiple single-loop controllers (see Chapter 2), and determining interaction among the variables, the relative gain array (RGA) and variations of it (Wolff et al., 1992; Skogestad and Wolff, 1992) is commonly applied. As RGA is a linear approach, the process model equations, which are non-linear, need to be linearised for different points of operation, as illustrated below. The FCC unit model may be considered to be composed of vector differential-algebraic-equations (DAEs), as follows:

$$\frac{dx}{dt} = f(x,u) \tag{5.1}$$

$$y = y(x,u) \tag{5.2}$$

with state (x), input (u) and output (y) vectors expressed by

$$x = \left[x_1,...,x_n\right] \tag{5.3}$$

$$u = \left[u_1,...,u_m\right] \tag{5.4}$$

$$y = \left[y_1,...,y_k\right] \tag{5.5}$$

Linearizing the system in the operating point (x_o, u_o) gives the following linear model

$$\frac{dx}{dt} = Ax + Bu \tag{5.6}$$

$$y = Cx + Du \tag{5.7}$$

$$A = \left[\frac{\partial f}{\partial x}\right]_{xo,uo} \quad C = \left[\frac{\partial y}{\partial x}\right]_{yo,uo}$$

$$B = \left[\frac{\partial f}{\partial u}\right]_{xo,uo} \quad D = \left[\frac{\partial y}{\partial u}\right]_{yo,uo} \tag{5.8}$$

The RGA matrix for a square (n x n) plant can be calculated using the following formula:

$$RGA = \left(-C \cdot A^{-1} \cdot B + D\right) \times \left(\left(-C \cdot A^{-1} \cdot B + D\right)^{-1}\right)^{T} \tag{5.9}$$

where the × symbol is the Hadamard product (element by element product) and A, B, C, and D are coefficient matrixes from the linear state space model.

For independent control loops, pairs where the input and output relative gain is close to 1, are the best. In contrast, pairs that exhibit relative gains that are negative in the steady state must be avoided (Bristol, 1966). Such a pairing will cause whole system or single loop instability in an integral control scheme or on removal of that specific loop (Grosdidier et al., 1985). Furthermore, process plants that exhibit high values of RGA, especially at high frequency, suffer inherently poor controllability, regardless of the control system used (Skogestad and Morari, 1987b). Moreover,

implementing decentralised control, where input and output pairs have low RGA values (compared to 1) in the bandwidth region, signals potential problems in stability (Hovd and Skogestad, 1992a,b).

Table 5.2 shows different control structures which were considered for control implementation From the RGA analysis the best results were obtained with control schemes 1 and 2 (Table 5.2) for which RGA matrix values close to 1 were obtained. Table 5.3 gives a suggested pairing for scheme 1 T_r-F_5, T_{reg}-*svsc*. In Table 5.4 the suggested pairing for scheme 2 T_r-F_5, T_{reg}-*svsc*, $cO_{2,sg}$-V_{14} is given. The results obtained with the other schemes from Table 5.4 were not conclusive since there are small and negative values, indicating that those configurations potentially would not work. These points out strong couplings between some of the control loops especially when three or more control loops are considered.

Table 5.2: Different control structure schemes for PID controller.

Control scheme	**1**	**2**	**3**	**4**	**5**
	(2x2)	**(3x3)**	(4x4)	(5x5)	(6x6)
Manipulated inputs	***F_5*, *svsc***	***F_5*, *svsc*, *V_{14}***	F_3, F_4, V_B, V_{11}	F_3, *svsc*, F_5, V_{14}, *svrgc*	F_3, F_4, *svrgc*, *svsc*, L_T,V_B
Controlled variables	***T_r*, *T_{reg}***	***T_r*, *T_{reg}*, *$cO_{2,sg}$***	T_r, P_6, $X_{(1)}$, $X_{(82)}$	T_r, T_{reg}, P_5, T_3, P_6	$X_{(1)}$, $X_{(82)}$, W_r, T_r, T_{reg}, W_{reg}

Table 5.3: RGA matrix of a sample 2X2 control scheme.

Controlled variable	**Manipulated Variables**	
	F_5	***svsc***
T_r	*1*	*0*
T_{reg}	*0*	*1*

Table 5.4: RGA matrix of a sample 3x3 control scheme.

Controlled variable	Manipulated Variables		
	F_5	*svsc*	V_{14}
T_r	*1*	*-0*	*0*
T_{reg}	*-0*	*1.1297*	*-0.1297*
$cO_{2,sg}$	*0*	*-0.1297*	*1.1297*

5.3 Advanced PID control of the FCCU

5.3.1 Design of the PID control algorithm

In the domain of controlling FCC units and achieving specific objectives, many approaches quite advanced techniques. A block diagram of a PID controller is presented in Figure 5.2, which illustrates this generic feedback controller, commonly used in industrial and process control applications. In this controller, the values of the measured process variable and the commanded set value are compared revealing a difference termed the "error", which the controller aims to reduce to a minimum through appropriate control inputs. The PID or three term algorithm involves proportional (P), integral (I), and derivative (D) constant values, which may be explained heuristically in that P is based on present error, I on past error accumulation, while D predicts future errors, according to the present rate of change (Taguchi and Araki, 2000). The process is adjusted by applying control actions, based on the weighted sum of these three constants, to a controlled element; for example, a valve or heating circuit power supply.

The PID controller does not require any prior knowledge of the process to be controlled, which is a major advantage (Bennett, 1993). The controller is tuned for the particular process by adjusting the values of the three parameters, and controller response may be defined according to responsiveness to error, set point overshoot, and degree of oscillation. However, despite its advantage in general applicability, PID control may not provide optimised operation or assure process stability.

The PID algorithm allows one or two of the three parameters to be disabled simply by assigning a zero value to the relevant constant, and hence may become a PD, PI, I or P controller accordingly. Due to the sensitivity of derivative action (D) to noise, it is quite common to encounter PI controllers. However, the integral (I) is important to enable command values to be achieved.

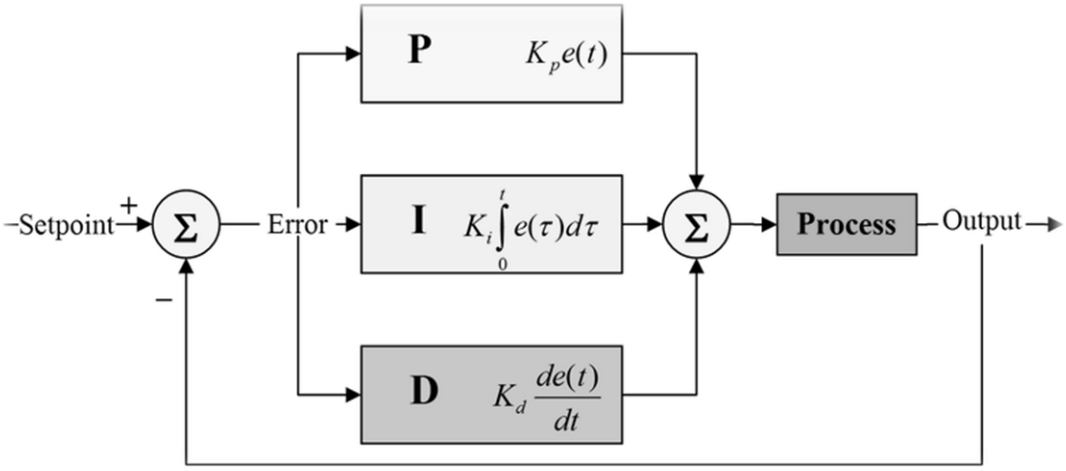

Figure 5.2: A block diagram of a PID controller.

The simulator described in the previous chapter was used to conduct simulations for closed-loop FCCU control. This used the MatLab-Simulink interface to apply an advanced PID algorithm (*discrete position algorithm with backward approximation and anti-windup*) that facilitates stability of the closed loop. Anti-windup in the algorithm was the main reason for the improved PID controller performance, and overcomes the physical limits associated with control elements. For example, a valve cannot exceed its fully closed or fully open positions, as this is physically impossible. The effect on control is severe, as the integral action may lead to instability; when the control element is saturated, simply by the fact that the output cannot change regardless of the input; this breaks the feedback loop. This unstable operating mode will cause a drift, involving high values, and even after the control element is desaturated, the system may take even longer to be restored to a stable state. Moreover, the control element may also experience, high and low value swings before recovery. Anti-windup, also termed tracking or back calculation, ensures that the integral is maintained at an appropriate value, once the control element saturates, which enables the controller to act properly, once again, after the error state changes **(**Bohn and Atherton, 1995).

5.3.2 Constrained optimization based MIMO PID tuning

The PID controller is in general a single input single output (SISO) controller which has a set of tuning parameters, which can be used to fine-tune the closed-loop response for good performance and stability. Tuning the multiple interacting PID loops is generally very difficult due to the high level of coupling between the loops.

In practice often the loops appear to be tuned independently, however when they are activated simultaneously the process can exhibit poor control performance or can be destabilized. To take the coupling between the loops into account the controllers should be tuned simultaneously. This work proposes a method for the tuning of the multiple PID control loops based on the use of a constrained optimization problem, which minimizes the overall integral square error (*OISE*) of the control loops defined as,

$$OISE = \sum_{i=1}^{N_L} \int_0^{t_f} (e_i(t))^2 dt \tag{5.10}$$

where $e_i(t)$ is the error function in the case of loop i, N_L is the number of PID loops and t_f is the time horizon on which the error is computed. From the objective function the control effort was omitted since the primary objective was to evaluate whether it is possible to find a set of tuning parameters, which would provide suitable control performance in a given input-output structure. However once a particular control architecture would be found, in a practical framework the control efforts could also be included in the objective function (5.10). The optimization problem for the tuning is expressed as follows

$$\min_{K_i, T_i} OISE \tag{5.11}$$

subject to:

$$k_{\min,i} \leq k_i \leq k_{\max,i} \tag{5.12}$$

$$T_{\min,i} \leq T_i \leq T_{\max,i}, \quad i = 1,2,\ldots,N_L \tag{5.13}$$

where K_i and T_i are the proportional gain and integral time, respectively, for the PID controller of loop i, and the constraints (5.12) and (5.13) sets the minimum and maximum limits on the tuning parameters. This is a highly nonlinear and nonconvex optimisation problem which may exhibit multiple local minimums, has the solution generally represents a complex numerical problem. Additionally due to the presence of constraints and input saturations the computations of the gradients for gradient-based optimisation approaches may be difficult. In this chapter a Genetic Algorithm-based optimisation framework is proposed for the tuning of MIMO interaction PID control systems.

The main advantages of the genetic algorithm (GA) include that it represents a global optimisation approach (although it does not guarantee that the final global optimum can be achieved within finite

number of iterations) and in the large numerical stability of the approach due its derivative-free nature (Schaffer, 1984; Kursawe, 1990; Hajela et al., 1992; Murata, 1997; Srinivas and Deb, 1994; Fonseca and Fleming, 1993; Horn and Nafploitis, 1993; Deb, 2001; Carlos et al., 2002; Goldberg, 1989; Holland, 1975; Petry et al., 1994; Davidor, 1991; Karr, 1992; Kacprzyk, 1995; Linkens and Nyongesa, 1995a; Linkens and Nyongesa, 1995b; Surmann et al., 1993).

The GA typically uses binary digits to form character strings to represent codes for potential (candidate) solutions in an optimisation. This character string, consisting of binary digits, is termed a 'chromosome', mirroring the terminology used in genetics. The candidate solution indicated by the chromosome is termed an 'individual', where the GA is concerned with many individuals gathered in a 'population'. The individuals in the population are iteratively modified and updated, in each step termed a generation, where the optimisation proceeds through a search for the best solutions. A fitness function within the GA assesses the individuals, and reveals the extent to which they are satisfactory; in addition, an objective function may be used for comparison in a classical approach to optimisation. The fitness function enables the GA concept of 'survival of the fittest' to be applied, where the algorithm seeks to achieve maximum fitness values rather than the classical optimisation approach of seeking to minimise some objective function. As such, specifying the fitness function is a vital aspect in GA design, leading to output of optimised solutions, and appropriate algorithm performance. In each iteration (generation), the GA evaluates the candidate solutions (individuals) by computing their fitness values, and then generating new individuals based on the old information.

The generation of new solutions is quite distinct in Gas compared to approaches in numerical optimisation. First, an initial population composed of individuals is generated, which describes the primary estimates regarding the optimisation. In each iteration step, the GA evaluates a group of solutions, as opposed to one solution, as is the case in gradient descent and similar approaches. The candidate solutions (individuals) are assessed by computing their fitness values, with new ones being formulated to form part of the subsequent generation. Given its distinct approach, the GA does not involve calculating the Hessian or Jacobian matrices, which may produce an ill-conditioned problem for a stiff and highly dimensional FCC unit model, negatively affecting the optimisation. In contrast, simulation has demonstrated that even with a small population, GA convergence may be rapid; 2x2 and 3x3 systems converged over 10 generations only to a global optimum (see Figures 5.3 - 5.4). The resulting tuning parameters for the individual PID loops are presented in Table 5.5. Tracking the evolution of fitness values (average and best) over successive generations reveals that within the initial generation, tuning parameters were quite close to the best,

and so no significant improvements were detected. This was because the initial tuning parameters had been obtained using standard (Ziegler-Nichols) methods for SISO systems applied to the individual controllers. Over the ten generations, there was a sharp decrease in mean fitness values, in parallel with convergence; this indicates that the parameters represent the global optimum, where all the individuals (candidate solutions) had been converging to the best solution, over successive generations. Furthermore, this demonstrated that for the system, individual and independent tuning of the controllers may result in achieving the same level of performance as simultaneous tuning of interacting controllers. In industry, the norm in the FCC unit is that PID controllers are tuned individually.

Table 5.5: Tuning parameters of the PID controllers.

Controller	**Parameters**								
Type	K_1	T_1 [s]	K_2	T_2[s]	K_3	T_3[s]	Td [s]	Tsamp [s]	OISE
3x3	0.0009	5.9	0.001	5.5	0.003	0.8	0	100	1.07 E5
2x2	0.0367	5.0	0.0004	63.953	-	-	0	100	8.081 E4

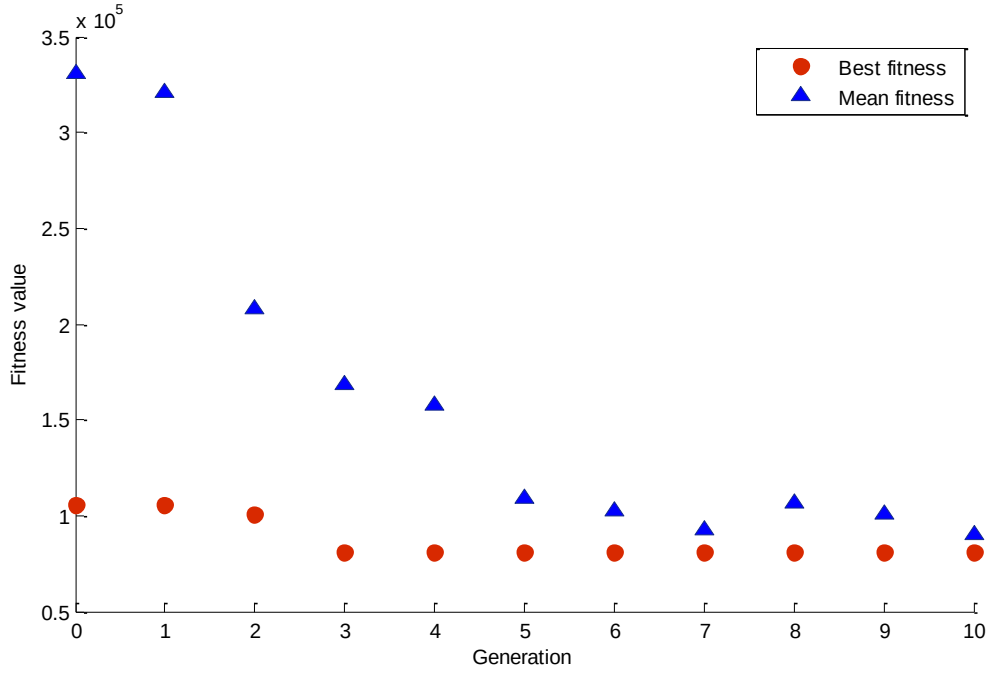

Figure 5.3: Fitness value for 2X2 PID controller system tuning.

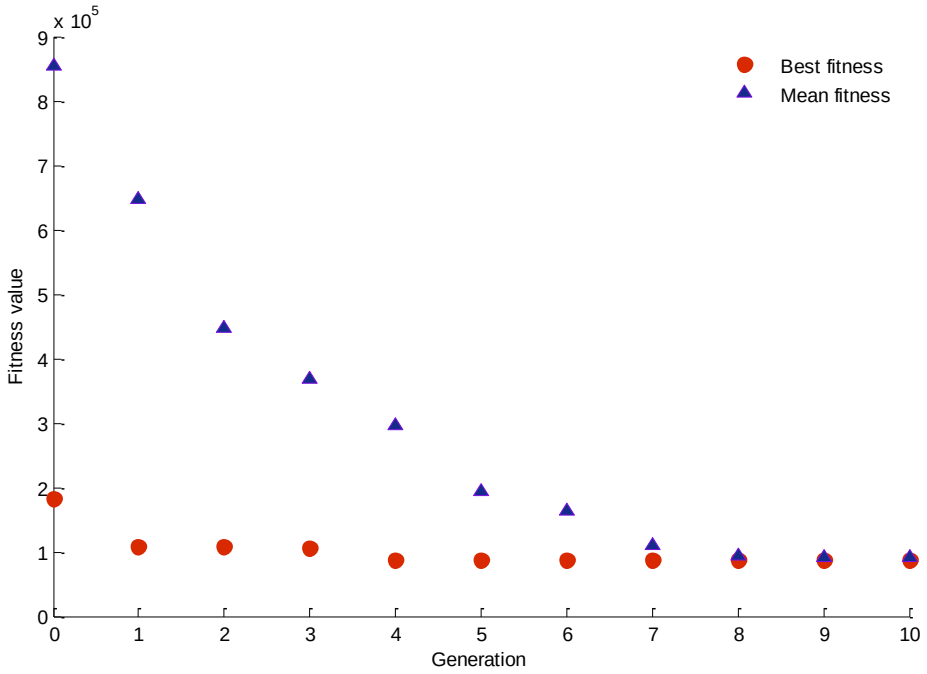

Figure 5.4: Fitness value for 3X3 PID controller system tuning

5.3.3 Multivariable PID control of the FCCU

3x3 structure

The MIMO closed loop system designed and implemented in Matlab/Simulink environment with the most common control scheme using PID controller is shown in Figure 5.5. Process simulations with three independent control loops were carried out. Based on the RGA results in Table 5.4 the following control pairings were used: T_r-F_5, T_{reg}-*svsc*, $cO_{2,sg}$-V_{14}. The control performance was evaluated in the case of regulatory (disturbance rejection) and servo control (set point tracking).

The regulatory control has been investigated in the case of a +5% disturbance in the feed oil composition represented by the coke production rate factor Ψ_f and in the case of a setpoint change as indicated in Table 5.6.

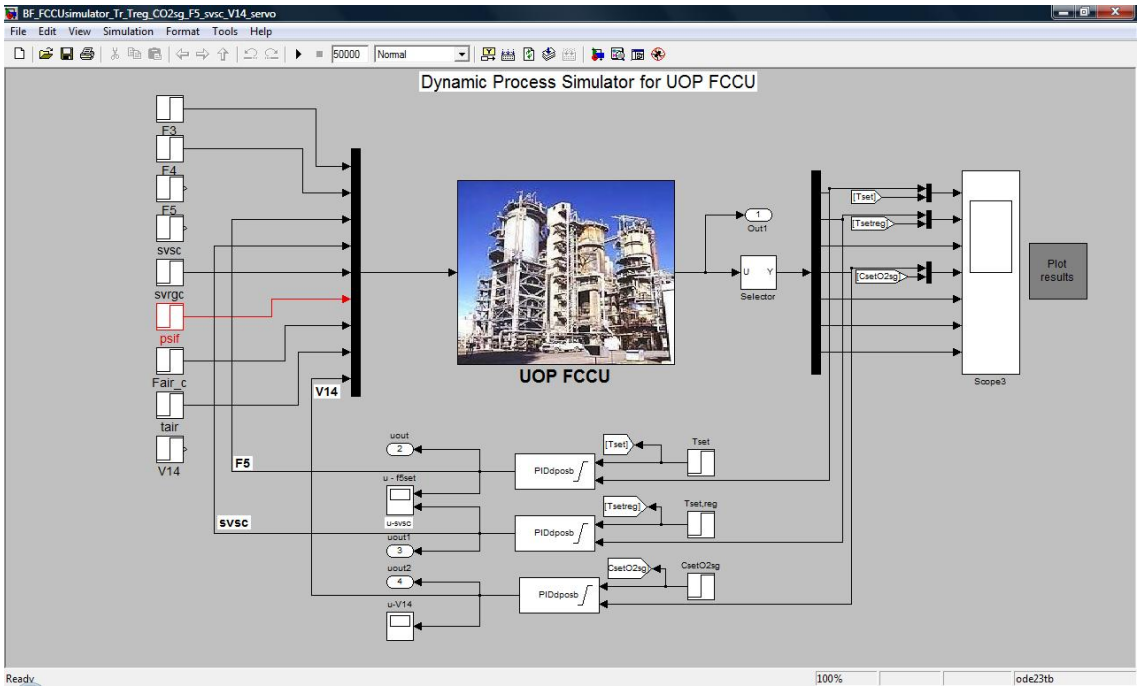

Figure 5.5: SIMULINK block diagram for the closed loop simulation with three PID controller loops.

Table 5.6: Tested data for 3 x 3 PID controllers in MIMO loops parameters.

Loop	Controlled variables	Manipulated variables	Disturbance	Control scenario	
				Servo, °C	**Regulatory,%**
1	T_r - T_{reg} -$cO_{2,sg}$	F_5 - *svrgc* - V_{14}	Ψ_f	$T_r \rightarrow 541.6$ $T_{reg} \rightarrow 737.7$ $cO_{2,sg} \rightarrow 4$	+ 5

In the case of the regulatory control scenario considered the +5% increase in coke formation factor in the feed oil occurs at time 1.5 h. The control system is able to maintain the controlled outputs within small variations, compared to the uncontrolled case (shown in Chapter 4). Variations are within 1-1.5 °C for the reactor temperature and bellow 4 °C for the regenerator temperature, whereas for the uncontrolled case these are around 5 and 8 °C, respectively. Whilst the CO_2 emission reaches similar maximum levels in the case of the controlled scenario as for the uncontrolled case, the control systems eventually brings the emission level down , below 4%.

Similar variations can be observed in the case of the CO emission, too. The variations in the product composition (Figure 5.7) are also relatively small. The settling time however is considerably long. It takes more than 6 hours for the control systems to bring the process back in the original operating point. Such a long period of operation with product specifications outside the required boundaries may lead to considerable economic effects. These results indicate that although the proposed control structure is able to eventually suppress the effect of the investigated disturbance on the process relatively well, this takes a significant amount of time, hence if the process is subject to frequent disturbances this may lead to poor overall control performance and potentially considerable economic and environmental losses.

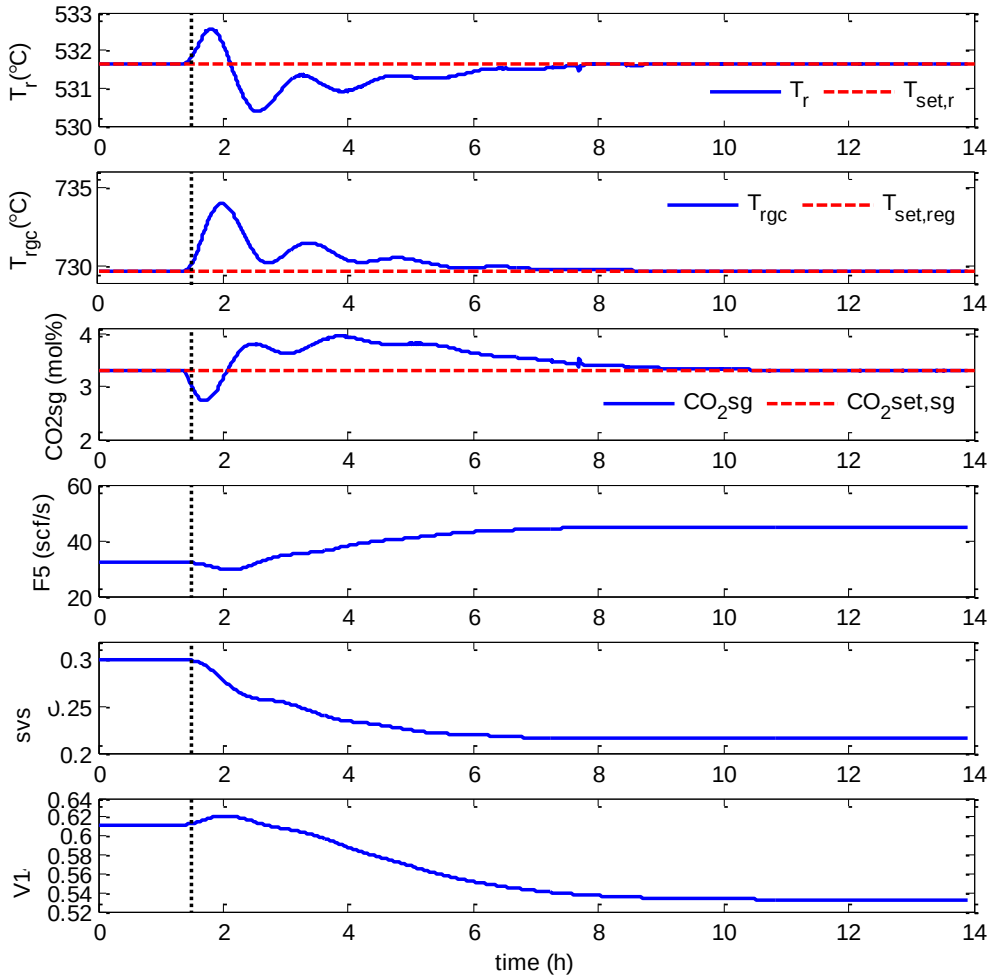

Figure 5.6: Performance of the regulatory controls for (T_r *vs.* F_5), (T_{reg} *vs. svsc*) and ($cO_{2,sg}$ *vs.* V_{14}) in the presence of step increase in the coking factor Ψ_f +5%, at t = 1.5 h.

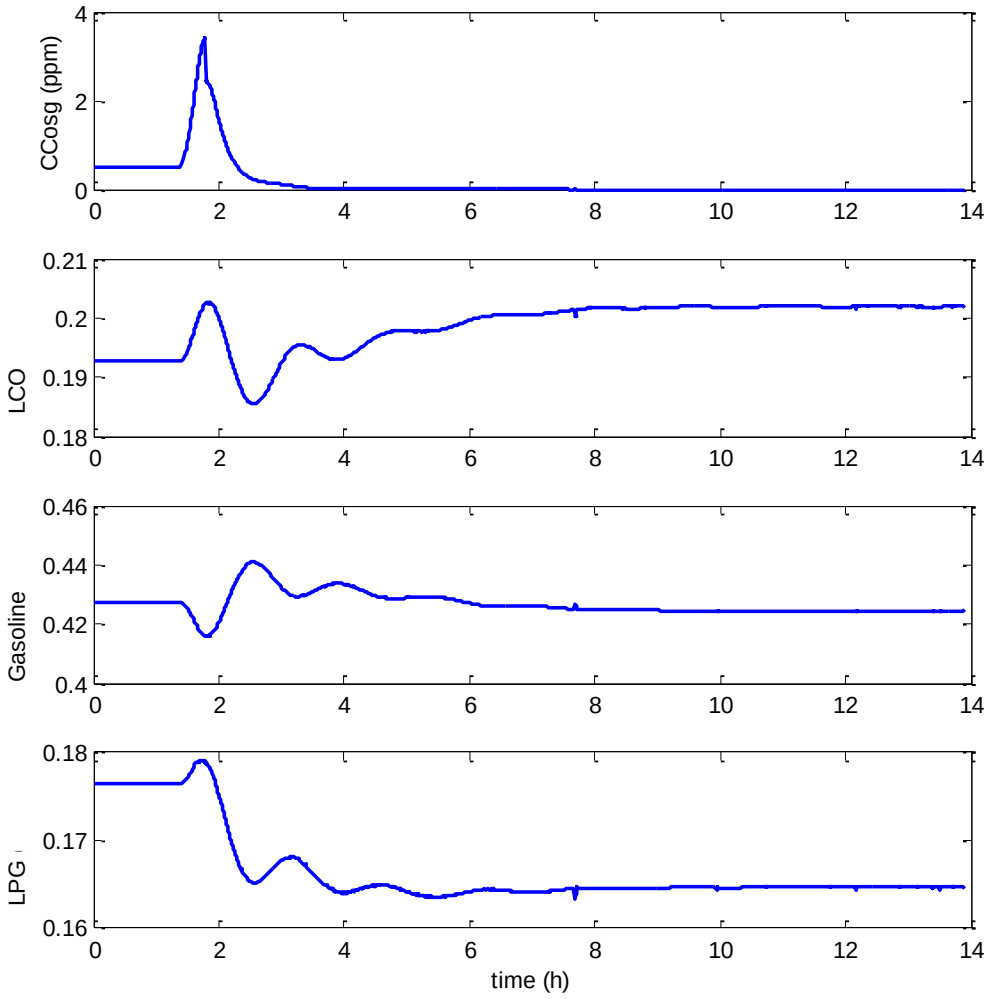

Figure 5.7: Dynamic behaviour of other uncontrolled process variables in the case of the disturbance rejection scenario in Figure 5.6.

In the case of the servo control scenario (tracking control), a positive setpoint change was applied to al three controlled variables at the same time. Figure (5.8) shows the results of the closed loop simulation indicating that whilst the control system eventually brings all three process outputs to the new setpoints this takes a variably long time. The reactor temperature is brought to the new setpoint within 2 hours whereas the regenerator temperature and cO_2 concentration takes considerably longer, about 6 hours for T_{reg} and 10 hours for cO_2. The effect of operating the system at the new setpoint values, on the product composition and *CO* emissions are shown on Figure 5.9.

.

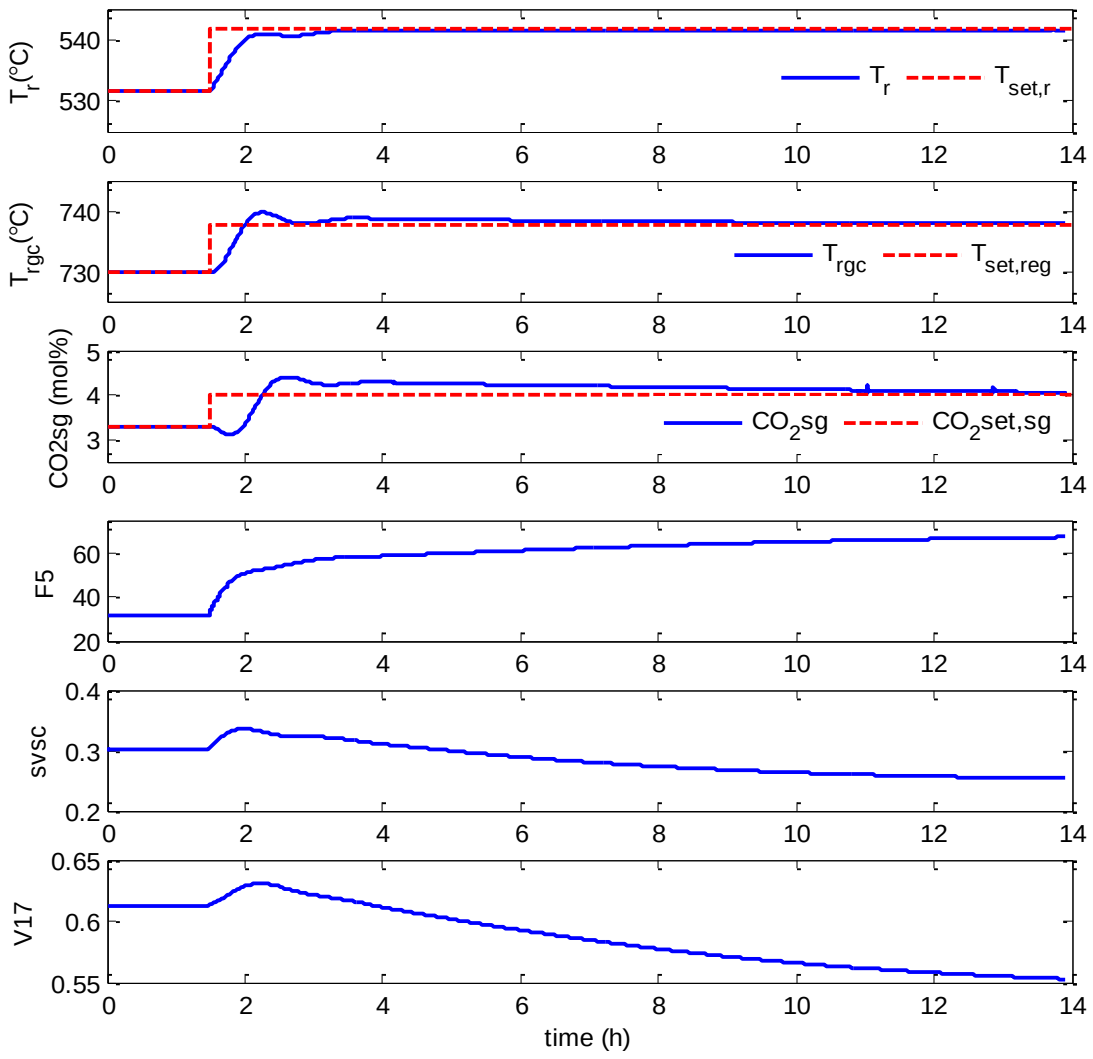

Figure 5.8: Performance of the servo control for (T_r vs. F_5), (T_{reg} vs. *svsc*) and ($cO_{2,sg}$ *vs.* V_{14}) in the presence of step increase, at t = 1.5 h.

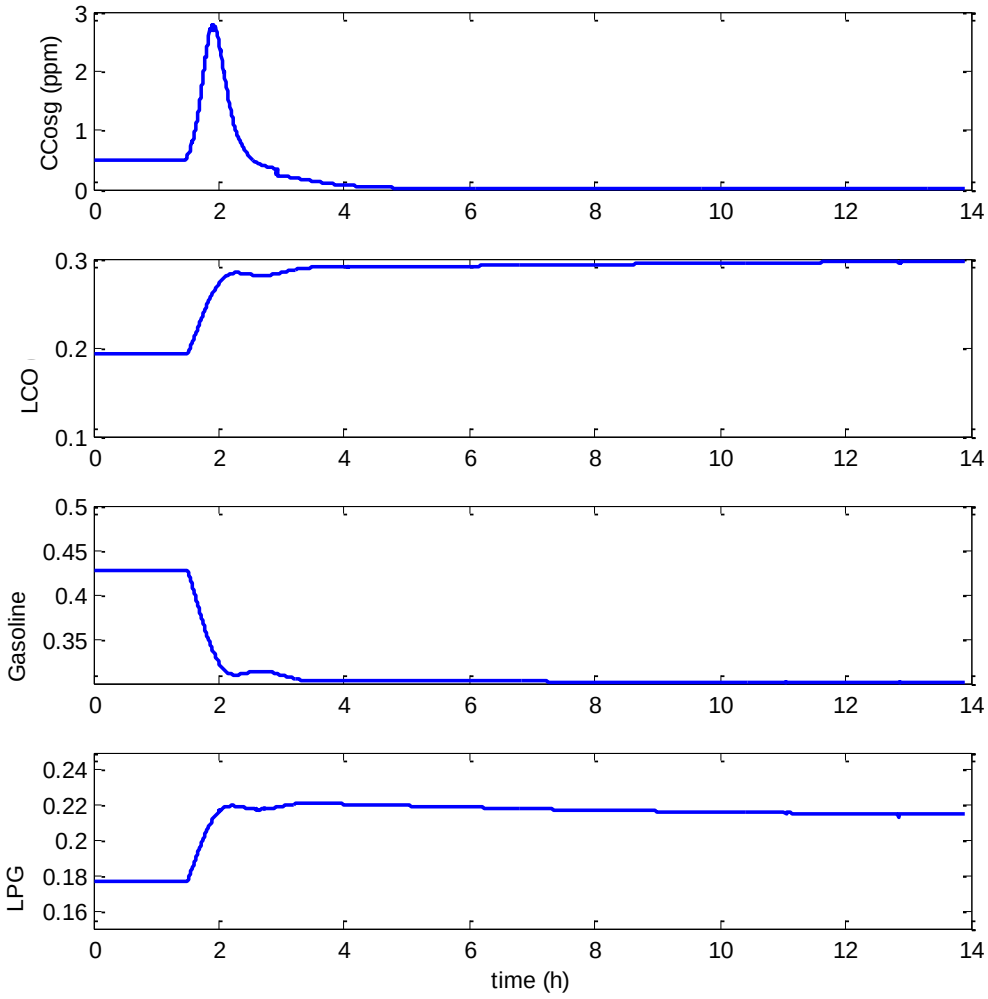

Figure 5.9: Dynamic behaviour of other uncontrolled process variables in the case of the setpoint tracking scenario in Figure 5.8.

2 x 2 Control Systems

The output variables considered in this study, T_r and T_{reg}, are strongly coupled, and a control that stabilizes one of the parameters may be able to stabilize inherently the other, too. The manipulated variables were chosen based on their behaviour and ability to stabilize the system as shown in the simulation results using the SISO PID control systems. Two 2x2 control structures were evaluated in the case of regulatory control and setpoint tracking as shown in Table (5.7). In the first structure evaluated the manipulated inputs *svrgc* and V_{14} were tested for the control of the reactor temperature and cO_2 concentration. Wolff *et al.* (1992) also proposed a similar control architecture

based on their analysis of the disturbance sensitivities for the FCCU system studied. The closed-loop simulation model was implemented using two separate PID control loops as shown in Figure (5.10) and the parameters were tuned using a tuning approach based on a Genetic Algorithm (GA).

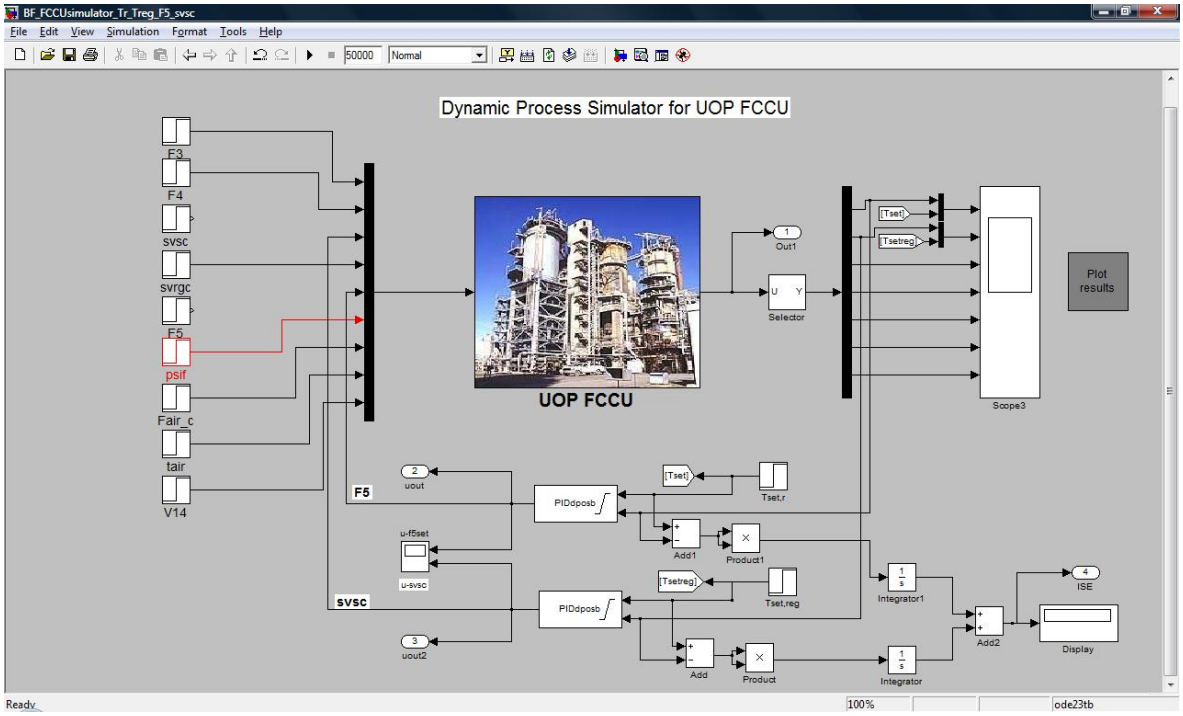

Figure 5.10: SIMULINK block diagram for the closed loop simulation with two PID controller loops.

Table 5.7: Tested data for PID controllers in MIMO loops parameters.

Loop	Controlled variables	Manipulated variables	Disturbance	Controller problem	
				Servo, °C	Regulatory, %
1	T_r - $cO_{2,sg}$	$svrgc - V_{14}$	Ψ_f	-	+ 5
2	T_r -T_{reg}	F_5 - $svsc$	Ψ_f	$T_r \rightarrow 541.6$ $T_{reg} \rightarrow 737.7$	+ 5

The simulation results are shown in Figures (5.11 – 5.16). Both control structures provide excellent performance. The plots clearly show that the T_r , T_{reg} and oxygen concentration can be controlled and brought to their steady states or new setpoints. Usually temperature control systems in large unit operations have a large time constant, but in the riser, the gas oil and catalyst flow rates are

very large, residence times are short, the cracking reactions are quick, therefore the riser outlet temperature reveals a quick response to the regenerated catalyst valve opening.

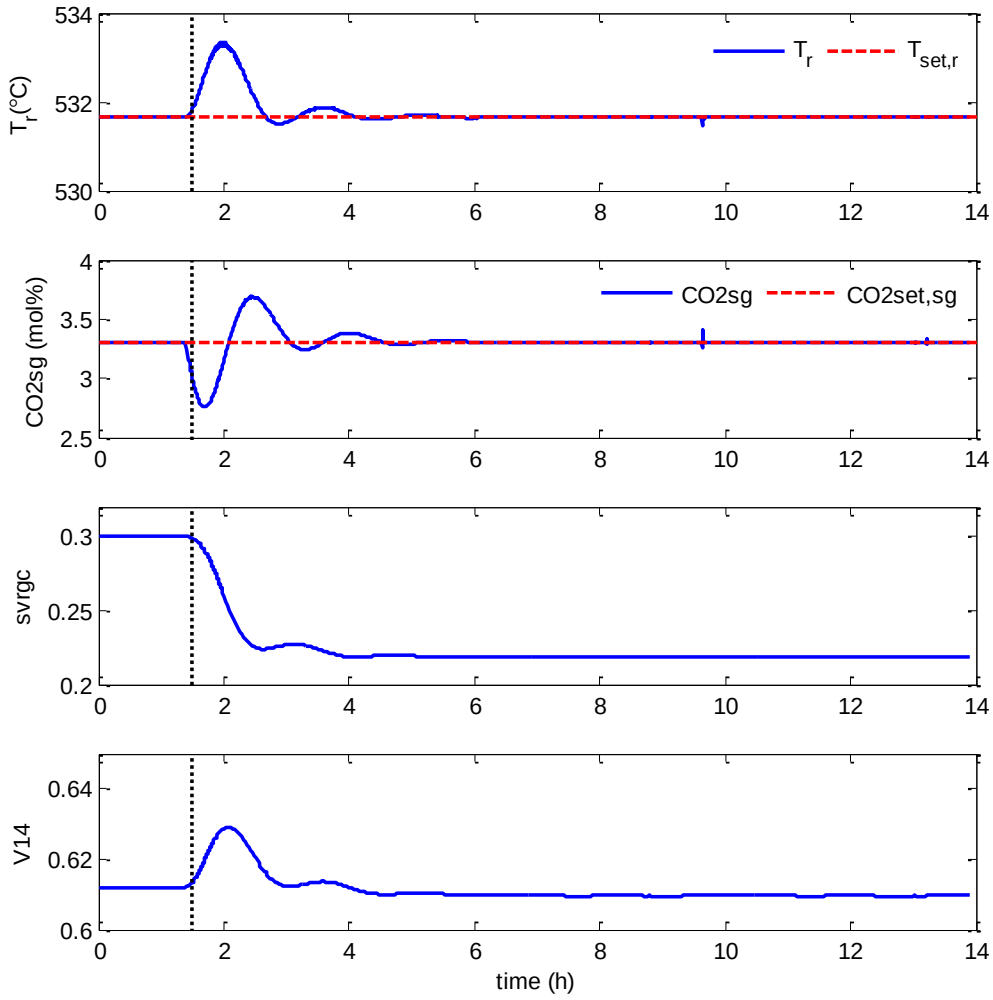

Figure 5.11: Model responses for the reactor T_r and regenerator $cO_{2,sg}$ temperatures by manipulated *svrgc* & V_{14} with changes in the coking factor Ψ_f +5%, at t = 1.5 h.

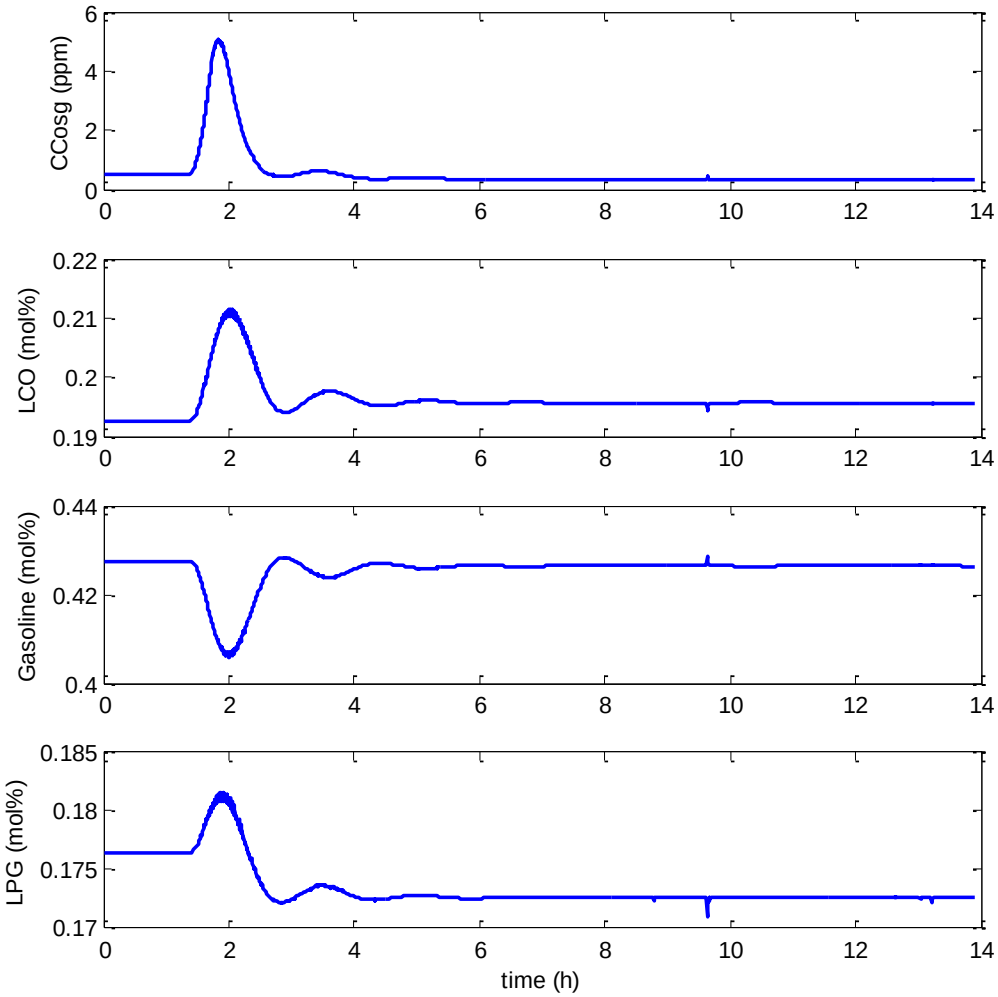

Figure 5.12: Dynamic behaviour of other uncontrolled process variables in the case the scenario in Figure 5.11.

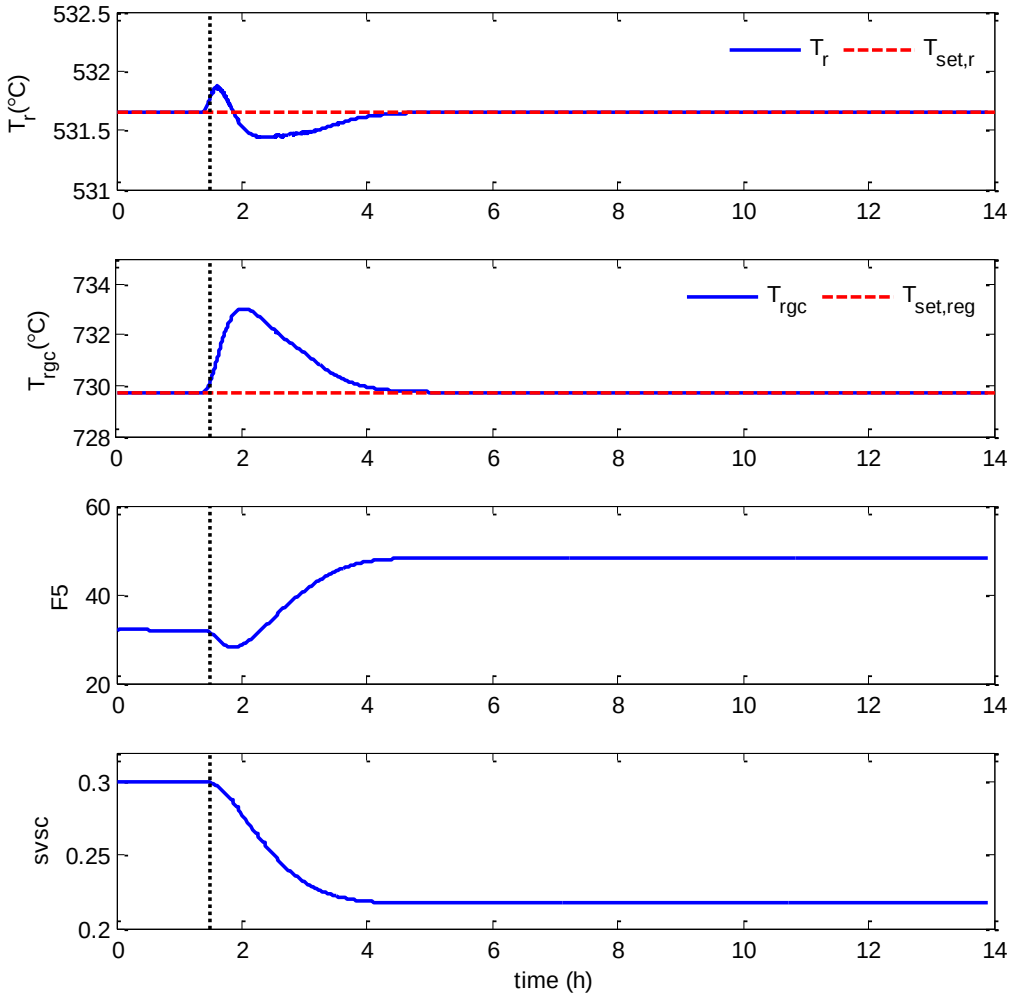

Figure 5.13: Model responses for the reactor T_r and regenerator T_{reg} temperatures by manipulated F_5 & *svsc* with changes in the coking factor Ψ_f +5%, at t = 1.5 h.

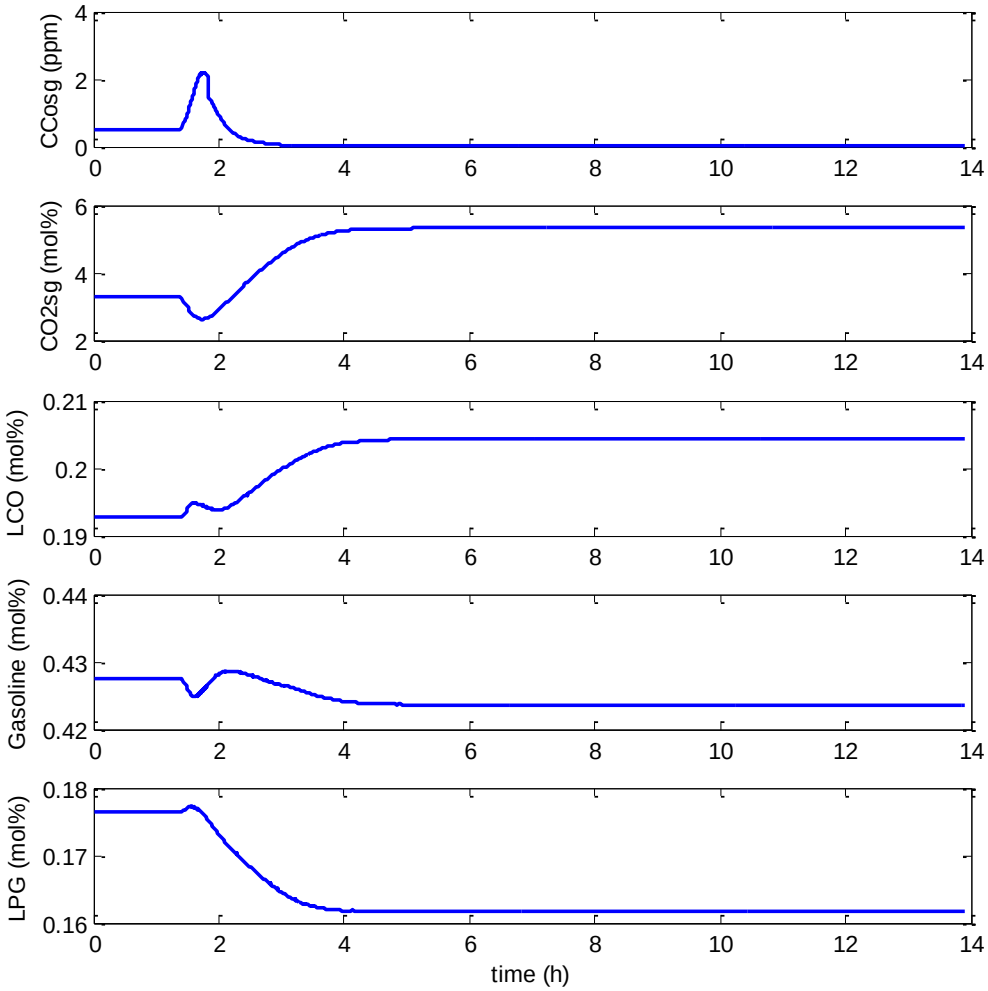

Figure 5.14: Dynamic behaviour of other uncontrolled process variables the case scenario in figure 5.13.

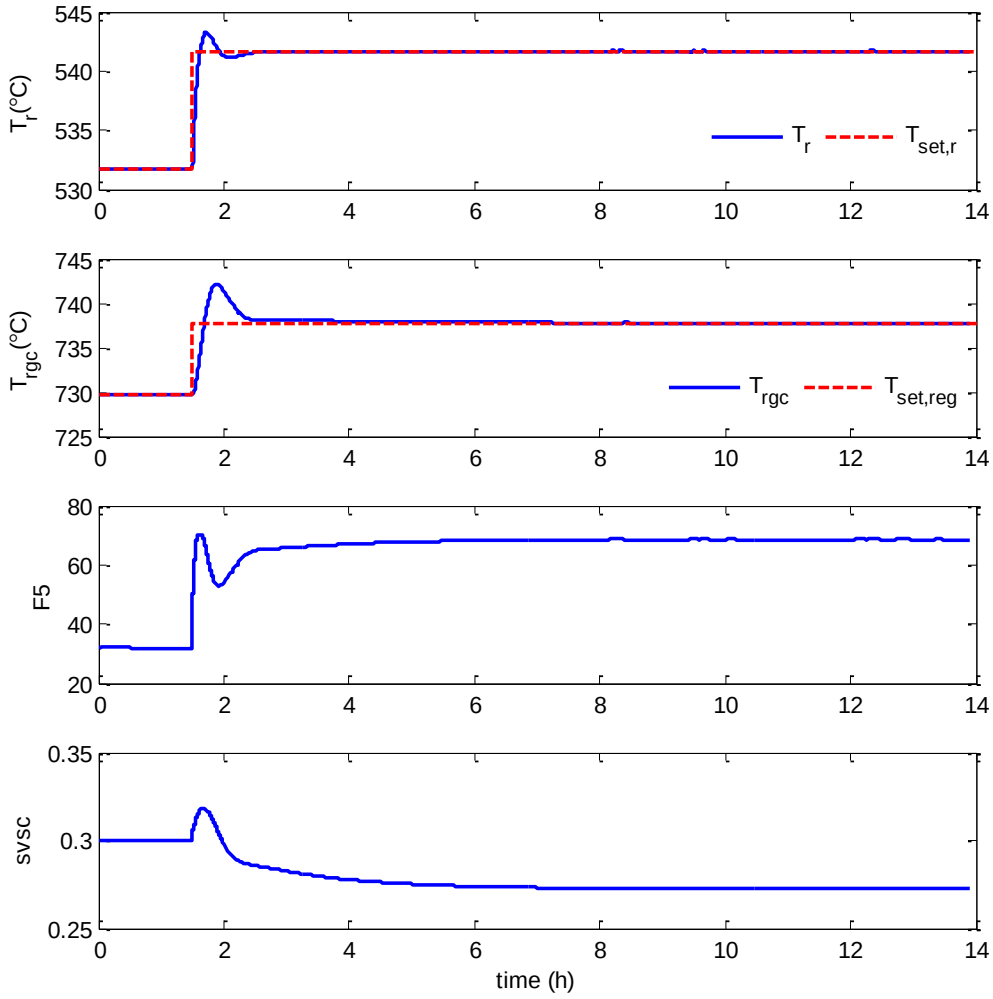

Figure 5.15: Performance of the servo control for (T_r *vs.* F_5) *and* (T_{reg} *vs. svsc) in* the presence of step increase, at t = 1.5 h.

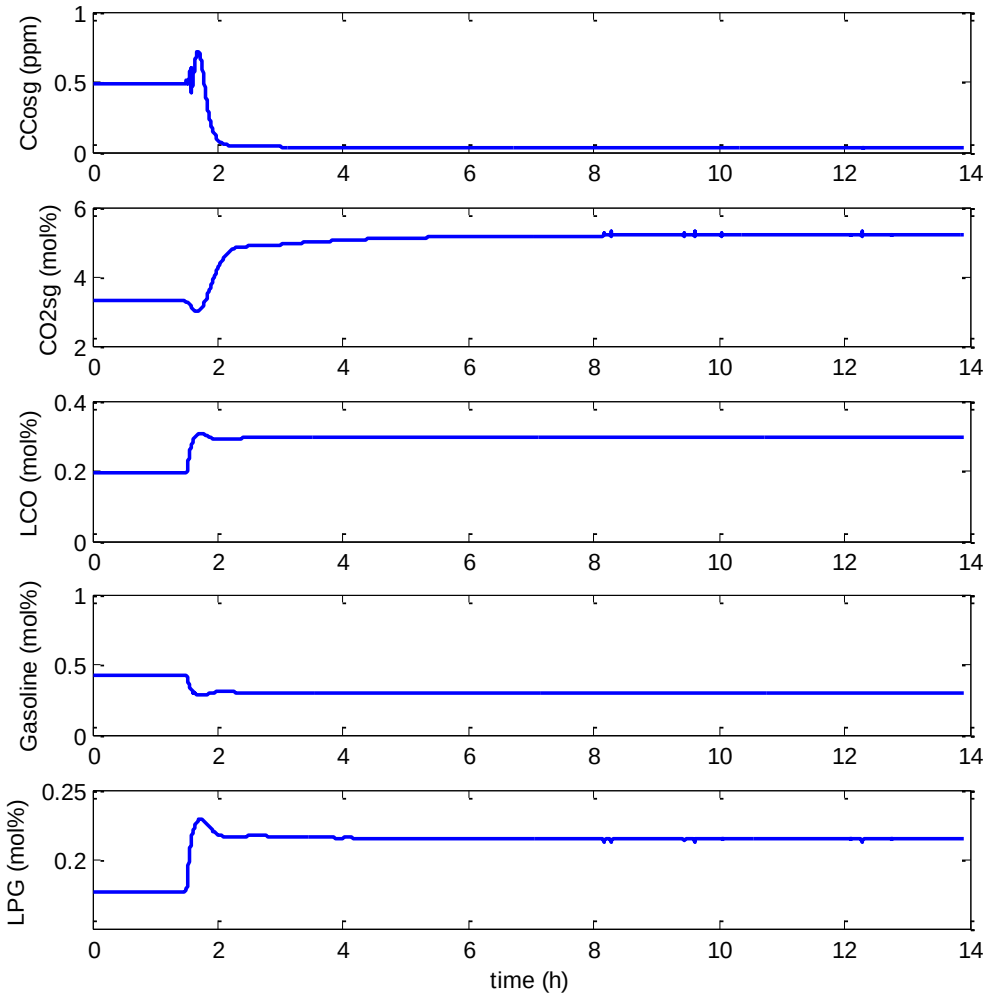

Figure 5.16: Dynamic behaviour of other uncontrolled process variables the case scenario in Figure 5.15.

5.4 Conclusions

The dynamic simulator was used to study the closed-loop dynamic behaviour of the process, using advanced PID controllers for the multivariable process plant. A simple RGA matrix based controllability analysis was performed in order to study the interdependence among the process variables. The PID algorithm was tried for different control structures. The results revealed the strong couplings among some of the control loops, which may lead to difficulties in tuning the individual control loops. A genetic algorithm based tuning approach is proposed to simultaneously

identify the controller parameters for the interacting SISO PID control loops. Sample 2x2 and 3x3 control schemes were evaluated for disturbance rejection and set point tracking. The results demonstrate that as the number of independent control loops increases, the performance of the PID controller scheme strongly deteriorates, as indicated, for example, by significantly increased settling time. While the control system is able to stabilize the system, the decreased performance in the case of frequent disturbances may lead to significant economic losses or negative environmental impact, providing incentives towards the implementation of more advanced multivariable control systems.

CHAPTER 6
MULTIVARIABLE LINEAR AND NONLINEAR MPC OF THE FCCU

6.1 Introduction

FCC unit control has been investigated by many workers, including the application of multivariate and nonlinear predictive control approaches (Alvarez-Ramirez et al., 1996; Aguilar et al., 1999; Abou-Jeyab and Gupta, 2001; Kiss and Szeifert, 1997; Balchen et al., 1992; Grosdidier et al., 1993). A multivariable control scheme was proposed for an industrial FCC unit with controls in the reactor and regenerator; it was concluded that this offered a robust solution resulting in good dynamic performance (Grosdidier et al. 1993). Temperature control of FCC units was also achieved using a state-space model based predictive controller, with the non-linear optimisation problem solved in real-time. Simulation studies demonstrated good closed loop performance. However, the model-based control schemes are characterised by high computational costs, due to the large numbers of process variables and the complex interactions between the controlled and manipulated variables (Balchen, 1992). Non-linear control, accommodating uncertainty, was also applied to the temperature control in the FCC regenerator and riser (Alvarez-Ramirez et al., 1996; Aguilar et al., 1999). The closed loop controllers developed using this concept were practical, and regulated the temperature near the set point. Hovd and Skogestad (1993) reported that the key to satisfactory control of the FCC units is in choosing the appropriate controlled variables for the linear model predictive control scheme investigated. It was demonstrated that control of FCC units presents a non-linear, multi-variable, complex dynamic problem, where the control loops frequently interact strongly. At the same time, FCC unit operation takes place in the presence of constraints, and so the control strategy must be designed to accommodate these complex input-output interactions, and to demonstrate robustness in face of operating non-linearity, and errors in models.

In the practical control of FCC units, as mentioned previously in Chapter 5, generally the preferred control loops are decentralised, temperature in the reactor and regenerator being the main parameters that need to be closely controlled (Christensen et al., 1999; Avidan and Shinnar, 1990). Temperature as an independent variable plays a critical role in adjusting the activity of the catalyst

in the steady state, and influences the product properties, such as octane number of gasoline. Moreover, process efficiency, conversion, and product yield, as well as plant safety are affected by the temperatures in the system. Therefore, in the key parts of the FCC unit, i.e. reactor, regenerator and riser, temperature needs to be controlled for optimal operation, and kept within the plant's design limits.

This meant that a new design and implementation of linear and non-linear controllers was needed to handle the challenging control problem for the FCC process. Furthermore, the strong nonlinearity of the FCC process and the presence of large number of operational, safety and environmental constraints require the use of a multivariate model-based controller. In this context, model predictive control (MPC) offers a promising solution to the FCC unit control, as it accommodates multiple inputs and outputs, constraints, and is an optimisation based strategy (Emad and Elnashaie, 1997; Karla and Georgakis, 1994).

Based on these preliminary aspects, two main types of model predictive control (MPC) approaches are investigated in this chapter: (i) linear model predictive control (LMPC) and (ii) nonlinear model predictive control (NMPC). The former approach is also investigated under the realistic scenario which considers model-plant mismatch, by using the linearized model in the LMPC scheme and using the complex first-principles nonlinear model for the plant simulator.

6.2 Linear MPC design and implementation

6.2.1 LMPC simulation using the linear model as plant

Linear Model Predictive Control (LMPC) is one of the most widely used advanced control methods in the chemical industry. Also referred as moving (receding) horizon control, has become an attractive control strategy especially for linear but also for nonlinear systems subject to input, state and output constraints. There are some features that individualize MPC in the field of control design making it attractive. In contrast to other feedback controllers that calculate the control action based on present or past information, MPC determines the control action based on the prediction of future dynamics of the system. Due to the future prediction, early control action can be taken accounting for future behaviour. In practice, most of the systems have to satisfy input, state or output constraints, resulting in limitations on achievable control performance (in the extreme case affecting the stability). The main idea of MPC is to calculate a set of future manipulated variable

moves (on the control horizon), which is calculated to minimize an objective function based on the sum of squares of the differences between model predicted outputs and a desired output variable trajectory over a prediction horizon (*p)*. The mathematical formulation of the LMPC problem is given in detail in Chapter 2.

As highlighted in Chapter 2, the tuning of a MPC is challenging, particularly in the multi-input-multi-output (MIMO) configuration, which is the most commonly used structure for MPC applications (Garcia et al., 1989; Semino and Scali, 1994; Lee and Yu, 1994). Potential tuning variables include the input and prediction horizons, designated *m* and *p* respectively, as well as sampling time, T_s The MIMO features of the problem present the difficulties in tuning, where changes in the variables influence control performance. The challenges are more significant, where model non-linearities exist (Chen and Allgower, 1997). The nature of these challenges dictates an iterative approach to MPC tuning, with further improvement in controller performance achieved through recursive simulations. The task of MPC tuning has been greatly facilitated with publication of MPC tuning guidelines (Karla and Georgakis, 1994; Semino and Scali, 1994; Chen and Allgower, 1997). In this case, choice of sampling time, T_s, is a compromise between potentially exceeding the computational capacity of the system, on one hand, and missing key data for the dynamic process, on the other.

Taking the existing tuning guidelines into account for the FCCU process a sampling time of T_s=100 *s* was selected. Similarly, since high values for prediction and control horizons (*p* and *m* respectively) result in greater computation, while small values leads to control that is "short-sighted", therefore, p = 20 was chosen, which with the sampling time of 100 *s* corresponds to a quarter (2000 *s*) of the open loop setting time of the process. Smaller values would result in a short term control view, and so more controlling effort; moreover, for these smaller values of *p*, constraint checking takes place over a small horizon, creating a dead zone where control is inefficient. At the same time, larger values of *p* (compared to the settling time) result in slow (but stabilising) control responses, which come at a greater computation cost. The value selected for the control horizon, *m* is 5, which was found to provide a suitable compromise between computational effort and enough degrees of freedom to stabilize the process and achieve the desired control performance. Values less than this resulted in inefficient control action with degrees of freedom that are insufficient, while larger values result in aggressive control actions.

Dynamic simulations were used to investigate various MPC schemes resulting in interesting results with practical implications in the industrial setting.

Control scheme selection

The process parameters (variables) that are seen to play a key role in proper operation of the FCC unit were identified from the published literature, and by analysing the commercial process (Rhemann et al., 1989; Yang et al., 1996). These process variables are controlled to ensure that the process is run safely and economically. The amount of catalyst or catalyst inventory in the reactor, W_r, is controlled to stabilise circulation of the catalyst, and also creates a buffer preventing disturbances due to coke deposition on the catalyst, as well as helping to stabilise the temperature from reactor to regenerator. In the regenerator, a controlled temperature regime is necessary, with T_{reg} at a set value, for the process of coke burn-off and consequent catalyst regeneration to achieve stability. Exceeding the limit of temperature permanently deactivates the catalyst, while a lower temperature prevents proper coke removal, and results of coke accumulation and gradual decrease in performance with time. The catalytic cracking reactions in the reactor also require good control of temperature, T_r, for efficient feedstock conversion. Another controlled process variable, stack gas oxygen concentration, $cO_{2,sg}$, is key to burning the coke, and as such maintaining the thermal balance, and maximising the combustion air blower load efficiency.

The manipulated process variables are independent variables selected for the practical reason that they can be modified, where the main ones are for catalyst, preheating furnace fuel, stack gas, and air vent flow rates. The catalyst flow, spent and regenerated, is controlled by slide valve positions, *svrgc* and *svsc* respectively. The flow of fuel to the preheating furnace, F_5, is a key variable in maintaining the FCC unit thermal balance. The flow of regenerator stack gas is controlled by the position of the stack gas valve, V_{14}. Similarly, the flow from the air vent is controlled by the position of the air vent valve position, V_7. The variables that represent potential sources of disturbances are ambient temperature, and the coking characteristics of the feedstock, i.e. rate of coking.

MPC is inherently a multivariate control scheme which can automatically deal with interactions between multiple inputs and outputs. Therefore in principle it is not necessary to choose input and output variables that correspond to a close to diagonal RGA matrix, representing decoupled non-interacting control loops, when MPC is applied directly at the basic level of the typical control hierarchy. However in most practical situations MPC is implemented on top of the basic control system which consists typically of single-input-single-output (SISO) control loops mainly based on PID controllers. Therefore in a practical industrial scenario before the implementation of the MPC the first step is to select the control loops at the basic control level.

The controllability study is the first step in control scheme selection, and has shown its effectiveness in both decentralised and multivariable control approaches (Hovd and Skogestad, 1991; Cristea and Agachi, 1996). In this step identifying the best input-output pairs with the highest sensitivities but minimal interactions, can significantly improve the control performance of the higher level MPC. In this context the RGA analysis facilitates the selection of the best manipulated variables influencing the controlled variables, and hence the most appropriate MPC scheme.

Based on this approach, a set of control schemes has been investigated. They have a different number of controlled/manipulated variables for square control structure (same number of inputs and outputs): 2x2, 3x3, 4x4, and non-square control structures (different number of manipulated inputs and controlled outputs): 2x4, schemes, presented briefly in Table 6.1.

Table 6.1: Input-output configurations tested with the MPC parameters used.

No	Control scheme	Controlled variables	Manipulated variables	MPC tuning parameters (duration, prediction and control horizons and Γ^u)
1	**2x2**	T_r - T_{reg}	F_5 - *svsc*	[8000 *s*, T_s = 40, p = 20, m = 5, Γ^u = 0.8]
2	**3x3**	T_r - T_{reg} - W_r	F_5 - V_{14} - *svsc*	[10000 s , (T_s = 80, p = 20, m = 2), Γ^u = 0.8]
3	**4x4**	T_r - T_{reg} - $cO_{2,sg}$ - W_r	*svrgc* - V_{14} - V_7 - *svsc*	[10000 s , (T_s = 80, p = 20, m = 5), Γ^u = 0.8]
4	**4x2**	T_r - T_{reg}	F_5 - *svrgc* - *svsc*- V_{14}	[8000 s , (T_s = 80, p = 20, m = 5), Γ^u = 0.8]

A linear model was used for the computation of the manipulated variables, obtained by the linearization of the non-linear model around the nominal operating point (Patwardhan et al., 1990). The RGA analysis was performed for all configurations. The result for control scheme 1 is given in Chapter 5, whereas the RGA matrix for the control structures 2 and 3 are given in Tables 6.2 and 6.3.

Representative results from the control schemes given in Table 6.1 are presented in Figures 6.1-6.10. Note that the input and output variables represented in the figures are deviation variables compared to their steady state values. This is due to the fact that the LMPC control design is

generally based on the linear model identified around a particular operating point. The controller was tested in different setpoint changes. Figure 6.1 and Figure 6.2 indicate that the 2x2 control scheme is able to provide a very good setpoint tracking, for a 10°C and 15°C change in the T_r and T_{reg} setpoints, respectively. The new setpoints are achieved quickly with no or minimal overshoot. Additionally, the MPC provides a good decoupling between the two control loops, shown by the relatively small disturbance in one of the controlled output when the setpoint changes for the other controlled outputs. This is mainly due to the fact that the input-output pairs are well-correlated according to the RGA analysis presented in Chapter 5. When the setpoint corresponding to any of the controlled outputs changes, both manipulating inputs must react, on one hand, to bring one of the outputs to the new setpoint value, and on the other hand to eliminate the effect of changes and maintain the other output at its original setpoint value. The control actions are smooth, indicating the control-change weight coefficient was chosen properly to achieve fast but stable closed-loop performance.

Figures 6.3 and 6.4 illustrate the performance of the 3x3 control scheme, which includes as an additional control output the inventory of catalyst in the reactor (W_r) and as an additional input the stack valve position (V_{14}). The setpoint tracking performance of the LMPC is very good, the new setpoints are achieved very fast, with no overshoot and with minimal interactions. It is interesting to observe that increasing the number of manipulating inputs the MPC controller is able to provide a significantly better decoupling of the controlled outputs compared to the 2x2 case. When the setpoint changes for the T_r or the T_{reg}, practically no disturbance can be observed in the other process outputs.

Similar observations are found by analyzing the results of the other 3x3 control structure on Figures 6.5 and 6.6. These results compared to the simulation results with the PID controllers for the same structure presented in Chapter 5, also indicate a significantly better performance. However, note that in the LMPC simulations no model-plant mismatch is assumed and the plant is represented by the linearized process model.

The results of the 4x4 control scheme are presented in Figures 6.7 and 6.8. These results also indicate that with the increase in the number of manipulating inputs the controller is able to provide better decoupling. In this control structure the fuel flow to the furnace (F_5) was eliminated from the manipulating inputs and the combustion air blower vent valve (V_7) and the regenerated catalyst valve (*svrgc*) were added instead. This, however, has led to a decrease in the controller performance compared to the 3x3 structure studied before. Although the observed interactions between the

controlled variables are minimal some of the process outputs settle slower to their new setpoint value (e.g. T_{reg}). This indicates that the F_5 is an important manipulating input, which should be kept in the MPC control scheme.

The 4x4 control scheme indicates the ability of this approach to maintain the stack gas oxygen concentration at a predefined value, which allows more efficient FCCU operation due to better use of air blower capacity, and leads to safer operation through control of the "afterburning" phenomenon.

One of the advantages of the MPC approach is that different number on manipulating and controlled variables can be used (non-square system) for control. This is an important property, given the previous observations that by increasing the number of manipulating inputs the decoupling between the controlled outputs can be improved. The simulations for the non-square 4x2 MPC scheme (4 inputs and 2 outputs) did reveal improvements compared to 2x2 or even to the 4x4 schemes, in providing better control performance. The advantage of using a control scheme with a higher number of manipulated than controlled variables is especially important when constraints on the manipulated variables are imposed. The surplus manipulated variables may be advantageous when one or more of the manipulated variables become restricted.

These results demonstrated the benefits of the model based multivariate control and the advantages of using excess of manipulated inputs. However the judicious selection of the manipulated inputs is emphasized, as it was indicated that the F_5 is an important parameter, which should be kept amongst the set of manipulated inputs to achieve the best control performance.

Table 6.2: RGA Matrix of 3X3 Control Scheme.

Controlled variable	**Manipulated Variables**		
	F_5	*svsc*	V_{14}
T_r	*1*	*0*	*-0*
T_{reg}	*-0*	*-0*	*1*
W_r	*0*	*1*	*-0*

Table 6.3: RGA Matrix of the 4x4 control scheme.

Controlled variable	Manipulated Variables			
	svrgc	V_7	V_{14}	***svsc***
T_r	*1*	*-0*	*-0*	*-0*
T_{reg}	*-0*	*0*	*1*	*0*
$cO_{2,sg}$	*-0*	*1*	*0*	*0*
W_r	*0*	*-0*	*-0*	*1*

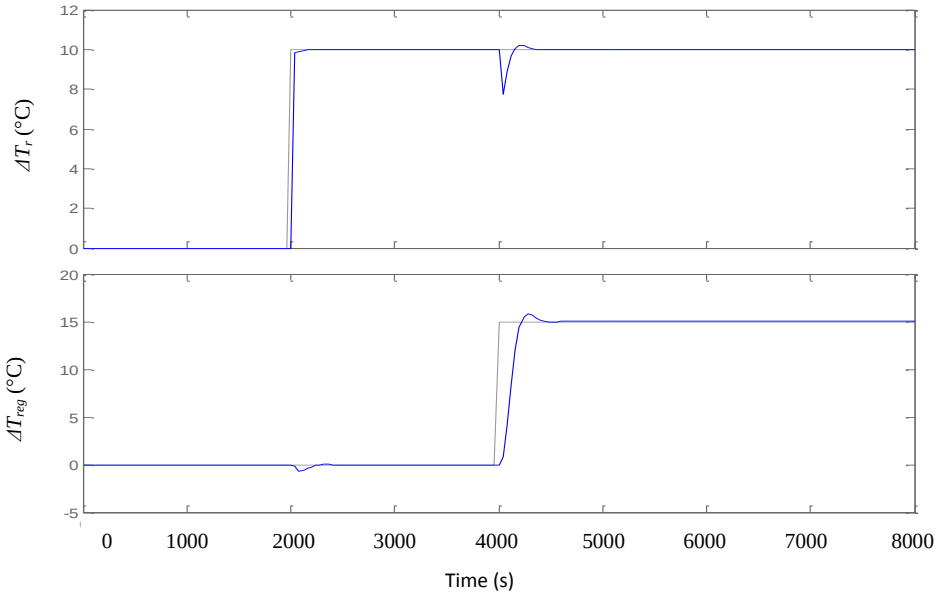

Figure 6.1: The 2x2 LMPC simulation results with the controlled variable response for setpoint change for T_r and T_{reg} at different times.

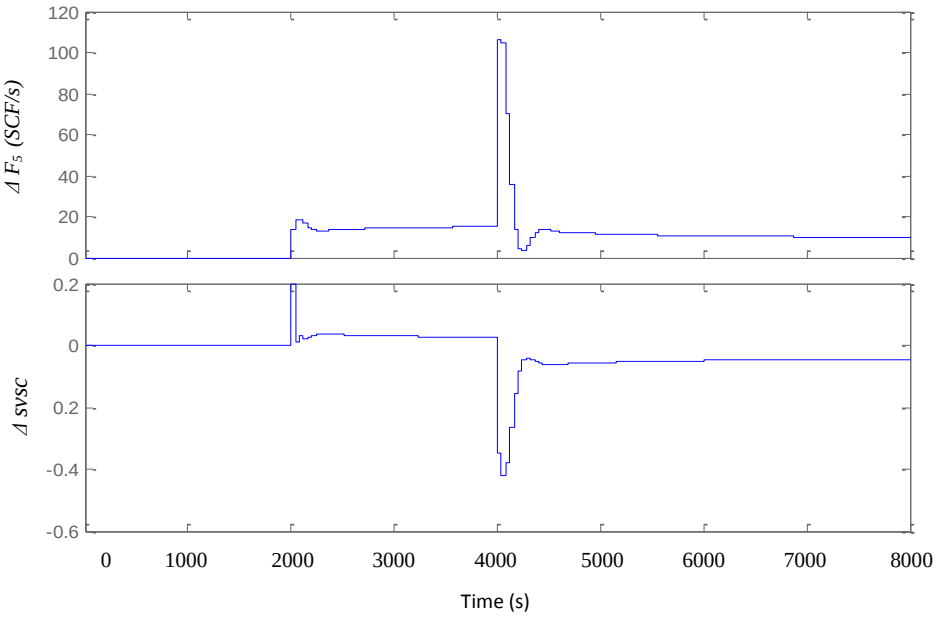

Figure 6.2: Manipulated variables for the 2x2 LMPC control scheme.

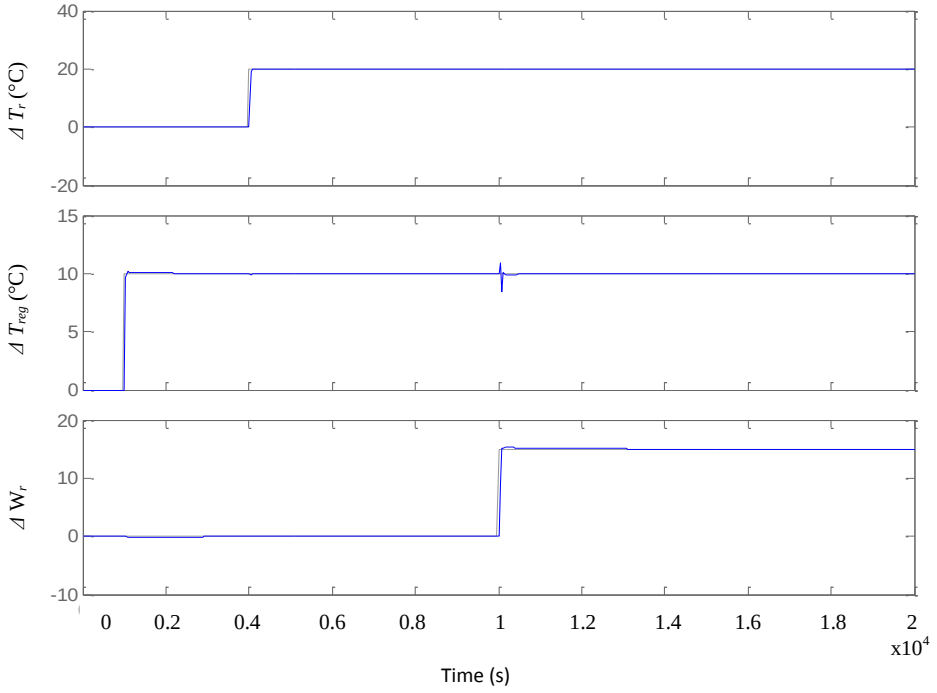

Figure 6.3: The 3x3 LMPC simulation results with the controlled variable response for setpoint change for T_r , T_{reg} and W_r at different times.

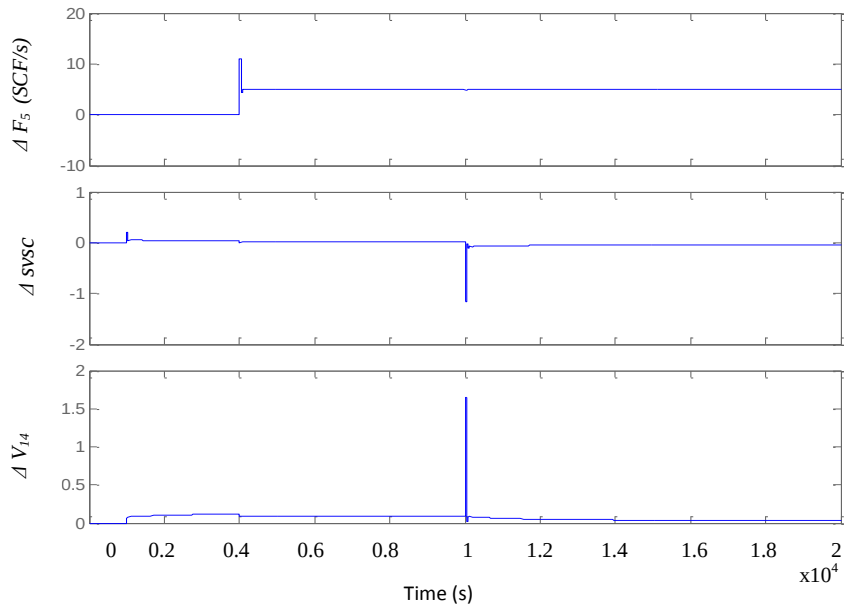

Figure 6.4: Manipulated variables for the 3x3 LMPC control scheme.

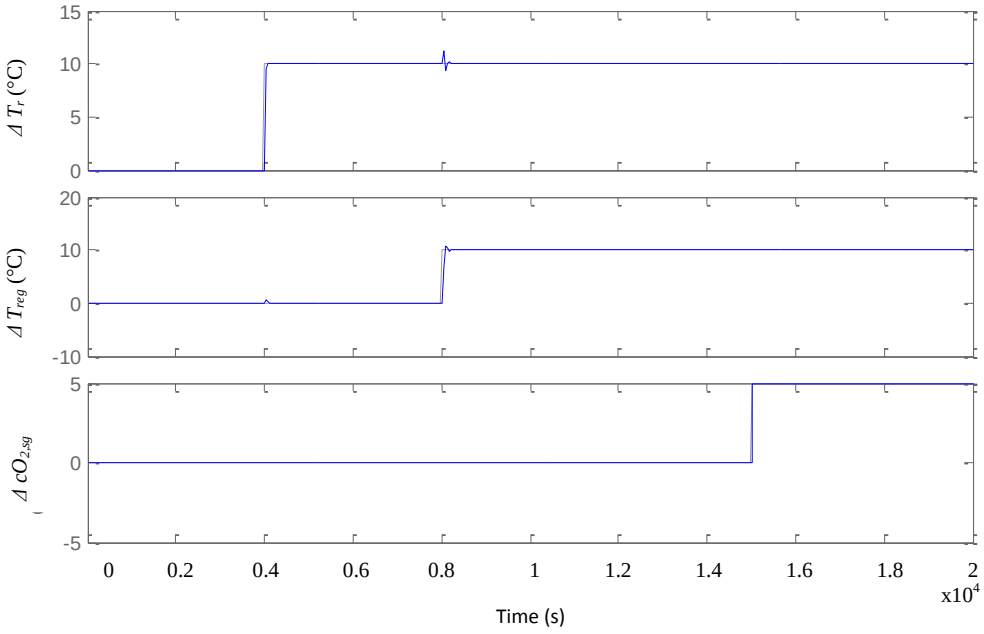

Figure 6.5: The 3x3 LMPC simulation results with the controlled variable response for setpoint change for T_r , T_{reg} and $cO_{2,sg}$ at different times.

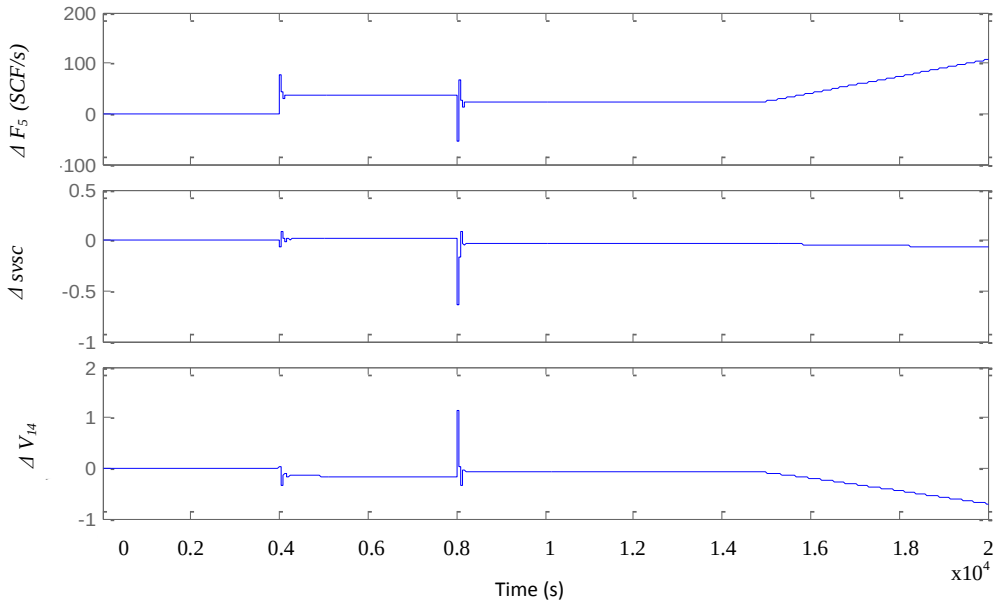

Figure 6.6: Manipulated variables for the 3x3 LMPC control scheme.

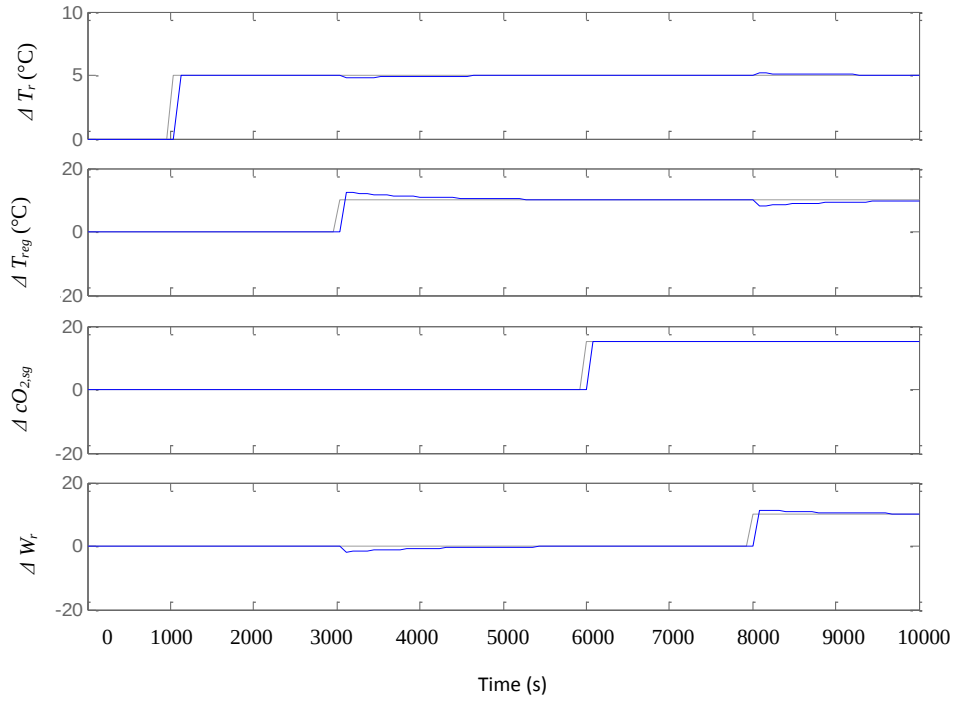

Figure 6.7: The 4x4 LMPC simulation results with the controlled variable response for setpoint change for T_r , T_{reg} , $cO_{2,sg}$ and W_r at different times.

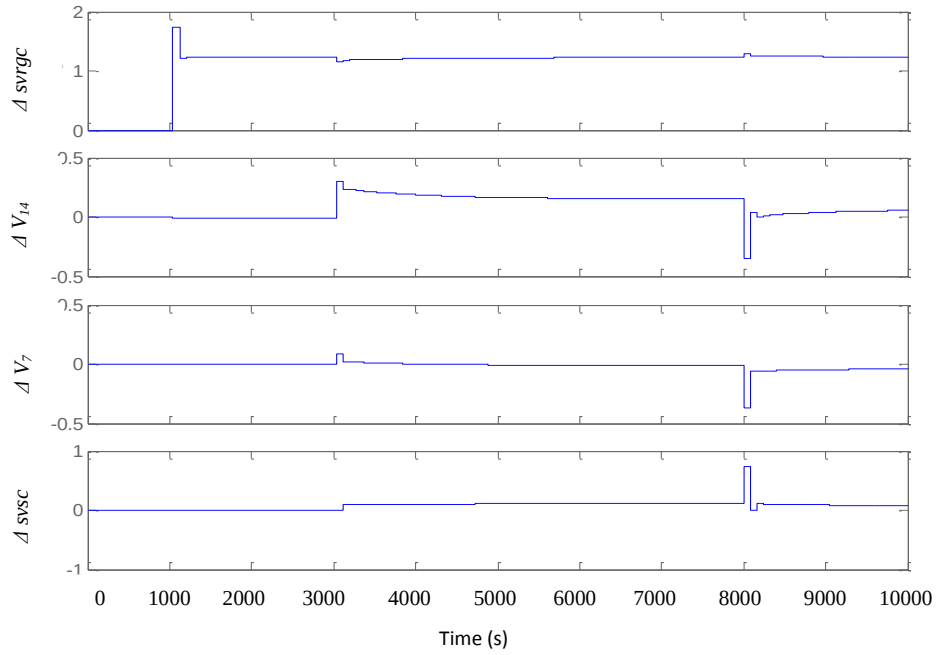

Figure 6.8: Manipulated variables for the 4x4 LMPC control scheme.

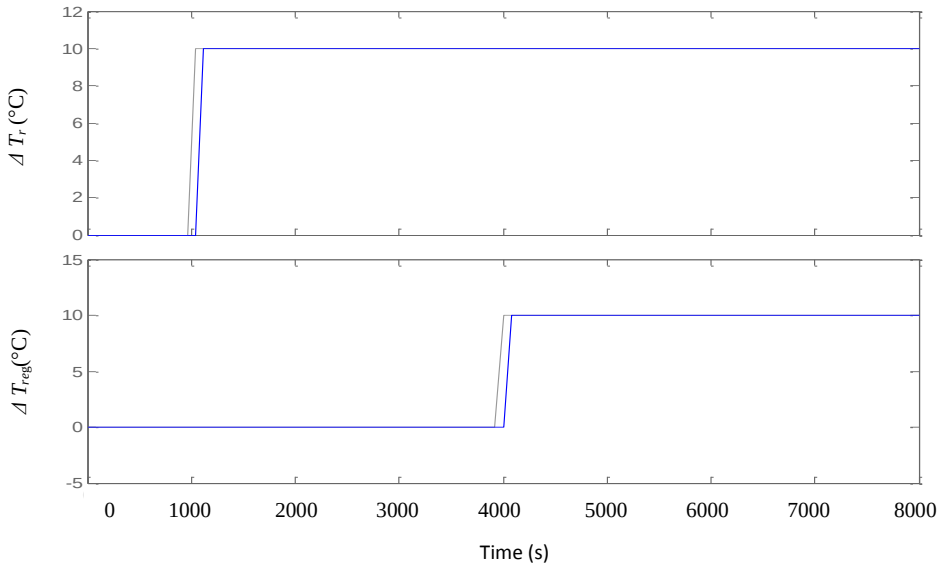

Figure 6.9: The non-square 4x2 MPC simulation results setpoint change for T_r and T_{reg} at different times.

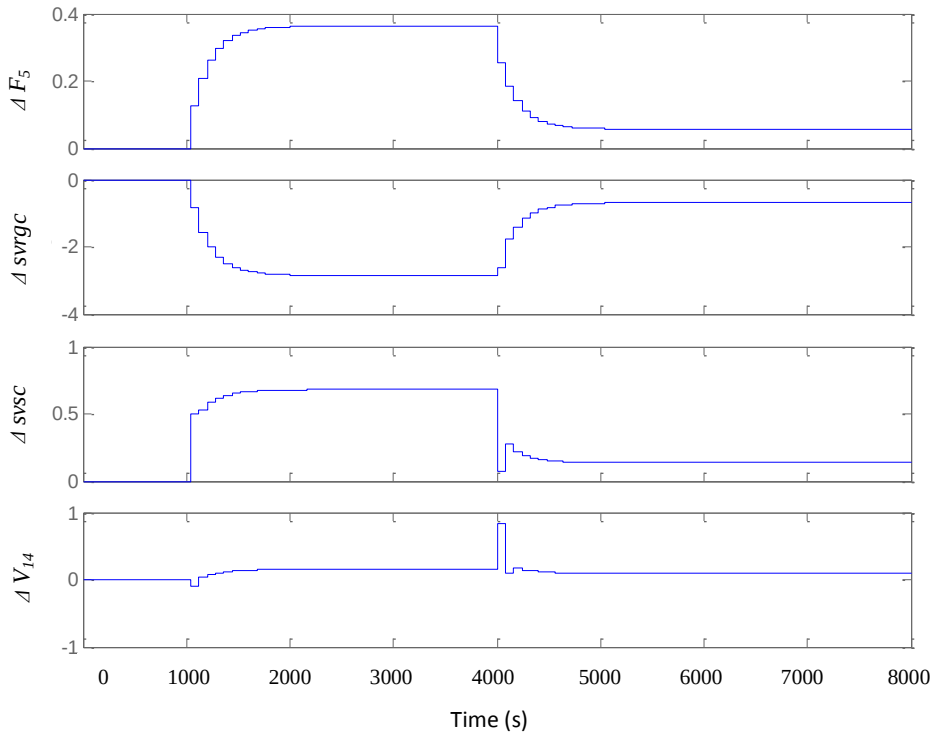

Figure 6.10: Manipulated variables for the non-square 4x2 control scheme.

6.2.2 Linear MPC applied to the nonlinear model-based plant simulator

In real model-based control application a mismatch always exists between the actual process and the model. The mismatch may be structural or parametric; the former is when process and model differ, whereas the latter is when parameter values differ between model and actual process. As the difference increases, the response of the closed loop will deteriorate, in terms of properties important to industrial implementation, namely overshoot and rise time. With a proper model, signifying little mismatch, the process exhibits minimal overshoot, and short rise time, but in the presence of mismatch and large perturbations, these cannot be maintained.

This study aimed to simulate the realistic scenario when model-plant mismatch exists, due to the application of the linear model predictive control to a real nonlinear plant. In this study the real-plant is represented by the detailed first-principles nonlinear model described in Chapter 3, whereas the model used in the controller is a linear model obtained via linearization of the nonlinear model. The Simulink block diagram with the implementation of this control scenario is shown in Figure

6.11 the 2x2 LMPC scheme with T_r and T_{reg} as the controlled outputs and F_5 *and svsc* as the manipulated inputs.

The result obtained in the case step change in the setpoint is presented in Figure 6.12. The MPC tuning was performed by choosing the output and input weights based on the maximum allowable deviation of the corresponding variables, followed by a trial and error refining step.

A very good control performance was achieved when the setpoint change was small as indicated in Figure 6.12. However if the magnitude of the setpoint change increases by 5 ◦C the LMPC fails to control this strongly nonlinear plant. This is expected since the predictions are based on the linear model obtained in the original operating point and as the process deviates from this operating point the model-plant mismatch increases and the control performance deteriorates. Generally these deviations and increasing model-plant mismatch may lead to stability problems in practical implementations. One approach to improve robust performance is to use different linearized models in the LMPC controller obtained in different operating points, and automatically choosing the corresponding model based on the operating region of the FCCU.

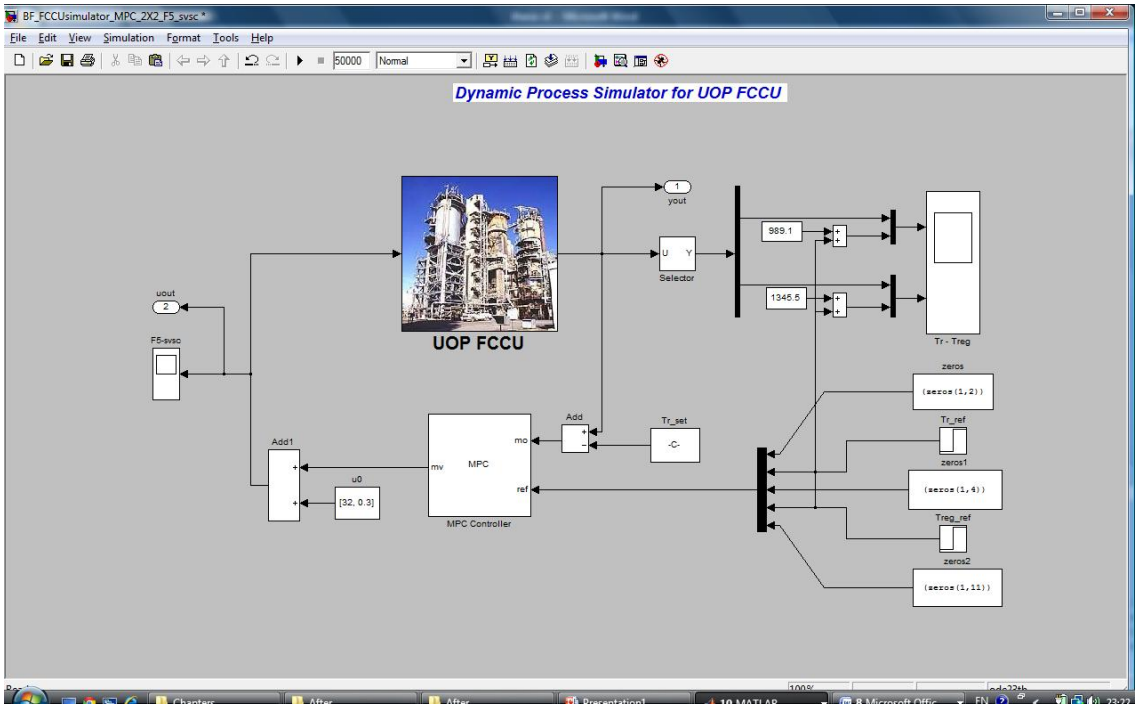

Figure 6.11: MPC block diagram for FCCU.

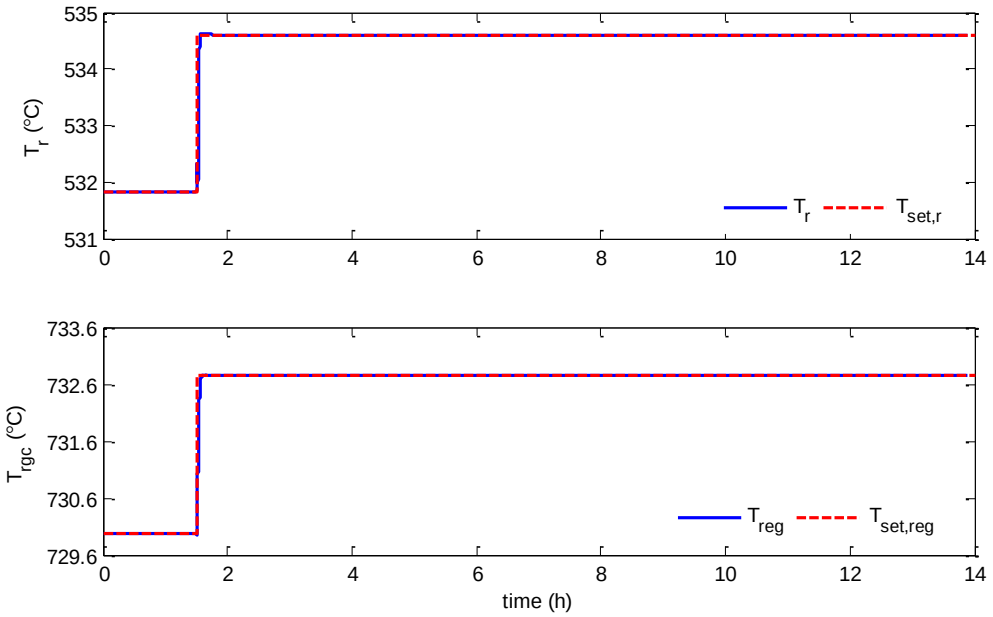

Figure 6.12: Simulation results with the LMPC applied to the plant represented by the nonlinear process model, in the case of setpoint changes in T_r and T_{reg} , at t=1.5 h.

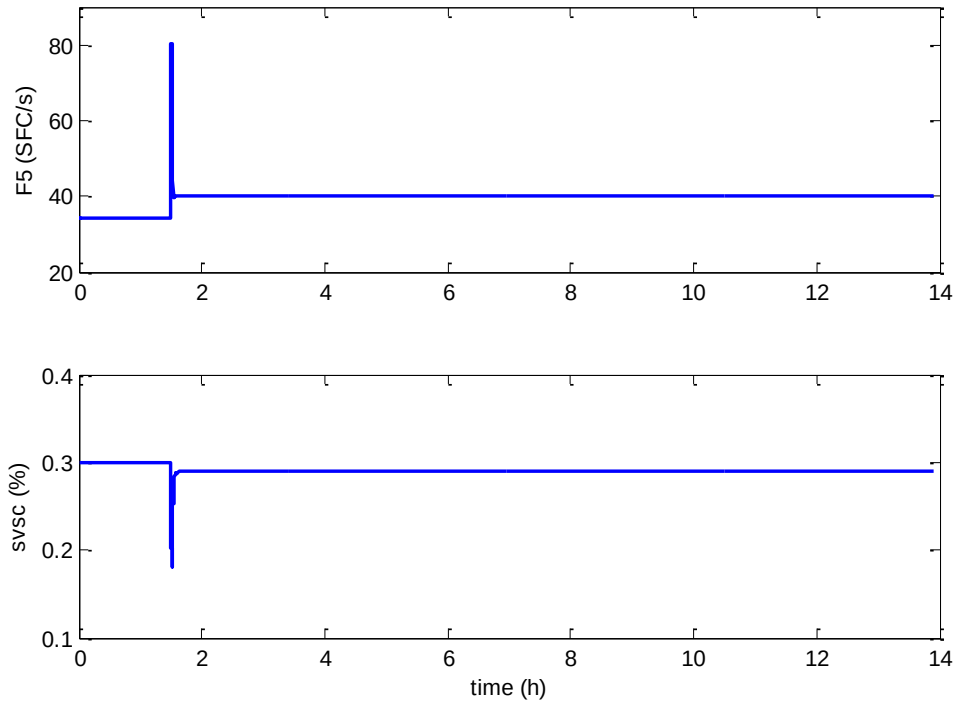

Figure 6.13: Manipulated variable response for set point change in the output, for 2x2 control scheme.

6.3 Nonlinear model predictive control (NMPC) of the FCCU

In this section, an efficient algorithm is presented and applied for the non-linear MPC of the FCCU. Chemical processes are typically non-linear, and as such, control system performance is generally governed by its ability to handle process non-linearity. Linear MPC schemes where linear models are used for prediction are in common use in various sectors, and so control issues, such as stability have been fully addressed. In contrast, non-linear MPC schemes are relatively new, appearing in the last twenty years, but with a growing base of applications (Agachi et al., 2006).

6.3.1 Efficient real-time iteration based NMPC approach

The optimal control problem to be solved on-line in every sampling time in the generic NMPC algorithm (Nagy et al., 2007) can be formulated as:

Problem $P_1(t_k)$:

$$\min_{u(t)\in\mathcal{U},\, t_k^F} \mathcal{H}(x(t), u(t); \theta) \tag{6.1}$$

subject to:

$$\dot{x}(t) = f(x(t), u(t); \theta), \tag{6.2}$$

$$y(t) = g(x(t), u(t); \theta), \tag{6.3}$$

$$x(t_k) = \hat{x}(t_k), \quad x(t_0) = \hat{x}_0, \tag{6.4}$$

$$h(x(t), u(t); \theta) \le 0, \quad t \in [t_k, t_k^F], \tag{6.5}$$

where $\mathcal{H}$ is the performance objective, t is the time, t_k is the time at sampling instance k, t_k^F is the final time at the end of prediction, $t_0 = 0$ is the initial time, $x(t) \in \mathbb{R}^{n_x}$ is the n_x vector of states, $u(t) \in \mathcal{U}$ is the n_u set of input vectors, $y(t) \in \mathbb{R}^{n_y}$ is the n_y vector of measured variables used to compute the estimated states $\hat{x}(t_k)$ with initial values $\hat{x}_0$, $\theta \in \Theta \subset \mathbb{R}^{n_\theta}$ is the n_θ vector of possible uncertain parameters, where the set Θ can be either defined by hard bounds or probabilistic, characterized by a multivariate probability density function. The function $f : \mathbb{R}^{n_x} \times \mathcal{U} \times \Theta \to \mathbb{R}^{n_x}$ is the twice continuously differentiable vector function of the dynamic equations of the system, $g : \mathbb{R}^{n_x} \times \mathcal{U} \times \Theta \to \mathbb{R}^{n_y}$ is the measurement equations function, and $h : \mathbb{R}^{n_x} \times \mathcal{U} \times \Theta \to \mathbb{R}^{c}$ is the vector of functions that describe all linear and nonlinear, time-varying or end-time algebraic constraints for the system, where c denotes the number of these constraints.

The objective function in the case the typical receding horizon NMPC with the aim to minimize deviations from the setpoints can be expressed as of can have the following general form:

$$\mathcal{H}(x(t),u(t);\theta)=\int_{t_k}^{t_k^F}(\left\|y\ -y^{ref}\right\|_{Q_y}^2+\left\|u\ -u^{ref}\right\|_{Q_u}^2+\left\|\frac{du}{dt}\right\|_{Q_{\Delta u}}^2)dt \tag{6.6}$$

where, y^{ref} and u^{ref} are the output and input references, respectively, and $Q_{y,}\ Q_u, Q_{\Delta u}$ are weighting matrixes.

Efficient optimization via direct multiple shooting

The optimal control problem $P_1(t_k)$ is an infinite dimensional problem, which except in a few very simple cases is impossible to solve. The main idea behind direct methods is based on transforming the original infinite dimensional problem $P_1(t_k)$ into a finite dimensional nonlinear programming problem (NLP) by formulating a discrete approximation to it that can be handled by conventional NLP solvers (Biegler, 2000). The time horizon $t\in\pi_k=[t_k,\ t_k^F]$ is divided into N_p subintervals (stages) $\pi_{k,i}=[t_{k,i},\ t_{k,i+1}]$, $i=0,1,\ldots,N_p-1$, with discrete time steps $t_k=t_{k,0}<t_{k,1}<\ldots<t_{k,i}<t_{k,i+1}<\ldots<t_{k,N_p-1}=t_k^F$. The infinite dimensional continuous control input $u_k(t)$ is then parameterized into a piecewise representation $\tilde{u}_{k,i}(t,\mathbf{p}_{k,i})$ for $t\in\pi_{k,i}$ with N_p local control parameter vectors $\mathbf{p}_{k,0},\mathbf{p}_{k,1},\ldots,\mathbf{p}_{k,N_p-1}$ with $\mathbf{p}_{k,i}\in\mathbb{R}^{n_p}$ and the optimization problem is solved with the local control parameter vectors being the decision variables. In most of the practical application piece-wise constant or piece-wise linear control parametrization is used. In the simplest case, using piecewise constant parameterization, we have $\tilde{u}_k(t,\mathbf{p}_{k,0},\ldots,\mathbf{p}_{k,N_p-1})\triangleq[u_k,u_{k+1},\ldots,u_{k+N_p-1}]$.

Problem $\tilde{P}_1(t_k)$ gives the general discrete time formulation of problem $P_1(t_k)$:

Problem $\tilde{P}_1(t_k)$:

$$\min_{u_k,u_{k+1},\ldots,u_{k+N_p}}\{\mathcal{M}^{k+N_p}(x_{k+N_p};\theta)+\sum_{j=k}^{k+N_p}\mathcal{L}_j(x_j,u_j;\theta)\}, \tag{6.7}$$

subject to:

$$G_k(x_k,u_k;\theta)=0, \tag{6.8}$$

$$H_k(x_k,u_k;\theta)\le 0, \tag{6.9}$$

where N_p is the number of stages in the prediction horizon $[t_k, t_k^F]$, $G_k : \mathbb{R}^{n_x} \times \mathcal{U} \times \Theta \rightarrow \mathbb{R}^{n_x+n_y}$ corresponds to all equality constraints resulted from the algebraic equations (6.3) of the model or from the discretized model equations, $H_k : \mathbb{R}^{n_x} \times \mathcal{U} \times \Theta \rightarrow \mathbb{R}^{c+2n_u}$ is the vector function of all inequality constraints (6.5), including the constraints on the inputs considering. We consider here that the set of possible inputs is given as hard bounds. It is assumed that the vector functions G and H are twice continuously differentiable. Sequential Quadratic Programming (SQP) is generally considered as the most efficient numerical method available to solve nonlinear optimization problems (NLP). It has been shown that SQP requires the fewest function evaluations to solve NLPs (Binder et al., 2001). SQP is a quasi Newton method that treats nonlinear optimization problems by solving a sequence of local linear-quadratic approximations. The Lagrangian of the optimization problem is approximated quadratically, typically by applying a numerical update formula. Constraints are approximated linearly. SQP methods generally apply the equivalent of Newton steps to the optimality conditions of the NLP problem achieving fast rate of convergence.

Several optimisation approaches have been proposed for the solution of the optimal control problem (6.7)-(6.9), including sequential approaches (Hicks and Ray, 1974; de Olivieara and Biegler, 1994), simultaneous approaches (Tsang et al., 1975; Biegler, 2000; Cuthrell and Biegler, 1989) and hybrid approaches such as direct multiple shooting (Bock and Plitt, 1984; Bock et al., 2000a; 2000b; Diehl, 2001; Diehl et al., 2002; E. ref 9).

Direct multiple shooting is one of the most efficient optimisation approaches available for the solution of the NMPC problems hence it was selected as the method applied in this work.The direct multiple shooting procedure consists of dividing up the time interval $[t_k, t_k^F]$ into *M* subintervals $[\tau_i, \tau_{i+1}]$ via a series of grid points $t_k = \tau_0 < \tau_1 < \tau_2 < \ldots < \tau_M = t_k^F$. Note that the grid points do not necessary correspond to the discretization points (N_p) in the definition of problem $\tilde{P}_1(t_k)$. Using a local control parameterizations a shooting method is performed between successive grid points (see Figure 6.14). The solution of the ODE on the M intervals are decoupled by introducing the initial values ω_i of the states at the multiple shooting nodes τ_i as additional optimization variables. The differential equations and cost on these intervals are integrated independently during each optimization iteration, based on the current guess of the control, and initial conditions ω_i. The continuity/consistency of the final state trajectory at the end of the optimization is enforced by adding consistency constraints to the nonlinear programming problem. The additional interior

boundary conditions, are incorporated into one large nonlinear programming problem (NLP) to be solved, which is given in a simplified form below (Nagy et al., 2007):

Problem P_2:

$$\min_{v} \mathcal{H}(v;\theta) \quad \text{subject to} \quad \begin{cases} G(v;\theta) = 0 \\ H(v;\theta) \le 0 \end{cases} \tag{6.10}$$

where the optimization variable v contains all multiple shooting state variables and controls

$$v = [\omega_0, u_0, \omega_1, u_1, \ldots, \omega_{M-1}, u_{M-1}, \omega_M]. \tag{6.11}$$

The discretized initial value problem and continuity constraints are included in the equality constraints:

$$G(v;\theta) = \begin{bmatrix} \omega_0 - \hat{x}(t_k) \\ \omega_{i+1} - x_i(t_{i+1};\omega_i, u_i) \\ y - g(\omega_i, u_i;\theta) \end{bmatrix} = 0, \tag{6.12}$$

and the inequality constraints are given by $H(v;\theta) = H(\omega_i, u_i;\theta) \le 0$, for $i = 0,1,\ldots,M$. The main idea of the direct multiple shooting algorithm is illustrated in Figure 6.14.

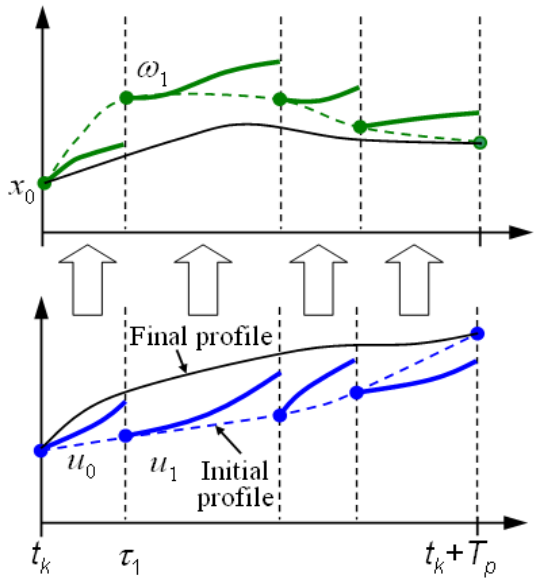

Figure 6.14: Illustration of the direct multiple shooting algorithm.

Real-time NMPC algorithm

The solution of problem P_2 requires a certain, usually not negligible, amount of computation time δ_k, while the system will evolve to a different state. In this case the optimal feedback control $u^{\star}(t_k) = [u_{0|t_k}, u_{1|t_k}, \ldots, u_{N_p|t_k}]$ computed in moment t_k corresponding to the information available up to this moment, will no longer be optimal. Computational delay δ_k has to be taken into consideration in real-time applications. In the approach used here, in moment t_k, first the control input from the second stage of the previous optimization problem, $u_{1|t_{k-1}}$, (which corresponds to the first stage of the current optimization) is injected into the process, and then the solution of the current optimization problem is started, with fixed $u_{0|t_k} = u_{1|t_{k-1}}$. After completion, the optimization idles for the remaining period of $t \in (t_k + \delta_k, t_{k+1})$, and then at the beginning of the next stage, at moment $t_{k+1} = t_k + \Delta t$, $u_{1|t_k}$ is introduced into the process, and the algorithm is repeated. This approach requires real-time feasibility for the solution of each open-loop optimization problems ($\delta_k \leq \Delta t$).

Initial value embedding strategy

The initial values embedding strategy originally proposed by Bock et al. (2000b), can significantly enhance computational performance. The approach is based on the fact that optimization problems at subsequent sampling times differ only by the initial values that are imposed through the initial value constraints. Accepting an initial violation of these constraints, the solution trajectory of the previous optimization problem can be used as an initial guess for the current problem. Since in the direct multiple shooting approach the decision variables include both the control input and the initial values of the states and the discretization points, for this approach to work efficiently the entire decision vector (control plus states) has to be initialized with the solution of the previous optimisation problem. Furthermore, all derivatives as well as an approximation of the Hessian matrix are already available for the solution trajectory from the previous step, and these can be used in the new problem. In this way the first QP solution can be performed without any additional ODE solution, leading to a computationally highly efficient approach (Diehl et al., 2002).

Solution tool for efficient BNMPC implementation

The solution of problem P_2 can be performed using various optimization packages. The NMPC tool, OptCon, (Nagy et al., 2004) based on the sequential-quadratic-programming (SQP) type optimizer HQP (*Franke et al.*), which is used in conjunction with the implicit differential-algebraic-equation (DAE) solver, DASPK, for robust and fast solution of the model equations (Li and Petzold, 1999), has been successfully applied in various applications including the control of an industrial pilot scale polymerization reactor (Nagy et al., 2007). OptCon includes a number of desirable features. In particular, the NMPC is based on first-principle or grey-box models, and the problem formulation is performed within Matlab® (The Mathworks Inc.), which is the most widely used modeling and control environment for control engineers. The model used in the controller has to be developed in the form of Simulink® (The Mathworks Inc.) "mex S-function" using C language. The S-function interface of the optimization tool provides convenient and fast connectivity with Matlab®. The NMPC implementation offers an efficient approach based on the direct multiple shooting algorithm, that exploits the special structure of optimization problem that arise in NMPC. The software uses low rank updates of the approximation of the Lagrangian Hessian of the nonlinear subproblems combined with a sparse interior point algorithm for the efficient treatment of the linear-quadratic subproblems in the nonlinear SQP iterations. Bounds and inequality constraints are handled using a barrier method and line search is used for global convergence of the SQP iterations. OptCon implements the real-time approach, and also provides an OPC connectivity, making it appropriate for rapid real-time prototyping of NMPC algorithms in industrial environment.

6.3.2 NMPC FCCU simulation results

The complex dynamic model of the FCCU was used in the NMPC algorithm. The 2×2 control structure is presented as one of the simulations performed. The two controlled variables are: reactor temperature T_r and regenerator temperature T_{reg}. The two manipulated inputs are: fuel flow F_5 and slide valve positions *svsc* on the spent catalyst circulation line. The coking rate factor Ψ_f change (5% step increase at moment t = 5000 s) has been selected as a typical disturbance. The control of presented variables is important for the efficient and safe operation of the unit, and has direct impact on the products yield. The reactor temperature has to be maintained at a certain level to provide a desired maximum conversion of the feed oil. Proper reactor and regenerator temperature

control also means good management of thermal energy. A set of tested scenarios is presented in Table 6.3.

Table 6.3: Tested scenarios for NMPC simulations.

Case	Disturbance	Setpoint change		NMPC tuning parameters (duration, prediction and control horizon and weight)
		Step increase	Step decrease	
1	N/A	T_r→551, at 2000 s T_{reg}→729, at 3000 s	T_r→547, at 4000 s T_{reg}→727, at 4000 s	[8000 s ,(T_s = 100, p = 5, m = 5), $Q_{\Delta u}$ = 10]
2	+ 5 %, at 5000 s	T_r→546.6, at 2000 s T_{reg}→741, at 3000 s	-	[8000 s , (T_s = 100, p = 10, m = 5), $Q_{\Delta u}$ = 10]

Two different scenarios are considered:

(i) **NMPC without anticipation –** in this case the setpoint change is treated as a disturbance which happens unexpectedly. The NMPC will react only after the setpoint change has been applied to the process.

(ii) **NMPC with anticipation** – in these simulations it is assumed that the moment when the setpoint change will occur is known beforehand, and is programmed in the NMPC controller. In this case the NMPC can take into account during the prediction the future changes in the setpoints and hence can react before the actual change happens, to achieve optimal performance.

Figure 6.14 illustrates the performance of the NMPC with both anticipation and no anticipation scenarios. The first setpoint change in T_r and T_{reg}, respectively, are considered known a priori and were programmed in the NMPC from the beginning of the simulation. Therefore the controller can react anticipating the change in the future resulting in very good setpoint tracking performance. The second simultaneous setpoint change at 4000 s, are considered as disturbance, in the sense that they are not programmed in the NMPC. This could correspond to a realistic scenario when sudden change in the operating conditions have to be applied immediately e.g. due to safety considerations. It can be seen that in this case the NMPC reacts with delay, since the change of the setpoint is only

detected at the next sampling time after the change occurred. Due to the real time iteration scheme, according to which the control action is implemented with one sampling period delay, the NMPC practically can only react to the unanticipated setpoint change after two sampling periods.

The CPU times corresponding to the NMPC calculations in each iterations and the number of SQP iterations are presented in Figure 6.16. It can be observed that the maximum number of iterations (set to 5 SQP iterations in these studies) is achieved when the setpoint changes occur, however the real-time iteration scheme and initial value embedding strategy allow the convergence of the optimisation problem over several iterations without considerable decrease in control performance. The maximum total computational time (approximately 65 s) is well below the sampling time of 100 s. The results demonstrate that the efficient optimisation scheme and tool used here can guarantee the real-time feasibility of the NMPC implementation, with very good control performance even for a model with a large number of ODEs.

Additionally the benefits of designing control systems in which a sepoint change can be programmed in with anticipation are highlighted. Since the control performance can be significantly improved if the predictive controller can take a future setpoint change into account, it is important to design the control systems to allow specifying the setpoint change *and* the time when that must occur, and operators need to be aware about the benefits of programming the future change into the controller in advance.

Figure 6.17 illustrates the results for case 2, considering NMPC with anticipation for setpoint change and in the case of a measured disturbance scenario. The setpoint change in the T_r is very well followed by the NMPC, however the control performance degrades when the change in T_{reg} occurs. Careful examination of the control variables show that one of the manipulated variables (*svsc*) saturates in this case, which causes the decreased tracking performance. At t= 5000 s a 5% increase in Ψ_f occurs. It is assumed that the disturbance is measured and the NMPC is able to reject the effect of the disturbance. The controller reacts to the disturbance as can be observed from the variation in the manipulated inputs, but no deviations in the controlled output is observed, indicating the excellent disturbance rejection ability of the NMPC system.

The NMPC provides stable closed-loop response in both simulate scenarios with very good setpoint tracking and disturbance rejection performances. The NMPC is able to provide a very good decoupled response with minimal disturbance in the controlled outputs when the setpoint change occurs for one of the outputs only.

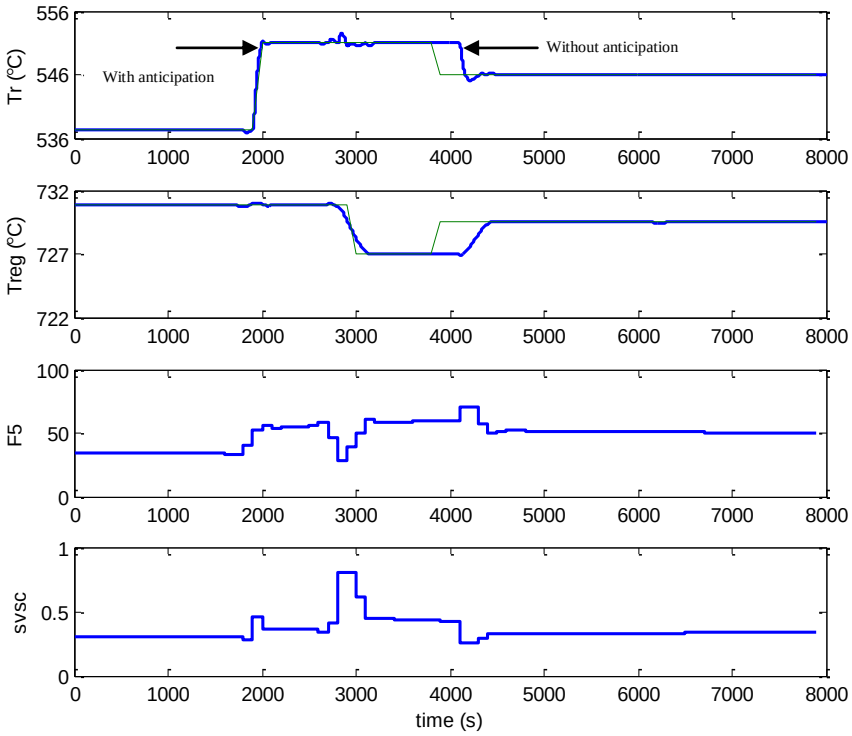

Figure 6.15: Performance of the NMPC in the case of setpoint change with and without anticipation.

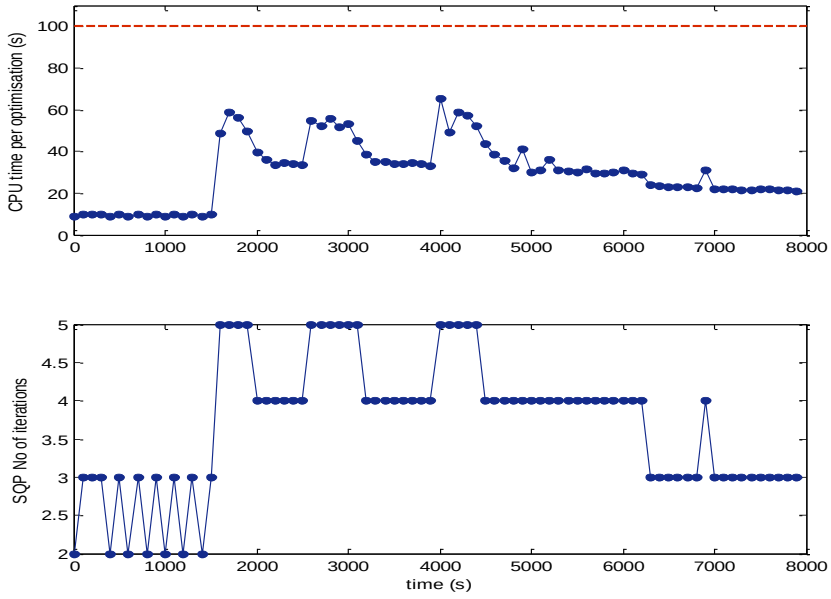

Figure 6.16: CPU times required for the optimisation problems of the NMPC

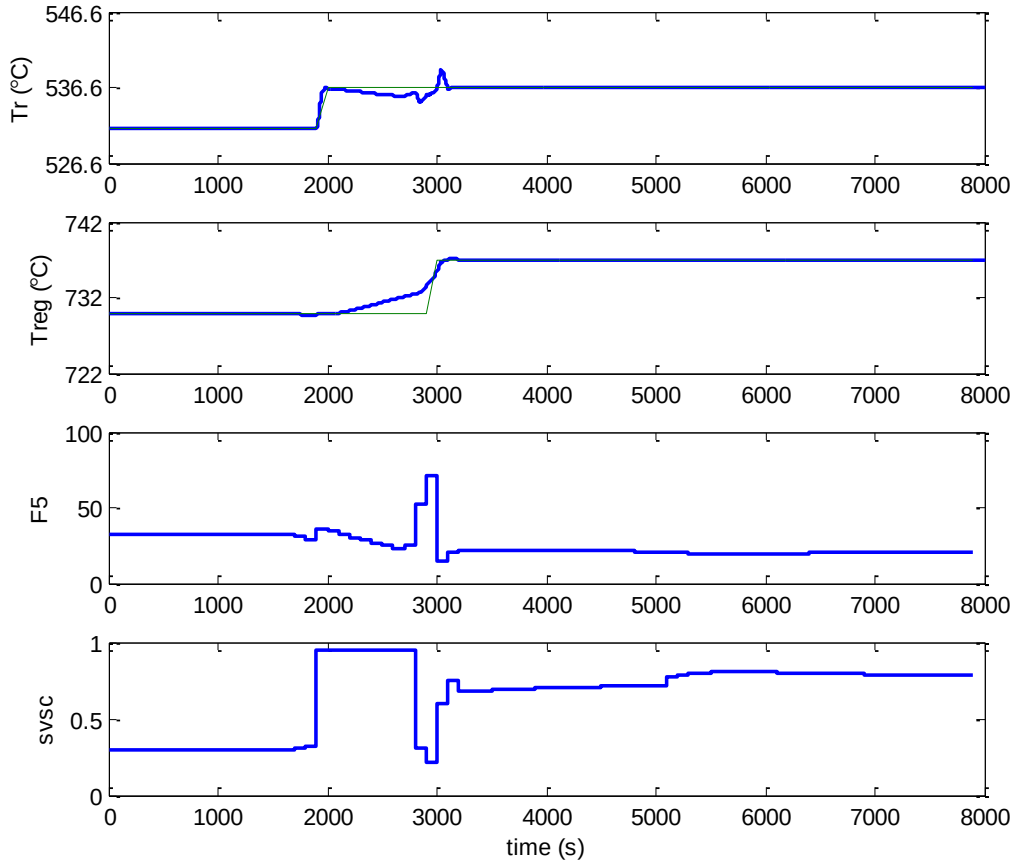

Figure 6.17: Performance of the NMPC in the case of setpoint change with anticipation and a measured disturbance (5 % step increase at t = 5000 *s* in Ψ_f).

6.4 Conclusions

The FCC unit is the most complex and challenging unit in a modern refinery. The success of any advanced control application (linear or nonlinear) on this unit depends on the ability to deal with the operating constraints, and to address the economic objectives.

A comprehensive analysis of several multivariate linear MPC (LMPC) schemes is presented. The results demonstrated the importance of including the fuel flow to the furnace among the manipulated input in a multivariate control scheme. The potential benefits of using non-square control structures are also demonstrated. The robust performance of the LMPC is evaluated in the case of model-plant mismatch, when the plant is represented by the complex nonlinear model, whilst using linear model for prediction in the MPC.

To further improve the control performance an efficient nonlinear model predictive control approach (NMPC) is implemented to the FCCU. The approach used is based on a real-time iterations scheme with initial value embedding, and is based on a highly efficient multiple shooting optimisation approach to achieve real-time feasibility. The efficient NMPC approach is evaluated for setpoint tracking and disturbance rejection. For setpoint tracking two different scenarios, with and without anticipation are considered. The results demonstrate that superior performance of the NMC scheme and highlight the importance of the implement setpoint changes into the controller in advance whenever this is possible to achieve better control performance.

Both NMPC and LMPC were superior, and it was also shown that NMPC provided better performance compared to LMPC. The performance advantage could be noted in terms of overshoot, settling time, and maintaining the controlled variables within the limiting constraints of the plant. Furthermore, the potential for practical implementation of the NMPC approach in the industrial context of complex chemical processes has been demonstrated. These results have demonstrated that the control structures proposed may be applied in industry in the form of a new scheme for controlling highly complex chemical processes.

CHAPTER 7
ECONOMIC OPTIMIZATION OF FCCU

7.1 Dynamic Real - time Optimization (DRTO)

In the process industry, a main challenge is to ensure optimal plant operation regardless of constantly varying materials and conditions, whether composition of feedstocks, rates of production, prices of material inputs and outputs, or energy availability. In this complicated context, the concept of Real-time Optimisation (RTO) was introduced in an attempt to ensure that a process is optimised for given economic constraints. The process is optimised through RTO, from the perspective of target profit or cost, and so profit-seeking enterprises can make sure that their plant is achieving optimal profitability, even as operating parameters and materials are subject to change. In typical form, RTO assumes that transient perturbations may be disregarded over a sufficiently large interval, as the process achieves the steady state. A typical RTO system consists of parts for detecting the steady state, acquiring and validating data, updating the process model, solving the optimisation problem, and applying operating policies (Adetola, 2008).

Given the surge in interest in Dynamic Real-Time Optimization (DRTO) or Non-linear Model Predictive Control (NMPC) for economic process optimisation (Backx et al., 2000; Helbig et al., 2000; Engell, 2007; Rawlings and Amrit, 2008; Zavala, 2008), efficient means to solve such optimisation problems have witnessed significant progress. Economic optimisation control schemes have advanced beyond the usual implementation of NMPC based on quadratic cost criteria that are minimised in terms of the deviation from a steady state set value. In economic NMPC all the dynamic degrees of freedom are considered in ensuring maximum economic profit over a specific time interval. A further point is that maximum profit is achieved at high frequency sampling rates, compared to the low sampling rates characteristic of conventional steady-state optimisation, and only during the process steady state. Therefore, DRTO effectively manages perturbations, and ensures that these are exploited optimally for maximum profit, compared to simple compensation for deviation from a steady state set value. However, sufficient research on DRTO and NMPC from an economic perspective has not been performed.

The strategy of DRTO based on an economic perspective was introduced (Helbig and Marquardt, 2007; Kadam and Marquardt, 2007), and is shown in Figure 7.1. Compared to the conventional approach, DRTO does not distinguish between dynamic and steady states, but engages in directly optimising the process according to economic criteria over the prediction horizon. Such a strategy involves calculating a solution to the NMPC problem utilising an economic objective function derived from first-principle dynamic models. In this context, process control actions are generated based on an economic objective; this particular control structure was first proposed by Morari et al. (1980).

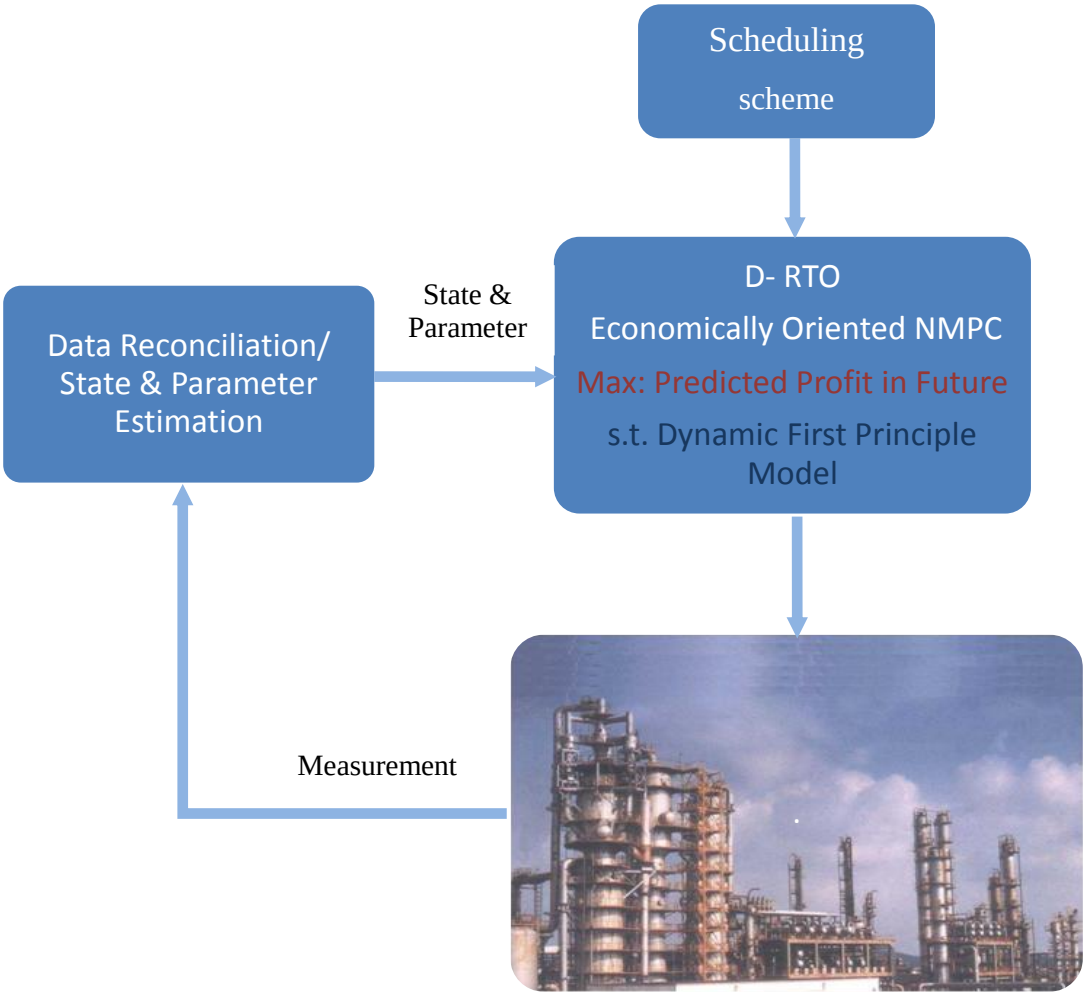

Figure 7.1: Illustration of D-RTO or Economically-Oriented NMPC

Over recent years, a number of workers have further refined DRTO or NMPC oriented towards profit maximisation. Such a control scheme was applied to a fluidized bed catalytic cracker (Zanin et al., 2000), while an MPC scheme integrating RTO was also proposed (Adetola and Guay, 2010).

Further progress took the form of a controller based on a receding horizon applied to constrained nonlinear process plant was also proposed (Angeli and Rawlings, 2010). For economically-optimised NMPC, an infinite-horizon formulation was proposed (Wurth et al., 2009). In an approach utilising a search technique for the general extremum, closed loop stability was studied with regard to optimisation from the economic perspective (Krstic and Wang, 2000). With the assumption of significant duality, an NMPC with an economic orientation was analysed in terms of nominal stability property (Diehl et al., 2010). Moreover, it was reported that multiple solutions result from formulations utilising linear economic objective functions, where a number of degrees of freedom remain to be optimised, and may be used to enhance operability through computing a second optimisation problem (Huesman et al., 2008). On the other hand, for efficient process economic optimisation, it has been reported that, at times, rapid achievement of the steady state may not be beneficial. Moreover, a turnpike-like trend results from an economic objective formulation (Rawlings and Amrit, 2008). While it seeks to follow a constant path, in the final part of the horizon, the trendline departs from the constant. Such a trend has also been previously reported in the economics literature, as being a feature of economic optimisation problems (Carlson et al., 1991).

A number of workers have addressed the problem of FCC process optimisation, where Rhemann et al. (1989) demonstrated an advanced control approach with systematic optimisation. In another study, a fitting model was used to derive five independent variables (preheat and reactor temperatures, and rate of feedstock, and HCO supply, as well as slurry recycling), where the generalised reduced gradient (GRG) technique was used to solve the economic objective function. Subsequently, optimised set values were input to the control system. For a residual catalytic cracking (RCC) unit, model-predictive control, with on-line optimisation, was applied (Cutler and Perry, 1983). This comprised a 40 equation, 20 independent variables, black box system for which a regression was performed using a large dataset covering different plants. The successive quadratic programming (SQP) technique was utilised to both formulate and solve the objective function containing constraints on variables; as a result, optimised set values for the process model-predictive controller were generated. The regression equation aspect of the optimisation scheme, means that not all the process behaviour is captured, which necessitates frequent updates of the model. An empirical model for predicting cracking products yield was combined with energy and mass balance, at macroscopic level, to form a Model IV FCC unit optimisation model (Ellis et al., 1998). Subsequently, a performance comparison was made between on-line and off-line optimisation, in terms of varying product pricing structure, and feedstock composition. However,

the work is not of direct industrial value, since the Model IV FCC unit lacks riser or slide valves, and is an outmoded plant type, which has been superseded by the upgraded FCC unit.

7.1.1 Integrated Real-Time Optimization and Control

The traditional approach to optimisation and control involves layers, in which the upper supervisory or optimisation layer is separate from the lower control layer; in this scheme, optimised control values are generated in the real-time optimisation (RTO) layer, and then passed down to the control layer for implementation. A steady state model is the basis for the RTO, and as such executed once the process achieves the steady state. In its separate layer, process control values are generated utilising a different model and frequencies. In this context, these two separate layers do not process the same data, which creates conflict and so predicted operating values may not be optimal; integrating both layers are still subject of research, and workers have attempted to tackle this systematically. The theory for such an integrated approach, in regard of performance and stability analysis, is well established. At present, two major classes have been proposed based on either model type or RTO execution frequency (Adetola, 2008).

1. *Single level strategy*: This approach involves the simultaneous solution of both the control and economic optimisation problems; this is achieved by including the economic objective term in the standard MPC objective function, and so a single algorithm MPC solves both problems (de Gouv'ea and Odloak, 1998; Zanin et al., 2002). This non-linear objective function contains both constraints that are steady state and dynamic, which must be resolved. In order to achieve the desired performance and stability, tuning of the relevant weighting factors is needed to properly implement this extended controller. The weighting factor values are determined by a significant amount of simulation (Zanin et al., 2002), which differs from a linear MPC scheme for which tuning is subject to specific guidelines. The single layer strategy allows rapid responses to changes in process variables, more so than in a two layer implementation. The disadvantage is that this strategy is only suitable for processes with short settling time, to which a linear model can be applied.

2. Two level strategy: This represents the classical hierarchical control structure, which aims to take into consideration the process' dynamic and non-linear behaviour. Typically, this approach is based on the idea of two levels; on the upper level, the economic optimisation as a dynamic process is addressed, while on the lower level, the non-linear MPC computations are performed (Kadam et al., 2002; Kadam et al., 2003; Zhu et al., 2004). Given the existence of two distinct layers, their

solution cycles need not follow the same sample intervals; hence, the RTO may be performed only when a disturbance or change occurs in the process conditions. As such, the RTO may be triggered by a disturbance sensitivity analysis, which detects persistent disturbances having high sensitivities (Kadam et al., 2002; Kadam et al., 2003). The RTO algorithm is based on dynamic models, in which appropriate set points are recalculated whenever economic benefits can be secured. A key factor in the success of this approach is the interaction of these two layers. The potential drawbacks to this approach revolve around the varying dynamic models that are applied.

The decomposition of the real-time economic optimisation of the process into a single layer or two has been proposed by many workers (Mohsen et al., 2011; Glauce et al., 2010; Wurth et al., 2009; Ioannis, 2005; Haruo et al., 2004; Zanin et al., 2002; Zanin et al., 2000; Loeblein and Perkins, 1999; Miriam et al., 1998; Robert et al., 1998).

7.2 Process optimizer for Economic NMPC of the FCCU

The FCC unit economic optimisation has a simple objective, to achieve the maximum profit from the process (Han et al., 2004). Therefore, the objective function seeks to maximise the difference between material and operating costs, and the market value of the products yielded by the process; this is given by:

$$\max_{u}\left\{ f\left(x,u,p\right)=-\sum_{p=1}^{N_{ps}} F_{pMF}w_{pMF}+\sum_{k=1}^{N_{fs}} F_{kFJ}w_{kFJ}+C_{opr}\left(x,u,p\right)\right\} \qquad (7.1)$$

where $F_{p\,MF}$ represents the product streams (LPG, gasoline, HCO and LCO); F_{kFJ} represents the feedstock streams (gas oil and slurry recycles); and C_{opr} represents the operating cost (cost of utility consumption and generation, and others).

A different objective function, which maximised the difference in feedstock and products value, was proposed (Umesh and Armando, 1998). In a simplification of the function, utility costs, comprising fuel, power consumption, etc, were considered negligible. However, the disadvantage in neglecting these terms is that a false premise will result, where using more power to produce a greater amount of products will be considered an optimum, while this is not actually the case, as there is a rise in cost associated, for example, with driving compressors at the maximum. Furthermore, there is an implicit assumption that the market has unlimited capacity to absorb whatever quantity of product is produced. Another assumption is that any unused feedstock is fully

recovered, and maintains its value. With the exception of wash oil and diesel feedstocks, the resulting cost function is given by:

$$C = \left(F_3 - F_{ugo}\right)v_3 - F_{gl}v_{gl} - F_{gs}v_{gs} \tag{7.2}$$

where F_3 flow of gas-oil feed, gal/s, F_{gl} flow of gasoline, gal/s, F_{gs} flow of lighter gas, gal/s, F_{ugo} flow of unused (uncracked) gas-oil, gal/s. v_3 value of gas-oil feed, \$/gal, v_{gl} value of gasoline, \$/gal, v_{gs} value of lighter gas, \$/gal.

Costs with respect to the manipulated variables and utilities can also be included for a more detailed representation of the actual costs.

7.2.1 One layer economic NMPC of the FCCU

In a hierarchical dynamic real-time optimisation and control scheme, the upper level is typically that of the optimisation algorithm, where the FCC optimum economic operating values are determined. The solution of the optimisation problem posed is achieved using the SQP algorithm, which incorporates an economic objective function, the process constraints set, and four decision variables addressed by the optimisation engine. The decision variables selected were the fuel flow rate, spent catalyst valve position, and the temperatures in the riser and regenerator. The existing typical constraints for an FCCU were described comprehensively by McFarlane et al. (1993). In this work, the manipulated variables and constraints selected for optimisation are presented in Table 7.1. Values were assigned to the different parameters, where the combustion air blower (operating range 60 ± 70 kg/s) was at maximum as indicated by a 100% open suction valve V_6; valve positions for the spent catalyst and regenerator were 0.3% open at the beginning; in operation, the wet gas compressor suction valve V_{11} was 95% open. The chosen combustion constraints followed the proposal by McFarlane et al. (1998), and comprised the choice of regenerator temperature and oxygen content of stack gas, or stack gas CO concentration of 350 ppm maximum. In the initial simulations, the stack gas CO concentration was used as a constraint in the DRTO. The variable process parameters were given by explicit expressions, following which the objective function was computed.

Table 7.1: Constrained and manipulated variables for application to FCC unit.

Constrained and manipulated variables	Min		Max
Fuel flow rate, SCF/s	10	F_5	70
Spent catalyst valve position, %	0.1	*svsc*	0.8
Oxygen concentration in stack gas valve, ppm	0	$cO_{2,sg}$	350
Regenerator temperature, °C	685	T_{reg}	760

In this work, simplified economic objective function was used, mainly focusing on optimising the product distribution, rather than taking production rates and cost of raw material or operational costs into account. The aim of this analysis was to show the advantage of adopting an economic NMPC strategy in order to adapt the operating conditions of the FCCU to obtain products that were adapted according to the varying trends in demand due to environmental, seasonal, or other changes. This objective function to be minimized is given by:

$$F_{econ} = w_1\, yhco + w_2\, ylco + w_3\, ygln + w_4\, yLPG + \\ + w_5\, ycoke + w_6 ycCO_{sg} + w_7 yCO_{2sg} \quad (7.3)$$

$$u_{min} \leq u \leq u_{max} \quad (7.4)$$

$$y_{min} \leq y \leq y_{max} \quad (7.5)$$

where $w_{1,2,\ldots\ i}$ cost related weighting coefficient. Three different scenarios were considered, corresponding to the scenarios in Table 7.2, represented by,

$$w_1 = [0\ -1\ 0\ 0\ 0\ 0\ 0] \quad (7.6)$$

$$w_2 = [0\ 0\ 0\ -1\ 0\ 0\ 0] \quad (7.7)$$

$$w_3 = [0\ 1\ 0\ 0\ 0\ 0\ 0] \quad (7.8)$$

The objective function presented here is typical of what is found in practice, in that a system of multiple variables requires real-time optimisation to achieve particular objectives that may vary, during the production, while being constrained in specific aspects. Two manipulated inputs were used in the control schemes evaluated, comprising of the fuel flow rate, u_1=F_5 (SCF/s), and spent catalyst valve position, u_2=*svsc* (%). The regenerator and reactor temperature are analysed during

the economic control scheme, since these represent the main controlled process outputs for the other control approaches, and their variations has a significant impact on the overall performance of the plant. Note however, that in the case of economic NMPC these outputs are not directly regulated.

A set of four cases were formulated for the optimisation of a FCC unit with a daily production of 46,000 barrels with the objective of profit maximisation. The optimisation cases were used to compare the performance of control algorithms for different market price scenarios (Table 7.2). The benchmark chosen for comparison was the first case, corresponding to a classical NMPC implementation which uses the advanced control algorithm to track predetermined but constant operating setpoints for the reactor and regenerator temperatures, similarly as described in Chapter 6. Although these values would in general be determined to achieve acceptable profit and performance corresponding to a particular raw material and operating conditions, this regulatory scheme is unable to adapt the operating conditions to achieve continuous profit optimisation.

Table 7.2: Scenarios of the operation studies

Case		Algorithms	Objective	Disturbance
1		NMPC	Benchmark study	Ψ_f + 5%
2	2.1	DRTO/NMPC	Maximize LCO	Ψ_f + 5%
	2.2	NMPC		
3	3.1	DRTO/NMPC	Maximize LPG	Ψ_f + 5%
	3.2	DRTO/NMPC with environmental constraint		
4		DRTO/NMPC	Minimize LCO	Ψ_f + 5%

The NMPC controller adopts the same tuning parameters and constraints as the DRTO/NMPC algorithm except for the weight of the economic components. The initial steady state of the FCC was given by: u_{ss} = [32 0.3] and for the reactor and regenerator temperatures, y_{ss} = [531.6 729.8] were used, which were also the setpoint values for the first, benchmark regulatory NMPC scenario. The prediction horizons used in the algorithm were: m = 3 and p = 3. The constraints on the manipulated inputs considered were: u_{max} = [70 0.8], u_{min} = [10 0.1]. In addition, the sampling period is equal to 100 s. The disturbance comprised 5% increase in the coking formation factor for all cases.

Case 1: Benchmark study using NMPC for regulatory control

This case presents the benchmark study when NMPC is used to regulate the reactor and regenerator temperature at their fixed setpoint values, and the control objective is to minimize any deviation from these setpoint values in the case of any process disturbance. The simulations performed are illustrated below in Figures 7.2 - 7.4. In Figure 7.2, the effect of the disturbance on the system's behaviour can be clearly seen. It is also clear that the controller can restore the temperatures by manipulating the inputs. The effects of corrective action can be seen as a decrease in LCO yield from 0.19 % to 0.17 % (Figure 7.3 (a)) and at the same time increasing LPG and gasoline percentage (Figure 7.3 (b and c)). Although this might be favoured, depending on the product requirement, but an undesirable significant increase in CO and decrease in O_2 amounts does not make this operating scenario feasible (Figure 7.4.(a and b)), due to potential violation of environmental constraints. Although this simulation scenario demonstrated the remarkable performance of the NMPC approach to keep the temperatures within very small variation around the setpoint (below ±0.2 °C compared to 5 °C in the open loop simulations shown in Chapter 4), the results emphasize several key observations:

(i) Good regulatory performance (maintaining the setpoint at its desired values) does not guarantee optimal operation of the plant in all disturbance scenarios. As it can be seen, in these results, despite the tight control of the process temperatures significant variations in the product distribution are caused by the disturbance related to the change in the quality of raw material.

(ii) Depending on the actual economic objective under which the FCCU operates at the moment when a disturbance occurs, from the economic operation point of view these disturbance can be differentiated as "beneficial" (good) and "harmful" (bad) disturbances, despite the fact that they both may cause deviation of the control system from its original setpoints. Note however that the same distrurbance may be considered "good" or "bad" depending of the economic objective under which the plant operates at the moment when the disturbance occurs. For example, if the FCCU operates under the economic objective expressed simply as to maximize the LPG concentration, a 5% increase in the coking factor, can be considered as a "beneficial" or "good" disturbance as it causes an increase in the LPG concentration (also shown in the case of the uncontrolled open loop simulations in Chapter 4). In this case, although the disturbance creates a deviation of the process temperatures from their original setpoints using control effort and utility costs to regulate the process at the original setpoint may actually reduce the economic objective than doing

no control at all. Certainly the process must be controlled under all conditions, but the control scheme should offer the possibility to adapt the operating conditions and potential exploit the effect of "beneficial" disturbance to achieve economically optimal operation, while maintain an operational, safety and environmental constraints.

(iii) Additional constraints e.g. related to environmental considerations should also be taken into account to achieve a globally optimal performance. Operating conditions which may maximize a particular economic objective related to the product composition but violate e.g. the furnace capacity to burn all resulting CO and hence violates environmental constraints are not acceptable.

In the following several economic NMPC scenarios are presented taking the aforementioned observations into account.

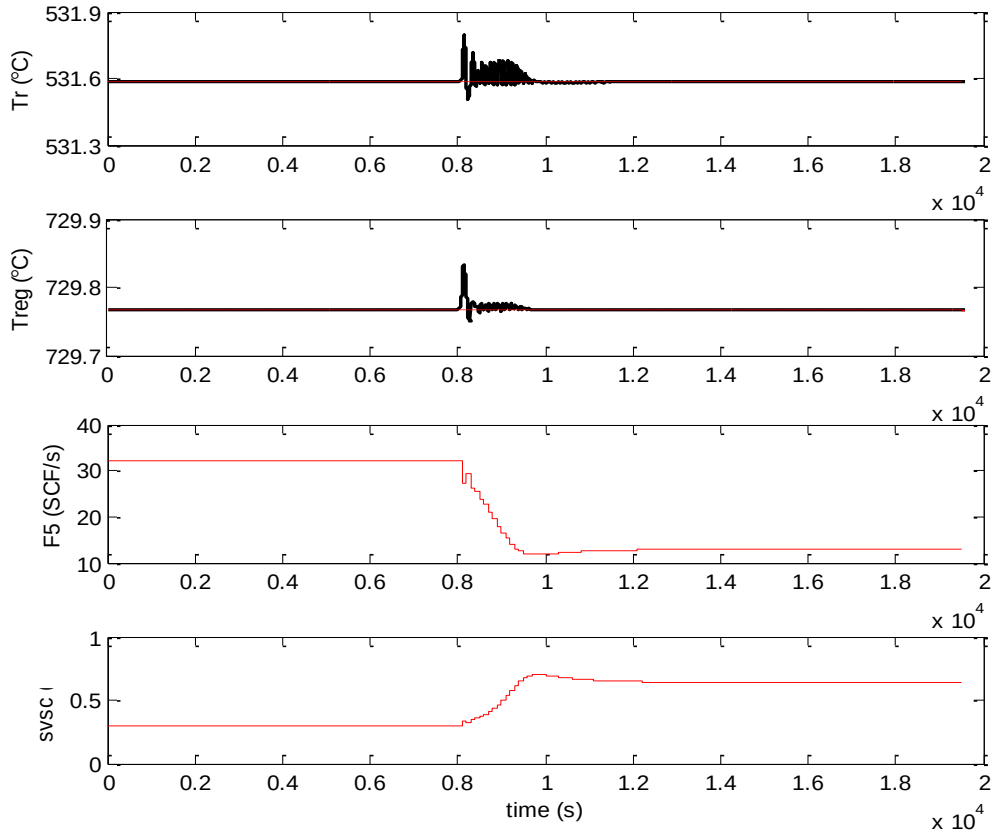

Figure 7.2: Controlled and manipulated variables responses for NMPC in presence of Ψ_f disturbance (5 % step increase at t = 8000 s).

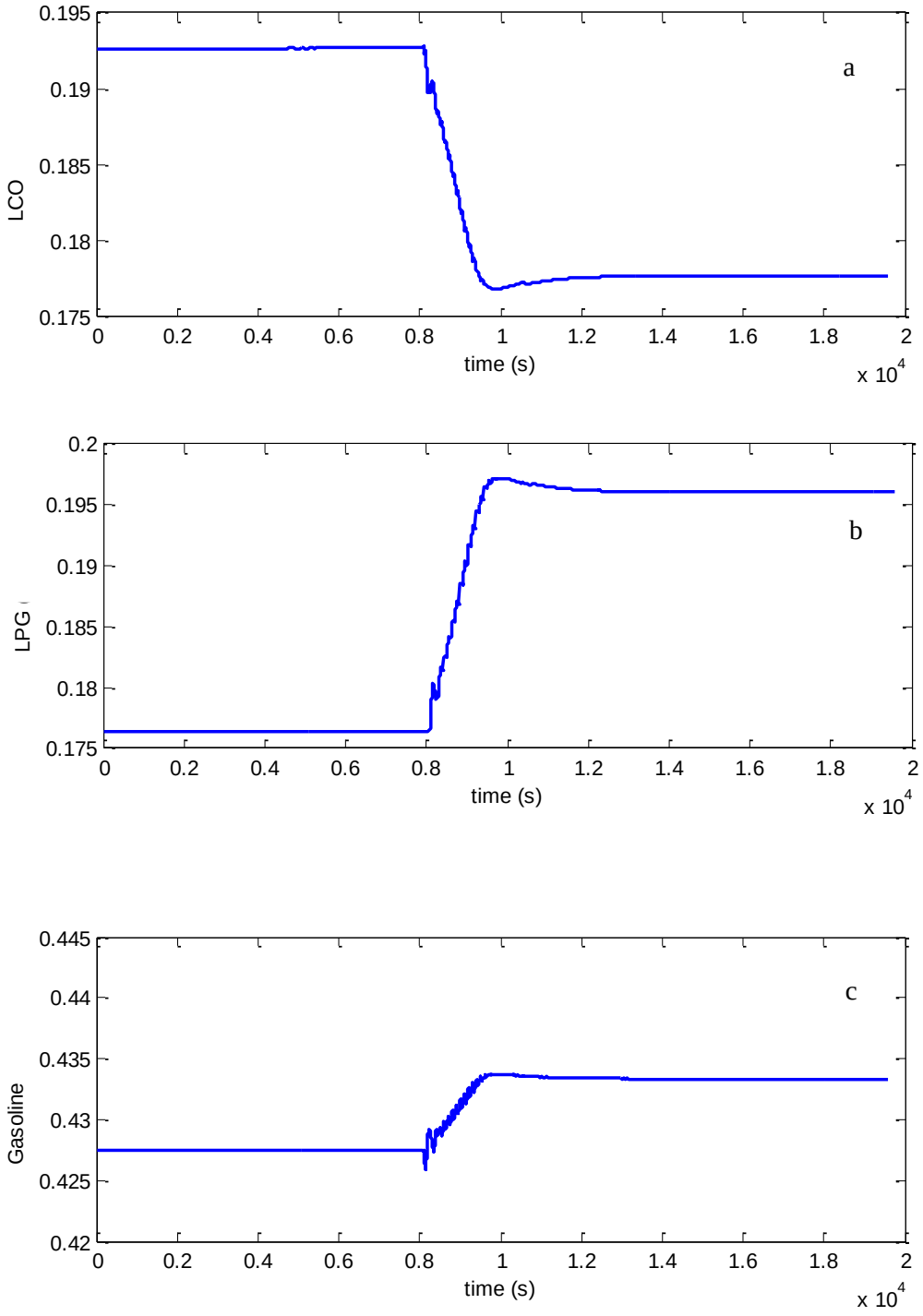

Figure 7.3: Model outputs dynamic responses for NMPC (a) LCO, (b) LPG, and (c) Gasoline.

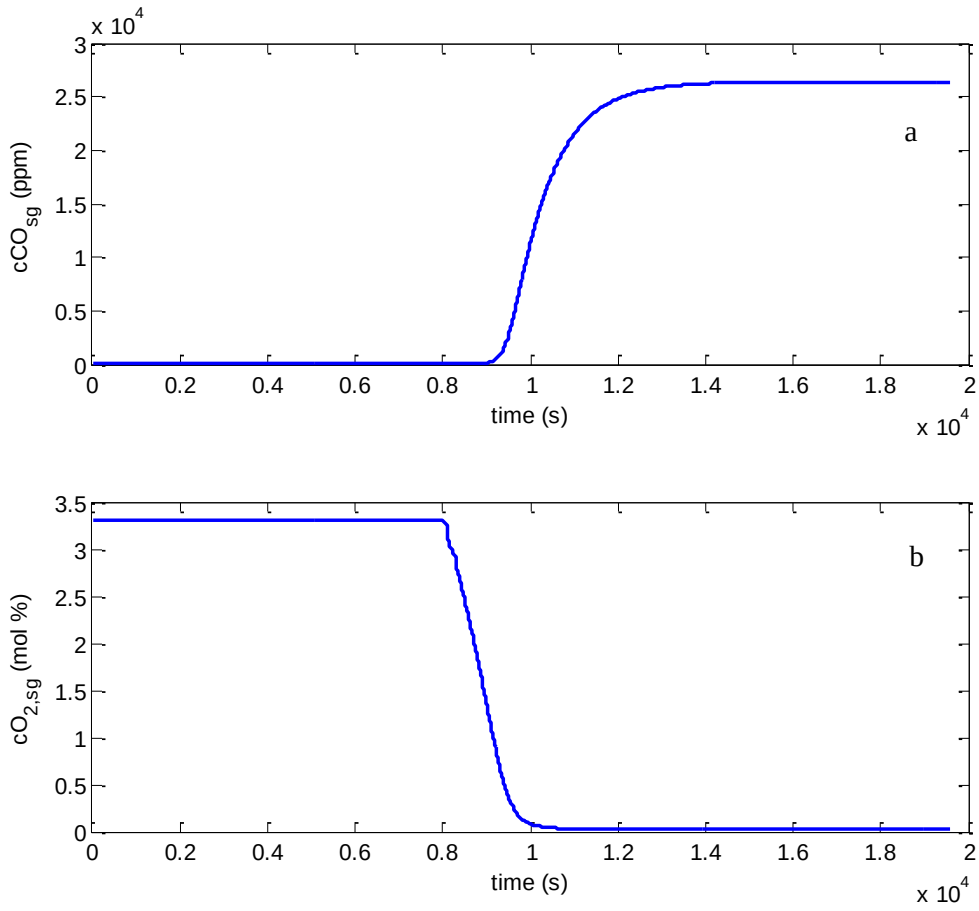

Figure 7.4: Model outputs dynamic responses for NMPC (a) cCO_{sg}. and (b) $cO_{2,sg}$.

Case 2: Economic NMPC (ENMPC) for maximization of LCO yield

This case presents a dynamic real time optimization strategy (DRTO), using the economic NMPC (ENMPC) concept presented before implemented to the simulated FCCU. First the ENMPC simulation is performed (case 2.1 in Table 7.2), and the results are shown in Figures 7.5 - 7.7, while the second (case 2.2 in Table 7.2), uses the typical regulatory NMPC bring the system to and keep at the optimal temperature profiles obtained by the ENMPC, but without taking into account the potential beneficial effect of a subsequent disturbance in the coking factor, as illustrated in Figures 7.8 – 7.10. Optimal conditions were obtained using the DRTO/ENMPC algorithm. The conditions at the optimal state were then used as the initial conditions for studying the effect of disturbances by using the NMPC technique for comparison with the DRTO/ENMPC.

In this case, the economic objective function is to maximise LCO concentration based on seasonal demand, especially in winter, where it is more valuable than other products. The tuning parameters adopted in the (DRTO/NMPC) algorithm are as follows: m = 3 and p = 3; the cost related weighting coefficient is $w_2 = [0\ -1\ 0\ 0\ 0\ 0\ 0]$; and the output constraints are defined as follows: y_{max} = [555 760] and y_{min} = [525 685].

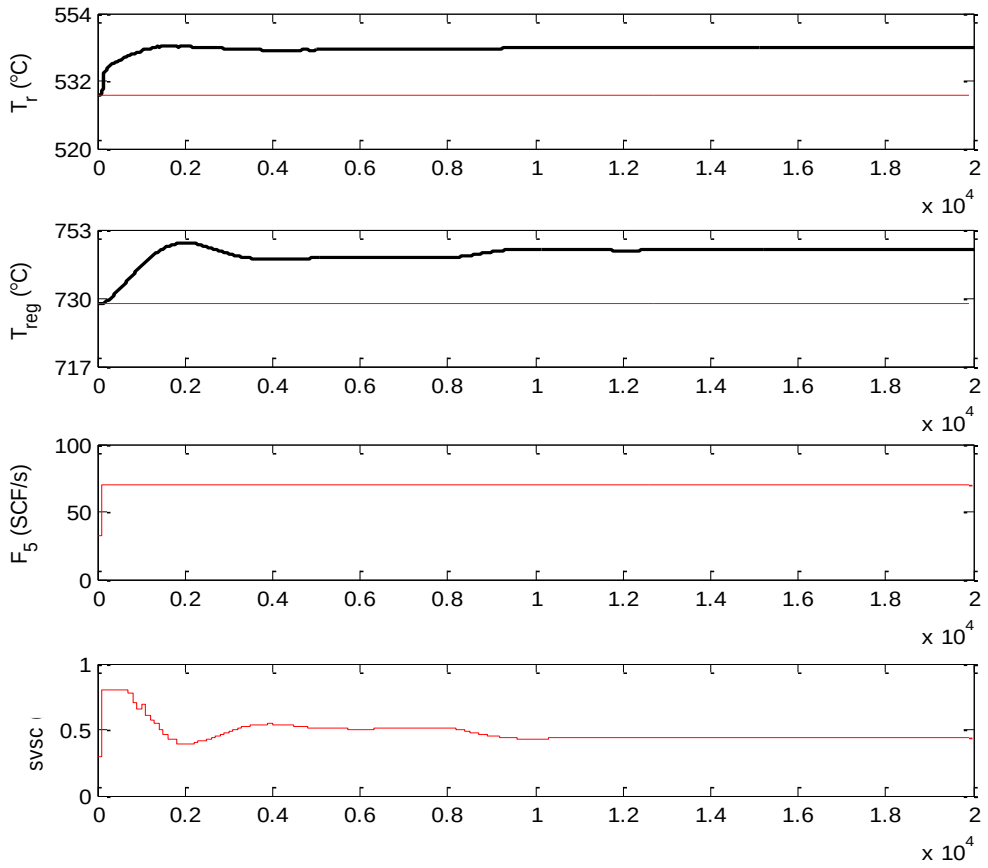

Figure 7.5: Controlled and manipulated variables responses for DRTO/ENMPC of maximizing LCO in presence of Ψ_f disturbance (5 % step increase at t = 8000 s).

In Figure 7.5, the reactor temperature can be seen to be adjusted by varying the parameters of heat balance in the system manipulated by the fuel flow rate F_5 controller and the svsc valve. The controller finds the new operating conditions which require increased operating temperature both in the reactor and regenerator, required to maximize the LCO concentration. The regenerator bed temperature need not be kept at the setpoint, but must be maintained within limits. Moreover, catalyst circulation decreases with increasing bed temperature since less catalyst is needed to

maintain the riser outlet temperature on target. A higher bed temperature, therefore, decreases the catalyst/oil ratio, which usually has undesirable effects on the product yields.

On the other hand, a low dense bed temperature is also undesirable, because it can force the regenerated catalyst slide valve to open fully, and can thereby limit the processing capacity of the unit. The F5 saturates during the control, indicating that the maximum fuel flow is required to raise the temperature to the economic optimum. Note that in these simulations the costs of utilities such as associated to the increase in F5 are neglected. After the process is brought to the new operating conditions that correspond to the particular fresh feed quality a disturbance in the raw material quality is simulated as a 5% increase in the coking factor. The ENMPC automatically adapted the operating conditions (e.g. increase mainly the regenerator temperature) to maintain economically optimal operations. This illustrates the working of the ENMPC, since when the coking factor of the raw material increases more coke is formed and hence higher temperature is needed to regenerated the catalyst. This new condition is automatically detected and found by the proposed ENMPC scheme.

The simulation results can be divided into two groups i.e. before and after disturbance at 8000s. For instance, in Figure 7.6 (a), the first part shows a sharp increase in LCO yield with a peak value of (0.39 %) at 2000s followed by a small decrease. This corresponds to the optimal LCO concentration corresponding to the raw material quality considered initially. In the second part after the disturbance developed, the LCO slightly increases and stabilizes at 0.365. The DRTO/ENMPC technique shows better performance for maximizing the LCO yield (0.365), as shown in Figure 7.6 (a), which is a significant increase compared with the previous LCO yield (0.17 %) obtained in the bachmark simulation when the process was regulated at the original steady state temperature setpoints (Figure 7.3 (a)). Figure 7.6 (b) also shows an increase in LPG yield before the disturbance, yet the yield was reduced slightly after the disturbance, but still remained greater than case 1 (0.196).

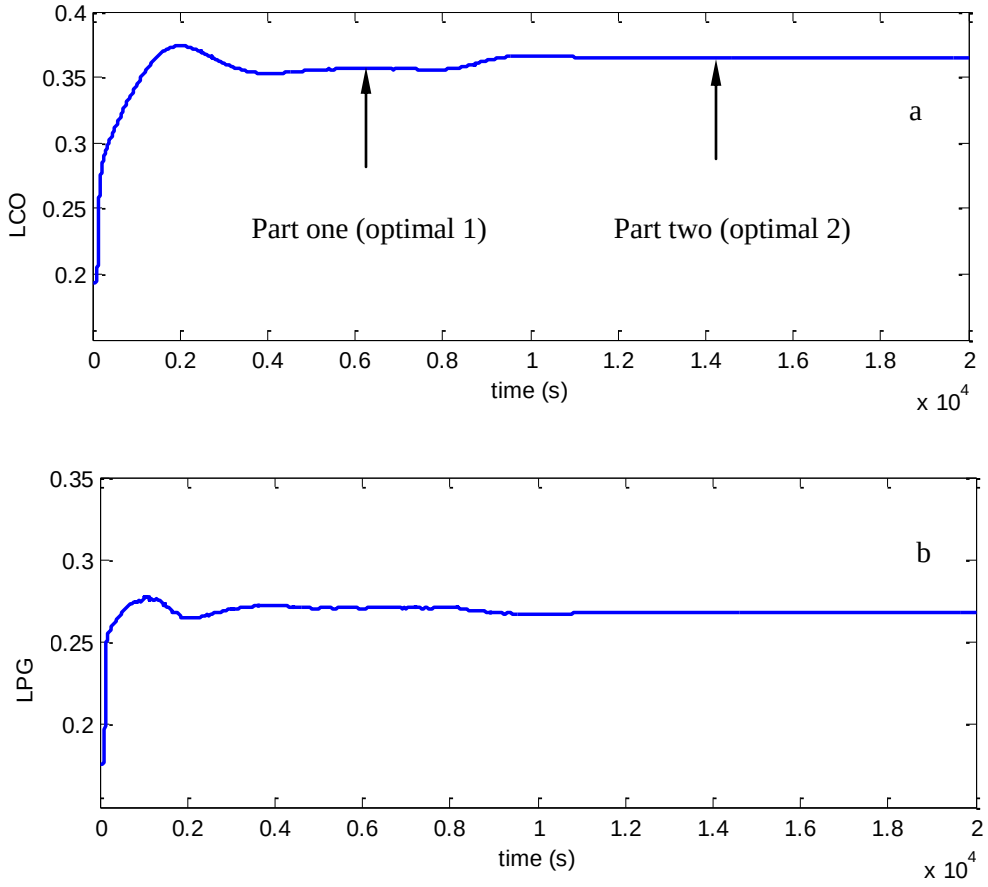

Figure 7.6: (a) LCO yield when the economic objective is to maximize LCO and (b) LPG yield.

Figure 7.7 (a) shows a significant decrease in gasoline yield in both parts, where the initial value was (0.42). This indicates that the operating conditions obtained from the optimization are not suitable for gasoline production, however this is expected as the objective focused only on maximizing the LCO content.

Figure 7.7 (b and c) illustrates an increase in CO emission (500 ppm), which exceeded the allowed emission limits (350 ppm). The controller was able to bring the CO to a lower level, however in a practical scenario temporary violation of the environmental constraint would have occurred resulting in the emission of a significant amount of CO gases into the environment. This emphasizes the importance of considering environmental constraints in the economic optimisation.

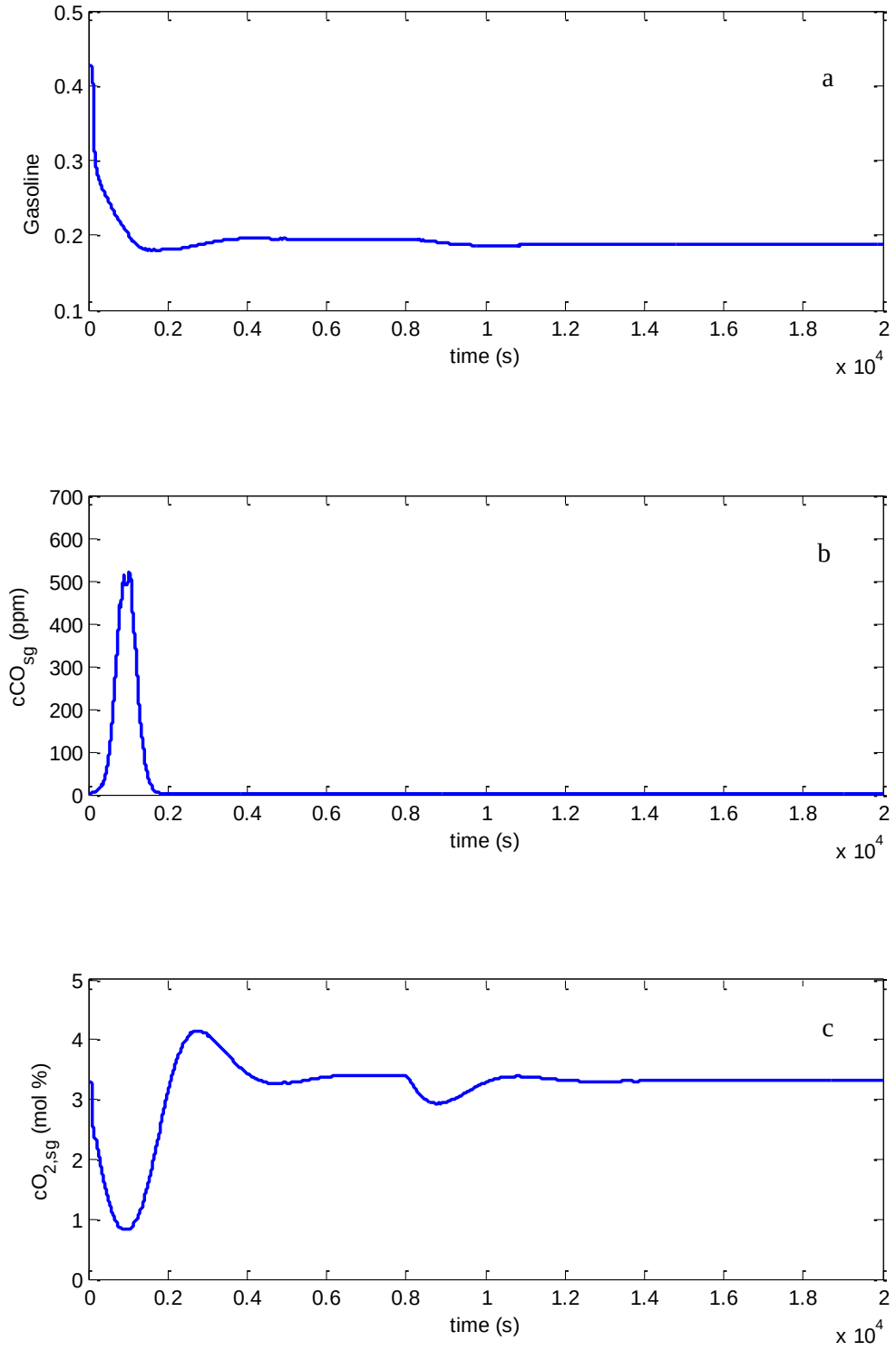

Figure 7.7: Model outputs dynamic responses for DRTO/NMPC (a) gasoline, (b) cCO_{sg} and (c) $cO_{2,sg}$.

The O_2 level rapidly decreases as the controller pushes more catalyst into the regenerator to maintain the regenerator temperature at the desired level. The oxygen concentration falls slightly when the disturbance is introduced, but returns to the pre-disturbance level after the controller's corrective action. This is the most important parameter in the regenerator and can vastly affect the operation of the unit. The main purpose of the regenerator is to burn off all the coke that has been formed during the course of the cracking reactions. The heat that is produced during the burning of coke in the regenerator is used to maintain the required temperature in the reactor for normal operation of the unit. It is also essential to ensure that all the coke is burnt off, or else the activity of the catalyst is reduced, and maintaining the reactor temperatures becomes difficult. The air rate to the regenerator is set to maintain a slight amount of excess O_2 in the regenerator flue gases. About 1-3% excess oxygen is maintained so as to ensure that all the coke in the spent catalyst is burnt off in the regenerator.

For comparison the results with regulatory NMPC (case 2.2) are shown in Figures 7.8-7.10. The steady state optimal controlled variables obtained from the DRTO/ENMPC algorithm were used as the setpoint temperature values for the regulatory NMPC. Figure 7.8 demonstrates the behaviour of the controlled and manipulated variables when they attempt to track the new setpoint values. The reactor temperature appears to follow the setpoint even in the presence of the disturbance. The regenerator temperature in the first part, before the disturbance, was brought to the new optimal steady state by the controller, but as the disturbance proceeded, it increased slightly, because more carbon was produced in the bed. Figure 7.9 (a) shows an increase in the LCO (0.33), and comparing it with the previous LCO yield (0.37) produced from DRTO/ENMPC proved that the proposed ENMPC approach gave an improvement in the LCO yield of 4 %, which is of significant value from the economic point of view, especialy considering the high-volume production of the FCCU. The results illustated that in this distrubance and objective scenario it is more economic to find a new opearting condition than to regulate the process at the previously deermined optimal setpoint values. The ENMPC approach was able to exploit the potentia beneficial effect of the distrubance and increased the LCO concentraion even further compared to the optimal value with the original raw material, whereas forcing the FCCU to operate at or close to the previously determined optimal temperature leads to an actual decrease in the the LCO concentration. Furthermore the ENMPC approach kept the CO emissions at a much lower level after the disturbance than the NMPC. Figure 7.9 (b) shows better LPG yield (0.2773) than that produced with DRTO/ENMPC, however this was not considered in the optimisation.

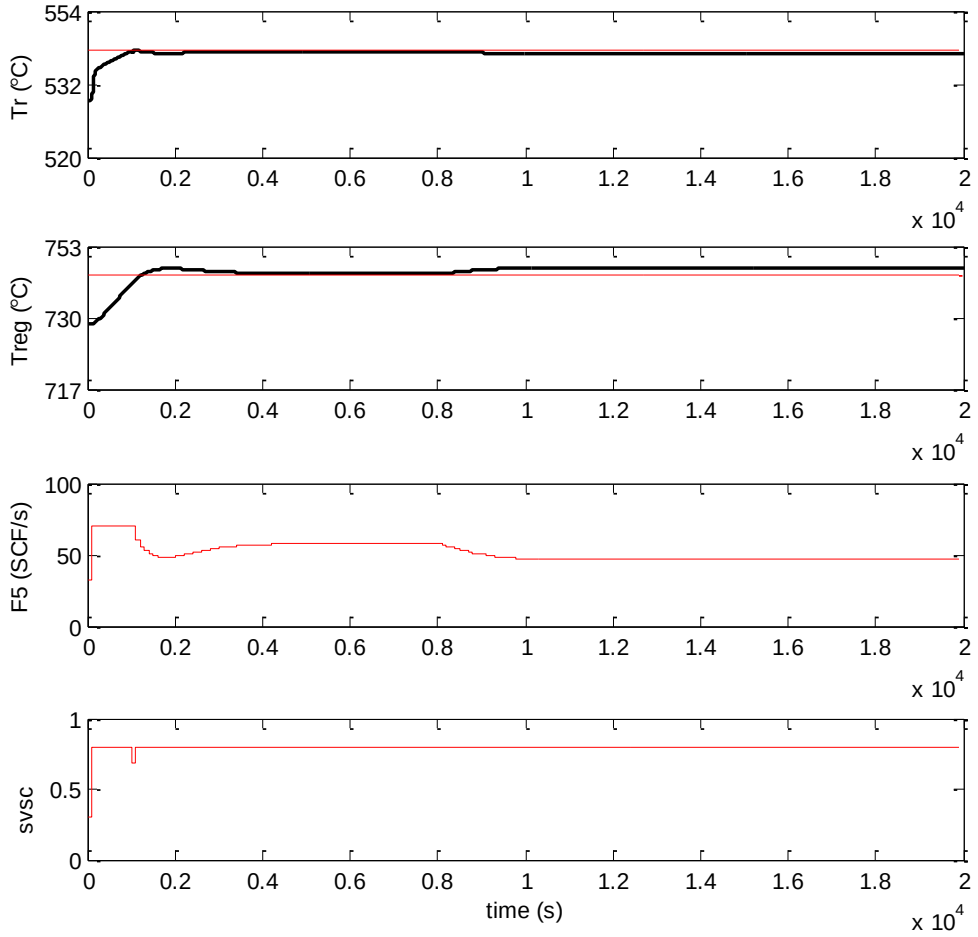

Figure 7.8: Controlled and manipulated variables responses for the regulatory NMPC using the setpoints determined by the ENMPC for the nominal raw material, in presence of Ψ_f disturbance (5 % step increase at t = 8000 s).

Figure 7.9 (c) also shows that the gasoline yield decreased to 0.2076, from its initial value 0.4275 and the DRTO/ENMPC value 0.1874. Figure 7.10 (a and b) shows an increase in CO emission (675 ppm) with decrease in oxygen concentration in the first part. In the second part, the O_2 stabilises at (1.347 %), while the CO decreases and stabilizes at (104 ppm), which is still significantly higher than in the case of the ENMPC. In the next case, discussed below, a constraint on CO emissions will be applied, to investigate the ability of the ENMPC to consider environmental constraints in the control problem.

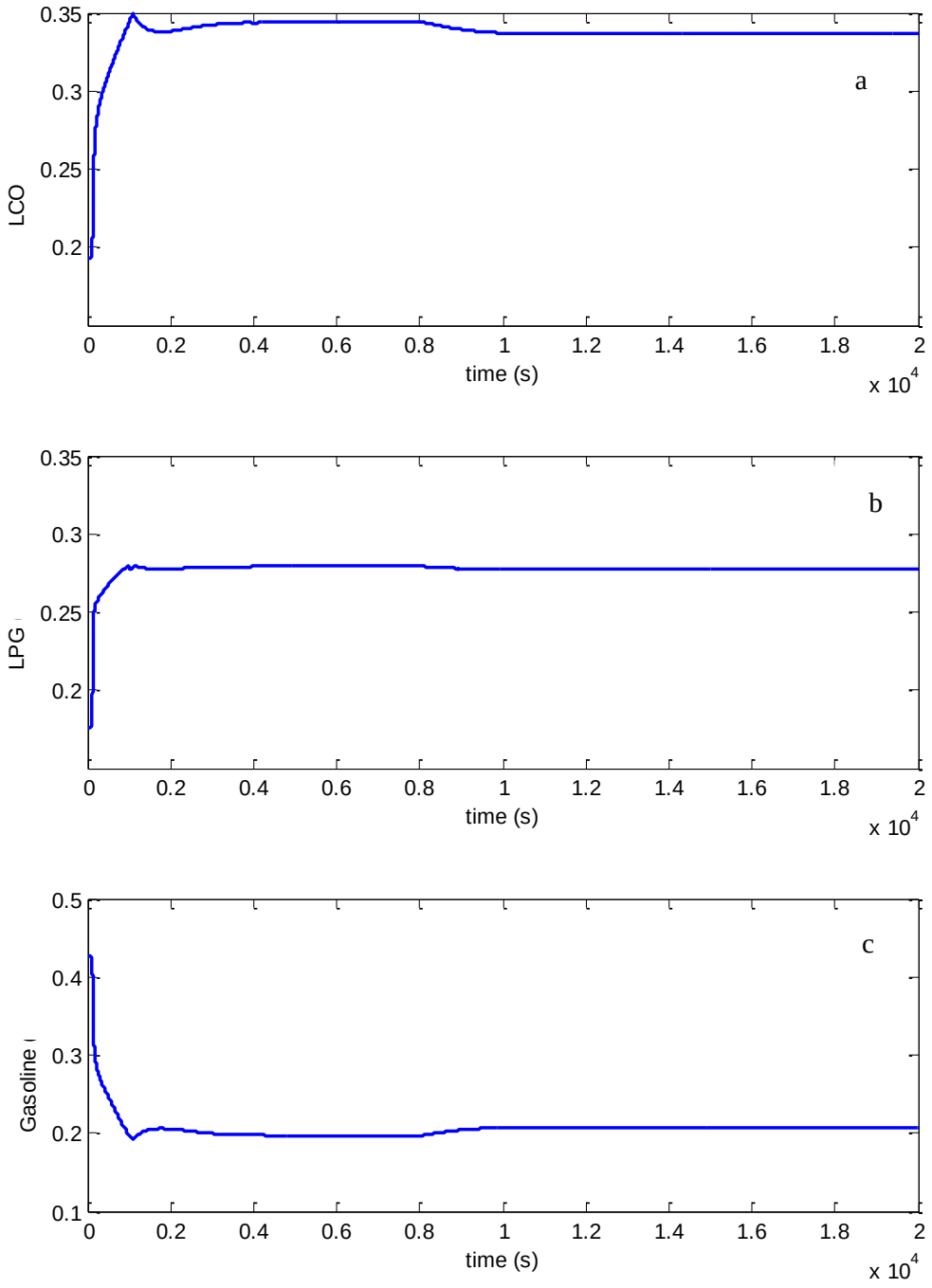

Figure 7.9: Model outputs dynamic responses for NMPC (a) LCO, (b) LPG and (c) gasoline.

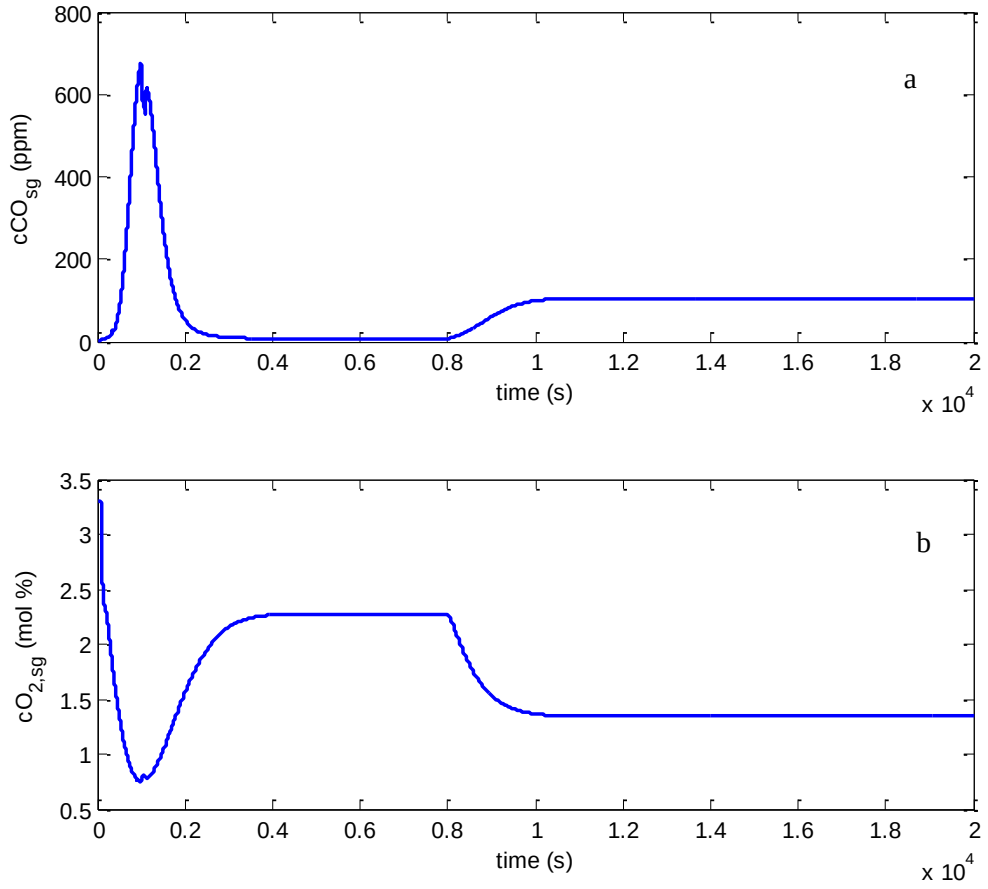

Figure 7.10: Model outputs dynamic responses for NMPC (a) cCO_{sg} and (b) $cO_{2,sg}$.

Case 3: Maximizing LPG yield using ENMPC with environmental constraints

DRTO/ENMPC of the FCCU without environmental constraint

Nowadays, the LPG product is one of most valuable products on world energy markets. In this case, the economic objective function aims to maximise LPG yield by using the proposed DRTO/ENMPC in the first scenario (case 3.1), and applying the environmental constraint on the CO emissions in the second scenario (case 3.2).

In the simulations carried out in both cases, the tuning parameters adopted in the (DRTO/ENMPC) algorithm were as follows: m = 3 and p = 3, and the cost related weighting coefficient is $w_4 = [0\ 0\ 0 - 1\ 0\ 0\ 0]$. The constraints on the manipulated inputs considered here are: u_{max} = [70 0.8], u_{min} = [10 0.1]. The output constraints are defined as follows: y_{max} = [560 760] and y_{min} = [525 685].

Figure 7.11 shows how the controlled and manipulated variables react to find the optimal operating condition to achieve maximum LPG yield.

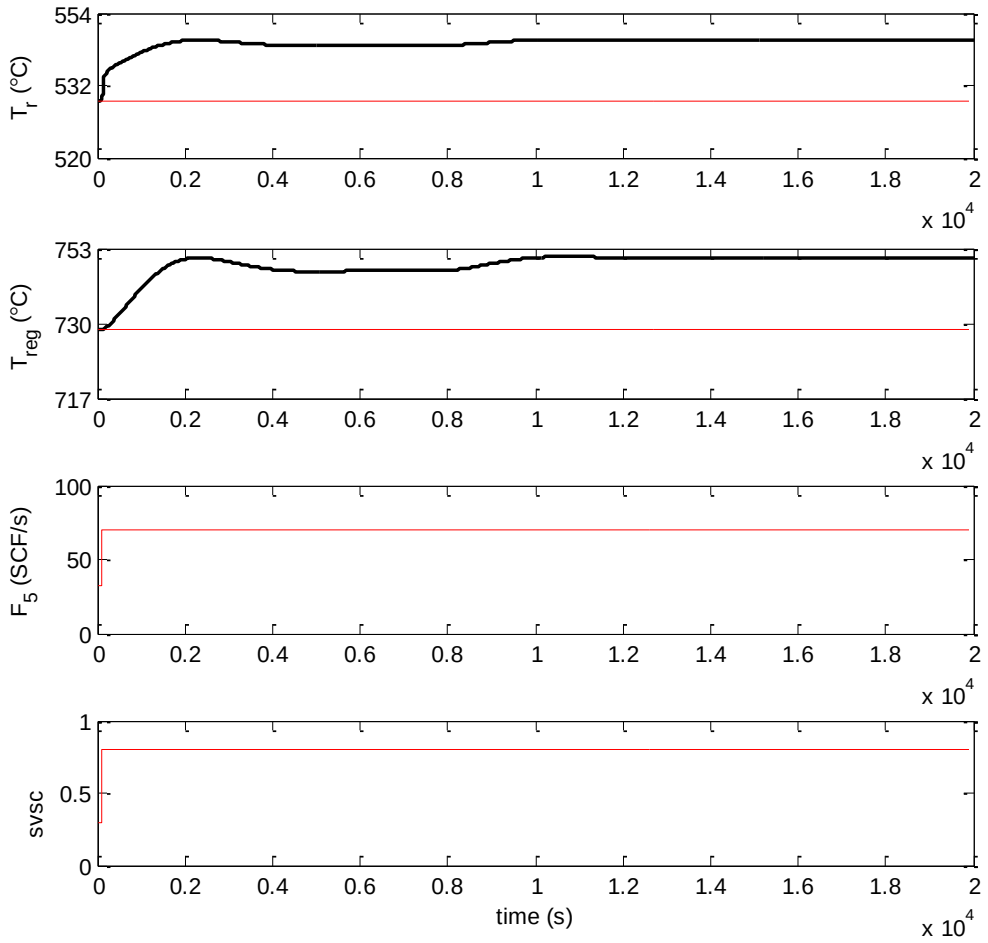

Figure 7.11: Controlled and manipulated variables responses for DRTO/ENMPC of maximizing LPG in presence of Ψ_f disturbance (5 % step increase at t = 8000 s).

In this case both manipulated inputs quickly reach their maximum values, indicating that the best operating condition to increase LPG production requires operating the unit close to the operating constraints. Figure 7.12 (a) indicates the significant increase in the LPG yield during the initial part of the simulation when the ENMPC is activated.

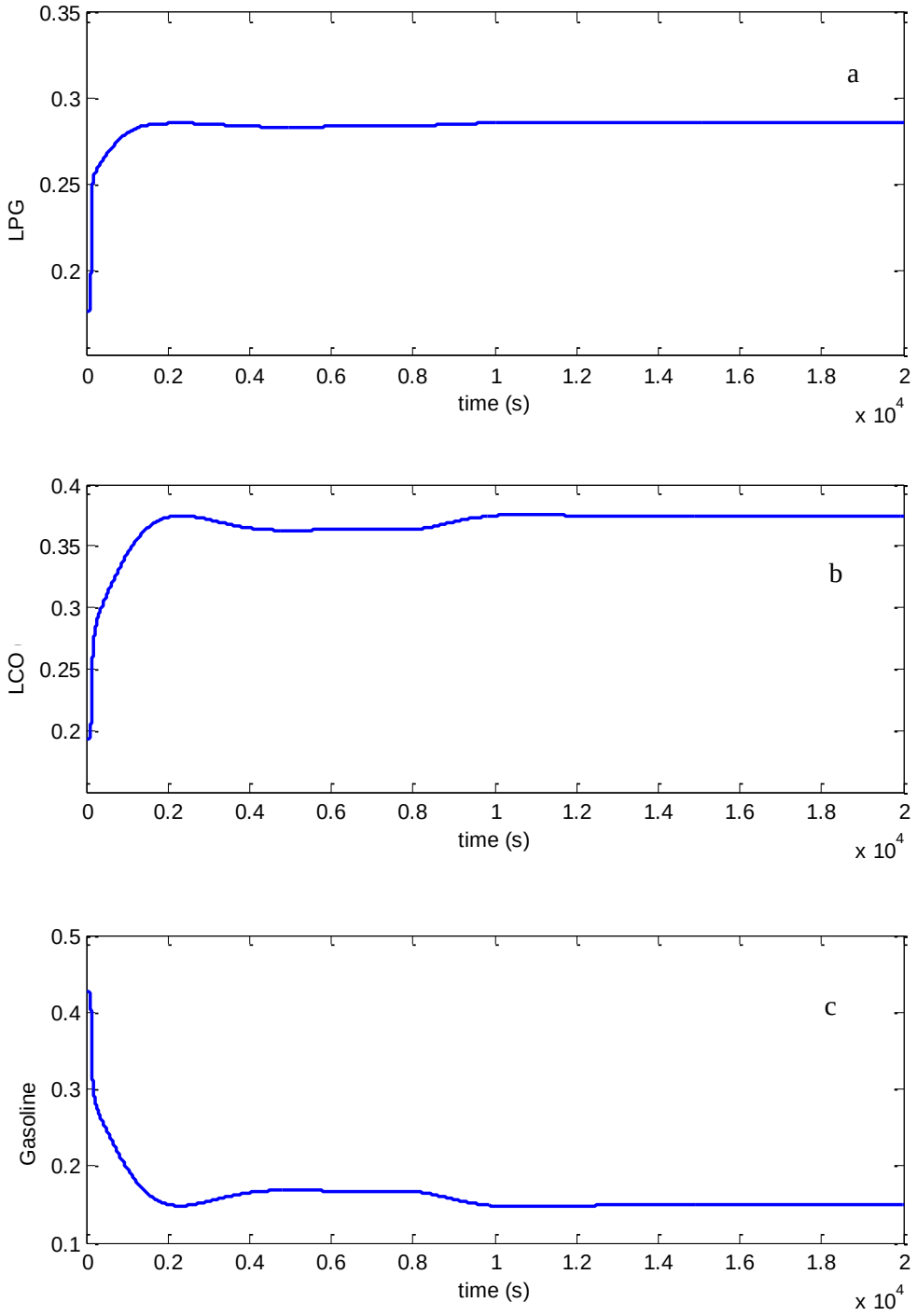

Figure 7.12: (a) LPG yield when the economic objective is to maximize LPG, (b) LCO and (c) gasoline.

A quick increase in LPG yield to the value of 0.29 at 2000 s followed by a small decrease can be observed, which corresponds to an approximately 14% increase in the LPG yield, that can correspond to considerable economic benefits. After the 5% disturbance in the coking factor occurs

a further increase can be observed and the LPG yield stabilises at 0.285. The limited variation after the disturbance is due to the fact that the manipulated inputs were saturated hence limiting the ability of the ENMPC to react to the disturbance. Nevertheless the ENMPC approach was able to recognize the beneficial effect of the disturbance and allowed both the reactor and regenerator temperatures to increase resulting in an additional increase in LPG yield.The first part in Figure 7.12 (b) shows a sharp increase in LCO yield, followed by a small decrease. In the second part, after the disturbance, the LCO yield slightly increases and stabilizes at 0.375 %. The DRTO/ENMPC technique, in this case, shows better performance not only for maximizing LPG, but also the LCO yield has increased more than the previous case 2 (0.365) as shown in Figure 7.6(a). Figure 7.12 (c) shows a significant decrease in gasoline yield in both parts of the simulation, before and after the disturbance, from the initial value 0.42 to 0.148, however this parameter was not considered in the optimisation.

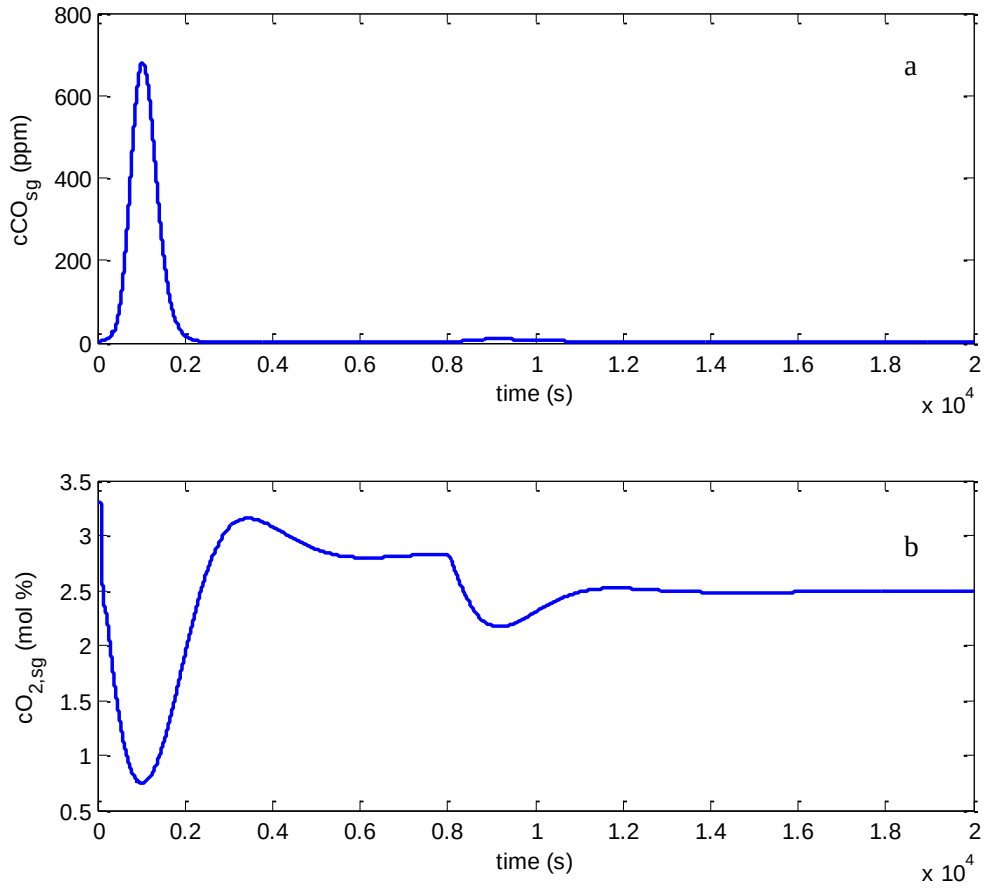

Figure 7.13: Model outputs dynamic responses for DRTO/ENMPC of (a) cCO_{sg} and (b) $cO_{2,sg}$.

Figure 7.13 (a) illustrates an increase in CO emission (681 ppm) as shown in the first part, which temporarily exceeds the allowed emission limits (350 ppm). Subsequently the controller was able to bring the CO to a lower level, however the temporary violation of the constraints could results in a significant amount of CO release into the atmosphere. The O_2 level, shown in Figure 7.13 (b), rapidly decreases to maintain the regenerator temperature at the desired level. The O_2 concentration goes down slightly when the disturbance began at 8000s and stabilizes at 2.48 %.

DRTO/ENMPC of the FCCU with CO environmental constraint

In this section, the same approach as in the previous case (case 3.1) was used, aiming to maximize the LPG yield by applying an environmental constraint for CO emissions (to keep CO concentration below 350 ppm). Figure 7.14 shows how the controller's corrective action with the temperatures worked to achieve the optimal operating condition values, while maintaining the environment constraints.

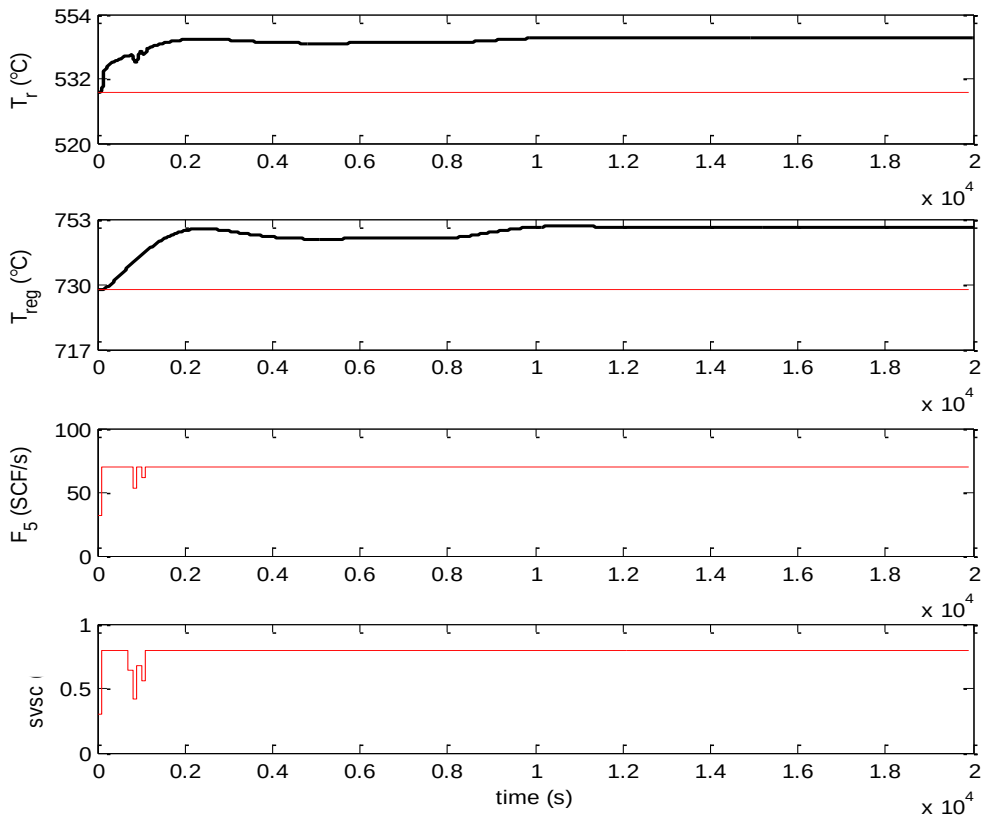

Figure 7.14: Controlled and manipulated variables responses for the DRTO/ENMPC of maximizing LPG with environmental constraints in the presence of Ψ_f disturbance (5 % step increase at t = 8000 s).

It can be clearly seen in Figures 7.15 (a, b and c) for LPG, LCO and gasoline yields respectively, that these were identical to the earlier values, especially in the second part. The first parts show that slight damping occurred, because of the controller's corrective actions to maintain the CO constraint limit, as shown in Figure 7.16 (a).

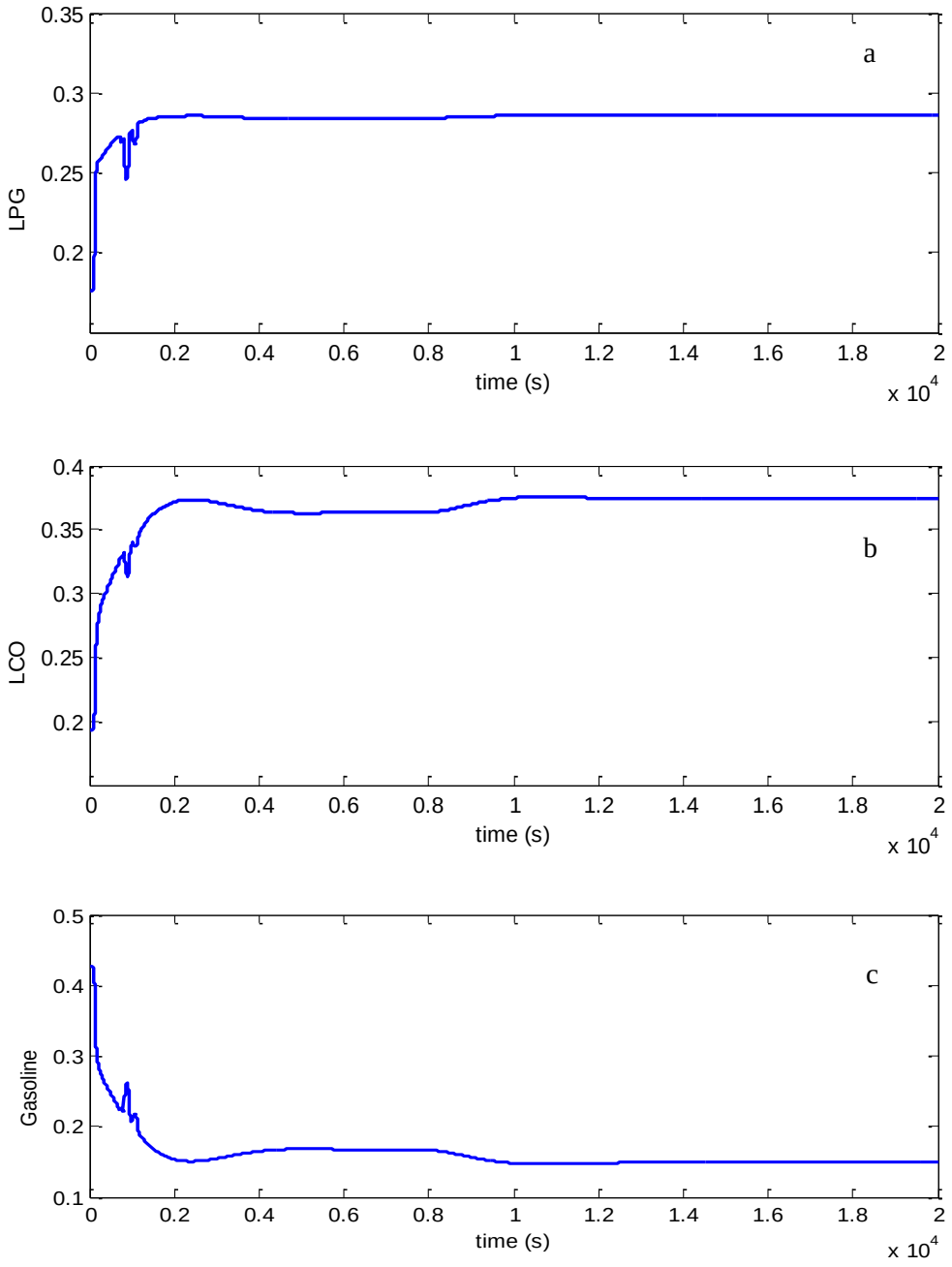

Figure 7.15: Model outputs dynamic responses for the DRTO/ENMPC (a) LPG, (b) LCO and (c) gasoline.

However, the re-circulation slide valve for spent catalyst, *svsc*, opened fully, as a control action, to allow more deposited catalyst to enter the upper regenerator section. After that, some of the hot catalyst from the upper zone was taken to the lower zone in the regenerator to maintain the required minimum temperature so that complete combustion is ensured. This is essential, because if the combustion is incomplete, then the coke balance in the catalyst will start burning in the dilute phase of the catalyst in the upper zone and in the flue gas lines. The heat that will be liberated during that burning will not be absorbed fully, as the density of catalyst in that area is very low.

This will result in a cyclone effect, and other hardware being exposed to very high temperatures causing mechanical damage. This phenomenon, as explained earlier, is called afterburning. In such cases, the re-circulation slide valve is opened so that the hot catalyst flows back to the lower section of the regenerator, thereby increasing temperature, which will result in more combustion taking place and all the C and CO is converted into CO_2.

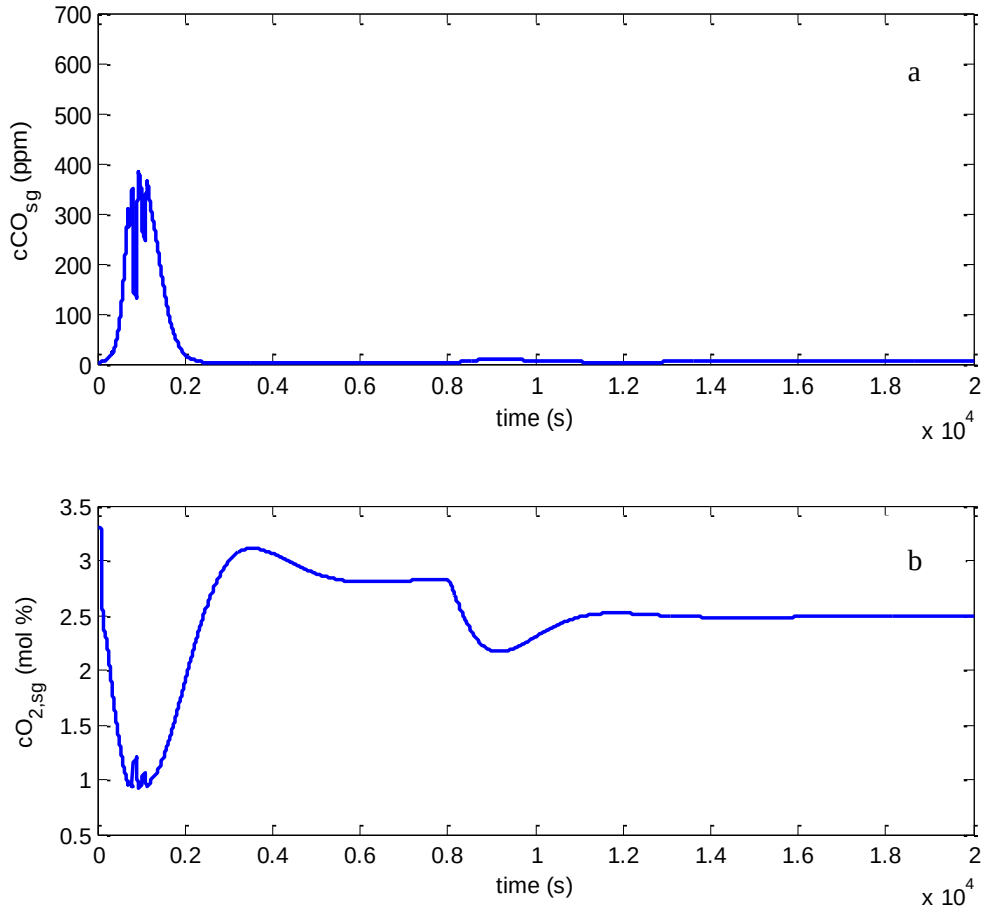

Figure 7.16: Model outputs dynamic responses for DRTO/NMPC of (a) cCO_{sg} and (b) $cO_{2,sg}$.

Case 4: DRTO/ENMP of the FCCU to minimize LCO yield to gain in Gasoline yield

In this case, the economic objective function is to minimize LCO based on seasonal demand. The cost related weighting coefficient is $w_2 = [0\ 1\ 0\ 0\ 0\ 0\ 0]$, and the constraints on the manipulated inputs, considered here are: u_{max} = [70 0.8], u_{min} = [10 0.1]. The output constraints are defined as follows: y_{max} = [555 760] and y_{min} = [525 685], and the sampling period is equal to 100 s. The coking formation factor disturbance has been applied by 5% increase at t = 8000s. Figure 7.17 shows how the controlled and manipulated variables react to find the optimal operating condition values to fulfil the economic objective function goal.

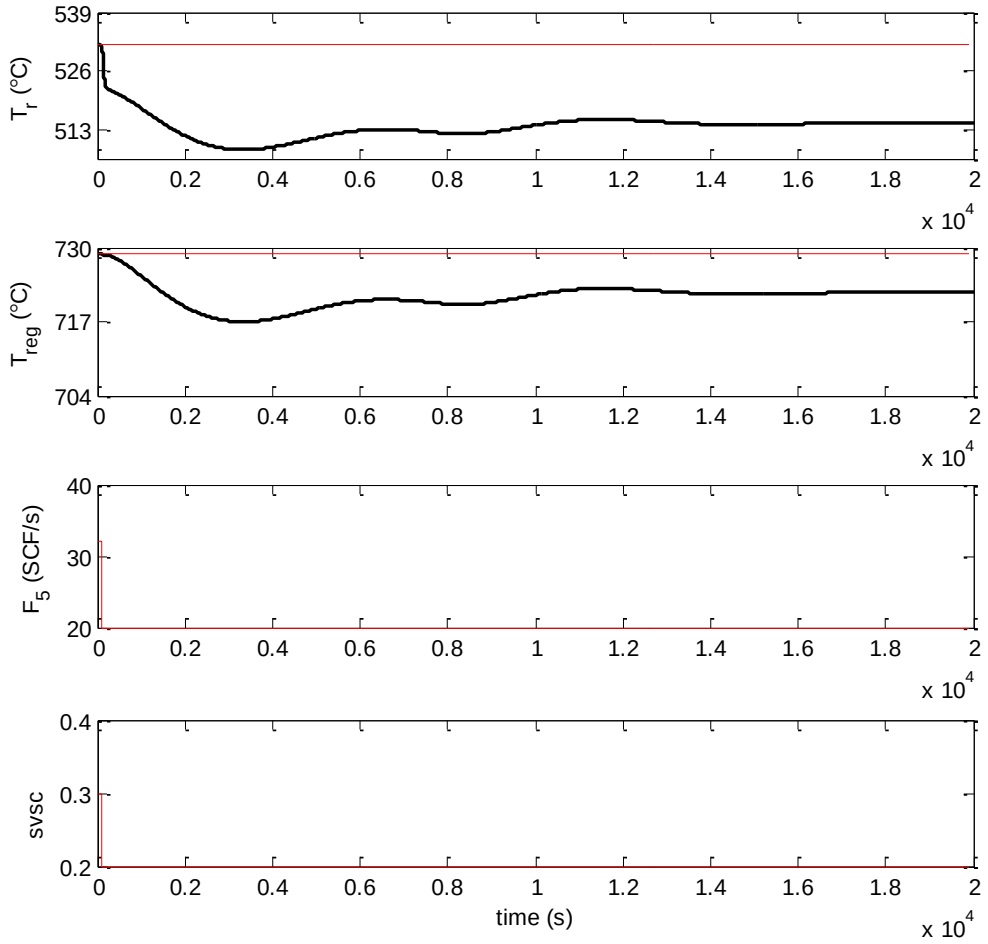

Figure 7.17: Controlled and manipulated variables responses for the DRTO/ENMPC of minimizing LCO in the presence of Ψ_f disturbance (5 % step increase at t = 8000 s).

Similarly to the previous case the manipulated inputs are saturated but this time at their minimum limits. This limits the performance of the ENMPC approach to achieve global optimum nevertheless the simulation results even under these constrained conditions show significant economic benefits.

The DRTO/NMPC technique appears to show the LCO yield being minimized to be able to maximize the gasoline yield.

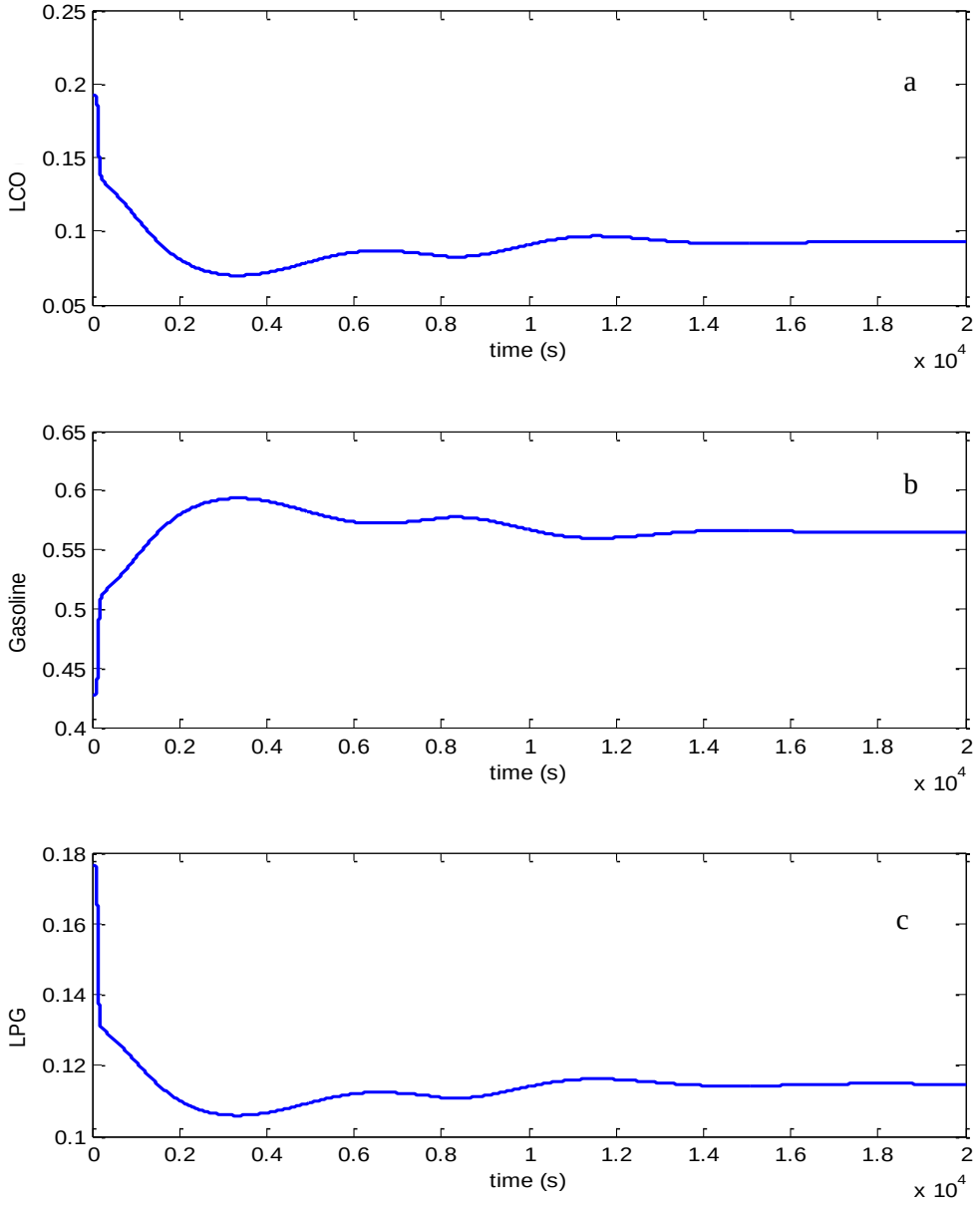

Figure 7.18: (a) LCO yield when the economic objective is to minimize LCO, DRTO/NMPC, (b) Gasoline and (c) LPG.

Figure 7.18 (a), indicates that a sharp drop in the LCO yield to 0.092 is obtained, which is a significant decrease compared with the LCO yield in case 1 (a decease with 17 % compare to the benchmark values (Figure 7.3 (a)). In Figure 7.18 (b), the first part shows a sharp increase in gasoline yield to 0.59 at 3000 s followed by a small decrease. In the second part, the gasoline decreases and stabilizes at 0.57. Figure 7.18 (c) shows a sharp decrease in LPG yield, before the disturbance, and the yield slightly increased, after the disturbance (to 0.11). However, this value is still lower than case 1 (0.19).

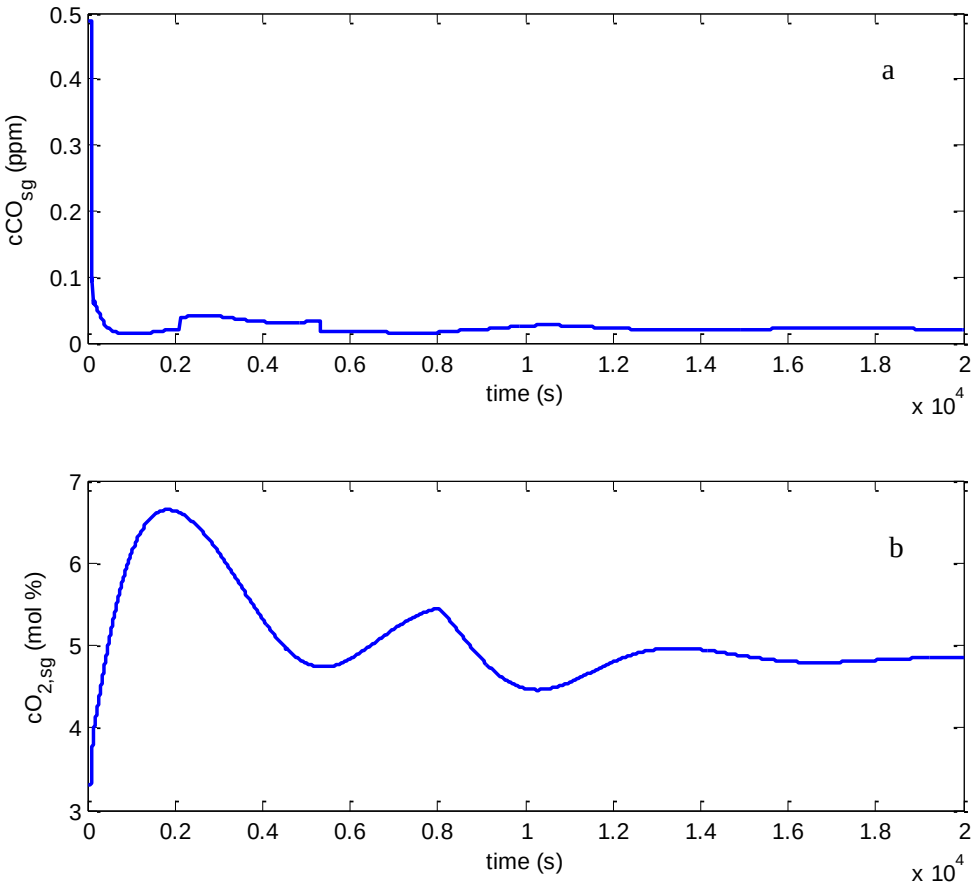

Figure 7.19: Model outputs dynamic responses for DRTO/NMPC of (a) cCO_{sg} and (b) $cO_{2,sg}$.

Figure 7.19 (a) illustrates a quick decrease in CO emission (to 0.015 ppm), as revealed in the first part, and continues to be much below the maximum emission limits. The O_2 level in Figure 7.19 (b) rapidly increases as the controller pushes less catalyst in the regenerator to maintain the regenerator temperature at the desired level, and consequently the reactor temperature. The oxygen concentration goes down slightly when the disturbance is introduced and stabilizes at (4.85 %).

However, the excess O_2 (4.85 %) in the stack gas is economically wasteful, since energy is expended to blow air into the regenerator vessel.

Table 7.3 summarises the results of cases obtained using RTO for different economic objective functions and NMPC controller that have been considered in this chapter.

Table 7.3: Summary of results

Cases			Variable						
			T_r (°C)	T_{reg} (°C)	LPG (%)	LCO (%)	Gasoline (%)	cCO_{sg} (ppm)	$cO_{2,sg}$ (%)
Case 1		Initial	531.6	729.8	0.176	0.193	0.427	0.489	3.3
		Optimal1	531.6	729.8	0.196	0.1777	0.4333	2.3e+4	0.0204
Case 2	2.1	Initial	531.6	729.8	0.176	0.193	0.427	0.489	3.3
		Optimal1	550.66	748.71	0.2706	0.356	0.1934	0.4512	3.4
		Optimal2	551.2	751.6	0.267	0.365	0.187	0.489	3.315
	2.2	Initial	551.2	751.6	0.176	0.193	0.427	0.489	3.3
		Optimal1	550.32	749.5	0.279	0.343	0.197	0.451	3.4
		Optimal2	551.2	751.6	0.277	0.336	0.207	104.8	1.347
Case 3	3.1	Initial	531.6	729.8	0.176	0.193	0.427	0.489	3.3
		Optimal1	553.28	751.9	0.283	0.363	0.166	1.85	2.8
		Optimal2	555.1	756.4	0.285	0.374	0.148	3.832	2.484
	3.2	Initial	531.6	729.8	0.176	0.193	0.427	0.489	3.3
		Optimal1	553.26	751.9	0.283	0.363	0.166	1.82	2.8
		Optimal2	555.1	756.4	0.285	0.374	0.148	3.832	2.484
Case 4		Initial	531.6	729.8	0.176	0.193	0.427	0.489	3.3
		Optimal1	526	725	0.112	0.086	0.572	0.0152	4.73
		Optimal2	516.7	715.2	0.115	0.093	0.59	0.021	4.852

7.3 Conclusions

The varying conditions on the market have encouraged the chemical processing industry to maximise the capabilities of the available plants. The productivity, and hence profitability, of high capital cost plant must be linked more closely to market demand, which can be achieved by

designing control strategies which are able to take these demands into account and set the operating conditions to provide optimal performance under changing market requirements.

In this work, a single layer, simplified, DRTO/ENMPC controller was studied. The controller proposed combines both on-line optimisation and control of multiple parameters with constraints. This allows simultaneous solution of both the control and optimisation problems as one. Initial results revealed that this optimising controller can bring a highly disturbed process to a stable state, as well as successfully controlling it at a new operating state, despite constraints, that satisfies specific economic criteria.

Optimisation of plant during dynamic operation creates new opportunities for maximising plant profitability and associated productivity. The novel concept of beneficial (good) and harmful (bad) disturbances is introduced and it is shown that the proposed approach is able to differentiate between these two scenarios, and potentially exploit the benefits of good disturbances, while maintaining the plant within the operating constraints. An additional benefit of the economic NMPC-based process simulator is its potential to be used as a practical tool for training plant operating personnel in the new plant operation regimes. Plant operating personnel can use the simulation tool to understand how the optimal operating conditions are achieved under different disturbances in the context of new operating constraints for the key process parameters, enhancing process understanding.

CHAPTER 8
CONCLUSIONS AND FUTURE WORK

This chapter provides an overview of the conclusions that can be drawn from the results of the work presented in this thesis. Some aspects of the work that require further development and improvement, which may form the basis for future investigations, are proposed.

8.1 Conclusions

The aim of this research project was to develop a mathematical model that can simulate the behaviour of the FCC unit, which consists of feed and preheat system, reactor (riser and stripper), regenerator, air blower, wet gas compressor, catalyst circulation lines, and the main fractionators. The model was subsequently used in studies of control and economic optimisation. The developed model is able to describe the complex dynamics of the reactor-regenerator system, and also includes the dynamic model of the fractionator, as well as a detailed five lump kinetic model for the riser (with components gas oil, gasoline, diesel, LPG and coke). This model is able to predict and describe the compositions of the final production rate, and the distribution of the main components in the final product. This allows the estimation of economic factors, related to the operation of the FCCU. This aim has been attained through successful achievements of the relevant objectives listed in Chapter 1 and individually presented in Chapters 2 to 7. The overall aim was to provide a systematic and comprehensive framework for robust economic control for optimal system operations. The main conclusions of the chapters and thesis are presented below.

In addition to an overview of some aspects of the advanced control processes as they currently stand, Chapter 2 also presented a comprehensive literature review of the development of linear and nonlinear model predictive control strategies. The detailed evaluation of the trends of industrial applications and preparation of the model predictive control approaches indicate that linear and nonlinear MPC are suitable technologies for the FCCU, with significant potential to increase the profitability and efficiency of the unit. This is part of the objective to gain knowledge and understanding of FCC unit behaviour, as well as its characteristics, so that these can be accounted for in the process controller design. The work has produced a compilation of literature methods for improving FCC unit productivity and efficiency that have been in use from 1941 to the present.

An original mathematical model for the FCC process was developed based on the momentum, mass, and energy dynamic balances, and incorporates process hydrodynamics, heat transfer, mass transfer and catalytic cracking kinetics based on a lumping strategy. Molecules and reactions are lumped according by their boiling point and treated as pseudo-components for a global description of the phenomena taking place in the reactor.

The FCCU mathematical model includes seven main components of the overal system: (1) feed and preheat system, (2) reactor (riser and stripper), (3) regenerator, (4) air blower, (5) wet gas compressor, (6) catalyst circulation lines, and (7) the main fractionator. The novelty of the model consists in that besides the complex dynamics of the reactor-regenerator system, it also includes the dynamic model of the fractionator, as well as a model capable of predicting the yields of valuable products and gasoline octane value, and a kinetic model for the riser section, which also incorporates the detailed effect of temperture on the product distribution. Different kinetic models where studied starting with the three lumped kinetic model, to a complex model with 13 lumped components. From the presented models, the five-lump (namely: gas oil, gasoline, diesel (LPG), gases and coke) kinetic model for the riser section was chosen to model the product composition in the FCC riser, since it corresponds to the available literature data and provides sufficient complexity to describe the yields of the key valuable products and gasoline octane value.

The dynamic simulator was used to study the dynamic behaviour of the process. A set of dynamic simulations were performed to study the dynamic response of the FCCU to disturbances. The selected disturbances reflect possible upsets that affect the normal operation of the unit, and were selected from a practical point of view, after several discussions and close cooperation with refinery personnel. Simulations demonstrate that the process is multivariable, strongly interacting and highly nonlinear. Inverse response behaviour has also been observed, indicating difficulties in the controller design. The simulation study showed that the developed simulator is sufficiently complex to capture the major dynamic effects that occur in an actual FCCU system and is able to depict the main dynamic characteristics of a typical commercial FCC process. The simulator includes all important economic, environmental and safety constraints of the overal system.

The developed simulator enables engineering and technical personnel to carry out research on the design, operation, performance, and development of a proper control system for a modern catalytic cracking unit. It could also be an efficient tool for training operating personnel.

As the catalytic cracking is achieved through endothermic reactions, operating the reactor at the highest possible temperature, allows greater productivity. At the same time, catalyst regeneration through coke burning also means that both reactor and regenerator should be operated at the highest temperature allowed by their metallurgical limits. Stack gas carbon monoxide concentration is also restricted due to environmental issues. A detailed dynamic FCC model and solver were implemented in the dynamic simulator (as described in Chapter 3). The model correlation equations relating to the transport and thermodynamic properties were derived from the published literature, directly or through a non-linear regression. The products composition was found to be significantly influenced by the disturbances applied in this study. Therefore, the disturbances have a huge impact on process economics due to the FCC unit's high production volume. Among the key disturbances studied is fresh feed coke formation factor, which has a large effect on the process variables. The FCC unit control must not only act to raise productivity, but must also ensure that the process is safe for the environment; stack gas CO concentration must be maintained below specific limits.

In applying advanced PID controllers to the multivariable process, the closed-loop dynamic behaviour was studied using the dynamic simulator. Analysis of the process controllability was performed using a simple RGA matrix, with the aim of exploring the interactions between the different process variables.The PID control approach was applied for several control structures, which demonstrated that between some loops there were strong couplings. This could complicate the tuning of individual loops. A genetic algorithm (GA) based optimsation approach was implemented to determine the tuning parameters for the interacting PID control loops. This approach was used to evaluate 2x2 and 3x3 control schemes in terms of setpoint tracking and distrubance rejection performance. The results of the simulation show that increasing the number of independent loops causes the PID controller performance to degrade significanty, as manifested in higher settling interval. It was found that the control system stabilised the process, yet in the presence of many disturbances, resulted in non-optimal operation resulting in negative environmental effects or economic losses. Therefore, applying advanced multivariable control systems to the control of the FCC unit is justified by the potential economic benefits to be achieved.

The benefits of model predictive control as the most commonly used multivariate control approach were demonstrated for the control of the FCCU. A detailed analysis of based on Linear MPC was

first performed which showed to advantages of using sets of control inputs and outputs based on relative well decoupled systems, which can offer suitable performance of the lower level basic control system, in a real industrial implementation. The study also indicated that the fuel flow in the preheater is a key manipulated input in the control of the reactor temperature which is one of the most important performance influencing process parameters. The benefits of non-square control architectures with larger number of manipulated variables than controlled outputs was shown to provide better decoupling between the controlled outputs than typical square control structures (same number of inputs and outputs). Simulation results also indicated the limited applicability of the linear MPC when applied to the nonlinear plant.

An efficient real-time nonlinear model predictive control (NMPC) strategy, based on efficient multiple shooting optimization was developed using a real-time iteration scheme. The performance of the proposed scheme was evaluated for the FCCU process. Based on this efficient approach a single layer, DRTO/ENMPC controller was investigated, which combines real-time optimisation with constrained multivariable control. Hence, this controller is able to simultaneously handle the process control and economic optimisation of the plant. The primary results show that such a controller is capable of stabilising a process and operating it within specified constraints to achieve defined economic objectives. Several simulated case studies have demonsted that applying a real-time model-based online optimisation scheme based on economic criteria can provide optimal process performance in case of changing quality of the raw material, while maintaining the process within operational and environmental constraints.

8.2 Recommendations for future work

The following aspects of the work presented in this thesis could be incorporated in future work:

1. The present work permits the study of some interesting aspects regarding the modelling and control of the catalytic cracking unit. One of these trends could be the improvement of the present model by applying a more complex kinetic model for the riser section, together with a more detailed model for the main fractionator and then model validation and optimization based on experimental data. This would allow an even more comprehensive investigation of the effects of changed operating conditions on the product distribution.
2. Another important development could be along the line of studies on thermal integration applied to the existing catalytic cracking model and NMPC control; results could lead to efficient use of raw material and energy, increased economic efficiency to reduce energy

and raw material consumption, reduction of operating costs or improvement of profit margins of the process.

3. Plant-wide control is one of the advanced trends being applied by refiners. These systems can look at large amounts of data, and are expected to make more consistent and logical decisions than people could or would concerning unit or plant-wide profitability. The presented study only used a 2x2 system for the economic control to provide a proof of concept of the benefits of the ENMPC approach. Future studies incorporating a more comprehensive plant-wide control scheme with multiple inputs and outputs in the ENMPC algorithms may provide additional benefits of the control scheme.
4. Evaluation of an output feedback scheme in the control approach applied that incorporates a state and parameter estimation step would significantly improve the robustness of the control scheme. In the present study state feedback was assumed, which is a realistic assumption considering that the main state variables modelled are measurable in the real plant, however the employment of state and parameter estimation approach (e.g. extended Kalman filter, or moving horizon estimation) would allow the use of more complex process models and confer adaptability to changind process conditions.
5. More detailed economic objectives could be included in the economic optimisation, taking into account production rates, operating and utility costs and other aspects that affect the profit of the plant.

As a final conclusion, it is important to emphasise that FCCU control continues to be a vital field with significant research problems, and a nonlinear model-based predictive control scheme that allows the incorporation of economic objectives has significant potential benefits to provide a positive step-change in the improvement of the current operating practices for industrial FCCUs.

References

1. Abou-Jeyab, R.A., and Y.P. Gupta. 2001.Constrained multivariable control of fluidized catalytic cracking process using linear programming. *Trans. I.Chem. Eng. A*, 79:274-282.

2. Adetola, V.A. 2008. PhD thesis, *Integrated real-time optimization and model predictive control under parametric uncertainties*, Queen's University, Kingston, Ontario, Canada.

3. Adetola, V. and M. Guay. 2010. Integration of real-time optimization and model predictive control. *Journal of Process Control* 20:125-133.

4. Agachi, S.P., Z.K. Nagy, M.V. Cristea, and A.I. Imre-Lucaci. 2006. *Model Based Control*, Wiley-VCH Verlag GmbH & Co. KGaA, 2006.

5. Aguilar, R., J. Gonzalez, M. Barron, and J. AlvarezRamirez. 1999. Control of a fluid catalytic cracking units based on proportional-integral reduced order observers", *Chem. Eng. J*. 75:77-85.

6. Alhumaizi, K. and S. Elnashaie. 1997. Effect of control loop configuration on the bifurcation behavior and gasoline yield of industrial fluid catalytic cracking (FCC) units, *Mathematicaland Coputer Modelling* 25(3):36-56.

7. Allgoewer, F., T.A. Badgwell, J.S. Qin, J.B. Rawlings and S.J. Wright. 1999. Nonlinear predictive control and moving horizon estimation – An introductory overview, in P.M. Frank (Ed.), *Advances in Control, Highlights of ECC'99*, Springer, 391-449.

8. Alsabei, R., Z.K. Nagy, and V. Nassehi. 2008. Process Simulators Based Control Design for a Fluid Catalytic Cracking Unit", *18th International Congress of Chemical and Process Engineering*, Prague, Czech Republic.

9. Alsabei, R., Z.K. Nagy, and V. Nassehi. 2009. Mathematical Modelling and Control of a UOP Fluid Catalytic Cracking Unit. *3rd Saudi International Conference*, University of Surrey, UK, 32.

10. Alsabei, R., Z.K. Nagy, and V. Nassehi. 2009. Multivariate Control Structure Synthesis for fluid catalytic cracking unit relative gain array. *Chemical Engineering*, D.B.Das, V. Nassehi, L. Deka, EUROSIS-ETI. *7th International Industrial Simulation Conference*. Loughborough. ISBN 978-90-77381-4-89.251-256.

11. Alsabei, R., Z.K. Nagy, and V. Nassehi. 2009. Process simulators based control design for Universal Oil Products FCCU", *Chemical Engineering*, 8th World Congress of Chemical Engineering (WCCE 8), Montréal, Canada, 2009.

12. Alvarez-Ramirez, J., R. Aguilar, and F. Lopez-Isunza. 1996. Robust regulation of temperature in reactor-regenerator fluid catalytic cracking units. *Ind. Eng. Chem. Res.* 35:1652-1659.

13. Ancheyta-Juarez, J. and R. Sotelo-Boyas. 2000. Estimation of kinetic constants of a five-lump model for fluid catalytic cracking process using simpler sub-models, *Energy & Fuels*, 14: 1226-1231.

14. Ancheyta-Juarez, J., F. Lopez-Isunza and E. Aguilar-Rodriguez. 1999. 5-Lump kinetic model for gas oil catalytic cracking. *Applied Catal. A: Gen.*177: 227-235.

15. Angeli, D. and J. Rawlings. 2010. Receding horizon cost optimization and control for nonlinar plants, in 'Proceedings of 8th IFAC Symposium on Nonlinear Control Systems (NOLCOS)', Bologna, Italy.

16. Ansari, R.M. and M.O. Tade. 2000. Constrained nonlinear multivariable control of a Fluid Catalytic Cracking Unit, *Journal of Process Control*. 10:539-555.

17. Arandes, J., M. Azokoiti, J. Bilbao, and H. de Lasa. 2001. Modeling FCC units under steady and unsteady-state conditions. *Can. J. Chem. Eng.*78:1025-1031.

18. Arandes, J.M. and H.I. de Lasa. 1992. Simulation and multiplicity of steady states in fluidized FCCUs. *Chem Eng Sci*. 47: 2535-2540.

19. Arandes, J.M., M.J. Azkoiti, J. Bilboa, and H.I. de Lasa. 2000. Modelling FCC units under steady and unsteady state conditions. *Can J Chem Eng*.78:111-123.

20. Araujo-Monroy, C., and F. Lopez-Isunza. 2006. Modeling and simulation of an industrial fluid catalytic cracking riser reactor using a lumping-kinetic model for a distinct feedstock. *Ind. Eng. Chem. Res.* 45:120-128.

21. Arbel, A., Z. Huang, I. H. Rinard, R. Shinnar, and A.V. Sapre. 1995. Dynamic and control of fluidized catalytic crackers. 1. Modeling of the current generation of FCC's, *Ind. Eng. Chem. Res.* 34(4):1228–1243.

22. Arkun, Y., J. Hollett, W.M. Canney, and M. Morari. 1986. Experimental study of internal model control, *Ind. Engng Chem. Process Des. Dev.*, 25:102-108.

23. Avidan, A.A., and R. Shinnar. 1990. Development of catalytic cracking technology: a lesson in chemical reactor design. *Ind. Eng. Chem. Res*. 29:931-942.

24. Backx, T., O. Bosgra, and W. Marquardt. 2000. Integration of model-predictive control and optimization of processes. In IFAC Symposium" Advanced Control of Chemical Processes", ADCHEM, 249-260. Pisa, Italy.

25. Balchen, J.G., D. Lungquist, and S. Strand. 1992. State-space predictive control. *Chem. Eng. Sci.,* 47:787-798.

26. Bennett, S. 1993. A history of control engineering, 1930-1955. IET.48.

27. Bequette, B.W. 1991. Nonlinear control of chemical processes - A review. *Ind. Eng. Chem. Res*. 30:1391-1413.

28. Bhattacharyya, A.A., G.M. Woltermann, J.S. Yoo, J.A. Karch, and W.E. Cormier. 1988. Catalytic SOx Abatement: The Role of Magnesium Aluminate Spinel in the Removal of SOx from Fluid Catalytic Cracking (FCC) flue gas, *Ind. Eng. Chem. Res.* 27(8):1356-1360.

29. Biegler, L.T. 2000. Efficient solution of dynamic optimization and NMPC problems. In F. Allgöwer and A. Zheng (Eds.), *Nonlinear Predictive Control,* Bagel, Birkhauser.

30. Biegler, L.T. 1984. Solution of dynamic optimization problems by successive quadratic programming and orthogonal collocation, *Comp. Chem. Eng.* 8:243.

31. Biegler, L.T. and J.B. Rawlings. 1991. Optimisation approaches to nonlinear model predictive control, *Proceedings of Conf. Chemical Process Control*, South Padre Island, Texas, 543-571.

32. Binder, T., L. Blank, H.G. Bock, et al. 2001. Introduction to model based optimization of chemical processes on moving horizons, In M. Groetschel, S.O. Krumke and J. Rambau (Eds.), *Online optimization of large scale systems*, Berlin, Springer.

33. Blanding, F. 1953. Reaction Rates in Catalytic Cracking of Petroleum. *Ind. Eng.Chem.* 45:1186-1197.

34. Bock, H.G. and K. Plitt. 1984. A multiple shooting algorithm for direct solution of optimal control problems. *Proc. 9th IFAC World Congress*, Budapest, Hungary.

35. Bock, H.G., I. Bauer, D. Leineweber, and J. Schloder. 1999. Direct multiple shooting methods for control and optimization in engineering, In *Scientific computing in chemical engineering II*, Volume 2, (F. Keil, W. Mackens, H. Vos, J. Werther, Eds.), Springer.

36. Bock, H.G., M. Diehl, D. Leineweber and J. Schlöder. 2000a. A direct multiple shooting method for real-time optimization of nonlinear DAE processes. in F. Allgöwer and A. Zheng (Edits.), *Nonlinear Predictive Control*, Birkhäuser, 245.

37. Bock, H.G., M. Diehl, J. Schlöder, F. Allgöwer, R. Findeisen, and Z. Nagy. 2000b. Real-time optimization and nonlinear model predictive control of processes governed by differential-algebraic equations. *Proc. Int. Symp. Adv. Control of Chemical Processes* (ADCHEM), Pisa, Italy, 695.

38. Bohn, C. and D.P. Atherton. 1995. An analysis package comparing PID anti-windup strategies. 15(2):34-40.

39. Bollas, G.M., A.A. Lappas, D.K. Iatridis, and I.A. Vasalos. 2007. Five-lump kinetic model with selective catalyst deactivation for the prediction of the product selectivity in the fluid catalytic cracking process. Research and Technology Hellas (CERTH). *Catalysis Today*. Thermi-Thessaloniki, Greece. 127: 31–43.

40. Bozicevic, J. and D. Lukec. 1987. Dynamic mathematical model for a fluid catalytic cracking process, *Trans Inst Meas Control* 9(1): 8-12.CPCL, 1999, FCC Operating Manual.

41. Brengel, D.D., W.D. Geider. 1989. Multistep nonlinear predictive controller, *Ind. Eng. Chem. Res*., 20:1812-1822.

42. Bristol, E.H. 1966. On a new measure of interactions for multivariable process control. *IEEE Trans. Autom. Control*, AC-11:133-134.

43. Brittain, J.E. 1977. *Turning Points in American Electrical History*, IEEE Press, New York, Sect. II-E.

44. Caldwell, J.M. and G.D. Martin. 1987. Online analyzer predictive control, *Sixth Annual Control Expo Conf.*, Rosemont, Illinois.

45. Campo, P.J. and M. Morari.1986. Inf-No rm formulation of model predictive control problems. *Proc. Am. Control Conf.,* Seattle, Washington. 339-343.

46. Carabineiro, H., C.I.C. Pinheiro, F. Lemos, and F. Ramoa Ribeiro. 2004. Transient microkinetic modelling of n-heptane catalytic cracking over H-USY zeolite, *Chemical Engineering Science*. 59:1221-1232.

47. Carlson, D.A., A.B. Haurie, and A. Leizarowitz. 1991. Infinite horizon optimal control. Springer Verlag.

48. Chang, S.S.L. 1961. *Synthesis of Optimum Control Systems*. McGraw-Hill, New York.

49. Chen H., C.W. Scherer, and F. Allgower. 1997. A game theoretic approach to nonlinear robust receding horizon control of constrained systems. In *Proc. Amer. Contr. Conf.*, 3073-3077, Albuquerque.

50. Chen J. and H. Cao. 1995. *Catalytic Cracking Technology and Engineering of Fluidized Catalytic Cracking*. China Petrochemical Press.788-864.

51. Chen, H. and F. Allgower. 1997. A quasi-infinite horizon nonlinear predictive control scheme for stable systems: Application to a CSTR, In *Proc. Int. Symp. Adv. Control of Chemical Processes, ADCHEM*. Banff, Canada. 471-476.

52. Chen, H. and F. Allgower. 1998. Nonlinear model predictive control schemes with guaranteed stability, In C. Berber, R. and Kravaris, editor, *Nonlinear Model Based Process Control*, 465-494. Kluwer Academic Publishers, Dodrecht.

53. Chen, H. and F. Allgower. 1996. A quasi-infinite horizon predictive control scheme for constrained nonlinear systems, In *Proc. 16th Chinese Control Conference*, Qindao.309-316.

54. Chen, H., C.W. Scherer and F. Allgower. 1998. A robust model predictive control scheme for constrained linear systems, In *5th IFAC Symposium on Dynamics and Control of Process Systems*, Korfu. *DYCOPS-5*, 60-65.

55. Cheng, W.C., G. Kim, A.W. Peters, X.Zhao, and K. Rajagopalan. 1998. Environmental FCC technology. *Catal. Rev. Sci. Eng*. 40: (1-2) 39-79.

56. Chisci, L.L., A. Lombardi, and E. Mosca. 1996. Dual-receding horizon control of constrained discrete time systems, *European Journal of Control*. 2: 278-285.

57. Christensen, G., M.R. Minas, K.J. Hickey, and S.F. Jaffe. 1999. Future directions in modeling the FCC process: An emphasis on product quality. *Chemical Engineering Science*, 54(13): 2753-2764.

58. Clarke, D.W. 1994. Advances in model-based predictive control. In D.W. Clarke, editor, *Advances in Model-Based Predictive Control.* Oxford University Press. 3-21.

59. Corella, J., E. Frances. 1991. In: M.L. Occelli (Ed.), Fluid Catalytic Cracking II (ACS Symposium Series 452). American Chemical Society, Washington, DC.452:165.

60. Corma, A., and J. Martinez-Triguero. 1994. Kinetics of gas oil cracking and catalyst decay on SAPO-37 and USY Molecular Sieves. *App. Catal.* 118:153-162.

61. Cristea, M.V. and S.P. Agachi. 1996. Controllability analysis of a model IV FCCU, in: *12th International Congress of Chemical and Process Engineering CHISA*, 10.

62. Cristea, M.V., S.P. Agachi, and V. Marinoiu. 2003. Simulation and Model Predictive Control of a UOP fluid catalytic cracking unit, *Chemical Engineering and Processing*. 42:67-91.

63. Cuthrell, J. and L. Biegler. 1989. Simultaneous optimization and solution methods for batch reactor profiles. *Comp. Chem. Eng.* 13(1/2):49-62.

64. Cutler, C.R. and B.L. Ramaker. 1980. Dynamic Matrix Control, a computer control algorithm, *Proceedings of Joint Automatic Control Conference.* San Francisco. 1: Paper No. WP5-B.

65. Cutler, C.R. and R.B. Hawkins. 1987. Constrained multivariable control of a hydrocracker reactor, *Proc. Am. Control Conf.,* Minneapolis, Minnesota, 1014-1020.

66. Cutler, C.R. and R.T. Perry. 1983. Real Time Optimization with Multivariable Control is Required to Maximize Profits. *Comp. Chem. Eng*. 7:663-1983.

67. Cutler, C., A. Morshedi, and J. Haydel. 1983. An industrial perspective on advanced control, in *AIChE Annual Meeting*, Washington, D.C.

68. Das, A., E., Baudrez, B. Marin, and G. Heynderickx. 2003. Three-dimensional simulation of a fluid catalytic cracking riser reactor. *Ind. Eng. Chem. Res.* 42:2602-2617.

69. Davidor, Y. 1991. Genetic Algorithms and Robotics: a heuristic strategy for optimization. Singapore: World Scientific.

70. De Gouv'ea M.T. and D. Odloak. 1998. One-layer real time optimization of LPG production in the fcc unit: Procedure, advantages and disadvantages. *Computers & Chemical Engineering*, 22:S191-S198.

71. De Lasa, H.I., A.F. Errazu, E. Barreiro, and S. Solioz. 1981. Analysis of fluidized bed catalytic cracking regenerator models in an industrial scale unit. *Can J Chem Eng*. 59: 549–553.

72. De Nicolao G., L. Magni, and R. Scattolini. 1996. On the robustness of receding horizon control with terminal constraints, *IEEE Trans. Automat. Contr*. 41(3):451-453.

73. De Nicolao G., L. Magni, and R. Scattolini. 1997. Stabilizing receding-horizon control of nonlinear time-varying systems, In *Proc. 4rd European Control Con- ference ECC'97.* Brussels.

74. De Nicolao, G., L. Magni, and R. Scattolini. 1998. Stability and Robustness of Nonlinear Receding Horizon Control, In *Proceedings of International Symposium on Nonlinear Model Predictive Control: Assessment and Future Directions* (F. Allgower and A. Zheng, Eds.). Ascona, Switzerland.77-90.

75. De Oliveira, N.M.C. and L.T. Biegler. 1995. An extension of Newton-type algorithms for nonlinear process control, *Automatica*. 31(2): 281-286.

76. De Oliveira, N.M.C., and L.T. Biegler. 1994. Constraint handling and stability properties of model-predictive control. *AIChE J.* 40(2):1138-1155.

77. De Oliveira, S.L. 1996. *Model predictive control for constrained nonlinear systems,* PhD thesis, Swiss Federal Institute of Technology (ETH), Zurich, Switzerland.

78. Deb, K. 2001. Multi-objective optimization using evolutionary algorithms. Chichester, UK: Wiley.

79. Diehl, M. 2001. *Real-Time Optimization for Large Scale Nonlinear Processes*. PhD Thesis, University of Heidelberg.

80. Diehl, M., H.G. Bock, J.P. Schlöder, R. Findeisen, Z. Nagy, F. Allgöwer. 2002. Real-time optimization and nonlinear model predictive control of processes governed by differential algebraic equations. *Journal of Process Control* 12:577-585.

81. Diehl, M., R. Amrit, and J. Rawlings. 2010. A lyapunov function for economic optimizing model predictive control. Accepted for Publication, IEEE Trans. on Auto.Cont.

82. Dulce, C.M. Silva, and Nuno M.C. Oliveira. 2002. Optimization and nonlinear model predictive control of batch polymerization systems, *Computers and Chemical Engineering*, 26:649-658.

83. Dupain, X., E.D. Gamas, R. Madon, C.P. Kelkar, M. Makkee, and J.A. Moulijn. 2003. Aromatic gas oil cracking under realistic FCC conditions in a microriser reactor. *Fuel.* 82(13):1559-1569.

84. Dupain, X., M. Makkee, and J.A. Moulijn. 2006. Optimal conditions in fluid catalytic cracking: a mechanistic approach. *Applied Catalysis.* 297:198-219.

85. Dupain, X., R. Krul, C. Schaverien, M. Makkee, and J. Moulijn. 2006. Production of clean transportation fuels and lower olefins from fischer-tropsch synthesis waxes undel fluid catalytic cracking conditions: the potential of highly paraffinic feedstock for FCC. *Applied Catalysis B: Enviromental*. 63(3-4):277-295.

86. E. ref 1. www. gasification. org/what is gasification/environmental_benefits. aspx.

87. E.ref 2. www. labbiokraftstoffe.de/downlods/PDF/fachinformation/suedzuckerbernardd.pdf.

88. E. ref 3. World Oil Outlook 2007, O PECS ecretariat2, 007 [date accessed2: 5/02/2008].

89. E. ref 4. www.chevron.com/products/prodserv/fuels/bulletin/motorgar/3%5Frefining%2 Dtesting/ Default. asp.

90. E. ref 5. www. chevron. com/products/about/Richmond/ about/what we do. Asp.

91. E. ref 6. www.uop.com/objects/1%20Emerg% 201nterlock%2OSystemp.dfl.

92. E. ref 7.www. uop. com/PetroFCC.

93. E. ref 8. www. maiglobal. com/news/wpss. pdfJ.

94. E.ref 9. Franke, R., E. Arnold and H. Linke. HQP: A solver for nonlinearly constrained large-scale optimization. http://hqp.sourceforge.net.

95. Edwards, W.M., and H.N. Kim. 1988. Multiple steady states in FCC unit operations. *Chem.Eng.Sci.* 43:1825.

96. Elamurugan, P., and D.D. Kumar. 2010. Modeling and Control of Fluid Catalytic Cracking Unit in Petroleum Refinery. *International Journal of Computer Communication and Information System (IJCCIS)* 2(1):976-1349.

97. Ellis, R.C., X. Li, and J.B. Riggs. 1998. Modelling and Optimization of a Model IV Fluidized Catalytic Cracking Unit. *AIChE Journal* 44(9):2068-2079.

98. Ellis, R.C., X. Li, and J.B. Riggs. 1998. Modelling and optimization of a model IV fluidized catalytic cracking unit. *American Institute of Chemical Engineers Journal* 44:2068.

99. Elshishini, E.E. and S.H. Elnashaie. 1990. Digital Simulation of Industrial Fluid Catalytic Cracking Units; Bifurcation and its Implications. *Chem .Eng. Sci.* 45:553.

100. Emad, E.A. and S.E. Elnashaie. 1997. Nonlinear model predictive control of industrial type IV fluid catalytic cracking units for maximum gasoline yield, *Ind. Chem. Eng. Res.* 36:389-398.

101. Eng, M.T., T.W. Cadman, and A.M. Kugelman. 1974. Nonlinear feedforward control of a fluidized catalytic cracking process. *ISA Trans.*13:232.

102. Engell, S. 2007. Feedback control for optimal process operation. *Journal of Process Control* 17:203-219.

103. Errazu, A.F., H.I. de Lasa, and F. Sarti. 1979. A fluidized bed catalytic cracking regenerator model grid effects, *Can J Chem Eng*. 57: 191-197.

104. Feng, W., E. Vynckier, and G. Froment. 1993. Single-event kinetics of catalytic cracking. *Ind. Eng. Chem. Res.* 32:2997-3005.

105. Findeisen, R. and F. Allgower. 1999. A procedure to determine a region of attraction for discrete time nonlinear systems, Technical Report #99.14, Automatic Control Laboratory, Swiss Federal Institute of Technology (ETH), Zurich, Switzerland.

106. Findeisen, R., and F. Allgower. 2000(a). Nonlinear model predictive control for index-one DAE systems, In *Nonlinear predictive control*, (F. Allgower and A. Zheng, Eds.), Birkhauser.

107. Findeisen, R., and J.B. Rawlings. 1997. Suboptimal infinite horizon nonlinear model predictive control for discrete time systems, Technical Report # 97.13, Automatic Control Laboratory, Swiss Federal Institute of Technology (ETH), Zurich, Switzerland,. *Presented at the NATO Advanced Study Institute on Nonlinear Model Based Process Control*.

108. Fisher, J.N. and S.L. Shah. 1986. Interaction analysis in multivariable control systems, *AIChE J*. 32:959-970.

109. Fonseca, C.M. and P.J. Fleming. 1993. Genetic algorithms for multi-objective optimization: formulation, discussion and generalization. In Proceedings of the Fifth International Conference on Genetic Algorithms, San Mateo, CA: Morgan Kaufmann, 416-423.

110. Ford, W.D., R.C. Reineman, I.A. Vasaloc, and R.J. Fahrieg. 1976. Modeling catalytic cracking regenerators. NPRA Annual Meeting.

111. Friedly, J.C. 1984. Use of the Bristol array in designing noninteracting control loops, A limitation and extension, *Ind. Eng. Chem. Process Des. Dev*. 23:469-472.

112. Fujiwara, M., D.L. Ma, T. Togkalidou, D.K. Tafti and R.D. Braatz. 2002. Identification of pharmaceutical crystallization processes. *Proc. of the IFAC World Congress on Automatic Control*, Elsevier Science Ltd., Oxford, UK, Paper T-Fr-A11.

113. Galan, O., J.A. 2000. Romagnoli, and A. Palazoglu, Robust H_∞ control of nonlinear plants based on multi-linear models: an application to a bench-scale pH neutralization reactor, *Chem. Eng. Sci.* 55:4435-4450.

114. Garcia, C.E. and A.M. Morshedi. 1986. Quadratic programming solution of dynamic matrix control (QDMC), *Proc. Am. Control Conf.,* San Diego, California; also *Chem. Engng Commun*. 46:73-87.

115. Garcia, C.E. and M. Morari. 1982. Internal model control-l. A unifying review and some new results, *Ind. Engng Chem. Process Des. Dev.* 21:308-323.

116. Garcia, C.E. and M. Morari. 1985a. Internal model control-2. Design procedure for multivariable systems, *Ind. Engng Chem. Process Des. Dev*. 24:472-484.

117. Garcia, C.E. and M. Morari. 1985b. Internal model control-3. Multivariable control law computation and tuning guidelines, *Ind. Engng Chem. Process Des. Dev.* 24:484-494.

118. Garcia, C.E., D.M. Prett, and M. Morari. 1989. Model Predictive Control: Theory and practice - A survey, *Automatica*. 25:335-347.

119. Garcia, C.E. 1984. Quadratic dynamic matrix control of nonlinear processes. An application to a batch reaction process, AIChE Annual Meeting, San Francisco, California.

120. Gary, J.H. and G.E. Handwerk. 1975. Petroleum refining Technology and Economics, Marcel Dekker, INC., New York. 86-87.

121. Gates, B. 1979. Chemistry of catalytic processes, McGraw-Hill book company, Gomez Prado J., UMIST dissertation, 2003.

122. Goldberg, D.E. 1989. Genetic Algorithms in Search, Optimization and Machine Learning. Addison-Wesley.

123. Gomez Prado J., UMIST dissertation, 2003.

124. Gomez-Prado J., N. Zhang and C. Theodoropoulos. 2006. Integrated feedstock characterization, kinetic modelling and process dynamics for FCC units. Conference proceedings of the 17th International Congress of Chemical and Process Engineering CHISA 2006, Prague, Czech Republic.

125. Gopaluni, R.B., R.S. Patwardhan and S.L. Shah. 2003. The nature of data pre-filters in MPC relevant identification - Open- and closed-Loop issues. *Automatica* 39(9):1617-1626.

126. Gros, S., B. Srinivasan and D. Bonvin. 2009. Optimizing control based on output feedback. *Comp. & Chem. Eng.* 33(1):191-198.

127. Grosdidier, P.M. Morari, and B.R. Holt. 1985. Closed loop properties from steady state gain information, *Ind. Eng. Chem. Fundam.* 24:221-235.

128. Grosdidier, P., A. Mason, A. Aitolahti, P. Heinonen, and V. Vanhamaki. 1993. FCC unit reactor-regenerator control. *Computers Chem. Engng.* 17(2):165-179.

129. Grosdidier, P., B. Froisy, and M. Hammann. 1988. The IDCOM-M controller, In T.J. McAvoy, Y. Arkun, and E. Zafiriou, edit. *Proceedings* of *the* 1988 *IFAC Workshop on Model Based Process Control.* Oxford, Pergamon Press. 31-36.

130. Guigon, P., and J.F. Large. 1984. Application of the Kunii-Levenspiel model to a multi-stage baffled catalytic cracking regenerator, *Chem Eng J.* 28:131-138.

131. Gupta, A. and D. Rao. 2003. Effect of feed atomization on FCC performance: simulation of entire unit, Chemical Engineering Science. 58:4567-4579.

132. Hagelberg, P. and I. Eilos, J. Hiltunen, K. Lipiäinen and V.M. Niemi, J. Aittamaa and A.O.I. Krause. 2002. Kinetics of catalytic cracking with short contact times. *Applied Catal.*223: 73-84.

133. Haggblom, K.E. 1994. Modeling of control structures for partially controlled plants, Prepr. IFAC Workshop on Integration of Process Design Control (IPDC'94). Baltimore, Maryland, USA.183-188.

134. Hajela, P., E. Lee, and C.Y. Lin. 1992. Genetic algorithms in structural topology optimization. In Proceedings of the NATO Advanced Research Workshop on Topology Design of Structures, Sesimbra, Portugal, 117-134.

135. Halvorsen, I.J. and S. Skogestad. 2000. Distillation Theory, In: Encyclopedia of Separation Science. D. Wilson (Editor), Academic Press.1117-1134.

136. Halvorsen, I.J. and S. Skogestad. 2003. Minimum Energy Consumption in Multicomponent Distillation. Part 1- Vmin Diagram for a Two-Product Column, *Industrial and Engineering Chemistry Research*. 42(3):594-604.

137. Han, I.S., C.B. Chung, and J.B. Riggs. 2000. Modeling of a fluidized catalytic cracking process, *Computers Chemical Engineering*. 24:1681-1687.

138. Han, I.S. and C.B. Chung. 2001. Dynamic modelling and simulation of a fluidized catalytic cracking process. *Chem. Eng. Sci.* 55:1951-1971.

139. Han, I.S. J. B. Riggsa, and Chang-Bock Chungb. 2004. Modeling and optimization of a fluidized catalytic cracking process under full and partial combustion modes. *Chemical Engineering and Processing.* 43:1063-1084.

140. Hassapis, G. 2003. Implementation of model predictive control using real-time multiprocessing computing, *Microprocessors and Microsystems*.27:327-340.

141. Heidarinejad, M., J. Liu, and P.D. Cristofides. 2011. Economic model predictive control of nonlinear process system using lyapunov thechniques. *AICHE Journal*, DOI 10.1002/aic.12672.

142. Helbig, A., O. Abel, and, W. Marquardt. 2000. Structural concepts for optimization based control of transient processes. In F. Allgöwer and A. Zheng (eds.), Nonlinear Model Predictive Control, Progress in Systems and Control Theory 26:295-311. Birkhauser, Basel.

143. Henson, A.M. 1998. Nonlinear model predictive control: current status and future directions, *Comp. Chem. Eng.* 23:187-201.

144. Hicks, G. and W. Ray. 1971. Approximation methods for optimal control synthesis. *Can. J. Chem. Eng*. 49:522-528.

145. Hicks, R.C., G.R. Worrell, and R.J. Durney. 1966. Atlantic Seeks Improved Control; Studies Analog-Digital Models. *Oil and Gas J.* 24:97.

146. Holland, J.H. 1975. Adaptation in natural and artificial systems. Ann Arbor: M I T Press.

147. Horn, J., and N. Nafploitis. 1993. Multiobjective optimization using the niched Pareto genetic algorithm. Technical Report 93005, IlliGAL, University of Illinois, Urbana-Champaign.

148. Hovd, M. and S. Skogestad. 1992. Simple frequency dependent tools for control system analysis, structure selection and design, *Automatica*, 28:989-996.

149. Hovd, M. and S. Skogestad. 1993. Procedure for regulatory control structure selection with application to the FCC process. *AIChE Journal*. 39(12):1938-1953.

150. Hovd, M., and S. Skogestad. 1991. Controllability analysis for the fluid catalytic cracking process, in: *AIChE* Annual Meeting, 17:/22, Los Angeles.

151. Hovd, M., and S. Skogestad. 1992a. Simple Frequency-Dependent Tools for Control System Analysis, Structure Selection and Design," *Automatica* 28: 989.

152. Hovd, M., and S. Skogestad. 1992b. Controllability Analysis for Unstable Processes," *IFAC Workshop* on *Interactions between Process Design and Process Control,* Pergamon Press, London, 49.

153. Huang, R., E. Harinathc, and L.T,. Biegler. 2011. Lyapunov stability of economically oriented NMPC for cyclic processes, *Journal of Process Control* 21:501-509.

154. Huesman, A.E.M., O.H. Bosgra, and P.M. den Hof. 2008. Integrating MPC and RTO in the process industry by economic dynamic lexicographic optimization; an open-loop exploration. In Proceedings of the AICHE Annual Meeting. Philadelphia, USA.

155. Humphries, A., and R.C. Skocpol. 2004. Fluid Cracking Catalysts design technology, *C.PG. Smit, PG. Connor, (Editors), Catalyst Courier*. 33:2004.

156. Imsland, L., R. Findeisen, E. Bullinger, F. Allgower, and B. A. Foss. 2003. A note on stability, robustness and performance of output feedback nonlinear model predictive control, *Journal of Process Control*.13:633–644.

157. Iscol L. 1970.The Dynamics and Stability of a Fluid Catalytic Cracker. Proc. 1970 JACC, session paper 23-B, 602.

158. Jacob, S., B. Gross, S. Voltz, and V. Weekman. 1976. A lumping and reaction scheme for catalytic cracking. *AIChEJ*. 22 (4):701-713.

159. Jacob, S.M., B. Gross, S.E. Voltz, and V.M. Weekman. 1976. A lumping and reaction scheme for catalytic cracking, *AIChE J*. 22(4):701-713.

160. Jia C., S. Rohani, and A. Jutan. 2003. FCC unit modeling, identification and model predictive control- a simulation study, *Chemical Engineering and Processing* 42: 311-325.

161. Jianping, Gao., Rohit Patwardhan, K. Akamatsu, Y. Hashimoto, G. Emoto, L. Shah Sirish, and Biao Huang. 2003. Performance evaluation of two industrial MPC controllers, *Control Engineering Practice*, in press.

162. John, T.M. and B.W. Wojciechowski. 1975. On identifying the primary and secondary products of the catalytic cracking of neutral distillates, *J. Catal.*, 37:240-250.

163. Kacprzyk, J. 1995. A modified genetic algorithm for multistage control of a fuzzy system. In Proceedings EUFIT'95, 1: Aachen, Germany, 463 – 6.

164. Kadam, J., W. Marquardt, M. Schlegel, T. Backx, O. Bosgra, P.-J. Brouwer, G. D¨unnebier, D. Hessem, A. Tiagounov, and S. de Wolf. 2003. Towards integrated dynamic real-time optimization and control of industrial processes, in I. E. Grossmann, C. M. McDonald (Eds.): FOCAPO, Proceedings of the Con- ference. 593-596.

165. Kadam, J. V. and W. Marquardt. 2007. Nonlinear model predictive cotnrol of the hashimoto simulated moving bed process, in R. Findeisen, F. Allgöwer, and L. Biegler, edits, 'Assessment and Future Directions of Nonlinear Model Predictive Control', Springer, 419–434.

166. Kadam, J., M. Schlegel, W. Marquardt, R. Tousain, D. Hessem, J. Berg, and O. Bosgra. 2002. A two-level strategy of integrated dynamic optimization and control of industrial processes - a case study, in J. Grievink, J. v. Schijndel (Eds.): European Symposium on Computer Aided Process Engineering. 12:511-516.

167. Kalra, L., and C. Georgakis. 1994. Effect of Process Nonlinearity on the Performance of Linear Model Predictive Controllers for the Environmentally Safe Operation of a Fluid Catalytic Cracking Unit, *Ind. Eng. Chem. Res*. 33:3063-3069.

168. Kambreck, F. 1991. Continuous mixtures in fluid catalytic cracking and extensions. Mobil workshop on chemical reaction in complex mixtures, Van Nostrand Reinhold, New York.

169. Karla, L., and C. Georgakis. 1994. Effect of process nonlinearity on performance of linear model predictive controllers for environmentally safe operation of a fluid catalytic cracking unit. *Ind. Eng. Chem. Res.* 33:3063-3069.

170. Karr, C.L. 1992. An adaptive system for process control using genetic algorithms .In IFAC Artificial Intelligence in Real-Time Control, Delft , The Netherlands.329-34

171. Katz, R.N. 2001. Advanced ceramics: Zeolites equal more miles per barrel, *ceramic Industry*. 151(12):16-20.

172. Keerthi, S.S. and E.G. Gilbert. 1988. Optimal infinite-horizon feedback laws for a general class of constrained discrete-time systems: Stability and moving-horizon approximations, *J. Opt. Theory and App.* 57 (2): 265-293.

173. Kirby, A. 2004. What to use when the oil runs out. BBC news online environment correspondent at http: //news. bbc. co. uk/l/hi/sci/tech/3623675. stm (date accessed: 10/03/2008).

174. Kiss, P., and F. Szeifert. 1998. Coordinated control of a fluid catalytic cracking unit. *Chem. Eng. Tech.* 21:515-521.

175. Kookos, I.K. 2005. Real time regulatory control structure selection based on economics. I*nd. Eng. Chem. Res.* 44:3993-4000.

176. Krishna, A.S. and E.S. Parkin. 1985. Modelling the regenerator in commercial fluid catalytic cracking units, *Chem Eng Prog.* 81(4):57-62.

177. Krstic, M. and H. Wang. 2000. Stability of extrmum seeking feedback for general nonlinear dynamic systems, *Automatica* 36:595-601.

178. Kumar, S., A. Chadha, R. Gupta, and R. Sharma. 1995. A process simulator for an integrated FCC-regenerator system, *Ind Eng Chem Res.* 34:3737-3748.

179. Kumar, V. and A.A. Sharma. 2001. A crude distillation unit model suitable for online applications, *Fuel Processing Technology*.73:1-21.

180. Kurihara H. 1967.Optimal Control of Fluid Catalytic Cracking Processes. Sc.D. Thesis, Massachusetts Institute of Technology.

181. Kursawe, F. 1990. A Variant of evolution strategies for vector optimization. In Parallel Problem Solving From Nature, I (PPSN-I), Dortmund, Germany, 193-197.

182. Kwon, W. H. 1994. Advances in predictive control: Theory and applications. In *1st Asian Control Conference*, Tokyo.

183. Larocca, M., S. Ng, and H. Lasa. 1990. Fast catalytic cracking of heavy gas oils: modelling coke deactivation, *Ind Eng Chem Res.* 29:171-180.

184. Le Lann M.V., M. Cabassud, and G. Casamatta. 1999. Modeling, optimization and control of batch chemical reactors in fine chemical production, *Annual Reviews in Control.* 23:25-34.

185. Lee J.H. and B. Cooley. 1996. Recent advances in model predictive control and other related areas. In J.C. Kantor, C.E. Garcia, and B. Carnahan, editors, *Fifth International Conference on Chemical Process Control - CPC V*, 201-216, *American Institute of Chemical Engineers*.

186. Lee J.H. 1998. Modeling and identification for nonlinear model predictive control: requirements, current status and future research needs, In *Proceedings of International Symposium on Nonlinear Model Predictive Control: Assessment and Future Directions* (F. Allgower and A. Zheng, Eds.). Ascona, Switzerland. 91-107.

187. Lee L., Y. Chen, T. Huang, W. Pan. 1989. Four-lump kinetic model fro fluid catalytic cracking process. *The Canadian Journal of Chemical Engineering.*67:615-619.

188. Lee, E. and F.R. Groves. 1985. Mathematical model of the fluidized bed catalytic cracking plant, *Transaction of the Society for Computer Simulation.* 3(3):219-236.

189. Lee, J.H. and Z.H. Yu. 1994. Tuning of model predictive controllers for robust performance, *Comp. Chem. Eng.* 18:15-37.

190. Lee, L., S. Yu, C. Cheng, and W. Pan. 1989a. Fluidized-bed catalyst cracking regenerator modelling and analysis, *Chem Eng J.* 40:71-82.

191. Lee, L., Y. Chen, T. Huang, and W. Pan. 1989b. Four-lump kinetic model for fluid catalytic cracking process. *Can J Chem Eng* 67:615-619.

192. Lee, W. and A.M. Kugelman. 1973. Number of steady-state operating points and local stability of open-loop fluid catalytic cracker, *Ind Eng Chem process Des Dev*. 12(2):197-204.

193. Levien, K.L. and M. Morari. 1987. Internal model control of coupled distillation columns. *AIChE Journal* 33(1):83–98.

194. Liao, Bo. 2008. Time optimal control of fluid catalytic cracking unit. Ph.D thesis. University of Toronto, Canada.

195. Linkens, D. A. and H. O. Nyongesa. 1995b. Genetic algorithms for fuzzy control - part 2: online system development and application. *IEE Proceedings on Control Theory Applications* 142(3):177-185.

196. Linkens, D. A. and H. O. Nyongesa. 1995a. Genetic algorithms for fuzzy control – part1: offline system development and application. *IEE Proceedings on Control Theory Applications* 142(3):161-175.

197. Lopez-Isunza, F. 1992. Dynamic modelling of an industrial fluid catalytic cracking unit, *Computers and Chemical Engineering* 16(1):S139-S148.

198. Lu, J. Z. 2001. Challenging control problems and emerging technologies in enterprise optimization, *Proceedings of the 6th IFAC Symposium on Dynamic and Control of Process Systems (DYCOPS-6.*23-34.

199. Luenberger, D.j. 1971. An introduction to observers. *IEEE Trans. Automat. Contr.* 16:596-602.

200. Magee, J.S. and M.M. Mitchell. 1993. Fluid catalytic cracking: science and technology. *Elsevier.* Amsterdam; New York.

201. Marques, D. and M. Morari. 1896. Model predictive control of gas pipeline networks, *Proc. Am. Control Conf.*, Seattle, Washington.349-354.

202. Marquis, P. and J.P. Broustail. 1988. SMOC, a bridge between state space and model predictive controllers: Application to the automation of a hydrotreating unit, In T.J. McAvoy, Y.Arkun, and E. Zafiriou, editors, *Proceedings of the 1988 IFAC Workshop on Model Based Process Control.* Oxford, Pergamon Press. 37-43.

203. Matsko, T. N. 1985. Internal model control for chemical recovery. *Chem. Engng Prog.* 81(12):46-51.

204. Mayne, D.Q. 2000. Nonlinear model predictive control: Challenges and opportunities, In F. Allgower and A. Zheng, editors, *Nonlinear Predictive Control.* Birkhauser, Basel.

205. Mayne, D.Q. and H. Michalska. 1990. Receding horizon control of nonlinear systems, *IEEE Trans. on Automatic Control.* 35(7):814-824.

206. Mayne, D.Q., J.B. Rawlings, C.V. Rao, P.O. Scokaert. 2000. Constrained model predictive control: Stability and optimality, *Automatica*. 36:789-814.

207. Mayne, D.Q. 1996. Nonlinear model predictive control: An assessment, In J.C. Kantor, C.E. Garcia, and B. Carnahanr editors, *Fifth International Conference on Chemical Process Control -CPC V.* 217-231, *American Institute of Chemical Engineers*.

208. Mayr, O. 1970. *The origins of feedback control*, M.I.T. Press, Cambridge, Mass.

209. McAvoy, T. 2002. Intelligent control applications in the process industries, *Annual Reviews in Control*. 26:75-86.

210. McAvoy, T.J. 1983. Interaction Analysis, Instrument Society of America, Research Triangle Park, USA.

211. McFarlane, R.C. and D.W. Bacon. 1989. Adaptive optimizing control of multivariable constrained chemical processes. 1. Theoretical development. Industrial and Engineering Chemistry Research 28:1828.

212. McFarlane, R.C. and R.C. Reineman, J.F. Bartee, and C., Georgakis. 1993. Dynamic simulator for a model IV Fluid Catalytic Cracking Unit, Computers Chemical Engineering, 17(3):275-300.

213. McFarlane, R.C., R.C. Reineman, J.F. Bartee and C. Georg akis. 1990. Dynamic simulation for a model IV fluid catalytic cracking unit. Presented at AIChE Meeting, Chicago Ill., paper 24d, 14-16.

214. McGreavy, C.and P.C. Isles-Smith. 1986. Modelling of a fluid catalytic cracker, *Transactions of the Institute of Measurement and Control* 8: 130-136.

215. Meadows, E. S. and J. B. Rawlings. 1993. Receding horizon control with an infinite horizon, In *Proc. Amer. Contr. Conf.* San Francisco. 2926-2930.

216. Meadows, E. S., M. A. Henson, J. W. Eaton, and J. B. Rawlings. 1995. Receding horizon control and discontinuous state feedback stabilization, *Int. J. Contr.* 62(5):1217-1229.

217. Meyers, R. A. 1997. Handbook of petroleum refining processes. 2nd edn. New York: McGraw-Hill.

218. Michaska, H., D.Q. Mayne. 1993. Robust receding horizon control of constrained nonlinear systems, *IEEE Transactions on Automatic Control*. 38(11):1623-1633.

219. Miriam Tvrzskh de GouvSa, and Darci Odloak. 1998. One-layer real time optimization of LPG production in the FCC unit: procedure, advantages and disadvantages. *Computers chum .Engng* 22:S191-S198.

220. Mohsen, M.S. and O.R. AI-Jayyousi. 1999. Brackish water desalination: an alternative for water supply enhancement in Jordan'', *Desalination* 124:163-174.

221. Morari, M. and J.H. Lee. 1997. Model predictive control: Past, present and future. In *Proc. PSE'97-ESCAPE-7 Symposium*, Trondheim.

222. Morari, M., G. Stephanopoulos, and Y. Arkun. 1980. Studies in synthesis of control structures for chemcial processes, part 1, *AIChE J.* 26:220-232.

223. Murata, T. 1997. Genetic algorithms for multi-objective optimization. Ph.D. Thesis, Osaka Prefecture University, Osaka, Japan.

224. Muske, K.R., J.W. Howse, G.A. Hansen and D.J. Cagliostro. 2000b. Model-based control of a thermal regenerator. Part 2: control and estimation, *Comp. Chem. Eng.*, 24:2507-2517.

225. Muske, K.R., J.W. Howse, G.A. Hansen, and D.J. Cagliostro. 2000a. Model-based control of a thermal regenerator. Part 1: dynamic model, *Comp. Chem. Eng.* 24:2519-2531.

226. Nagy, Z. and S. Agachi. 1997. Model Predictive Control of a PVC Batch Reactor, *Comp. Chem. Eng.* 21(6):571-591.

227. Nagy, Z. K. 2001. Model Predictive Control techniques for chemical processes. PhD Thesis. University of Clujnapoca.

228. Nagy, Z. K. and S. P. Agachi. 2004. Model based control of chemical processes. Press Universitara Clujeană.

229. Nagy, Z.K. and R.D. Braatz. 2003. Robust nonlinear model predictive control of batch processes, *AIChE J.* 49(7):1776-1786.

230. Nagy, Z.K. and F. Allgower. 2007. A nonlinear model predictive control approach for robust end-point property control of a thin film deposition process. *International Journal of Robust and Nonlinear Control* 17:1600-1613.

231. Nikolaou, M. 2001. Model Predictive Controllers: A Critical Synthesis of Theory and Industrial Needs. *Advances in Chemical Engineering Series.*

232. O'Connor, P., P. Imhof, and S.J. Yanik. 2001. Catalyst assembly technology in FCC. In Fluid Catalytic Cracking V. Materials and Technologh Innovations; Occelli, M.L., O'Connor, P., Eds.; Studies in Surface Science and Catalysis; *Elsevier*.134.

233. Oliveira, L. 1987. Estimate of parameters and Evaluation Model Catalytic cracking. MSc Thesis (in Portuguese), Univ. Federal do Rio de Janeiro, Brazil.

234. Oliveira, L. and E.C. Biscaia. 1989. Catalytic cracking kinetic models parameter estimation and model evaluation. *Ind. Eng. Chem. Res.* 28:264-271.

235. Oliveira, L.L., E.C. Biscaia. 1989. Ind. Eng. Chem. Res. 28:264.

236. Pan Y., J.H. Lee. 2003. Recursive data-based prediction and control of product quality for a PMMA batch process, *Chemical Engineering Science*. 58:3215- 3221.

237. Paraskos, J.A., Y.T. Shah, J.D. McKinney, and N.L. Carr. 1976. A kinematic model for catalytic cracking in a transfer line reactor, *Ind Eng Chem Process Des Dev.* 15(1):165-169.

238. Park Myung-June, Hyun-Ku Rhee. 2003. Property evaluation and control in a semibatch MMA/copolymerization reactor, *Chemical Engineering Science*.58:603-611.

239. Parrish, J.R. and C.B. Brosilow. 1985. Inferential control applications, *Automatica.* 21:527-538.

240. Patwardhan, A.A., J.B. Rawlings, and T.F. Edgar. 1990. Nonlinear model predictive control, *Chem. Eng. Comm.* 87:123-141.

241. Petry, E.E., B.P. Buckles, D. Prabhu, R. George, and R. Srikanth. 1994. Fuzzy clustering with genetic search. In Proceedings of the First IEEE Conference on Evolutionary Computation,1: 46-50.

242. Pitault, I., D. Nevicato, M. Forissier, and J. Bernard. 1994. Kinetic model based on a molecular description for catalytic cracking of vacuum gas oil. *Chem. Eng. Sci*. 49(24A):4249-4262.

243. Pohlenz, J. B. 1963. How Operational Variables Affect Fluid Catalytic Cracking. *Oil Gas J.* 61 :(13), 124-143.

244. Poloski, A. P., and J. C. Kantor. 2003. Application of model predictive control to batch processes, *Computers and Chemical Engineering*. 27:913-926.

245. Prett, D.M. and R.D. Gillette. 1979. Optimization and constrained multivariable control of a catalytic cracking unit, *AIChE National Meeting*, Houston; Texas; also *Proc. Joint Aut. Control Conf.*, San Francisco, California.

246. Lee, W. and A.M., Kugelman. 1973. Number of steady-state operating points and local stability of open- loop fluid catalytic cracker. *Ind. Eng. Chem. Process Des. Dev.* 12: 197-204.

247. Qin S.J. and T. Badgewell. 2003. A survey of industrial model predictive control technology. *Control Engineering Practice* 11:733-764.

248. Qin, S.J. and T.A. Badgwell. 2000. An overview of nonlinear model predictive control applications. In F. Allgower and A. Zheng, editors, *Nonlinear Predictive Control*, Birkhauser, Basel.

249. Rahul B. Kasat, Santosh K. Gupta. 2003. Multi-objective optimization of an industrial fluidized-bed catalytic cracking unit (FCCU) using genetic algorithm (GA) with the jumping genes operator.*Computers and Chemical Engineering* 27:1785-1800.

250. Rawlings, J. and R. Amrit. 2009. Optimizing process economic performance using model predictive control, in L. Magni, D. M. Raimondo and F. Allgöwer, edits, 'Assessment and Future Directions of Nonlinear Model Predictive Control', Springer, 119-138.

251. Rawlings, J.B. and R. Amrit. 2008. Optimizing process economic performance using model predictive control. In Assessment and Future Directions of Nonlinear Model Predictive Control. Pavia, Italy.

252. Rhemann, H., G. Schwartz, T. Badgwell, M. Darby, and D. White. 1989. On-line FCCU advanced control and optimization, Hydrocarbon Processing 64-71.

253. Richalet, J., A. Rault, J.L. Testud, and J. Papon. 1978. Model Predictive Heuristic Control: application to industrial processes, *Automatica*. 14:413-428.

254. Roman, R., Z. Nagy, M. Cristea, and S. Agachi. 2009. Dynamic modelling and nonlinear model predictive control of a Fluid Catalytic Cracking Unit, 2009, *Computers and Chemical Engineering*. 33(3):605-617.

255. Sadeghbeigi, R. 1995. Fluid catalytic cracking handbook. Houston, Tex.: Gulf Pub. Co.

256. Sadeghbeigi, R. 2000. Fluid Catalytic Cracking Handbook - Design, Operation and Troubleshooting of FCC Facilities, second edition. Gulf professional publishing.

257. Saxton, A.L. and A.C. Worley. 1970. Modern catalytic cracking design, *Oil and Gas J.* 68:82-99.

258. Schaffer, J.D. 1984. Some experiments in machine learning using vector evaluated genetic algorithms. Ph.D. Thesis, Vanderbilt University, Nashville, TN.

259. Scherzer, J. 1990. Octane-enhancing, zeolitic FCC catalysts: scientific and technical aspects / Julius Scherzer M. Dekker, New York.

260. Secchi, A.R., M.G. Santos, G.A. Neumann, and J.O. Trierweiler. 2001. A dynamic model for a FCC UOP stacked converter unit, *Computers and Chemical Engineering*, 25:851-858.

261. Sekia, Hiroya, Morimasa Ogawab, Satoshi Ooyamab, Kouji Akamatsub, Masahiro Ohshimac, and Wang Yang. 2001. Industrial application of a nonlinear model predictive control to polymerization reactors, *Control Engineering Practice*. 9:819-828.

262. Semino, D. and C. Scali. 1994. A method for robust tuning of linear quadratic optimal controllers. *Ind. Eng. Chem. Res.* 33:889-895.

263. Serti-Bionda, K., Z. Gomzi, and M. Muzic. 2010. Modeling of Gas Oil catalytic cracking in a fixed bed reactor using a five-lump kinetic model, *Chemical Engineering Communications* 197(3):275-288.

264. Shah, Y.T., G.T. Huling, J.A. Paraskos, and J.D. McKinney. 1977. A kinematic model for an adiabatic transfer line catalytic cracking reactor. *Ind Eng Chem Process Des Dev*. 16(1):89-94.

265. Shinskey F.G. 1979. Process, Control Systems, 2nd ed, McGraw Hill, New York.

266. Shinskey F.G. 1984. Distillation Control, 2nd ed, McGraw Hill, New York.

267. Shouche Manoj S., Hasmet Genceli, and Michael Nikolaou. 2002. Effect of on-line optimization techniques on model predictive control and identification (MPCI), *Computers and Chemical Engineering*.26:1241-1252.

268. Shridar, R. and D.J. Cooper. 1997. A tuning strategy for unconstrained SISO model predictive control, *Ind. Eng. Chem. Res*.36:729-746.

269. Silverman, B.W. 1986. Density estimations for statistics and data analysis, *Mnonogr. Stat. Appl. Prob.* 26:175. Chapman and Hall, London.

270. Silverman, L.D., W.S. Winkler, J.A. Tiethof, A. Witoshkin. 1986. NPRA Annual Meeting, Los Angeles, March 23-26; AM-86-62.

271. Skogestad, S. and M. Morari. 1987. Implications of large RGA elements on control performance, Ind. Eng. Chem. Res.26, 2323-2330.

272. Skogestad, S., and E.A. Wolff. 1992. Controllability Measures for Disturbance Rejection. IFAC *Workshop on Interactions between Process Design and Process Control,* Pergamon Press, London, 23-29 (1992).

273. Skogestad, S., and M. Morari. 1987a. Effect of Disturbance Direction on Closed Loop Performance. *Ind. Eng. Chem. Res.* 26:2029.

274. Skogestad, S., and M. Morari. 1987b. Implications of Large RGA Elements on Control Performance. *Ind. Eng. Chem. Res.* 26(11):2323.

275. Srinivas, N., and K. Deb. 1994. Multi-objective optimization using nondominated sorting in genetic algorithms. *Evolutionary Computation* 2:221.

276. Surmann, H., A. Kanstein and K.Goser. 1993. Self-organizing and genetic algorithms for an automatic design of fuzzy control and decision systems. In *Proceedings of First European Congress on Intelligent Techniques and Soft Computing*, 2:1097-1104.

277. Taguchi, H. and M. Araki. 2000. Two-Degree-off freedom PID controllers - Their functions and optimal tuning. In IFAC Digital Control: Past, Present and Future of PID Control. Terrassa, Spain.

278. Takatsuka, T., S. Sato, Y. Morimoto, and H. Hashimoto. 1987. *Int. Chem. Eng*. 27:107.

279. Takatsuka, T., S. Sato, Y. Morimoto and H. Hashimoto. 1987. A reaction model for fluidized-bed catalytic cracking of residual oil. *Int Chem Eng*. 27:107-116.

280. Tasoti, V. 2007. Enhancement of environmental security by mathematical modelling and simulations of processes, NATO Security through Science Series, 47-56.

281. Tominaga, H., and M. Tamaki. 1997. Chemical reaction and reactor design. *J. Wiley. Chic ester*, England; New York.

282. Tsang, T., D. Himmelblau, and T. Edgar. 1975. Optimal control via collocation and non-linear programming. *Int. J. Contr.* 21:763-768.

283. Umesh K. Chitnis and Armando B. Corripio. 1998. On-line optimization of a model IV fluid catalytic cracking unit, ISA Transactions 37: 215-226, USA.

284. Van Brempt, Wim Ton Backx, Jobert Ludlage, Peter Van Overschee, Bart De Moor, and R. Tousain. 2001. A high performance model predictive controller: application on a polyethylene gas phase reactor. *Control Engineering Practice* 9:829-835.

285. Wang, D. and J.A. Romagnoli. 2003. Robust model predictive control design using a generalized objective function. *Comp. & Chem. Eng.* 27:965-982.

286. Weekman, V. and D. Nace. 1970. Kinetics of catalytic cracking selectivity in fixed, moving and fluid bed reactorsA. *IChEJ*. 16:397-404.

287. Weekman, V.W. and D.M. Nace. 1970. Kinetics of catalytic cracking selectivity in fixed, moving and fluid bed reactors, *AIChE J.* 16: 397-404.

288. Witcher, M.F. and T.J. McAvoy. 1977. Interacting control systems - Steady state and dynamic measurement of interaction, *ISA Transactions* 16:35-41.

289. Wolff, E. A., S. Skogestad, M. Hovd, and K. W. Mathisen. 1992. A Procedure for Controllability Analysis," *IFAC Workshop on Interactions between Process Design and Process Control*, Pergamon Press, London, 127-132.

290. Würth, L., J. B. Rawlings, and W. Marquardt. 2009. Economic dynamic real-time optimization and nonlinear model predictive control on infinite hoirzons, in 'International Symposium on Advanced Control of Chemical Process', Istanbul, Turkey.

291. Würth, L., J.B. Rawlings, and W. Marquardt. 2009. Economic dynamic real-time optimization and nonlinear model predictive control on infinite hoirzons, in: Proceedings

of the International Symposium on Advanced Control of Chemical Process, Istanbul, Turkey, 2009.

292. Xu, Ch., J. Gao, S. Zhao, and Sh. Lin. 2005. Correlation between feedstock SARA components and FCC product yields. *Fuel* 84:669-674.

293. Yang, S., X. Wang, C. McGreavy. 1996. A multivariable coordinated control system based on predictive control strategy for FCC reactor-regenerator system, *Chem. Eng. Sci.*51:2977-2982.

294. Yen, L. C., R. E. Wrench, and A. S. Ong. 1988. Reaction Kinetic Correlation Equation Predicts Fluid Catalytic Cracking Coke Yields. *Oil & Gas J.* 86:67.

295. Yu, C.C., and W.L. Luyben. 1987. Robustness with respect to integral controllability, *Ind. Eng. Chem. Res.* 26:1043-1045.

296. Zafiriou, E., and M. Morari. 1986. Design of robust digital controllers and sampling-time selection for SISO systems, *Int. J. Control* 44(3):711-735.

297. Zanin, A.C., and M. Tvrzská de Gouvêa, and D. Odloak. 2002. Integrating real-time optimization into the model predictive controller of the FCC system. *Control Engineering Practice* 10:919-931.

298. Zanin, A.C., M.T. Gouvêa, and D. Odloak. 2002. Integrating real-time optimization into the model predictive controller of the FCC system. *control engineering practice* 10:819.

299. Zanin, A., M. Gouvˆea, and D. Odloak. 2000. Integrating real-time optimization into the model predictive controller of the FCC system. *Cont. Eng. Practice* 10:819-831.

300. Zavala, V. M., E. M. Constantinescu, T. Krause, and M. Anitescu. 2009. On-line economic optimization of energy systems using weather forecast information. *Journal of Process Control* 19:1725-1736.

301. Zavala, V. 2008. Computational Strategies for the Optimal Operation of Large-Scale Chemical Processes. Ph.D. thesis, Carnegie Mellon University.

302. Zhang, W.D., Y.X. Sun, and X. M. Xu. 1996. Modified PID controller based on H infinity theory. *IEEE Int. Conf. on Ind. Tech.* 9-12.

Appendix

The following MATLAB codes for main model which contains the main FCC Unit (7) parts with 5-lump riser model.

```
function [sys,
X0]=fccmodcol2(t,X,u,flag,disturban
ce);

persistent ft xO2sg xCOsg xCO2sg
fsc frgc cO2sg cCOsg yhcofinal
ylcofinal yglnfinal
%    Constants

%    feed system constants

f1set = 13.8;
f2set = 0.0;
%f3set = 126.0;
%f4set = 5.25;

%    preheat system constants

%f5set  =  34.0;
taufo  =   60.0;
taufb  =  200.0;
UAf    =   25.0;
temph1 =  460.9;
DHfu   = 1000.0;
a1     =    0.15;
a2     =  200.0;

%    reactor and fractionator
constant

%psif   = 1.0;
Aris   = 12.3;%9.6
hris   = 129.4;%60;
rov    = 0.57;
ropart = 68;
c1     = 7.12e-3;%8.84e-3;
c2     = 3.8e-5;%4.0e-5;
tref   = 999;%999;
mcpeff = 10000;
cpc    = 0.31;
tbase  = 959;
cpfl   = 0.82;
tbasef = 700;
t4     = 572;
cpsv   = 0.80;
cpsl   = 0.80;
Qsr    = 412.0;
cpfv   = 0.81;
Qfr    = 309;
dtstrp = 10;
k12    = 0.5;
patm   = 15;%14.7;
dpfrac = 9;
astr   = 70.9;%60;
eloi   = 11.5;%124.5;
estrp  = 26.2;%130;

%     wet-gas compressor constants

pvru = 101.;
k11  = 1.5;
k13  = 0.01;

%     ubend constants

roc    = 45;
areaur = 6.7;%3.7;
areaus = 8.2;%5.2;
lur    = 44;%56;
lus    = 30.2;%56;
furgc  = 17;
fusc   = 47;
R      = 10.73;
vslip  = 2.2;
g      = 32.2;
Asvsc  =930;%749;
Asvrgc = 930;%533;

%     Regenerator constans

ch      = 0.075;
mh      = 2;
cpc     = 0.31;
Qe      = 556;
areg    = 706.5;%590;
zlp     = 11;
ztop    = 106;%52;%47;
zcyc    = 103;%50;%45;
dH1     = 46368;
dH2     = 169080;
cpH2O   = 8.62;
cpN2    = 7.22;
cpCO    = 7.28;
cpCO2   = 11;
cpO2    = 7.62;
dHH     = 60960;
```

```
cpair   = 7.08;
tair    = 416;
mi      = 200000;
fof     = 424;
zsp     = 13;
hsp     = 20;
asp     = 7;
k14     = 1.1;
alp     = 8.73;
taufill = 40;
hlift   = 34;
etap    = 40.3;%155;
elift   = 61;%134;

%    airblowers

k6     = 250;
k7     = 25;
%k8     = 10;
k9     = 10;
kca    = 40;
tatm   = 75;
tcombd = 190;
vcombs = 40;
vcombd = 1000;
kavg   = 1.39;
polef  = 1;
samin  = 5000;
samax  = 6100;
sb     = 5950;
klift  = 5;
tliftd = 225;
vliftd = 200;
kcla   = 0.01;
kila   = 0.005;


V6    = 1.0;
V7    = 0.0;
V8    = 0.0;
V9    = 0.0;
V11   = 0.95;
V12   = 0;
V13   = 0.0;
Vlift = 0.42;
dpset = -3.37;

%coloana
NT=41;
% Location of feed stage (stages
are counted from the bottom):
NF=21;
% Number of components
NC=3;

% Relative volatilities:
alpha=[alpha1 alpha2...alphaNC]
alpha=[2.0 1.5 1.0];
%F=0.33;


%     Algebraic equations

if abs(flag) == 1

   %   state variables

     for i=1:82
         x(i)=X(i);
     end
     for i=83:123
         M(i)=X(i);
     end
     T2   = X(124);
     T3   = X(125);
     Tr   = X(126);
     Csc  = X(127);
     Wr   = X(128);
     P5   = X(129);
     P7   = X(130);
     Treg = X(131);
     Crgc = X(132);
     Wreg = X(133);
     Wc   = X(134);
     Wsp  = X(135);
     P6   = X(136);
     n    = X(137);
     P2   = X(138);
     vsc  = X(139);
     vrgc = X(140);
     P1   = X(141);
     fcol = X(142);

%intrari
     f3      = u(1);
     f4      = u(2);
     svsc    = u(3);
     svrgc   = u(4);
     LT      = u(5);
     fair_c  = u(6);
     f5set   = u(7);
     psif    = u(8);

      VB     = 0.4;
     V14     = 0.612;

 %disturbances

%     if t>30000
%    dpfrac=10.45; %13; %10; %9.75;
```

```
% end
%
%      if t>=10000
%     psif = 0.5;
%     end
%
     %if t>=300 & t<=3900
        % tatm=tatm+30/28800*(t-
300);
        %elseif t>3900
        % tatm=tatm+30*3600/28800;
        %end


%   2.2  feed system equations

f1 = f1set;
f2 = f2set;
%f3 = f3set;
%f4 = f4set;

%   2.3  Preheat system computing

f5    = f5set;

dtin  = T3-temph1;
dtout = T3-T2;
tln   = (dtin-
dtout)/(log(dtin/dtout));
Qloss = a1*f5*T3-a2;

%   2.4 General equations

%  regenerator computing used in
ubend and other

prgb = P6 + Wreg/144/areg;
f7   = kca*sqrt(max(0,P2-prgb));
rog  =
520*P6/(379*14.7*(Treg+459.6));

p4   = P5+dpfrac;
dprr = P6-p4;

fsg = k14*V14*sqrt(max(0,P6-patm));

% regenerator equations using total
air flowrate

% ft       = f7;
% fair     = f7/29;
ft       = f7 + fair_c;
fair     = ft/29;
vs       = 0.5*(fsg+fair)/rog/areg;
rocdil   = -0.878+0.582*vs;
epsf     = 0.332+0.06*vs;
rocdens  = ropart*(1-epsf);
zbed     =
min(zcyc,(2.85+0.8*vs+(Wreg-
rocdil*areg*zcyc)/...
            (areg*rocdens))*1/(1-
rocdil/rocdens));
pblp     = P6;
me       = areg*vs*rocdil;
roag     = 29*P6/R/(Tr-
dtstrp+459.6);

%   2.5    ubend equations

%     computing fsc

fsc        = vsc*areaus*roc;
Msc        = (Wr +
areaus*lus*roc)/g;
deltapsc   = 144*(p4-pblp) +
Wr/astr+(estrp-elift)*roc;
deltapsvsc =
((50*0.453*60/0.7/900)^2)*((fsc/svs
c/Asvsc)^2)/roc;
fmicsc     = (deltapsc -
144*deltapsvsc)*areaus -
vsc*lus*fusc;

%     computing frgc

frgc  = vrgc*areaur*roc;

vris  = (f3+f4)/rov+frgc/ropart;
roris = (f3+f4+frgc)/vris;
prb   = P5+dpfrac+roris*hris/144;


Mrgc       = (max(0,Wsp) +
areaur*lur*roc)/g;
deltaprgc  = 144*(P6-
prb)+(max(0,Wsp))/asp + (etap-
eloi)*roc;
deltapsvrgc =
((50*0.453*60/0.7/900)^2)*((frgc/As
vrgc/svrgc)^2)/roc;
fmicrgc    = (deltaprgc -
144*deltapsvrgc)*areaur -
vrgc*lur*furgc;

%   2.6 wet-gas compressor
equations

crw    = pvru/P7;
hwg    = 182922.1*(crw^(0.0942)-1);
```

```
fsucwg = 11600+sqrt(max(0,1.366e+8-
0.1057*hwg^2));
f11    = 2.636e-6*fsucwg*P7;
fV13   = k13*V13*pvru;

%   2.7 airblowers equations

if V6 > 0.5
         fpp6 = exp(2*log(0.15)*(1-
V6));
else
         fpp6 = 0.3*V6;
end
if V7 > 0.5
        fpp7 = exp(2*log(0.15)*(1-
V7));
else
        fpp7 = 0.3*V7;
end

Pbase = 14.7*P2/P1;
Fsucn_comb =
45000+sqrt(max(0,1.581e+9-
1.249e+6*(Pbase)^2));
f6   =
0.0451*P1*Fsucn_comb/(tatm+460);
fV7  = k7*fpp7*sqrt(max(0,P2-
patm));
fV6  = k6*fpp6*sqrt(max(0,patm-
P1));

%reactorul cu riser cu 5 componenti

COR=frgc/(f3+f4);
tc=Aris*hris/vris;

k1=1.54;
k2=5;
k3=0.55;
khco=7.09;
k4=0.35;
k5=0;
k6=0;
k7r=0.25;
k8=0;
kd=6.25;
alfa=18.5;
xhco=0.19;

CTO=COR;

yhco0=0.95;
ylco0=0.035;
ygln0=0.01;
ygas0=0;
ycoke0=0;
ficoke0=1;
teta0=0;

step=0.01;

No_of_elemnts = fix(tc/step);

yhco   = zeros(1,No_of_elemnts);
ylco   = zeros(1,No_of_elemnts);
ygln   = zeros(1,No_of_elemnts);
ygas   = zeros(1,No_of_elemnts);
ycoke  = zeros(1,No_of_elemnts);
ficoke = zeros(1,No_of_elemnts);

yhco(1)=yhco0;
ylco(1)=ylco0;
ygln(1)=ygln0;
ygas(1)=ygas0;
ycoke(1)=ycoke0;
ficoke(1)=ficoke0;

t=0;
timp(1) = 0;

cont = 1;
while t <= tc
     cc=0.68*(1-exp(-30*t));
   ficonv=exp(-(kd*cc));

dyhco=((-(k1+k2+k3)*(yhco(cont)-
xhco))*ficonv-(k7r*(yhco(cont)-
xhco))*ficoke(cont))*CTO;
dylco=((k1*(yhco(cont)-xhco)-
k4*ylco(cont))*ficonv-
(k8*ylco(cont))*ficoke(cont))*CTO;
dygln=(k2*(yhco(cont)-
xhco))*ficonv*CTO;
dygas=(k3*(yhco(cont)-
xhco)+k4*ylco(cont))*ficonv*CTO;
dycoke=(k7r*(yhco(cont)-
xhco)+k8*ylco(cont))*ficoke(cont)*C
TO;
dficoke=-alfa*ficoke(cont);

yhco(cont+1)=yhco(cont)+step*dyhco;
ylco(cont+1)=ylco(cont)+step*dylco;
ygln(cont+1)=ygln(cont)+step*dygln;
ygas(cont+1)=ygas(cont)+step*dygas;
ycoke(cont+1)=ycoke(cont)+step*dyco
ke;
ficoke(cont+1)=ficoke(cont)+step*df
icoke;

t=t+step;
```

```
timp(cont+1) = t;
cont = cont + 1;
end

yhcofinal=yhco(end);
ylcofinal=ylco(end);
yglnfinal=ygln(end);
ygasfinal=ygas(end);
ycokefinal=ycoke(end);
ficokefinal=ficoke(end);
timp=timp(end);
frhco=yhcofinal/(yhcofinal+ylcofina
l+yglnfinal+ygasfinal);
frlco=ylcofinal/(yhcofinal+ylcofina
l+yglnfinal+ygasfinal);
frgas=ygasfinal/(yhcofinal+ylcofina
l+yglnfinal+ygasfinal);
frglngas=(yglnfinal+ygasfinal)/(yhc
ofinal+ylcofinal+yglnfinal+ygasfina
l);
frtotal= frhco+frlco+frglngas;
quf=frhco+frlco+frglngas-frgas;
zF=[frglngas frlco frhco];

fb      = (psif*f3 + 3*f4 + 2*f1 -
0.8*f2)/(f3 + f4);
wris    = frgc*Aris*hris/vris;
whsv    = 3600*(f3+f4)/wris;
taur    = wris/60/frgc;
fcoke   =
(1.3557*(f3+f4)*fb*taur^(-
1.98431))/(100*whsv);
fwg     = (f3+f4)*(c1+c2*(Tr-
tref));
Qrgc    = frgc*cpc*(Treg-tbase);
Qrin    = Qrgc+f3*cpfl*(T2-tbasef);
Qcatout = frgc*cpc*(Tr-tbase);
Qslurry = f4*(cpsv*(Tr-tref)+Qsr);
Qff     = f3*(cpfv*(Tr-tref)+Qfr);
dhcrack = 172.7+3*(Tr-tref);
Qcracking = (f3+f4)*dhcrack;
Qrout     =
Qcatout+Qslurry+Qcracking+Qff;
Qr      = Qrin-Qrout;
tsc     = Tr-dtstrp;
fV12 = k12*V12*sqrt(P5-patm);

if V11 <= 0.5
         fppwg = 0.3*V11;
else
         fppwg =
exp(2*log(0.15)*(1-V11));
end

fV11 = k11*fppwg*sqrt(max(0,P5-
P7));

fH   = fsc*(Csc-Crgc)*ch;
epse =
min(1,max(epsf,epsf+(1.904+0.363*vs
-0.048*vs^2)/zbed));

z    = 0;
treg = Treg;
xCO  = 0;
xCO2 = 0;
%xO2  = 1/fair*(0.21*fair-0.25*fH);
xO2  = max(0,1/fair*(0.21*fair-
0.25*fH));%% s-a modificat de mine
stepz = 0.2;

while z < ztop
  if z<zcyc
      deltaz = 1;
  else
      deltaz = 0;
  end
      cpz =
0.79*cpN2+xCO*cpCO+xCO2*cpCO2+xO2*c
pO2+...

(0.25*cpH2O*fH+deltaz*cpc*me)/fair;

      k1 = 6.9547*exp(19.88-
34000/(treg+459.6));
      k2 = 0.69148*exp(15.06-
25000/(treg+459.6));
      k3 = 0.6412*P6*exp(25.55-
45000/(treg+459.6));

%
      if z<=zbed
         rob = 1-epse;
      else
        rob  = (1-epse)*exp(-
1000*fair/(areg*vs*rocdil)*(z-
zbed));
      end

     dxO2z  = (100*(-0.5*k1-
k2)*rob*Crgc-k3*xCO)*xO2/vs;
     dxCOz  = (100*k1*rob*Crgc-
2*k3*xCO)*xO2/vs;
     dxCO2z = -dxO2z - 0.5*dxCOz;
    if z <= zbed
      dtregz = 0;
    else
      dtregz =
(dH1*dxCOz+dH2*dxCO2z)/cpz;
```

```
    end

  xO2  = xO2+dxO2z*stepz;
  xCO  = xCO+dxCOz*stepz;
  xCO2 = xCO2+dxCO2z*stepz;
  treg = treg+dtregz*stepz;

       if xCO < 0
          xCO = 0;
       end
       if xO2 < 0
          xO2 = 0;
       end
       if xCO2 < 0
          xCO2 = 0;
       end
       if z > zcyc
         rob  = 0;
         tcyc = treg;
       end
     z = z + stepz;
end

xO2sg   = xO2;
xCOsg   = xCO;
xCO2sg  = xCO2;

Qfg     =
(fair*(xO2sg*cpO2+xCOsg*cpCO+xCO2sg
*cpCO2+0.79*cpN2)+0.5*cpH2O*fH)*(tc
yc-tbase);
Qsc     = fsc*cpc*(tsc-tbase);
Qc      =
fair*(xCOsg*dH1+xCO2sg*dH2);
Qh      = fH*dHH;
Qair    = fair*cpair*(tair-tbase);
Qoutreg = Qfg+Qrgc+Qe;
Qinreg  = Qair+Qh+Qc+Qsc;
Qreg    = Qinreg-Qoutreg;
lsp     = max(0,Wsp)/roc/asp;
d       = min(3,hsp-lsp);
fsp     =
max(0,fof*sqrt(asp)*(zbed-zsp)-
4925-20*(3-d)); % - 27;
cO2sg   = 100*fair*xO2sg/fsg;
cCOsg   =
1e+6*28*xCOsg/(28*xCOsg+44*xCO2sg+3
2*xO2sg+22.12);
vregg   = areg*zcyc-areg*zbed*(1-
epse);
%fcol= f3+f4+frgc-fsc-fwg;
%coloana
KcB=10;  KcD=10;
% controller gains
MDs=0.1; MBs=0.1;
% Nominal holdups - these are
rather small
Ds=0.165; Bs=0.165;
% Nominal flows
MB=X((NC-1)*NT+1);
MD=X(NC*NT) ;   % Actual reboiler
and condenser holdup
D=Ds+(MD-MDs)*KcD ;   % Distillate
flow
B=Bs+(MB-MBs)*KcB ;            %
Bottoms flow
x=X(1:(NC-1)*NT);
% Liquid compositions from btm to
top
M=X((NC-1)*NT+1:NC*NT);
% Liquid hold up from btm to top

% Rearrange elements of composition
vector (x) for later use
Iu=[1:NT]'*ones(1,NC-
1)+NT*ones(NT,1)*[0:NC-2];
x=(x(Iu))';
% THE MODEL

% Vapour-liquid equilibria
(multicomponent ideal VLE,
Stichlmair-Fair, 'Distillation', p.
36, 1998)
y=(alpha(1:NC-
1)'*ones(1,NT).*x)./(ones(1,NC-
1)'*(1+(alpha(1:NC-1)-1)*x));
 % Vapor Flows assuming constant
molar flows
i=1:NT-1;    V(i)=VB*ones(1,NT-1);
i=NF:NT-1;   V(i)=V(i) + (1-
quf)*fcol*0.4535/178;
% Liquid flows are given by
Franci's Weir Formula
L(i)=K*Mow(i)^1.5
% Liquid flow L(i) dependent only
on the holdup over the weir Mow(i)
% M(i)= Mow(i) + Muw(i) (Total
holdup = holdup over weir + holdup
below weir)
Kuf=21.65032/60;
% Constant above feed
Kbf=29.65032/60;
% Constant below feed
%Kuf=19/60;     %pt. dpfrac=9.0
% Constant above feed
%Kbf=27/60;     %pt. dpfrac=9.0
% Constant below feed
Muw=0.1;
% Liquid holdup under weir (Kmol)
```

```
i=2:NF;      L(i)= Kbf*(M(i)-
Muw).^1.5;     % Liquid flows below
feed (Kmol/min)
i=NF+1:NT-1; L(i)= Kuf*(M(i)-
Muw).^1.5;     % Liquid flows above
feed (Kmol/min)
L(NT)=LT;
% Condenser's liquid flow
(Kmol/min)
% Time derivatives from material
balances for
% 1) total holdup and 2) component
holdup

% Column
j=2:NT-1;
dMdt(j) = L(j+1)          - L(j)
+ V(j-1)          - V(j);

for i=1:NC-1;
for j=2:NT-1;
dMxdt(i,j) = L(j+1)*x(i,j+1)  -
L(j)*x(i,j)   + V(j-1)*y(i,j-1)
- V(j)*y(i,j);
end
end

% Correction for feed stage
% The feed is assumed to be mixed
into the feed stage

dMdt(NF) = dMdt(NF)  +
fcol*0.4535/178;

dMxdt(:,NF)=dMxdt(:,NF)+(fcol*0.453
5/178)*zF(1:NC-1)';

% Reboiler (assumed to be an
equilibrium stage)
dMdt(1) = L(2) - V(1)        - B;

i=1:NC-1;
dMxdt(i,1)= L(2)*x(i,2) -
V(1)*y(i,1) - B*x(i,1);
 % Total condenser (no equilibrium
stage)
dMdt(NT) = V(NT-1) - LT  - D;

i=1:NC-1;
dMxdt(i,NT)= V(NT-1)*y(i,NT-1) -
LT*x(i,NT) - D*x(i,NT);

% Compute the derivative for the
mole fractions from d(Mx) = x dM +
M dx
dxdt=(dMxdt-x.*(ones(NC-
1,1)*dMdt))./(ones(NC-1,1)*M');

% Rearrange elements of composition
vector (dxdt) for later use
Ix=[1:(NC-1)*NT]';
W=dxdt';
dxdt=W(Ix);

dT2   = (temph1+UAf*tln/f3-
T2)/taufo;
dT3   = (f5*DHfu-UAf*tln-
Qloss)/taufb;
dTr   = (Qrin-Qrout)/mcpeff;
dCsc  = (frgc*Crgc+fcoke-fsc*Csc-
Csc*(frgc-fsc))/Wr;
dWr   = frgc-fsc;
dP5   = 0.833*(fwg-fV11-fV12+fV13);
dP7   = 5*(fV11-f11);
dTreg = (Qinreg-
Qoutreg)/((Wreg+max(0,Wsp))*cpc+mi)
;
dCrgc = (fsc*Csc-fH-
(max(0,fsp)*Crgc+12*fair*(xCOsg+xCO
2sg))-Crgc*...
         (fsc-max(0,fsp)))/Wreg;
dWreg = fsc-max(0,fsp);
dWc   = fsc*Csc-fH-
(max(0,fsp)*Crgc+12*fair*(xCOsg+xCO
2sg));
dWsp  = max(0,fsp)-frgc;
dP6   = (R*(n*(Qinreg-
Qoutreg)/((Wreg+max(0,Wsp))*cpc...
+mi)+(Treg+460)*(fair-fsg)))/vregg;
dn    = fair-fsg;
dP2   =
R*(tcombd+460)/29/vcombd*(f6-fV7-
f7);
dvsc  = fmicsc/Msc;
dvrgc = fmicrgc/Mrgc;
dP1   = R*(tatm + 460)*(fV6-
f6)/(29*vcombs);
dfcol = f3+f4+frgc-fsc-fcol;
%sys = [dxdt;dMdt'];
sys =
[dxdt;dMdt';dT2;dT3;dTr;dCsc;dWr;dP
5;dP7;dTreg;dCrgc;dWreg;...
dWc;dWsp;dP6;dn;dP2;dvsc;dvrgc;dP1;
dfcol];

%i=1:123;
 %X =
[x;M;T2;T3;Tr;Csc;Wr;P5;P7;Treg;Crg
c;Wreg;Wc;Wsp;P6;n;P2;vsc;vrgc;P1;f
col];
```

```
 elseif flag == 0
  sys = [142 0 142+11 8 0 0];


X0 = [

    4.102805762039235e-001
    5.250768045383215e-001
    6.090295678210853e-001
    6.647184711852767e-001
    6.999136517544166e-001
    7.218309205578514e-001
    7.355425780052245e-001
    7.442398214671327e-001
    7.498489420584803e-001
    7.535247153536314e-001
    7.559668699297101e-001
    7.576074667588276e-001
    7.587190211488416e-001
    7.594769446441061e-001
    7.599961569859209e-001
    7.603530400594605e-001
    7.605989356947257e-001
    7.607686491186187e-001
    7.608859237989325e-001
    7.609670311072776e-001
    7.610231583520370e-001
    7.935100634028763e-001
    8.202657175072821e-001
    8.418073423207758e-001
    8.589595228917157e-001
    8.726250679955578e-001
    8.836454796758728e-001
    8.927370216494378e-001
    9.004757439591793e-001
    9.073081306860253e-001
    9.135718798231480e-001
    9.195182605182517e-001
    9.253321212605720e-001
    9.311482385285077e-001
    9.370639780922759e-001
    9.431487644117131e-001
    9.494509921460599e-001
    9.560029811652185e-001
    9.628244826189277e-001
    9.699251398615792e-001
    9.773062150484678e-001
    1.530244978499652e-001
    1.541263538337487e-001
    1.459528257717734e-001
    1.344903117907614e-001
    1.233999670224613e-001
    1.141560945015914e-001
    1.070097723447256e-001
    1.017107298678100e-001
    9.787644439610779e-002
    9.514324975575179e-002
    9.321328685875070e-002
    9.185882971957438e-002
    9.091210762040128e-002
    9.025217387431267e-002
    8.979299824849162e-002
    8.947390960606379e-002
    8.925236108228883e-002
    8.909862784488616e-002
    8.899199577167828e-002
    8.891805499293592e-002
    8.886679315082846e-002
    9.271398485781029e-002
    9.511705265421500e-002
    9.620994638509704e-002
    9.617527103715355e-002
    9.519883982471469e-002
    9.344428455716700e-002
    9.104331179342076e-002
    8.809543157234483e-002
    8.467221514355509e-002
    8.082300408083755e-002
    7.658048860952456e-002
    7.196550956157456e-002
    6.699093505992447e-002
    6.166468549993386e-002
    5.599205504002732e-002
    4.997748248122757e-002
    4.362590131499029e-002
    3.694376848976960e-002
    2.993984307260207e-002
    2.262576268252438e-002
    9.284641325253319e-002
    1.099044817624081e+000
    1.099044817624081e+000
    1.099044817624082e+000
    1.099044817624082e+000
    1.099044817624083e+000
    1.099044817624083e+000
    1.099044817624084e+000
    1.099044817624084e+000
    1.099044817624084e+000
    1.099044817624084e+000
    1.099044817624084e+000
    1.099044817624084e+000
    1.099044817624083e+000
    1.099044817624083e+000
    1.099044817624082e+000
    1.099044817624082e+000
    1.099044817624081e+000
    1.099044817624081e+000
    1.099044817624080e+000
    1.099044817624080e+000
    1.023048680803940e+000
```

```
    1.023048680803940e+000
    1.023048680803940e+000
    1.023048680803940e+000
    1.023048680803940e+000
    1.023048680803940e+000
    1.023048680803940e+000
    1.023048680803940e+000
    1.023048680803940e+000
    1.023048680803940e+000
    1.023048680803940e+000
    1.023048680803940e+000
    1.023048680803940e+000
    1.023048680803940e+000
    1.023048680803940e+000
    1.023048680803940e+000
    1.023048680803940e+000
    1.023048680803940e+000
    9.529993506207503e-002
    7.826027736455383e+002
    1.659564334971949e+003
    9.932070027620795e+002
    3.901281291711348e-003
    2.225473104525494e+005
    1.579229601661189e+001
    1.557926799156491e+001
    1.064425988191907e+003
    1.952728693846411e-003
    3.927528423494652e+005
    1.845380965498859e+003
    3.243834313719916e+003
    2.786505547810026e+001
    2.566492705837050e+002
    3.479018022391441e+001
    4.055562514970572e+000
    4.963524272053554e+000
    1.492154586174961e+001
    8.300000000000543e+001
 ];

elseif flag == 3

    for i=1:82
         x(i)=X(i);
     end
     for i=83:123
         M(i)=X(i);
     end
     T2   = X(124);
     T3   = X(125);
     Tr   = X(126);
     Csc  = X(127);
     Wr   = X(128);
     P5   = X(129);
     P7   = X(130);
     Treg = X(131);
     Crgc = X(132);
     Wreg = X(133);
     Wc   = X(134);
     Wsp  = X(135);
     P6   = X(136);
     n    = X(137);
     P2   = X(138);
     vsc  = X(139);
     vrgc = X(140);
     P1   = X(141);
     fcol = X(142);
     p4   = P5+dpfrac;
dprr = P6-p4;
  if t==0
    ft    =7.002416469083545e+001;
    xO2sg = 9.426727601699798e-002;
    xCOsg = 4.259398111910952e-008;
    xCO2sg = 9.308933947905657e-
002;
    fsc = 1.496502568024175e+003;
    frgc = 1.496502568024172e+003;
    cO2sg = 9.426727601699826e+000;
    cCOsg = 4.079815564345754e-002;
    yhcofinal= 1.899999980733520e-
001;
    ylcofinal = 7.899168031516896e-
002;
   yglnfinal = 5.383451451188887e-
001;

   frglngas = 0.56952817544156;
   frlco = 0.17262037126428;
   frhco = 0.25785145329416;
   quf = 0.93122462693013;
   ygasfinal = 6.607188611783442e-
02;
   ycokefinal = 3.430893910662157e-
02;

 end
sys=[X];
sys =
[X;ft;xO2sg;xCOsg;xCO2sg;fsc;frgc;c
O2sg;cCOsg;yhcofinal;ylcofinal;ygln
final];

else

 sys = [];
 end
```

LIST OF PUBLICATIONS

Conference papers:

Alsabei, R., Z.K. Nagy, and V. Nassehi. 2008. Process simulators based control design for a fluid catalytic cracking unit. 18th International Congress of Chemical and Process Engineering, Prague, Czech Republic.

Alsabei, R., Z.K. Nagy, and V. Nassehi. 2009. Process simulators based control design for universal oil products FCCU. Chemical Engineering, 8th World Congress of Chemical Engineering (WCCE 8), Montréal, Canada.

Alsabei, R., Z.K. Nagy, and V. Nassehi. 2009. Multivariate control structure synthesis for fluid catalytic unit Using Relative Gain Array. Chemical Engineering, D.B. Das, V. Nassehi, L. Deka, EUROSIS-ETI 2009, 7th International Industrial Simulation Conference, Quality Hotel, Loughborough, 251-256, ISBN 978-90-77381-4-89.

Alsabei, R., Z.K. Nagy, and V. Nassehi. 2009. Mathematical modelling and control of a UOP fluid catalytic cracking unit. Chemical Engineering, Saudi Students Club & Schools in UK and Ireland, 3rd Saudi International Conference, University of Surrey, UK, 32.

Alsabei, R., Z.K. Nagy, and V. Nassehi. 2010. Linear model predictive control of a fluid catalytic cracking unit. Chemical Engineering, Saudi Students Club & Schools in UK and Ireland, 4th Saudi international conference, University of Manchester, UK.

Alsabei, R., Z.K. Nagy, and V. Nassehi. 2010. Model based control of a UOP fluid catalytic cracking unit. Chemical Engineering Conference, Loughborough University, UK.

Conference Presentations:

Alsabei, R., Z.K. Nagy, and V. Nassehi. 2008. Process Simulators Based Control Design For a Fluid Catalytic Cracking Unit. 18th International Congress of Chemical and Process Engineering, Prague, Czech Republic.

Alsabei, R., Z.K. Nagy, and V. Nassehi. 2009. Process simulators based control design for universal oil products FCCU. Chemical Engineering, 8th World Congress of Chemical Engineering (WCCE 8), Montréal, Canada.

Alsabei, R., Z.K. Nagy, and V. Nassehi. 2009. Multivariate control structure synthesis for fluid catalytic unit using relative gain array. Chemical Engineering, D.B. Das, V. Nassehi, L. Deka, EUROSIS-ETI 2009, 7th International Industrial Simulation Conference, Quality Hotel, Loughborough, 251-256, ISBN 978-90-77381-4-89.

Alsabei, R., Z.K. Nagy, and V. Nassehi. 2009. Mathematical modelling and control of a UOP fluid catalytic cracking unit. Chemical Engineering, Saudi Students Club & Schools in UK and Ireland, 3rd Saudi International Conference, University of Surrey, UK, 32.

Poster Presentations:

Alsabei, R., Z.K. Nagy, and V. Nassehi. 2010. Linear model predictive control of a fluid catalytic cracking unit. Chemical Engineering, Saudi Students Club & Schools in UK and Ireland, 4th Saudi international conference, University of Manchester, UK.

Alsabei, R., Z.K. Nagy, and V. Nassehi. 2010. Model based control of a UOP fluid catalytic cracking unit. Chemical Engineering Conference, Loughborough University, UK.

Journal Paper:

Alsabei, R., Z.K. Nagy, and V. Nassehi. 2011. Economic optimization based model predictive control of a fluid catalytic cracking unit. Chemical Engineering and Processing (under review).

Awards and Prizes:

Gold poster award in Engineering at 4th Saudi International Conference, University of Manchester, UK, 2010.

Award of excellence from Saudi Cultural Bureau in London, UK, 2011.